



Existence and construction of Chebyshev nets with singularities and application to gridshells

Yannick Masson

► To cite this version:

Yannick Masson. Existence and construction of Chebyshev nets with singularities and application to gridshells. Mathematics [math]. Université Paris Est, École des Ponts Paris Tech, 6-8 avenue Blaise Pascal, 77455 Marne La Vallée, 2017. English. NNT: . tel-01676984v1

HAL Id: tel-01676984

<https://theses.hal.science/tel-01676984v1>

Submitted on 14 Jan 2018 (v1), last revised 9 Apr 2018 (v2)

HAL is a multi-disciplinary open access archive for the deposit and dissemination of scientific research documents, whether they are published or not. The documents may come from teaching and research institutions in France or abroad, or from public or private research centers.

L'archive ouverte pluridisciplinaire **HAL**, est destinée au dépôt et à la diffusion de documents scientifiques de niveau recherche, publiés ou non, émanant des établissements d'enseignement et de recherche français ou étrangers, des laboratoires publics ou privés.

UNIVERSITÉ — PARIS-EST

École Doctorale: Mathématiques et Sciences et Technologies
de l'Information et de la Communication

THÈSE DE DOCTORAT
Spécialité : Mathématiques appliquées

Présentée par

Yannick Masson

**Existence et construction de réseaux
de Chebyshev avec singularités et
application aux gridshells**

Thèse dirigée par Olivier Baverel et Alexandre Ern au CERMICS,
École des Ponts ParisTech

Soutenue le 9 Juin 2017 devant un jury composé de :

M. Pierre Alliez	INRIA Sophia-Antipolis	Rapporteur
M. Olivier Baverel	École des Ponts ParisTech	Codirecteur de thèse
M. Alexandre Ern	École des Ponts ParisTech	Directeur de thèse
M. Laurent Hauswirth	Université Paris-Est Marne-la-Vallée	Examinateur
M. Tim Hoffmann	Technische Universität München	Rapporteur
M. Arthur Lebée	École des Ponts ParisTech	Invité
Mme. Pooran Memari	École Polytechnique	Examinaterice
M. Laurent Monasse	École des Ponts ParisTech	Examinateur
M. Thilo Rörig	Technische Universität Berlin	Examinateur

Remerciements

This Thesis has been supported by a PhD fellowship from Labex MMCD (Modeling and Experiments for Durable Construction) in the framework of the French “Programme des Investissements d’Avenir ANR-11-LABX-022-01”. This support is gratefully acknowledged.

This Thesis has also benefited from the on-site collaborations stimulated by the Labex Bezout on Mathematics, Informatics and their common applications. In particular, the scientific progress of the Thesis was discussed (more or less every two months) within a Supervision Committee composed of experts in Numerical Analysis (A. Ern and L. Monasse, CERMICS Laboratory, University Paris Est, ENPC), in Structural Engineering (O. Baverel, A. Lebée, Navier laboratory, University Paris Est, ENPC), and in Discrete Geometry (L. Hauswirth, LAMA Laboratory, University Paris Est Marne la Vallée). This Interdisciplinary Committee has been extremely useful to broaden the perspective and to elaborate on many seminal ideas developed in this Thesis. I am thankful to all the members of this Committee for the time they have dedicated to this Thesis, in discussing ideas, formalizing them and writing them up.

I would like to thank Pierre Alliez and Tim Hoffmann for having accepted to review this manuscript. I am looking forward to their comments. I also would like to thank Pooran Memari and Thilo Röhrig for having accepted to participate in the Defense Committee and I am looking forward in engaging discussions with them.

[Personal thanks to be completed]

Résumé

Les réseaux de Chebyshev sont des systèmes de coordonnées sur les surfaces que l'on obtient par cisaillement d'un domaine du plan. Ceux-ci sont utilisés en particulier pour modéliser les gridshells qui constituent une construction architecturale notamment reconnue pour son faible coût environnemental. La difficulté principale dans la conception des gridshells est le manque de diversité des formes accessibles. En effet, bien que toute surface admette localement en tout point un réseau de Chebyshev, l'existence globale de ce type de coordonnées n'est possible que sur un ensemble restreint de surfaces. La recherche de conditions suffisantes pour l'existence globale de réseaux de Chebyshev est toujours d'actualité. Un des résultats de cette thèse est l'amélioration de ces conditions. Les possibilités d'améliorations en ce sens étant néanmoins limitées, nous élargissons la perspective en considérant des réseaux de Chebyshev avec singularités. Notre résultat principal est l'existence de réseaux de Chebyshev avec singularités coniques, lisses par morceaux, sur toute surface dont la courbure totale positive est inférieure à 2π et dont la courbure totale négative est finie. Notre preuve est constructive, ce qui permet de déterminer ces réseaux dans des cas pratiques. Nous avons implémenté un cas particulier de notre algorithme dans le logiciel Rhinoceros et nous présentons des exemples de réseaux construits par cette méthode.

Abstract

Chebyshev nets are coordinate systems on surfaces obtained by pure shearing of a planar domain. These nets are used in particular to model gridshells, an architectural construction which is well-known for its low environmental impact. The main issue when designing a gridshell is the lack of diversity of the accessible shapes. Indeed, although any surface admits locally a Chebyshev net at any point, the global existence for these coordinate systems is only possible for a restricted set of surfaces. The research for sufficient conditions ensuring the global existence of Chebyshev nets is still ongoing. A result achieved in this thesis is an improvement on these conditions. Since the improvement in this direction seems to be rather limited, we broaden the perspective by introducing Chebyshev nets with singularities. Our main result is the existence of a global Chebyshev net with conical singularities on any surface with total positive curvature less than 2π and with finite total negative curvature. Our proof is constructive, so that this method can be applied to practical cases. We have implemented a special instance of this algorithm in the software Rhinoceros and some discrete Chebyshev nets constructed using this method are presented.

Table of contents

List of figures	i
1 Introduction	1
1.1 Les gridshells	1
1.1.1 Généralités	2
1.1.2 Conception : la recherche de forme	5
1.2 Surfaces paramétrées et systèmes de coordonnées	9
1.3 Les réseaux de Chebyshev	11
1.3.1 Brève introduction	11
1.3.2 Propriétés	14
1.3.3 Discréétisation : la méthode du compas	17
1.3.4 État de l'art sur l'existence	18
1.4 Résultats principaux et plan du manuscrit	19
2 Smooth Chebyshev nets defined by dual boundary conditions	21
2.1 Introduction	21
2.2 Preliminary results	22
2.2.1 Splitting the surface into two components	22
2.2.2 Solution to Servant's equations	23
2.3 Existence of a Chebyshev net on each half-surface	24
2.3.1 Global injectivity of the map φ	24
2.3.2 Hazzidakis' formula on the dual	24
2.3.3 Angle distribution along the dual curve	26
2.4 Proof of the main theorem	26
3 Conical singularities	29
3.1 Chebyshev coordinates	29
3.1.1 Introduction	29
3.1.2 Construction of Chebyshev nets with conical singularities	31
3.2 Global surface parametrization and conical singularities	35
3.2.1 From local to global coordinate systems	36
3.2.2 Singularities of globally compatible coordinate systems	39
3.3 Properties of Chebyshev globally compatible atlases with conical singularities	48
3.4 Some technical results	53
3.4.1 From globally compatible atlases to local homeomorphisms	53
3.4.2 Proof of Proposition 3.15	57

Table of contents

3.4.3 Proof of Proposition 3.31	58
4 Smooth Chebyshev nets defined by primal boundary conditions	67
4.1 Preliminaries	67
4.1.1 Informal statement of the main result	67
4.1.2 Functional spaces and statement of the main result	70
4.2 Construction of a Chebyshev net from its angle distribution	71
4.2.1 Construction of curves from their geodesic curvature	72
4.2.2 Construction of the parametrization	77
4.2.3 Regularity of the candidate Chebyshev nets	79
4.2.4 From integrability conditions to Chebyshev nets	80
4.3 Existence and uniqueness of angle distribution	86
4.3.1 Local existence of a solution	86
4.3.2 Extension to rectangles	91
4.3.3 Proof of the main result	93
5 Construction of Chebyshev nets with singularities	95
5.1 Introduction	95
5.2 Chebyshev nets on broken half-surfaces	96
5.2.1 Construction on a sector	97
5.2.2 Construction on a broken half-surface	101
5.3 Splitting of a surface into geodesic broken half-surfaces	103
5.3.1 Splitting of broken half-surfaces	103
5.3.2 Recursive splitting	106
5.4 Proof of the main theorem	109
5.4.1 Existence of a Chebyshev net with conical singularities	109
5.4.2 Piecewise smooth Chebyshev nets on broken half-surfaces	111
6 Construction of discrete Chebyshev nets with singularities	121
6.1 Discrete Chebyshev nets with conical singularities	121
6.1.1 Compass method	121
6.1.2 Discrete Chebyshev nets given by two primal curves	123
6.1.3 Junction of discrete Chebyshev nets and conical singularities	124
6.2 An algorithm for Chebyshev nets with one conical singularity	125
6.2.1 Splitting the surface into sectors	127
6.2.2 Algorithm	129
6.3 Numerical results	129
6.4 Additional functionalities	131
6.4.1 Other types of boundary conditions	131
6.4.2 Rosette singularities	135
7 Perspectives	139
7.1 Possible extensions of our results	139
7.2 Existence and construction of Chebyshev nets	140
7.3 Conception of Algorithms	140

References	143
-------------------	------------

List of figures

1.1	Mise en forme d'un gridshell : déformation élastique d'une grille de poutres (Créteil, 2013)	2
1.2	Position des extrémités des poutres fixée au sol [18]	3
1.3	Un gridshell après contreventement [21]	3
1.4	Gridshell de Mannheim [17, p.19]	5
1.5	Intérieur du Savill Building [17, p.29]	5
1.6	La grille de poutres assemblée dans le plan sur un domaine $U_{\text{gs}} \subset (\mathbb{R}^+)^2$	7
1.7	Méthode du filet suspendu et gridshell correspondant [17, p.131]	8
1.8	Les singularités génériques des réseaux de Chebyshev	13
1.9	Un réseau de Chebyshev sur la sphère [25]	14
1.10	Un réseau de Chebyshev sur le caténoïde	14
1.11	Un réseau de Chebyshev sur une surface de translation	15
1.12	Illustration du transport parallèle de $\partial_u \varphi$ le long de $\varphi(u_1, \cdot)$	16
1.13	Schéma des angles entre les lignes de coordonnées d'un réseau de Chebyshev sur Ω	17
1.14	Méthode du compas avec des conditions au bord de type primal (les conditions au bord sont les courbes en rouge)	18
2.1	Scheme of the Hazzidakis' formula on triangle ABC	25
3.1	Illustration of the angles between the coordinate curves of a Chebyshev net on Ω	30
3.2	Illustration of an O-polyhedral surface	32
3.3	Three polygons of an O-surface	32
3.4	A vertex p_e^1 of an O-polyhedral surface ($\lambda_1 = \theta_{1,1} + \theta_{1,2} + \theta_{1,3} = 2\pi$)	32
3.5	Illustration of the equivalence table T of a Chebyshev net with one conical singularity on the plane	33
3.6	A Chebyshev net with one conical singularity on Enneper's surface	34
3.7	Chebyshev nets with singularities: junction of 5 mappings on Enneper's surface (top) and junction of 3 mappings on the sphere (bottom)	34
3.8	Illustration of the four types of orthogonal polygons in \mathbb{R}^2	35
3.9	A Chebyshev net with two conical singularities on the sphere: the image by φ of the orthogonal polygons are delimited by the red curves	36
3.10	Illustration of two compatible nets on M [31, p.3]	37
3.11	Illustration of a GC atlas that does not contain a global coordinate system	38
3.12	A GC atlas on the cylinder of revolution	39
3.13	A GC atlas on the torus	39
3.14	Generic singularities of Chebyshev nets	40

3.15 An example of singularity at once in the usual sense and in the present meaning on a Chebyshev net $\bar{\varphi}$	40
3.16 A representation of the cone of interior angle λ : the rays (OA) and (OB) are isometrically identified as a single line	41
3.17 Illustrations of conical surfaces isometrically embedded in \mathbb{R}^3	42
3.18 Representation of the branch-cut domain $\bar{V} \subset C_\lambda$ with its associated global isometry $Is(C_\lambda, \bar{V})$ in principal subcases	43
3.19 Illustration of the set $\bar{V}_{\theta_0, \delta}$ introduced in Definition 3.22	44
3.20 Illustration of the GC atlas induced by the complex square root	45
3.21 Illustration of the mapping $\bar{\varphi}: C_{4\pi} \rightarrow \mathbb{C}$ defined from the square root	46
3.22 A GC atlas with one singularity defined on \mathbb{R}^2 by the mapping τ of Example 3.32	49
3.23 Illustration of the Hazzidakis formula	50
3.24 A Chebyshev GC atlas with a conical singularity of valence 8 on Enneper's surface	51
3.25 Illustration of the proof of the smoothness of $\bar{\varphi} _{\bar{V}_{m,1}}$ at 0	51
3.26 Illustration of the angles $\{\theta_\alpha\}_{1 \leq \alpha \leq n}$ of a conical singularity (proof of Proposition 3.37)	52
3.27 Illustration of $\bar{\varphi}(\bar{V}_{\alpha_0,2})$ (proof of Proposition 3.37)	53
3.28 Illustration of the total transition mapping [47]	54
3.29 Illustration of the open covers $\{\Omega_i\}_{1 \leq i \leq N}$ and $\{\tilde{\Omega}_\alpha\}_{1 \leq \alpha \leq \tilde{N}}$ ($n_{\alpha+1} = n_\alpha + 2$)	55
3.30 Illustration of the branch-cut	59
3.31 Illustration of the construction of the mapping $\tilde{\psi}_2$	61
3.32 Construction of the mapping ψ_{cyl} (proof of Lemma 3.44)	63
3.33 Illustration of the sets $\bar{\Omega}_0$ and D	66
4.1 Illustration of the coordinate curves of a Chebyshev net φ	69
4.2 Illustration of the construction of the family of curves σ_1	72
4.3 Illustration of the construction of the parametrization φ_ω	77
5.1 Illustration of the total turn angle $\tau(\eta)$	96
5.2 Illustration of a Chebyshev net φ on a sector Q of exterior angle ψ	97
5.3 Illustration of the parallel transport of $\partial_u \varphi$ along $\varphi(u_1, \cdot)$	98
5.4 Illustration of the Hazzidakis formula	99
5.5 Illustration of the Hazzidakis formula in the sector Q	100
5.6 Illustration of a geodesic N -half-surface B_c with $N=4$	101
5.7 Illustration of the sectorization $Q(B_c, p_2)$ of a N -half-surface B_c with $N=4$	102
5.8 Illustration of the two possible cases for the splitting in Theorem 5.16 ($N=4$)	104
5.9 Illustration of the possible splittings of a N -half-surface with $N=4$ (proof of Theorem 5.16)	105
5.10 Illustration of the splitting of Theorem 5.18	107
5.11 Illustration of the recursive splitting used for the proof of Theorem 5.20	110
5.12 An example of skeleton	111
5.13 Illustration of the construction of the Chebyshev net with conical singularities (the crosses are the vertices)	112
5.14 Illustration of the notation of Lemma 5.24	113

5.15	Parallel transport of η_1 and η_2 along each other ($N_1 = 1$, $N_2 = 2$): numbering of the double induction process	114
5.16	Illustration of the parallel transport of $\eta_{2,1}$ along $\eta_{1,1}$ ($N_1 = 1$, $N_2 = 1$)	115
5.17	Illustration of the recursive parallel transport of η_2 along $\eta_{1,1}$ ($N_1 = 1$, $N_2 = 2$)	116
6.1	The surface used for the conception of the forum constructed for the Soliday's festival (Rhinoceros software)	122
6.2	Illustration of the compass method with the primal boundary conditions given by the red curves	123
6.3	A Chebyshev net constructed with the primal boundary conditions given by the red curves (view 2 of Figure 6.1)	124
6.4	Junction of two discrete Chebyshev nets (view 1)	125
6.5	Connectivity of a discrete Chebyshev net at a conical singularity point of valence 5	126
6.6	Junction of 6 discrete Chebyshev nets defined by the primal boundary conditions given by the red curves forming two singularity points (view 1)	126
6.7	A discrete Chebyshev net with one conical singularity of valence 6 (view 1)	127
6.8	Illustration of the Hazzidakis formula on the parallelogram $ABCD$	127
6.9	Illustration of the surface splitting into sectors	128
6.10	A Chebyshev net with one singularity on Enneper's surface of order 3	129
6.11	A Chebyshev net with one singularity on Enneper's surface of order 5	131
6.12	A Chebyshev net with one singularity on a surface with positive and negative curvature	132
6.13	Illustration of the one-sided compass method with the dual boundary conditions given by the curve and the angles in red	133
6.14	A Chebyshev net constructed with the dual boundary conditions given by the red curve and a constant angle (view 1)	134
6.15	A discrete Chebyshev net defined by a closed dual curve (in red) on the sphere .	134
6.16	Grid formed by the diagonals of the discrete cylinder	135
6.17	Illustration of the one-sided compass method with mixed boundary conditions .	135
6.18	A Chebyshev net constructed with the mixed boundary conditions given by the red curves (view 1)	136
6.19	A discrete Chebyshev net with a rosette singularity defined by a small closed dual curve (view 1)	137
6.20	A neighborhood of a rosette singularity	137
6.21	A rosette singularity reduced to a point	138
6.22	A junction of discrete Chebyshev nets defined by the primal boundary conditions given by the red curves forming a rosette-type singularity	138
7.1	Illustration of a Chebyshev net with two conical singularities of valence 3 joined by a coordinate curve	140

Chapter 1

Introduction

Nous présentons en premier lieu dans cette introduction un certain type de constructions architecturales : les gridshells. La conception d'un gridshell élastique nécessite une attention particulière sur le choix de la forme de cette construction. Les problématiques de recherche de forme pour les gridshells ont motivé cette thèse. Ces constructions sont obtenues par la déformation élastique d'une grille de poutres, que nous supposerons incompressibles et inextensibles, assemblées dans le plan. Nous présentons dans la section 1.1 une introduction à ce type de construction. Nous y mettons en avant l'importance de la recherche de forme dans la conception de ces structures. La déformation de la grille, appelée mise en forme du grishell, est modélisée par un type particulier de systèmes de coordonnées : les réseaux de Chebyshev. Ainsi, la recherche d'une surface accessible par gridshell passe par la construction d'un réseau de Chebyshev sur celle-ci. Dans la section 1.2, nous présentons quelques notions sur les surfaces et sur les systèmes de coordonnées nécessaires pour la présentation des réseaux de Chebyshev. Ces derniers sont introduits dans la section 1.3. Après avoir énoncé les principales problématiques de cette thèse, nous indiquons dans cette section quelques propriétés satisfaites par les réseaux de Chebyshev. Un état de l'art sur l'existence de ces réseaux sur une surface donnée est ensuite présenté. Enfin, nous présentons la méthode du compas : une méthode numérique permettant la discrétisation des réseaux de Chebyshev. Nous terminons ce chapitre en présentant les résultats obtenus au cours de cette thèse ainsi qu'un résumé des chapitres suivants (section 1.4).

Les gridshells

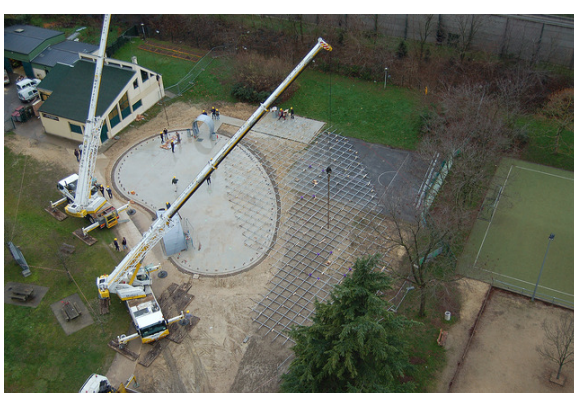
Nous présentons un aperçu des enjeux concernant la recherche de forme appliquée aux gridshells. Nous exposons en premier lieu dans la section 1.1.1 une brève introduction au concept de gridshell. Nous y définissons tout d'abord le terme gridshell puis nous présentons le procédé permettant leur construction. Ensuite, nous indiquons les différents avantages inhérents à ces constructions. Enfin, nous présentons quelques réalisations de gridshells. Dans un second temps, nous nous rapprochons en section 1.1.2 des problématiques amenant à l'étude des réseaux de Chebyshev : la recherche de forme. Ainsi, nous détaillons tout d'abord les différents aspects de la recherche de forme appliquée aux gridshells : les contraintes à satisfaire, mais aussi les objectifs à atteindre. Nous rappelons ensuite les principales méthodes utilisées à ce jour pour la recherche de forme de gridshells. Nous renvoyons à la thèse de Cyril Douthe [17] pour plus de détails sur la conception et la construction des gridshells.

Généralités

Nous commençons par définir le concept de gridshell.

Définition

Les gridshells peuvent être définis de la manière suivante : un gridshell est une structure obtenue par assemblage de poutres en une grille ayant un comportement mécanique de coque discrète. Ceci explique la juxtaposition des deux mots “grid” (grille) et “shell” (coque). Une définition plus précise est donnée par Frei Otto dans [39] : “Un gridshell est une structure de barres, courbe dans l'espace. Les barres forment une grille plane avec une maille rectangulaire et un espacement constant entre chaque noeud.” Ainsi, le terme de gridshell fait également références aux méthodes de construction permettant d'obtenir cette structure. Une méthode consiste à déformer une grille de poutres assemblée dans le plan (voir la figure 1.1). Cette déformation est appelée mise en forme de la structure. Aussi, nous utiliserons le terme raideur pour référer à la résistance d'un matériau ou d'une structure à une déformation. Quelques remarques faisant ressortir les



(a) Grille de poutres assemblée sur le sol [20]



(b) Déformation élastique de la grille de poutres [19]

Fig. 1.1 Mise en forme d'un gridshell : déformation élastique
d'une grille de poutres (Créteil, 2013)

caractéristiques des gridshells peuvent maintenant être faites à propos de cette mise en forme :

1. Tout d'abord, le choix de la forme a une place prépondérante dans la conception des gridshells. En effet, nous soulignons que la rigidité de la structure dépend principalement de cette forme.
2. Ensuite, pour pouvoir procéder à cette mise en forme, il est nécessaire que les poutres vérifient certaines propriétés. Celles-ci doivent tout d'abord être élancées et avoir une faible raideur en flexion. Aussi, ces poutres doivent être en capacité de subir une grande déformation élastique avant rupture. Finalement, afin d'assurer la rigidité de la structure, les poutres doivent avoir une grande raideur en traction/compression. Le choix des matériaux est donc essentiel pour la conception d'un gridshell. Ces propriétés peuvent être observées notamment dans certains bois ou certains matériaux composites qui, dans la majorité des cas, sont les matériaux utilisés pour ces constructions.
3. Enfin, les formes accessibles par gridshells sont des formes issues de cette déformation. Cela induit une restriction sur les formes accessibles que nous détaillons ci-dessous.

Ces trois points sont nécessairement à prendre en compte lors de la phase de conception d'un gridshell. Ainsi, le concept de gridshell regroupe aussi bien la structure que les matériaux choisis, mais aussi le procédé de mise en forme et le choix de la forme, contraint par ce procédé.

Méthode de construction

Le principe de construction est relativement simple et peut être résumé comme suit : on assemble tout d'abord deux directions de poutres sur le sol afin de former une grille. La jonction des poutres est faite par des articulations. Ces dernières permettent un cisaillement entre les deux directions de poutres et donc, grâce à la faible raideur en flexion, la déformation de cette grille. On déforme ensuite la grille afin d'obtenir la forme finale du gridshell, préalablement choisie. Cette étape peut nécessiter l'intervention de grues ou de tours de levage pour des constructions de grande échelle, comme on peut le voir sur la figure 1.1.

Une fois la forme obtenue, l'extrémité de chacune des poutres est fixée au sol, ce qui permet de rendre la structure suffisamment rigide pour ne plus nécessiter l'intervention des engins de levage, et ce grâce au choix d'une forme assurant une grande rigidité à la structure. On peut voir un gridshell à ce moment de la construction dans la figure 1.2. La structure ainsi fixée conserve une très faible raideur en cisaillement. En effet, les articulations joignant les poutres permettent toujours des cisaillement : la structure n'a pas encore un comportement de coque. C'est pourquoi on ajoute ensuite une troisième direction de poutres, dite de contreventement, dans une des deux directions diagonales de la grille (voir figure 1.3). Cette triangulation des mailles permet à la grille d'avoir un comportement de coque et d'augmenter ainsi considérablement la rigidité de la structure (l'augmentation de la raideur pouvant aller de un à vingt [3]). On recouvre finalement la structure d'un revêtement qui peut être une toile, cette étape terminant la construction. On peut voir quelques réalisations de gridshells dans la sous-section 1.1.1.4.



Fig. 1.2 Position des extrémités des poutres fixée au sol [18]

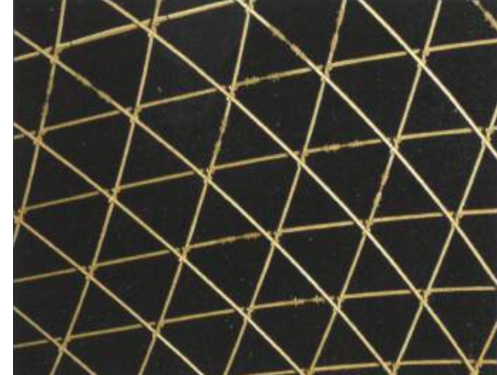


Fig. 1.3 Un gridshell après contreventement [21]

Défis et intérêts des gridshells

Comme nous allons le voir tout au long de ce manuscrit de thèse, la conception d'un gridshell s'avère complexe, notamment à cause des difficultés dues au choix de la forme. Mais d'autres difficultés concernant la conception et la construction de gridshells peuvent aussi être rencontrées. Notamment, les matériaux utilisés pour les gridshells, comme les matériaux composites verre/résine [17, Chap. 2], sont nouveaux dans le domaine du génie civil. Ensuite, la grille

de poutres réalisant de grands déplacements, la simulation de son comportement mécanique et notamment de sa stabilité nécessite une adaptation des méthodes de calculs à ce type de mécanique non-linéaire (voir par exemple [17, Chap. 3]). Soulignons que les gridshells présentent de nombreux intérêts par rapport à d'autres types de constructions plus classiques, qui motivent ces efforts d'adaptation. Ainsi, deux types d'avantages concernant les gridshells peuvent être mis en avant : le premier concerne la méthode de construction et le second réside dans la légèreté de la structure.

Tout d'abord, en ce qui concerne la méthode de construction, le premier grand intérêt est qu'elle est relativement simple et peu coûteuse. En effet, cette construction peut se faire en très peu de temps et demande un outillage peu important. Un second avantage de ce type de construction est qu'il permet de couvrir de grands espaces, libres de tout support. Pour finir, le démontage, voire le recyclage, des gridshells est tout aussi simple : il suffit de défaire les liaisons entre l'extrémité des poutres et le sol. La grille peut ensuite être repliée (très faible raideur en cisaillement des jonctions) ou désassemblée.

Regardons maintenant le deuxième grand avantage de ces constructions : leur légèreté. Pour commencer, la légèreté d'une structure est généralement définie comme le rapport entre le poids propre de celle-ci et les charges variables (charge que doit supporter la structure, vent, neige,...). Ainsi, notons que meilleure est la rigidité structurelle, plus légère sera la structure. En effet, cette rigidité permet une réduction du dimensionnement et donc une réduction du poids propre de la structure. En ce sens, pour concevoir des structures légères, Jörg Schlaigh donne quatre éléments principaux à prendre en compte [17, Chap. 1] :

1. La flexion des éléments qui doit être minimisée, ceci dans le but de mieux répartir les contraintes dans la structure.
2. Les matériaux de la structure qui doivent être choisis en prenant en compte les efforts qu'ils ont à subir et leurs propriétés mécaniques.
3. La précontrainte des éléments de la structure qui est à utiliser judicieusement afin d'obtenir une meilleure rigidité de ces éléments.
4. La forme de la structure qui doit être prise en compte, dans le même but de répartir de manière optimale les efforts dans celle-ci. En ce sens, il faut privilégier les surfaces à double courbure (courbure de Gauss non-nulle). Cette double courbure permet en effet à la structure d'avoir un comportement membranaire exploitant au mieux les propriétés du matériau (une grande raideur en traction/compression et en cisaillement de la structure).

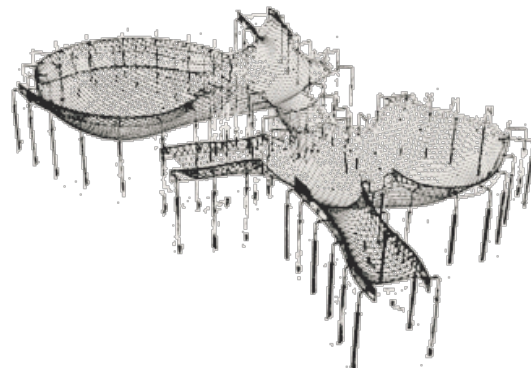
Les gridshells ont été conçus en ce sens et la recherche de forme, préalable à la construction d'un gridshell, permet d'optimiser ces différents points. Cette optimisation permet d'assurer une grande rigidité structurelle à la construction, aussi appelée rigidité géométrique dans la suite. Qui plus est, la quantité de matériaux est aussi considérablement réduite grâce à l'utilisation d'une structure de grille au lieu d'une coque continue. Pour finir, nous soulignons aussi la légèreté des matériaux utilisés (bois, matériaux composites verre/résine). Le poids propre de la structure est donc, de ce fait, très réduit, rendant le ratio définissant la légèreté d'une structure très élevé. Ceci fait du gridshell une structure très attractive dans ce contexte.

Quelques réalisations de gridshells

Une des premières réalisations de grande ampleur est le gridshell de Mannheim construit pour une exposition en 1975. La figure 1.4a est une vue aérienne de cette construction et on peut observer une maquette ayant servi à sa conception en figure 1.4b. Nous renvoyons à la sous-section 1.1.2.2 pour une explication de cette maquette.



(a) Vue aérienne du gridshell



(b) Maquette du gridshell

Fig. 1.4 Gridshell de Mannheim [17, p.19]

Le Savill Building du parc de Windsor construit en 2006 est un second exemple de gridshell que l'on peut observer sur la figure 1.5.

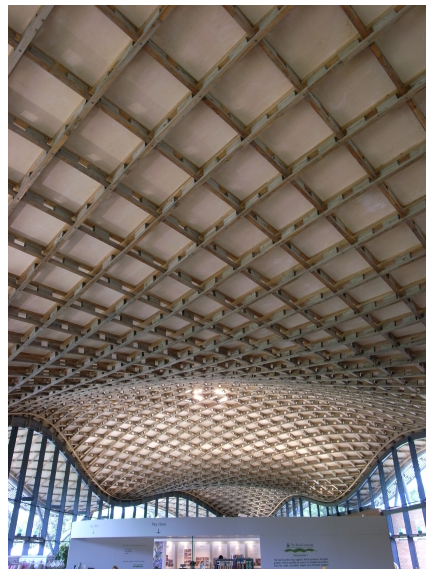


Fig. 1.5 Intérieur du Savill Building [17, p.29]

Conception : la recherche de forme

Nous nous intéressons maintenant à la recherche de forme : la recherche de surfaces accessibles par le procédé de mise en forme des gridshells. Nous décrivons dans un premier temps les contraintes devant être satisfaites par la forme du gridshell dans la sous-section 1.1.2.1. D'autres aspects doivent aussi être pris en compte par le concepteur comme la rigidité géométrique de la structure finale. Nous présentons un aperçu des différentes méthodes utilisées à ce jour pour cette recherche de forme en sous-section 1.1.2.2.

Des contraintes mécaniques et géométriques

Nous exposons maintenant les contraintes sur les formes que l'on peut obtenir par gridshell. Pour commencer, nous soulignons que les formes accessibles par ce procédé sont soumises à deux types de contraintes. Premièrement, celles-ci sont obtenues par la mise en forme : déformation élastique d'une grille de poutres assemblée dans le plan. Ainsi, cette contrainte, dite géométrique, est définie par les propriétés mécaniques des poutres (incompressibilité et inextensibilité) ainsi que par le type d'assemblage de la grille (articulations). La deuxième contrainte concerne la stabilité mécanique du gridshell. En effet, la structure doit être en équilibre avant même la prise en compte de la troisième direction de barres (contreventement) afin d'obtenir une structure ayant une grande rigidité. Il s'agit ainsi d'une contrainte qui ne peut être vérifiée qu'après simulation. Cette contrainte, que nous qualifierons de mécanique, ne sera pas détaillée dans ce manuscrit. Nous renvoyons à la thèse de Cyril Douthe [17, Chap. 3] pour un algorithme permettant de simuler les gridshells. C'est donc la contrainte géométrique à laquelle nous nous intéressons maintenant. Ainsi, nous considérons uniquement la mise en forme et nous ignorons la question de la stabilité mécanique de la structure.

Tout d'abord, en raison de la différence d'échelle entre la raideur en flexion et en tension/compression dans les poutres, nous simplifions le comportement mécanique de ces dernières en supposant que la raideur en tension/compression est infinie. L'incompressibilité et l'inextensibilité des poutres est ainsi imposée et la déformation d'une poutre de longueur $L > 0$ est donc définie par une courbe paramétrée par longueur d'arc

$$\gamma: [0, L] \rightarrow \mathbb{R}^3, \quad \text{avec } |\gamma'(s)| = 1 \text{ pour tout } s \in [0, L]. \quad (1.1)$$

Ensuite, l'assemblage de la grille dans le plan est réalisé par des articulations, ce qui induit une très faible raideur en cisaillement que nous supposons nulle. La mise en forme d'un gridshell est la déformation élastique de chacune des poutres de manière à préserver leurs longueurs, mais aussi la position des jonctions entre celles-ci. Étant élastique, cette déformation sera supposée lisse. Nous supposons de plus pour simplifier que la grille est régulière, c'est-à-dire que les poutres ne sont pas courbées dans le plan et que la distance $h > 0$ entre celles-ci est constante. Cette distance reste ainsi constante au cours de la déformation grâce à la préservation de la longueur des poutres. Dans ce cas, l'angle entre les deux directions de poutres est constant et un simple cisaillement nous ramène au cas où les mailles sont des carrés. Plaçons-nous donc dans ce cas et notons $U_{\text{gs}} \subset (\mathbb{R}^+)^2$ le domaine connexe et borné sur lequel est assemblé la grille de poutres. Nous notons $N_1 \geq 1$ et $N_2 \geq 1$ le nombre de poutres dans les directions verticales et horizontales respectivement. Nous supposons maintenant que les poutres sont initialement positionnées sur les domaines

$$D_{1,i}(U_{\text{gs}}) = U_{\text{gs}} \cap (\{ih\} \times \mathbb{R}^+), \quad D_{2,\alpha}(U_{\text{gs}}) = U_{\text{gs}} \cap (\mathbb{R}^+ \times \{\alpha h\}), \quad (1.2)$$

où $i \in \{1, \dots, N_1\}$ et $\alpha \in \{1, \dots, N_2\}$ sont respectivement l'indexation des poutres dans les directions verticales et horizontales. L'assemblage des poutres dans le plan est illustré dans la figure 1.6. Nous notons ensuite, pour tout $i \in \{1, \dots, N_1\}$, $\gamma_{1,i}: D_{1,i}(U_{\text{gs}}) \rightarrow \mathbb{R}^3$ et, pour tout $\alpha \in \{1, \dots, N_2\}$, $\gamma_{2,\alpha}: D_{2,\alpha}(U_{\text{gs}}) \rightarrow \mathbb{R}^3$ les positions respectives des poutres dans ces deux directions après mise en forme. Cela nous permet finalement, en supposant que h est petit, de définir une application

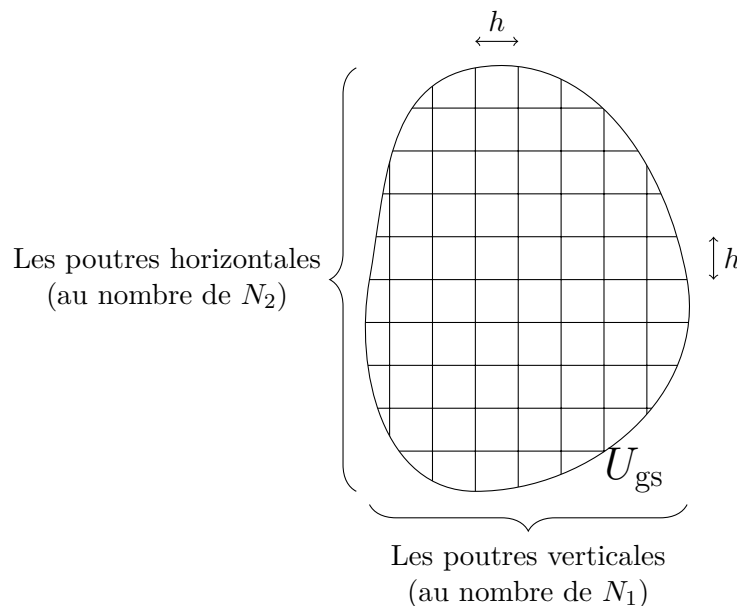


Fig. 1.6 La grille de poutres assemblée dans le plan sur un domaine $U_{\text{gs}} \subset (\mathbb{R}^+)^2$

lisse $\varphi: U_{\text{gs}} \rightarrow \varphi(U_{\text{gs}}) \subset \mathbb{R}^3$ telle que

$$\begin{aligned}\varphi(ih, y) &= \gamma_{1,i}(y), & \text{pour tout } y \in D_{1,i}(U_{\text{gs}}) \text{ et } i \in \{1, \dots, N_1\}, \\ \varphi(x, \alpha h) &= \gamma_{2,\alpha}(x), & \text{pour tout } x \in D_{2,\alpha}(U_{\text{gs}}) \text{ et } \alpha \in \{1, \dots, N_2\}.\end{aligned}\quad (1.3)$$

Cette application modélise la position du gridshell dans \mathbb{R}^3 . Ainsi, un gridshell est représenté par :

- son domaine de définition U_{gs} ;
- les courbes $\{\gamma_{1,i}\}_{1 \leq i \leq N_1}$ et $\{\gamma_{2,\alpha}\}_{1 \leq \alpha \leq N_2}$ le composant ou, de manière équivalente, par une application $\varphi: U_{\text{gs}} \rightarrow \varphi(U_{\text{gs}}) \subset \mathbb{R}^3$ définie à partir de celles-ci.

Notons finalement que, afin de bien prendre en compte toutes les contraintes géométriques dues à la mise en forme, il faudrait aussi imposer sur chacune des poutres une courbure maximale au delà de laquelle les poutres peuvent se détériorer. Il serait aussi souhaitable d'introduire un angle de cisaillement minimal, ceci dans le but de prendre en compte les contraintes liées aux jonctions. En effet, ces deux propriétés mécaniques sont aussi des contraintes sur la déformation définie par φ . Ces deux points peuvent néanmoins être vérifiés *a posteriori*. Ainsi, dans un souci de simplification, ils ne sont pas considérés dans cette modélisation.

Les différentes méthodes

Le but de la recherche de forme est de satisfaire les contraintes géométriques et mécaniques tout en ayant une grande rigidité géométrique. De plus, il est souhaitable de laisser du choix dans la forme afin de donner un peu de liberté au concepteur de la structure. Nous décrivons ci-dessous les méthodes les plus importantes permettant de trouver des formes satisfaisant ces contraintes et objectifs.

La première méthode consiste à idéaliser le comportement des poutres du gridshell par un comportement de fil, tout en choisissant une forme permettant à cette approximation d'être

justifiée *a posteriori*. Ainsi, avec cette méthode, dite du filet suspendu, la contrainte géométrique est satisfaite, tandis que la contrainte mécanique est analysée *a posteriori*. L’expérience est réalisée de la manière suivante : on choisit un domaine $U_{\text{gs}} \subset (\mathbb{R}^+)^2$ et on assemble une grille de fils formant des mailles orthogonales (le filet) sur ce domaine U_{gs} . L’extrémité des fils est ensuite attachée à un support puis le filet est suspendu. Finalement, on ajuste la longueur de chacune des cordes afin que celles-ci soient sans bosse (relativement tendues). Ainsi, les paramètres de recherche permettant d’obtenir différentes formes sont :

- l’image de l’extrémité des fils $\varphi(\partial U_{\text{gs}})$, c’est-à-dire les points où le filet est attaché au support ;
- le domaine U_{gs} , bien que ce choix ne soit pas complètement libre puisque ce domaine évolue au cours de l’expérience.

Cette méthode, illustrée dans la figure 1.7, a l’avantage d’être simple, mais permet difficilement de parcourir l’ensemble des formes accessibles et n’assure pas nécessairement la stabilité de la forme obtenue.

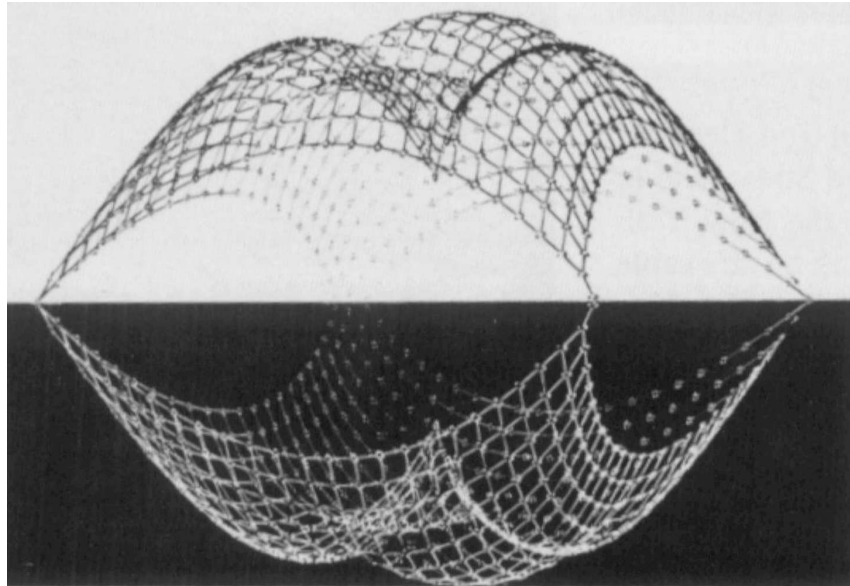


Fig. 1.7 Méthode du filet suspendu et gridshell correspondant [17, p.131]

Une seconde méthode permet de pallier en partie les deux difficultés ci-dessus : la méthode dite à contour libre. Il s’agit ici de prendre en compte la raideur en flexion, bien que faible, des poutres dans l’expérimentation, qui devient cette fois numérique. Le réseau de poutres est simulé par ordinateur afin de déterminer une statique de ce système qui réponde aux attentes des concepteurs. Cette prise en compte de la raideur en flexion permet de libérer de nombreux paramètres de recherche imposés dans la méthode précédente. Notamment, l’image du bord $\varphi(\partial U_{\text{gs}})$ peut être laissée libre (dans un domaine du plan par exemple) puisque la raideur en flexion va imposer la position de l’extrémité des poutres. Ainsi, dans cette méthode, les contraintes géométriques et mécaniques sont toutes deux vérifiées. Il reste donc à parcourir les formes accessibles afin d’optimiser la rigidité géométrique. Une analyse de cette méthode, ainsi que des différents paramètres de recherche permettant de parcourir les formes disponibles, peut être trouvée dans [17, section 4.3].

Cette méthode présente toujours le désavantage de ne pas pouvoir déterminer au préalable la forme du gridshell. Ainsi, une troisième méthode, que nous développons dans ce manuscrit, permet cette fois de fixer la forme désirée $M \subset \mathbb{R}^3$. Cette méthode est par exemple utilisée dans [21] où la forme M est issue d'une optimisation sur des critères mécaniques. Nous notons aussi ce parti pris de fixer la forme dans [13, 34, 35] où des méthodes d'optimisation sont utilisées pour concevoir des gridshells. Ce choix *a priori* de la forme complexifie considérablement la contrainte géométrique. Cette dernière se ramène dans ce cas à la question suivante :

Question 1.1. Existe-t-il $U_{\text{gs}} \subset (\mathbb{R}^+)^2$ et $\varphi: U_{\text{gs}} \rightarrow M$ vérifiant les contraintes :

- (1.3) et (1.2) sur l'assemblage des poutres réalisé par des articulations sur le domaine U_{gs} ;
- (1.1) sur l'inextensibilité des poutres.

Si la réponse à cette question est positive, il serait aussi souhaitable de savoir si la solution vérifie la contrainte mécanique de stabilité. Cette problématique reste ouverte et nous nous concentrerons dans cette thèse sur la première question, à savoir est-ce que M vérifie les contraintes géométriques ? Nous étudions pour cela les réseaux de Chebyshev qui sont au cœur de cette problématique. Une introduction à ce type de systèmes de coordonnées sur les surfaces est présentée dans la section 1.3.

Surfaces paramétrées et systèmes de coordonnées

Nous présentons maintenant quelques notions et propriétés concernant la géométrie des surfaces : système de coordonnées, application de Gauss, courbure, etc. Les notations que nous utiliserons dans la suite du manuscrit sont aussi introduites dans cette section.

Nous précisons tout d'abord que nous ne définissons pas dans la suite toutes les notions utilisées et nous renvoyons vers des ouvrages de géométrie comme [16] ou [22] pour une définition de ces notions. Nous appelons surface une variété connexe bidimensionnelle notée M , munie d'une métrique notée g . La surface est donc définie par le couple (M, g) . S'il n'y a pas d'ambiguité, nous la noterons simplement M . Les surfaces considérées sont supposées orientées et lisses. Nous précisons que le mot voisinage référera dans la suite à un voisinage ouvert. Une première propriété vérifiée par M est l'existence en tout point d'un système local de coordonnées :

Propriété 1.2 (Système local de coordonnées). *Pour tout $p \in M$, il existe un voisinage (ouvert) $\Omega \subset M$ de p et un C^∞ -difféomorphisme $\varphi: U \subset \mathbb{R}^2 \rightarrow \Omega$. Le couple (Ω, φ) est appelé système local de coordonnées de M en p .*

L'ensemble des systèmes locaux de coordonnées d'une surface est appelé atlas. Ces systèmes vérifient la propriété de compatibilité suivante :

Propriété 1.3 (Cartes C^∞ -compatibles). *Soient (Ω_i, φ_i) , (Ω_j, φ_j) deux systèmes locaux de coordonnées de M tels que $\Omega_i \cap \Omega_j \neq \emptyset$. Alors, l'application*

$$\varphi_j^{-1} \circ \varphi_i: \varphi_i^{-1}(\Omega_i \cap \Omega_j) \rightarrow \varphi_j^{-1}(\Omega_i \cap \Omega_j) \quad (1.4)$$

est un C^∞ -difféomorphisme et ces systèmes de coordonnées sont dits C^∞ -compatibles.

Un espace tangent à M peut être défini en chaque point $p \in M$. Il est noté $T_p M$ et le fibré tangent à M , défini par $\cup_{p \in M} T_p M$, est noté TM . Comme la surface est munie d'une métrique g , nous utiliserons les notations suivantes : pour tous $p \in M$ et $X_p, Y_p \in T_p M$,

$$\langle X_p, Y_p \rangle_g := g(X_p, Y_p), \quad |X_p|_g^2 := g(X_p, X_p).$$

Nous noterons, pour tous $X, Y \in \mathbb{R}^2$, $\langle X, Y \rangle$ le produit scalaire euclidien et $|X|$ la norme euclidienne. Soient maintenant $(M_1, g_1), (M_2, g_2)$ deux surfaces et $F: M_1 \rightarrow M_2$ une application lisse. L'application tangente à F est notée : $dF: TM_1 \rightarrow TM_2$ et, pour tout $p \in M_1$, la restriction de dF à $T_p M_1$ est notée $dF_p: T_p M_1 \rightarrow T_{F(p)} M_2$. L'application F est appelée isométrie locale lorsqu'elle vérifie, pour tous champs de vecteurs X, Y sur M_1 et en tout point de M_1 ,

$$\langle dF(X), dF(Y) \rangle_{g_2} = \langle X, Y \rangle_{g_1}.$$

Une application qui est à la fois une isométrie locale et une bijection est appelée isométrie globale (sous-entendu, sur son image). Nous notons u et v les deux composantes de \mathbb{R}^2 . Soient X et Y deux champs de vecteurs sur M . Nous notons $D_X Y$ la dérivation covariante de Y dans la direction X . Soit (Ω, φ) un système local de coordonnées et soient les champs de vecteurs $e_1 := \partial_u \varphi$ et $e_2 := \partial_v \varphi$ définissant une base de $T_p M$, pour tout $p \in \Omega$. En utilisant la notation d'Einstein, nous notons $[X, Y]$ le crochet de Lie de X et Y , exprimé dans le système de coordonnées (Ω, φ) par

$$[X, Y] = (X^j \partial_j Y^i - Y^j \partial_j X^i) e_i,$$

où $X = X^i e_i$ et $Y = Y^i e_i$. De plus, nous notons X^\perp le champ de vecteurs vérifiant $\angle(X, X^\perp) = \frac{\pi}{2}$ en tout point $p \in M$ tel que $X_p \neq 0$. Soit $\gamma: I \subset \mathbb{R} \rightarrow M$ une courbe paramétrée par longueur d'arc. Nous appelons courbure géodésique de γ la fonction $\kappa: I \rightarrow \mathbb{R}$ définie par

$$\kappa(t) = \langle \gamma''(t), \gamma'^\perp(t) \rangle_g,$$

pour tout $t \in I$.

Supposons maintenant que la surface M soit plongée dans \mathbb{R}^3 . Ainsi, il existe un système local de coordonnées (Ω, φ) au voisinage de tout point $p \in M$, avec $\varphi: U \subset \mathbb{R}^2 \rightarrow \Omega \subset \mathbb{R}^3$ et Ω un ouvert de M . Le plan tangent en $p = \varphi(u, v)$, est défini par $T_p M = \text{vect}(\partial_u \varphi, \partial_v \varphi)$, l'espace vectoriel engendré par $\partial_u \varphi(u, v)$ et $\partial_v \varphi(u, v)$ dans \mathbb{R}^3 . Comme M est plongée dans \mathbb{R}^3 , la métrique g_p en $p \in M$ est définie par la restriction à $T_p M$ de la métrique euclidienne sur \mathbb{R}^3 . Le système de coordonnées (Ω, φ) induit une métrique sur U rendant φ isométrique. Cette métrique est appelée première forme fondamentale et notée I_p au point $p \in M$, l'indice p étant omis quand il n'y a pas d'ambiguïté. La métrique I a la forme suivante :

$$I = E du^2 + 2Fdudv + Gdv^2, \quad \text{avec } E = |\partial_u \varphi|^2, \quad F = \langle \partial_u \varphi, \partial_v \varphi \rangle, \quad G = |\partial_v \varphi|^2.$$

De plus, le plan tangent $T_p M$ est indépendant du système de coordonnées (Ω, φ) et nous notons donc $N(p)$ la normale à $T_p M$. Cette application $N: M \rightarrow S^2$, où S^2 est la sphère unitaire de \mathbb{R}^3 , est appelée application de Gauss et est définie par

$$N(p) = \frac{\partial_u \varphi \times \partial_v \varphi}{|\partial_u \varphi \times \partial_v \varphi|}(u, v), \quad \text{avec } p = \varphi(u, v).$$

Notons maintenant II_p la seconde forme fondamentale définie en $p \in M$ par

$$II_p(X_p, Y_p) = -\langle dN_p(X_p), Y_p \rangle = \langle S_p(X_p), Y_p \rangle_g, \quad \forall X_p, Y_p \in T_p M,$$

où $S_p \in \mathcal{L}(T_p M)$ est un endomorphisme de $T_p M$ appelé opérateur de forme en p . Dans le système de coordonnées (Ω, φ) , la seconde forme est notée

$$II = e du^2 + 2f dudv + g dv^2, \text{ avec } e, f, g : M \rightarrow \mathbb{R}.$$

L'opérateur de forme $S(p)$ est symétrique donc diagonalisable dans une base orthogonale pour la métrique g . Nous notons cette base $(v_1(p), v_2(p))$. Les deux valeurs propres associées $\lambda_1(p), \lambda_2(p) \in \mathbb{R}$ sont appelées courbures principales de la surface. Dans le cas où $\lambda_1(p) \neq \lambda_2(p)$, les vecteurs propres $(v_1(p), v_2(p))$ sont définis de manière unique (à normalisation près) et appelés directions principales de courbure. Dans le cas contraire, le point $p \in M$ est dit ombilic. Finalement, nous notons respectivement $K = \lambda_1 \lambda_2$ et $H = \frac{\lambda_1 + \lambda_2}{2}$ la courbure de Gauss et la courbure moyenne de la surface.

Les réseaux de Chebyshev

Nous présentons maintenant une introduction aux réseaux de Chebyshev. Dans un premier temps, nous introduisons brièvement dans la section 1.3.1 ces systèmes de coordonnées et nous exposons un aperçu des problématiques de cette thèse. Quelques exemples de réseaux de Chebyshev sur des surfaces avec symétries sont aussi présentés. Dans un second temps, nous énonçons dans la section 1.3.2 quelques propriétés satisfaites par ces systèmes de coordonnées que nous utiliserons dans ce manuscrit. Puis, nous présentons dans la section 1.3.3 la méthode du compas qui permet de construire des réseaux de Chebyshev discrets. Finalement, nous présentons un état de l'art sur la construction de réseaux de Chebyshev dans la section 1.3.4.

Brève introduction

De la contrainte géométrique aux réseaux de Chebyshev

Nous revenons dans ce paragraphe à la question 1.1 modélisant les contraintes géométriques de la recherche de forme pour les gridshells. Ainsi, nous reprenons les notations introduites dans la sous-section 1.1.2.1 et nous notons $M \subset \mathbb{R}^3$ la surface que l'on souhaite construire par gridshell. Pour commencer, cette question peut être reformulée sous la forme suivante : pour un $h > 0$ fixé, existe-t-il $U_{\text{gs}} \subset (\mathbb{R}^+)^2$ et $\varphi : U_{\text{gs}} \rightarrow M$ tels que

$$\begin{aligned} \left| \frac{d}{du} \varphi(u, \alpha h) \right| &= 1 \text{ pour tout } u \in D_{2,\alpha}(U_{\text{gs}}) \text{ et } \alpha \in \{1, \dots, N_2\}, \\ \left| \frac{d}{dv} \varphi(ih, v) \right| &= 1 \text{ pour tout } v \in D_{1,i}(U_{\text{gs}}) \text{ et } i \in \{1, \dots, N_1\}, \end{aligned}$$

où $N_1, N_2 \geq 1$, $(D_{1,i}(U_{\text{gs}}))_{1 \leq i \leq N_1}$ et $(D_{2,\alpha}(U_{\text{gs}}))_{1 \leq \alpha \leq N_2}$ ont été introduits dans la sous-section 1.1.2.1. Ainsi, en supposant h petit, on se ramène à la question suivante :

Question 1.4. Soit M une surface. Existe-t-il un ouvert $U_{\text{gs}} \subset \mathbb{R}^2$ et une application $\varphi : U_{\text{gs}} \rightarrow M$ tels que

$$|\partial_u \varphi|_g(u, v) = |\partial_v \varphi|_g(u, v) = 1, \quad (1.5)$$

pour tout $(u, v) \in U_{\text{gs}}$.

Notons ici que la modélisation faite ci-dessus reste valable dans le cas de jonctions de fils inextensibles et incompressibles. Les tissus sont donc des exemples de structures pouvant être modélisées d'une manière similaire, dans le cas où le glissement entre les fils est négligé. Ainsi, la question 1.4 a été initialement posée en 1878 par P.L. Chebyshev lors d'un exposé dont le thème était la coupe des vêtements [25]. En supposant de plus que $(\partial_u \varphi, \partial_v \varphi)$ forme une famille libre pour tout $(u, v) \in U$, le couple (M, φ) est un système de coordonnées de la surface M appelé réseau de Chebyshev.

La première problématique est de savoir s'il existe, et en tout point p d'une surface M , un système local de coordonnées de Chebyshev. La réponse est positive, comme on peut le voir dans la proposition ci-dessous, dont la première preuve a été apportée en 1902 par Bianchi [5].

Proposition 1.5. *Soient M une surface et $p \in M$. Il existe un ouvert U de \mathbb{R}^2 , un voisinage $\Omega \subset M$ de p et un système local de coordonnées (Ω, φ) de M tels que $\varphi: U \rightarrow \Omega$ satisfasse (1.5), pour tout $(u, v) \in U$.*

Nous renvoyons à [25] pour une ébauche de preuve pour cette proposition et une approche historique des réseaux de Chebyshev. Une fois l'existence locale assurée, la problématique principale est celle de l'existence globale d'un réseau de Chebyshev sur une surface donnée : peut-on trouver une carte globale (M, φ) vérifiant (1.5) ? Cette problématique, centrée sur l'existence d'un système de coordonnées, est développée dans le chapitre 2. Dans le chapitre 3, cette question est généralisée en considérant les lignes de coordonnées comme une entité. Ainsi, il n'est pas nécessaire que ces lignes de coordonnées soient définies par un unique système de coordonnées et on se ramène au problème suivant :

Question 1.6. *Soit M une surface. Existe-t-il un ensemble de systèmes de coordonnées $\{(\Omega_i, \varphi_i)\}_{i \in E}$, avec $\cup_{i \in E} \Omega_i = M$, tel que φ_i satisfasse (1.5) pour tout $i \in E$ et tel que les lignes de coordonnées “recollent” sur les domaines d’intersection des Ω_i ?*

Pour le moment, cette question est présentée de manière informelle et nous renvoyons au chapitre 3 pour plus de précisions sur le passage du local au global. Dans la section 1.3.4, nous remarquerons que toutes les surfaces ne permettent pas de répondre positivement à la question 1.6. Cela se traduit par l'apparition de singularités sur les réseaux de Chebyshev définis sur les surfaces ne satisfaisant pas ces contraintes. Afin d'illustrer ces singularités, nous notons $\omega = \angle(\partial_u \varphi, \partial_v \varphi)$ l'angle entre les lignes de coordonnées de l'application $\varphi: U \subset \mathbb{R}^2 \rightarrow \varphi(U) \subset M$ vérifiant (1.5). Les points de singularités de φ sont l'ensemble des points où cette application n'est plus un C^1 -difféomorphisme. Généralement, ces singularités peuvent être de deux types différents appelés plis ($\omega = \pi$) et fronces ($\omega = 0$) [25]. Ces deux types de singularités sont présentés sur la figure 1.8. Ainsi, afin de ne pas avoir une trop grande restriction sur les surfaces accessibles, nous sommes amenés à considérer les réseaux de Chebyshev avec singularités. Les singularités des systèmes de coordonnées sont introduites dans le chapitre 3.

Quelques exemples

Nous présentons dans cette section des constructions de réseaux de Chebyshev connus pour des surfaces particulières. Nous ne prétendons pas à l'exhaustivité des différentes symétries permettant l'existence de ces réseaux. Seuls quelques exemples introduisant les réseaux de Chebyshev sont présentés ci-dessous.

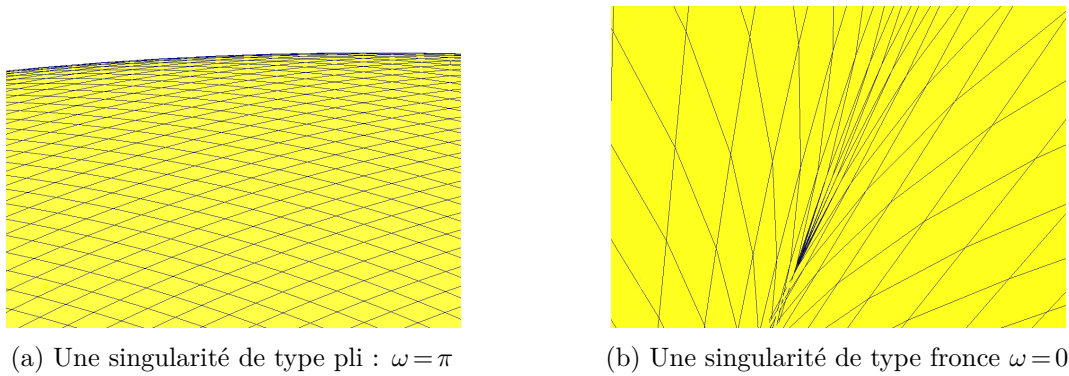


Fig. 1.8 Les singularités génériques des réseaux de Chebyshev

1.3.1.2.1 Les surfaces de révolution Le premier exemple est celui des surfaces de révolution. Soit tout d'abord $\gamma: I \subset \mathbb{R} \rightarrow \mathbb{R}^2$, avec $\gamma = (\gamma_x, \gamma_y)$, une courbe lisse du plan paramétrée par longueur d'arc. Ensuite, soient $U = [0, 2\pi] \times I$ et M la surface de révolution définie par la paramétrisation $\psi: U \rightarrow M \subset \mathbb{R}^3$, avec

$$\psi(u, v) = \left(\cos(u)\gamma_x(v), \sin(u)\gamma_x(v), \gamma_y(v) \right).$$

L'espace tangent de M est donc engendré en chaque point $\psi(u, v) \in M$ par les vecteurs

$$\partial_u \psi = \left(-\sin(u)\gamma_x(v), \cos(u)\gamma_x(v), 0 \right), \quad \partial_v \psi = \left(\cos(u)\gamma'_x(v), \sin(u)\gamma'_x(v), \gamma'_y(v) \right).$$

Ces champs de vecteurs satisfont $\langle \partial_u \psi, \partial_v \psi \rangle = 0$, $|\partial_u \psi|^2 = |\gamma_x|^2$ et $|\partial_v \psi|^2 = 1$. Nous définissons, pour tout $\alpha > 0$, l'ouvert

$$U_\alpha = \left\{ (u, v) \in U \mid (\alpha \gamma_x(v))^2 < 4, \gamma_x(v) \neq 0 \right\} \subset U.$$

De plus, soient $\tilde{X}_\alpha, \tilde{Y}_\alpha: \psi(U_\alpha) \rightarrow \mathbb{R}^3$ les champs de vecteurs sur $\psi(U_\alpha)$ définis par

$$\tilde{X}_\alpha = \alpha \partial_u \psi, \quad \tilde{Y}_\alpha = \sqrt{4 - \alpha^2 |\gamma_x|^2} \partial_v \psi.$$

Alors les champs de vecteurs $\tilde{X}_\alpha, \tilde{Y}_\alpha$ satisfont $\langle \tilde{X}_\alpha, \tilde{Y}_\alpha \rangle = 0$, $[\tilde{X}_\alpha, \tilde{Y}_\alpha] = 0$ et

$$|\tilde{X}_\alpha|^2 + |\tilde{Y}_\alpha|^2 = \alpha^2 |\gamma_x|^2 + 4 - \alpha^2 |\gamma_x|^2 = 4.$$

Ainsi, les champs de vecteurs $X_\alpha = \frac{\tilde{X}_\alpha + \tilde{Y}_\alpha}{2}$ et $Y_\alpha = \frac{\tilde{X}_\alpha - \tilde{Y}_\alpha}{2}$ vérifient $|X_\alpha| = 1$, $|Y_\alpha| = 1$ et $[X_\alpha, Y_\alpha] = 0$. On en déduit donc l'existence d'un système de coordonnées $\varphi_\alpha: V_\alpha \subset \mathbb{R}^2 \rightarrow \psi(U_\alpha)$ tel que $\partial_u \varphi_\alpha = X_\alpha$ et $\partial_v \varphi_\alpha = Y_\alpha$. L'application φ_α est de plus, par définition, un réseau de Chebyshev. Nous remarquons que les points $(u, v) \in \text{cl}(U_\alpha) \cap U$, avec $\text{cl}(U_\alpha)$ l'adhérence de U_α , sont des points où l'application φ_α n'est plus un C^1 -difféomorphisme. En effet, les vecteurs X_α et Y_α ne forment pas une base de $T_{\varphi_\alpha(u,v)} M$ en ces points. Ces derniers sont donc des points de singularité de l'application φ_α .

Nous présentons maintenant deux applications permettant la construction de réseaux de Chebyshev. Tout d'abord, soit $\gamma_1 = (\gamma_{1,x}, \gamma_{1,y}): [-\frac{\pi}{2}, \frac{\pi}{2}] \rightarrow \mathbb{R}^2$ la courbe définie par $\gamma_1(t) = (\cos(t), \sin(t))$. La surface de révolution définie par γ_1 est S^2 , la sphère unitée de \mathbb{R}^3 . Un exemple de réseau de Chebyshev sur la sphère construit par cette méthode est présentée sur la figure 1.9. On peut

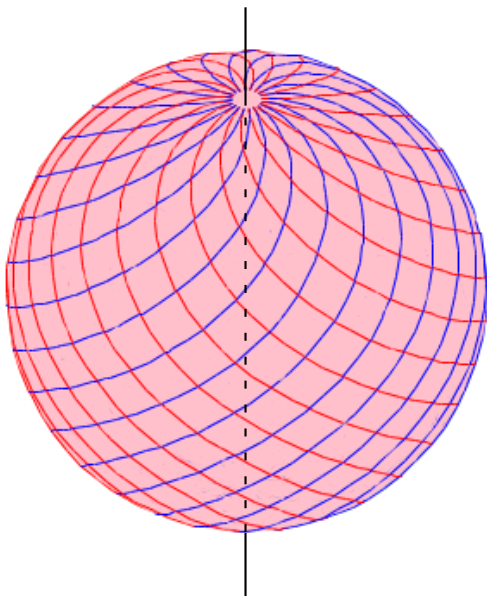


Fig. 1.9 Un réseau de Chebyshev sur la sphère [25]

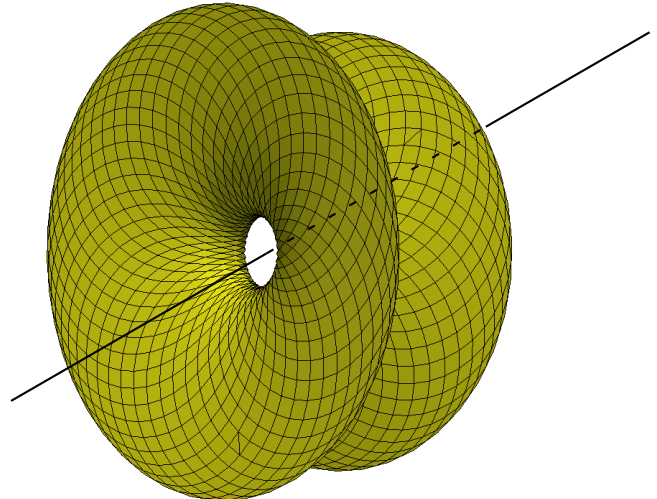


Fig. 1.10 Un réseau de Chebyshev sur le caténoïde

observer sur ce réseau un point de singularité à chaque pôle. Ces points correspondent au cas $\gamma_{1,x}=0$ et la singularité ainsi définie est dite de type rosace. Un second exemple est donné par la courbe $\gamma_2=(\gamma_{2,x}, \gamma_{2,y}):\mathbb{R}\rightarrow\mathbb{R}^2$ obtenue par reparamétrisation par longueur d'arc de la courbe $\tilde{\gamma}_2:\mathbb{R}\rightarrow\mathbb{R}^2$ définie par $\tilde{\gamma}_2(t)=(t, \cosh(t))$, pour tout $t\in\mathbb{R}$. La surface de révolution définie par γ_2 est le caténoïde. Nous présentons sur la figure 1.10 le réseau de Chebyshev φ_{α_0} , avec $\alpha_0<1$, construit sur cette surface. On peut observer sur cette figure des lignes de la surface le long desquelles l'angle entre les lignes de coordonnées est π . Ces lignes, dites de pli, correspondent à l'ensemble des points tels que $(\alpha_0\gamma_{2,x})^2=4$. Finalement, nous observons que, en réduisant α_0 , le domaine de définition U_{α_0} de φ_{α_0} est agrandi et on peut construire de cette manière un réseau de Chebyshev sur tout domaine borné de la surface. De même que pour la sphère, il est par contre impossible de trouver un réseau de Chebyshev global sur le caténoïde.

Les surfaces de translation

Les surfaces de translation sont d'autres exemples de surfaces sur lesquelles on peut construire un réseau de Chebyshev. Ainsi, soient deux courbes $\gamma_1:I_1\subset\mathbb{R}\rightarrow\mathbb{R}^3$ et $\gamma_2:I_2\subset\mathbb{R}\rightarrow\mathbb{R}^3$ paramétrées par longueur d'arc. Dès lors que, pour tout $(u, v)\in I_1\times I_2$, on a $\gamma'_1(u)\times\gamma'_2(v)\neq 0$, avec \times le produit vectoriel, ces deux courbes permettent de définir une surface de translation M . Celle-ci est définie par la paramétrisation $\psi:I_1\times I_2\rightarrow M\subset\mathbb{R}^3$, où $\psi(u, v)=\gamma_1(u)+\gamma_2(v)$, pour tout $(u, v)\in I_1\times I_2$. Ainsi, on a $\partial_u\psi=\gamma'_1$ et $\partial_v\psi=\gamma'_2$ et ψ est donc un réseau de Chebyshev. Un exemple de surface de translation est donné par les courbes $\gamma_1:\mathbb{R}\rightarrow M$ et $\gamma_2:\mathbb{R}\rightarrow M$ respectivement définies par $\gamma_1(u)=(u, 0, \sin(u))$ et $\gamma_2(v)=(0, v, \sin(v))$. Le réseau de Chebyshev ψ de cette surface est présenté dans la figure 1.11.

Propriétés

Nous présentons maintenant certaines propriétés satisfaites par les réseaux de Chebyshev. Soit $\varphi:U\subset\mathbb{R}^2\rightarrow\Omega\subset M$ un réseau de Chebyshev, c'est-à-dire un système de coordonnées (Ω, φ)

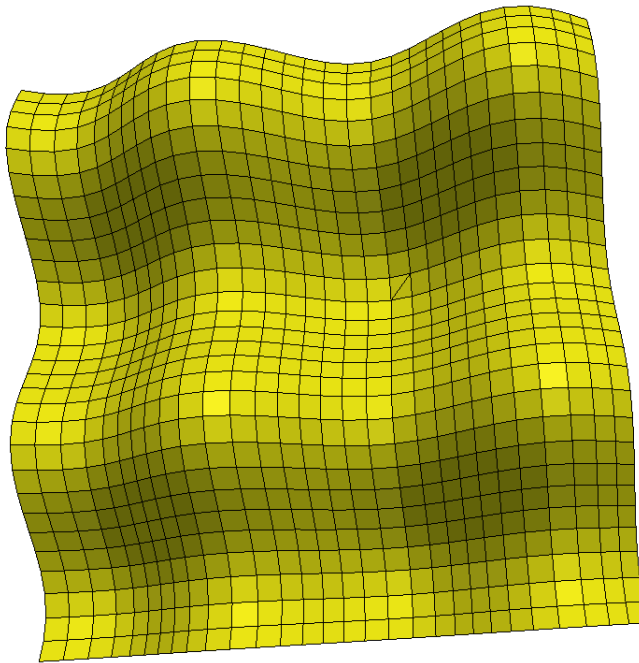


Fig. 1.11 Un réseau de Chebyshev sur une surface de translation

satisfaisant

$$|\partial_u \varphi|_g(u, v) = |\partial_v \varphi|_g(u, v) = 1, \quad (1.6)$$

pour tout $(u, v) \in U$. Nous notons $\omega: U \rightarrow (0, \pi)$ la distribution d'angles définie par $\omega(u, v) = \angle(\partial_u \varphi, \partial_v \varphi)(u, v)$, pour tout $(u, v) \in U$. Alors, la première forme fondamentale s'écrit dans ce système de coordonnées :

$$I = du^2 + 2 \cos(\omega) du dv + dv^2.$$

La courbure de Gauss $K: U \rightarrow \mathbb{R}$ de cette métrique I est

$$K = \frac{\partial_{uv}\omega}{\sin(\omega)}.$$

Soit maintenant (Ω, ψ) , avec $\psi: \tilde{U} \subset \mathbb{R}^2 \rightarrow \Omega$, un système de coordonnées. Notons que l'on peut exprimer (Ω, φ) dans le système de coordonnées (Ω, ψ) par le biais de l'application $\psi^{-1} \circ \varphi: U \rightarrow \tilde{U}$. Une propriété importante satisfaite par un réseau de Chebyshev est que les lignes de coordonnées en u sont transportés parallèlement le long des lignes de coordonnées en v , et inversement. Cela s'exprime dans le système de coordonnées (Ω, ψ) par l'équation de Servant énoncée dans la propriété ci-dessous.

Propriété 1.7 (Transport parallèle et équation de Servant). *En dérivant la condition (1.6), on obtient $D_{\partial_u} \partial_v \varphi = 0$, D_{∂_u} étant la dérivation covariante dans la direction de $\partial_u \varphi$. Ainsi, en exprimant (Ω, φ) dans un système de coordonnées (Ω, ψ) , on obtient que l'application $f = \psi^{-1} \circ \varphi: U \rightarrow \tilde{U}$ satisfait l'équation de Servant*

$$\frac{\partial f_i}{\partial u \partial v} + \sum_{k,l=1}^2 \Gamma_{k,l}^i(f) \frac{\partial f_k}{\partial u} \frac{\partial f_l}{\partial v} = 0, \quad \text{pour } i = 1, 2, \quad (1.7)$$

où $\Gamma_{k,l}^i: \tilde{U} \rightarrow \mathbb{R}$, pour $i, k, l \in \{1, 2\}$, sont les symboles de Christoffel exprimés dans le système de coordonnées (Ω, ψ) .

En utilisant la propriété 1.7, on obtient de plus la propriété suivante sur les lignes de coordonnées des réseaux de Chebyshev.

Propriété 1.8 (Courbure géodésique des lignes de coordonnées). *Soit $\varphi:U \subset \mathbb{R}^2 \rightarrow \varphi(U) \subset M$ une application satisfaisant (1.6) and soient $(u_1, v_1) \in \mathbb{R}^2$ et $(u_2, v_2) \in \mathbb{R}^2$. Nous notons $\omega:U \rightarrow \mathbb{R}/2\pi\mathbb{Z}$ la distribution d'angles définie par $\omega(u, v) = \angle(\partial_u \varphi, \partial_v \varphi)(u, v)$, pour tout $(u, v) \in U$. Alors, en supposant que u_1, v_1 et v_2 sont tels que $\{u_1\} \times [v_1, v_2] \subset U$, on a*

$$\omega(u_1, v_2) = \omega(u_1, v_1) - \int_{-v_2}^{-v_1} \kappa_v,$$

où $\kappa_v:[-v_2, -v_1] \rightarrow \mathbb{R}$ est la courbure géodésique de la courbe $\eta_1:[-v_2, -v_1] \rightarrow M$ définie par $\eta_1(v) = \varphi(u_1, -v)$, pour tout $v \in [-v_2, -v_1]$. Cette propriété, illustrée en figure 1.12, résulte du transport parallèle de $\partial_u \varphi$ le long de η_1 . De plus, en supposant que u_1, u_2 et v_1 sont tels que $[u_1, u_2] \times \{v_1\} \subset U$, on a

$$\omega(u_2, v_1) = \omega(u_1, v_1) - \int_{u_1}^{u_2} \kappa_u,$$

où $\kappa_u:[u_1, u_2] \rightarrow \mathbb{R}$ est la courbure géodésique de la courbe $\eta_2:[u_1, u_2] \rightarrow M$ définie par $\eta_2(u) = \varphi(u, v_1)$, pour tout $u \in [u_1, u_2]$.

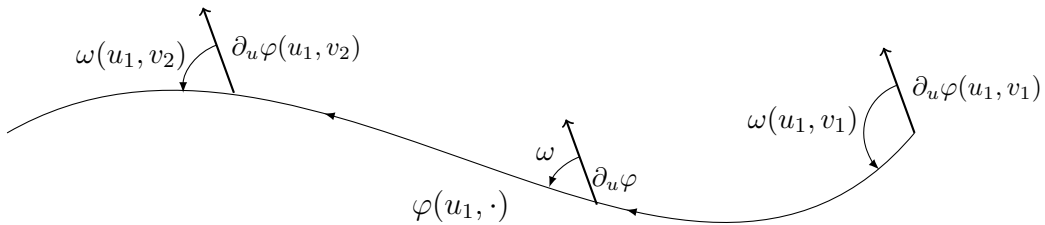


Fig. 1.12 Illustration du transport parallèle de $\partial_u \varphi$ le long de $\varphi(u_1, \cdot)$

Nous présentons maintenant la formule d'Hazzidakis [28] reliant les angles entre les lignes de coordonnées des réseaux de Chebyshev et la courbure de Gauss de la surface. Les notations introduites pour exprimer cette formule sont présentées dans la figure 1.13.

Propriété 1.9 (Formule d'Hazzidakis). *Soit $U = [0, L_1] \times [0, L_2]$, avec $L_1, L_2 > 0$, et soit $\varphi:U \rightarrow \varphi(U) \subset M$ un réseau de Chebyshev. Nous notons $\Omega = \varphi(U)$ et nous définissons les cinq points suivants*

$$A = \varphi(0, 0), \quad B = \varphi(L_1, 0), \quad D = \varphi(0, L_2), \quad C = \varphi(L_1, L_2).$$

Les angles (dans $(0, \pi)$) entre les lignes de coordonnées en ces points sont respectivement notés

$$\omega_A = \omega(0, 0), \quad \omega_B = \omega(L_1, 0), \quad \omega_D = \omega(0, L_2), \quad \omega_C = \omega(L_1, L_2).$$

Ces angles satisfont la formule d'Hazzidakis

$$\omega_A + \omega_C = \omega_B + \omega_D - \int_{\Omega} K dA. \tag{1.8}$$

Nous remarquons finalement que les réseaux de Chebyshev sont utilisés pour paramétriser les surfaces à courbure de Gauss constante négative. Voir par exemple [8, 6] ou [9, Sec. 1.6, 4.2]. La

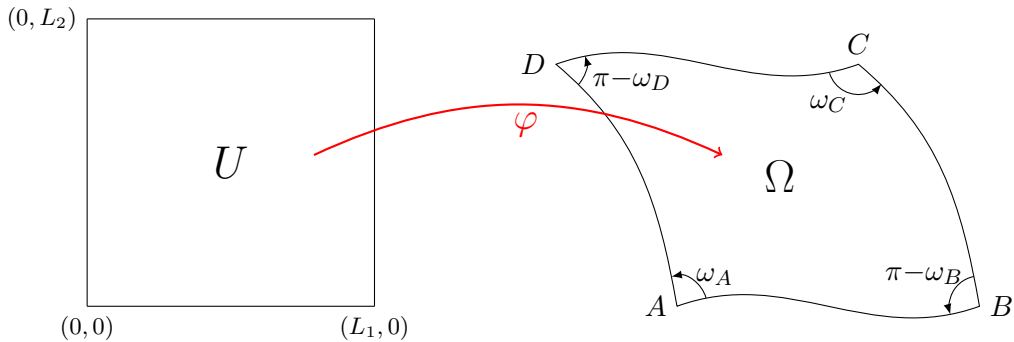


Fig. 1.13 Schéma des angles entre les lignes de coordonnées d'un réseau de Chebyshev sur Ω

discrétisation de ces surfaces se ramène ainsi à la discrétisation de l'équation de Sine-Gordon étudiée par Hirota [29]. Des classes spéciales de ces surfaces ont été étudiées par Hoffmann [30] et Pinkall [41].

Discrétisation : la méthode du compas

Nous présentons une méthode permettant de discrétiser les lignes de coordonnées d'un réseau de Chebyshev (Ω, φ) , avec $\varphi: U \subset \mathbb{R}^2 \rightarrow \Omega$. Nous notons $h > 0$ le pas de la discrétisation. La méthode présentée ci-dessous permet d'approcher la grille $\varphi(U \cap h\mathbb{Z}^2)$ par approximation de la condition (1.6). Pour illustrer la méthode, nous prenons maintenant les quatre points de U suivants :

$$A = (u, v), \quad B = (u + h, v), \quad C = (u + h, v + h), \quad D = (u, v + h).$$

En supposant h assez petit, le point $\varphi(C)$ est approché par un point de M à une distance h des points $\varphi(B)$ et $\varphi(D)$. Nous supposons de plus que h est assez petit pour que les distances de la surface soient assez proches des distances de \mathbb{R}^3 . Ainsi, cette approximation est donnée par l'unique point (en dehors de $\varphi(A)$) à l'intersection de la surface et des deux sphères de rayon h centrées en $\varphi(B)$ et en $\varphi(D)$. La donnée des trois points $\varphi(A)$, $\varphi(B)$ et $\varphi(D)$ permet donc de déterminer de manière unique une approximation de $\varphi(C)$.

Nous présentons cette méthode dans le cadre des conditions au bord dites de type primal. Nous renvoyons au chapitre 6 pour une présentation de la méthode du compas avec d'autres types de conditions au bord. Ainsi, soient $\gamma_1: [0, L_1] \rightarrow M$, avec $L_1 > 0$, et $\gamma_2: [0, L_2] \rightarrow M$, avec $L_2 > 0$, deux courbes de la surface et posons $D = [0, L_1] \times [0, L_2]$, $N_1 = \lfloor \frac{L_1}{h} \rfloor$ et $N_2 = \lfloor \frac{L_2}{h} \rfloor$. Alors la grille associée au réseau de Chebyshev φ est donnée par l'application $\mathcal{P}: \{1, \dots, N_1\} \times \{1, \dots, N_2\} \rightarrow M$ vérifiant

$$\begin{aligned} \mathcal{P}(i, 1) &= \gamma_1(ih), \text{ pour tout } i \in \{1, \dots, N_1\}, \\ \mathcal{P}(1, j) &= \gamma_2(jh), \text{ pour tout } j \in \{1, \dots, N_2\}. \end{aligned} \tag{1.9}$$

Nous notons maintenant $\mathcal{P}_{i,j}^h \in M$, avec $i \in \{1, \dots, N_1\}$ et $j \in \{1, \dots, N_2\}$, un tableau vérifiant les conditions au bord (1.9). Alors, les trois points $\mathcal{P}_{1,1}^h$, $\mathcal{P}_{1,2}^h$ et $\mathcal{P}_{2,1}^h$ permettent de déterminer uniquement, par la méthode énoncée précédemment, le point $\mathcal{P}_{2,2}^h \in M$. Nous notons d_E la distance euclidienne de \mathbb{R}^3 . En répétant l'opération, on détermine donc entièrement l'application

\mathcal{P}^h telle que

$$\begin{aligned} d_E(\mathcal{P}_{i,j}^h, \mathcal{P}_{i+1,j}^h) &= h, \text{ pour tout } i \in \{1, \dots, N_1 - 1\} \text{ et } j \in \{1, \dots, N_2\}, \\ d_E(\mathcal{P}_{i,j}^h, \mathcal{P}_{i,j+1}^h) &= h, \text{ pour tout } i \in \{1, \dots, N_1\} \text{ et } j \in \{1, \dots, N_2 - 1\}. \end{aligned}$$

La grille \mathcal{P}^h ainsi construite est donc une approximation de la grille \mathcal{P} associée au réseau de Chebyshev $\varphi: D \rightarrow M$. Notons que le pavage de la surface M formé par \mathcal{P}^h est constitué de losanges de \mathbb{R}^3 . Cette méthode est schématisée dans la figure 1.14.

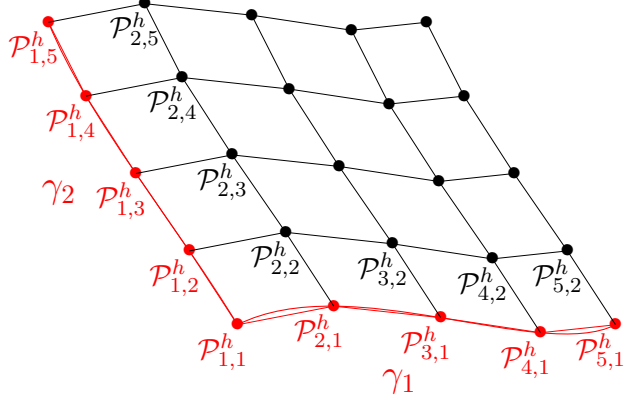


Fig. 1.14 Méthode du compas avec des conditions au bord de type primal
(les conditions au bord sont les courbes en rouge)

État de l'art sur l'existence

Nous présentons maintenant les principaux résultats concernant l'existence de réseaux de Chebyshev : étant donné une surface M , nous cherchons un réseau de Chebyshev $\varphi: U \subset \mathbb{R}^2 \rightarrow M$. Cette problématique a été présentée dans la question 1.4. Le premier résultat d'existence d'un réseau de Chebyshev sur une surface générale est donné par Bakelman [2] où il est montré que toute surface M homéomorphe au plan, complète et satisfaisant la condition

$$\int_M K^\pm < \frac{\pi}{2}, \quad (1.10)$$

avec $K^+ = \max(K, 0)$ et $K^- = \max(-K, 0)$, admet un réseau de Chebyshev. Nous précisons que ce résultat est présenté dans le cadre plus général des surfaces d'Alexandrov [1] et il ne garantit pas que φ soit lisse sur une surface (lisse). Le premier résultat d'existence d'un réseau de Chebyshev lisse a été obtenu, sous les mêmes conditions, par Samelson et Dayawansa [43]. Tandis que la preuve de Bakelman est géométrique, la preuve de [43] est analytique. Il y est prouvé que, pour des conditions au bord données (présentées dans le chapitre 2), il existe une unique solution à l'équation de Servant (1.7). Ensuite, il est montré que, sous les conditions (1.10) sur M , il existe des conditions au bord permettant d'assurer que la solution soit un C^∞ -difféomorphisme. La borne permettant l'existence est ensuite améliorée par Burago *et al.* [14]. En effet, il est montré l'existence d'un réseau de Chebyshev $\varphi: U \subset \mathbb{R}^2 \rightarrow M$ sur toute surface (d'Alexandrov) M homéomorphe au plan, complète satisfaisant

$$\int_M K^\pm < 2\pi.$$

De même que pour la construction de Bakelman, sur laquelle s'appuie cette construction, le réseau de Chebyshev obtenu est non lisse. On peut voir par la formule d'Hazzidakis que, dans le cas où le signe de la courbure est constant, ce résultat est optimal.

Résultats principaux et plan du manuscrit

Nous présentons finalement un résumé des travaux effectués dans le cadre de cette thèse. Ces travaux sont regroupés dans les cinq chapitres suivants. Dans le premier de ces chapitres, nous nous concentrons sur l'existence d'un système global de coordonnées de Chebyshev, dans la continuité de [43]. Nous élargissons ensuite les perspectives en introduisant les singularités coniques dans le chapitre 3. La construction de réseaux de Chebyshev avec singularités coniques est présentée dans le chapitre 5. Dans ce but, nous montrons préalablement dans le chapitre 4 l'existence d'un unique réseau de Chebyshev satisfaisant des conditions au bord dites de type primal. Le dernier chapitre est une application numérique des résultats précédents. Plus précisément, nous résumons le contenu de ces chapitres ci-dessous.

- Nous présentons dans le chapitre 2 une amélioration de la borne (1.10) sur la courbure de la surface M assurant l'existence d'un réseau de Chebyshev lisse sur M . Ainsi, en se basant sur [43], nous considérons les conditions au bord dites de type dual et nous présentons une variante de la formule d'Hazzidakis (1.8) nous permettant de contrôler les angles entre les lignes de coordonnées du réseau de Chebyshev construit à partir de ces conditions au bord. Ce chapitre, publié dans Journal of geometry [37], a pour résultat principal le théorème suivant :

Theorem 1.10 (Existence d'un réseau de Chebyshev global). *Soit M une surface ouverte, complète et simplement connexe de régularité C^∞ . Supposons que $\int_M |K| < 2\pi$. Alors il existe un réseau de Chebyshev global sur M .*

- Dans le chapitre 3, après avoir défini les réseaux de Chebyshev avec singularités coniques, nous présentons un cadre théorique permettant le passage du local au global dans la définition des systèmes de coordonnées. Dans ce but, nous introduisons les systèmes de coordonnées globalement compatibles. Nous introduisons aussi la notion de singularité des systèmes de coordonnées. Nous présentons finalement quelques propriétés spécifiques aux singularités des réseaux de Chebyshev justifiant la définition de singularités coniques initialement introduite.
- Nous construisons dans le chapitre 4 des réseaux de Chebyshev à partir de conditions au bord de type primal. Ainsi, nous montrons par une construction géométrique se basant sur [25] que le problème consistant à chercher un réseau de Chebyshev satisfaisant des conditions au bord de type primal est bien posé au sens de Hadamard : à conditions au bord fixées, il y a existence et unicité d'un réseau de Chebyshev et celui-ci dépend continûment de ces conditions au bord. Ce résultat est énoncé dans le théorème suivant :

Theorem 1.11 (Existence et unicité d'un réseau de Chebyshev). *Soit M une surface ouverte, complète et simplement connexe. Soient $\eta_1 : [-L_1, 0] \rightarrow M$, avec $L_1 \in \mathbb{R}_*^+ \cup \{\infty\}$, et $\eta_2 : [0, L_2] \rightarrow M$, avec $L_2 \in \mathbb{R}_*^+ \cup \{\infty\}$, deux courbes lisses de courbure géodésique $\kappa_1 : [-L_1, 0] \rightarrow \mathbb{R}$ et $\kappa_2 : [0, L_2] \rightarrow \mathbb{R}$ telles que $\eta_1(0) = \eta_2(0)$. Supposons que $\angle(\eta'_1(0), \eta'_2(0)) \in (0, \pi)$. Alors, il*

existe une unique distribution lisse d'angles $\omega : D \rightarrow \mathbb{R}/2\pi\mathbb{Z}$, avec $D = [0, L_2] \times [0, L_1]$, satisfaisant la formule d'Hazzidakis (1.8), avec $\varphi : D \rightarrow M$ l'unique application lisse satisfaisant les conditions au bord

$$\begin{aligned}\varphi(u, 0) &= \eta_2(u), \quad \forall u \in [0, L_2], \\ \varphi(0, v) &= \eta_1(-v), \quad \forall v \in [0, L_1],\end{aligned}$$

et tel que ses lignes de coordonnées en v soient paramétrées par longueur d'arc et aient une courbure géodésique $\kappa_2^{\text{map}} : D \rightarrow \mathbb{R}$ satisfaisant $\kappa_2^{\text{map}}(u, v) = \partial_v \omega(u, v)$ pour tout $(u, v) \in D$.

Supposons de plus qu'il existe $\tilde{D} = [0, \tilde{L}_2] \times [0, \tilde{L}_1]$, avec $\tilde{L}_1 \in (0, L_1]$ et $\tilde{L}_2 \in (0, L_2]$, tel que $0 < \omega(u, v) < \pi$, pour tout $(u, v) \in \tilde{D}$. Alors, l'application φ satisfait

$$|\partial_u \varphi|_g(u, v) = |\partial_v \varphi|_g(u, v) = 1,$$

pour tout $(u, v) \in \tilde{D}$. De plus, φ dépend continuement des conditions au bord η_1 et η_2 .

- Dans le chapitre 5, nous construisons des réseaux de Chebyshev avec singularités coniques (voir la définition 3.5 du chapitre 3) sur des surfaces à courbure négative dominante. Le résultat principal de ce chapitre est énoncé dans le théorème suivant :

Theorem 1.12. *Soit M une surface lisse, ouverte, complète et simplement connexe. Supposons que M satisfasse*

$$\int_M K^+ < 2\pi, \quad \int_M K^- < \infty.$$

Alors il existe un réseau de Chebyshev avec singularités coniques lisse par morceau sur M .

Nous soulignons finalement que la preuve du théorème présentée dans ce chapitre est constructive.

- Nous appliquons dans le chapitre 6 les résultats précédents pour construire par ordinateur des réseaux de Chebyshev. En effet, un programme permettant la construction de réseaux de Chebyshev avec singularités coniques à partir d'entrées fournies par l'utilisateur a été développé au cours de cette thèse. Ces entrées constituent les données d'un des différents types de conditions au bord que nous présentons dans ce chapitre. Le programme a été relié à un logiciel de conception assisté par ordinateur utilisé dans le domaine de l'architecture : Rhinoceros. Nous décrivons tout d'abord dans ce chapitre un algorithme permettant de déterminer automatiquement des conditions au bord amenant à la construction de réseaux de Chebyshev avec singularités coniques sur toute surface M satisfaisant $\int_M K^- < \infty$ et ayant une courbure positive suffisamment bien répartie. Nous présentons dans un second temps des résultats numériques obtenus par ce programme. Finalement, nous décrivons quelques fonctionnalités supplémentaires présentes dans ce programme comme la construction de singularités dites de type rosace.

Chapter 2

Smooth Chebyshev nets defined by dual boundary conditions

This chapter corresponds to an article written with Laurent Monasse. It has been published in Journal of geometry.

Abstract:

We prove the existence of a global smooth Chebyshev net on complete, simply connected surfaces when the total absolute curvature is bounded by 2π . Following Samelson and Dayawansa, we look at Chebyshev nets given by a dual curve, splitting the surface into two connected half-surfaces, and a distribution of angles along it. An analogue to the Hazzidakis' formula is used to control the angles of the net on each half-surface with the integral of the Gaussian curvature of this half-surface and the Cauchy boundary conditions. We can then prove the main result using a theorem about splitting the Gaussian curvature with a geodesic, obtained by Bonk and Lang.

Introduction

In this paper we call *surface* a Riemannian 2-manifold, whose metric will be denoted g , and we consider complete, simply connected surfaces. A Chebyshev net Φ on a surface is a parameterization of the surface satisfying

$$\forall(u^1, u^2) \in \mathbb{R}, \quad \left| \partial_u \Phi(u^1, u^2) \right|_{g(\Phi(u^1, u^2))} = \left| \partial_v \Phi(u^1, u^2) \right|_{g(\Phi(u^1, u^2))} = 1, \quad (2.1)$$

which means that length is preserved in two directions, called the *primal coordinates*. Let $\Omega(u^1, u^2)$ be the angle between the coordinate curves at $\Phi(u^1, u^2)$.

A question of interest both for the existence of bi-Lipschitz maps [14] and for applications in textile or architectural shape design [25, 18] is the existence of a Chebyshev net on a given surface. While local existence of a Chebyshev net holds for all surfaces [5], two approaches have been explored to obtain global existence. The first approach relies on a geometric proof on more general Alexandrov surfaces. The first result on global existence of a Chebyshev net on complete and simply connected Alexandrov surfaces has been obtained by Bakelman [2]. Existence is proved on every sector Q_α delimited by two geodesics crossing at an angle α such that $\int_{Q_\alpha} K^+ < \alpha$ and $\int_{Q_\alpha} K^- < \pi - \alpha$, where K^+ and K^- denote, respectively, the positive and negative parts of the Gaussian curvature K . A global Chebyshev net is then obtained on the

surface for $\alpha = \pi/2$. Burago, Ivanov and Malev [14] improved this result by showing that a complete and simply connected Alexandrov surface M admits a global Chebyshev net under the relaxed constraints $\int_M K^+ < 2\pi$ and $\int_M K^- < 2\pi$, but this net is not necessarily smooth on a Riemannian surface as the coordinate curves might present kinks at the boundaries between adjacent sectors.

A second analytical approach was developed by Samelson and Dayawansa [43] using the dual coordinates. A geodesic cutting the surface into two connected components \mathcal{R}^+ and \mathcal{R}^- is chosen as a dual curve. In each connected component, existence and uniqueness of a smooth solution to Servant's equations (see (2.5) below) in the dual coordinates is proved for any smooth distribution of angles along the dual curve. Then, choosing a constant angle $\pi/2$ along the geodesic and using an estimate on the angle Ω of the net on \mathcal{R}^\pm , it is shown that the solution to Servant's equations is a diffeomorphism under the condition that $\int_{\mathcal{R}^\pm} K^+ < \pi/2$ and $\int_{\mathcal{R}^\pm} K^- < \pi/2$. In the present paper, we add some arguments to the proof to improve this result by relaxing the constraints on the integrals of the Gaussian curvature. Our main result is the following:

Theorem 2.1. *Let M be a complete, simply connected, C^∞ surface. Suppose that $\int_M |K| < 2\pi$. Then M admits a global Chebyshev net.*

Let us note that the Hazzidakis' formula [28] suggests that this result is optimal in the sense that a smooth global Chebyshev net does not exist on a complete, simply connected surface M such that $\int_M |K| > 2\pi$.

The paper is organized as follows. In Section 2.2, we restate two existing results in a form that is useful for our purpose. The first one is that the estimates obtained on half the surface in [43] can be doubled using a theorem proved by Bonk and Lang [11] stating that the surface can be split by a geodesic into two connected components (called half-surfaces) such that each component contains half of the integral of K^+ and K^- on the surface. The second result concerns the existence (and uniqueness) of a smooth solution to Servant's equations proved in [43] which we restate by specifying the boundary conditions from the choice of a dual curve and an arbitrary smooth angle distribution on that curve. Then in Section 2.3, we prove the existence of a Chebyshev net on each half-surface. To that end, we first observe that it is sufficient to keep the angles Ω of the net uniformly away from 0 and π for Φ to be a global diffeomorphism. This means that no nonlocal self-intersection of the parameterization can occur when Φ is locally injective everywhere. Proving an analogue to the Hazzidakis' formula in the dual coordinates, we are able to choose an adequate (constant) angle distribution on the dual geodesic curve to control the angles in each half-surface. Finally, we conclude the proof in Section 2.4 by assembling the intermediate results.

Preliminary results

In this section, we restate two existing results on splitting the surface into two components and on the solution to Servant's equations.

Splitting the surface into two components

We give a restatement of [11, prop. 6.1] applied to the continuous nonnegative function K^- .

Proposition 2.2. Let M be a smooth, complete surface homeomorphic to the plane. Suppose that $\int_M K^+ < 2\pi$ and $\int_M K^- < \infty$. Then there exists a properly embedded, complete geodesic γ , splitting M into two connected components M_1 and M_2 such that

$$\int_{M_1} K^+ = \int_{M_2} K^+, \quad \int_{M_1} K^- = \int_{M_2} K^-. \quad (2.2)$$

Solution to Servant's equations

Following Samelson and Dayawansa [43], we introduce the change of variables $D:(u^1, u^2) \mapsto (x^1, x^2) = (u^1 - u^2, u^1 + u^2)$ to the *dual coordinates*. We use upper case letters Φ and Ω for the primal parameterization and angle between primal coordinate curves, lower case letters $\varphi = \Phi \circ D^{-1}$ and $\omega = \Omega \circ D^{-1}$ for their dual counterparts. The first fundamental form in a Chebyshev net is then

$$g = (du^1)^2 + 2 \cos(\Omega(u^1, u^2)) du^1 du^2 + (du^2)^2 \quad (2.3)$$

$$= \sin^2\left(\frac{\omega(x^1, x^2)}{2}\right) (dx^1)^2 + \cos^2\left(\frac{\omega(x^1, x^2)}{2}\right) (dx^2)^2. \quad (2.4)$$

A derivation of (2.1) along coordinates (u^1, u^2) leads to Servant's equations, expressed here in the dual coordinates (x^1, x^2) ,

$$\partial_{yy}^2 \varphi^i - \partial_{xx}^2 \varphi^i + \sum_{k,l=1}^2 \Gamma_{k,l}^i(\varphi) (\partial_y \varphi^k \partial_y \varphi^l - \partial_x \varphi^k \partial_x \varphi^l) = 0, \quad \text{for } i=1, 2, \quad (2.5)$$

where $\Gamma_{k,l}^i$ denote the Christoffel symbols, together with the Cauchy boundary conditions

$$\begin{cases} \varphi(x^1, 0) = \gamma(x^1), \\ \partial_y \varphi(x^1, 0) = \psi(x^1), \end{cases} \quad \forall x^1 \in \mathbb{R}, \quad (2.6)$$

for given functions $\gamma, \psi : \mathbb{R} \rightarrow M$. The following result on smooth solutions with smooth boundary conditions is proved in [43].

Proposition 2.3. Assume that γ, ψ are C^∞ functions. Then there exists a unique C^∞ solution φ to (2.5)-(2.6).

The primal parameterization $\Phi = \varphi \circ D$, where φ is the solution to (2.5)-(2.6), is then a Chebyshev net if and only if (2.1) is satisfied by Φ on the boundary. This is expressed, on the dual coordinates, by

$$\begin{cases} \langle \partial_x \varphi(x^1, 0), \partial_y \varphi(x^1, 0) \rangle_{g(\varphi(x^1, 0))} = 0, \\ |\partial_x \varphi(x^1, 0)|_{g(\varphi(x^1, 0))}^2 + |\partial_y \varphi(x^1, 0)|_{g(\varphi(x^1, 0))}^2 = 1, \end{cases} \quad \forall x^1 \in \mathbb{R}. \quad (2.7)$$

But (2.7) is equivalent to the existence of an arc length parameterized curve $\tilde{\gamma}$ and an angle distribution $\bar{\omega} : \mathbb{R} \rightarrow (0; \pi)$ along $\tilde{\gamma}$ such that

$$\begin{cases} \varphi(x^1, 0) = \tilde{\gamma}(\alpha(x^1)), \\ \partial_y \varphi(x^1, 0) = \cos\left(\frac{\bar{\omega}(x^1)}{2}\right) n(\alpha(x^1)), \end{cases} \quad \forall x^1 \in \mathbb{R}, \quad (2.8)$$

where $t(x^1)$ is the tangential vector to $\tilde{\gamma}$ at x^1 , $n(x^1)$ is the normal vector to this curve at x^1 such that $(t(x^1), n(x^1))$ is positively oriented, and

$$\alpha(x^1) = \int_0^{x^1} \sin\left(\frac{\bar{\omega}(s)}{2}\right) ds.$$

Moreover, we have $\bar{\omega}(x^1) = \omega(x^1, 0)$ where ω is the angle between the primal coordinate curves. The Cauchy boundary conditions for Servant's equations (2.5) satisfying the Chebyshev property (2.1) are now prescribed by specifying

- an arc length parametrized curve $\tilde{\gamma}: \mathbb{R} \rightarrow M$;
- an angle distribution $\bar{\omega}: \mathbb{R} \rightarrow (0; \pi)$ uniformly bounded away from 0 and π .

We will say that a map $\varphi: \mathbb{R} \rightarrow M$ is a local Chebyshev net on M if it satisfies Servant's equations (2.5) with Cauchy boundary conditions (2.8).

Existence of a Chebyshev net on each half-surface

In this section we prove the existence of a Chebyshev net on each half-surface. The key ingredient is a new Hazzidakis-type formula on the dual (see Lemma 2.5) which allows us to specify a suitable angle distribution along the geodesic (see Lemma 2.7).

Global injectivity of the map φ

Lemma 2.4. *Let M be a complete, simply connected, C^∞ surface. A mapping $\varphi: \mathbb{R} \rightarrow M$ satisfying (2.1) is a global Chebyshev net if it satisfies*

$$\exists \varepsilon > 0 \quad s.t. \quad \varepsilon < \omega(x^1, x^2) < \pi - \varepsilon, \quad \forall (x^1, x^2) \in \mathbb{R} \quad (2.9)$$

where ω is the angle of the map defined in (2.3).

Proof. Let ds^2 be the metric (2.3) associated with φ . Since ω satisfies (2.9), (\mathbb{R}, ds^2) is a geodesically complete, simply connected, C^∞ surface. Moreover, $\varphi: (\mathbb{R}, ds^2) \rightarrow M$ is a local isometry. That φ is a global isometry follows from [22, prop. 2.106]. Hence $\varphi: \mathbb{R} \rightarrow M$ is a global Chebyshev net. \blacksquare

Hazzidakis' formula on the dual

Lemma 2.4 shows that the map φ can be proved to be a diffeomorphism by deriving a uniform estimate on the angle ω of the net. To this purpose, we derive an equivalent to the Hazzidakis' formula in the dual coordinates. We derive the result from the classical relation (see for instance [44]):

$$\partial_{uv}^2 \Omega(u^1, u^2) = -K \left(\Phi(u^1, u^2) \right) \sin(\Omega(u^1, u^2)). \quad (2.10)$$

Lemma 2.5. *Let φ be a local Chebyshev net of M . Define the three points $A = \varphi(x_0, y_0)$, $B = \varphi(x_0 + h, y_0)$, and $C = \varphi(x_0 + \frac{h}{2}, y_0 + \frac{h}{2})$. Consider the dual line $\gamma = \varphi(\cdot, y_0)$ (containing the points A and B) and let ABC be the triangle delimited by the two primal lines AC and BC and the dual line γ , depicted on Figure 2.1. Then the following holds:*

$$\forall (x_0, y_0) \in \mathbb{R}, \quad \forall h > 0, \quad \omega(x_0 + \frac{h}{2}, y_0 + \frac{h}{2}) = \frac{\omega(x_0, y_0) + \omega(x_0 + h, y_0)}{2} + \int_{AB} k_\gamma - \int_{ABC} K,$$

where ω is the angle of the net introduced in (2.3) and k_γ is the geodesic curvature of γ defined as

$$k_\gamma = -\frac{1}{|\partial_x \varphi|_{g(\varphi)}} \left\langle \partial_x \left(\frac{\partial_x \varphi}{|\partial_x \varphi|_{g(\varphi)}} \right), \frac{\partial_y \varphi}{|\partial_y \varphi|_{g(\varphi)}} \right\rangle_{g(\varphi)}$$

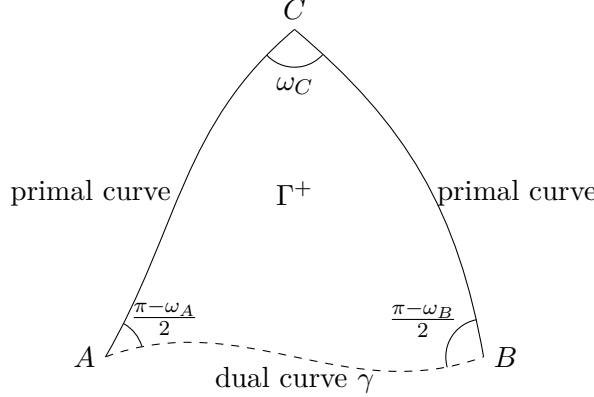


Fig. 2.1 Scheme of the Hazzidakis' formula on triangle ABC

The proof of Lemma 2.5 hinges on the following lemma.

Lemma 2.6. *Let $\varphi: \mathbb{R} \rightarrow M$ be a local Chebyshev net of M . The following holds for all $y_0 \in \mathbb{R}$:*

$$\partial_y \omega(\cdot, y_0) = 2k_\gamma \sin\left(\frac{\omega(\cdot, y_0)}{2}\right). \quad (2.11)$$

Proof. Define $\partial_x := \partial_x \varphi$ and $\partial_y := \partial_y \varphi$. Using the commutation of ∂_x and ∂_y , we obtain

$$\begin{aligned} \partial_x \left\langle \frac{\partial_x}{|\partial_x|_{g(\varphi)}}, \partial_y \right\rangle_{g(\varphi)} &= \left\langle \partial_x \left(\frac{\partial_x}{|\partial_x|_{g(\varphi)}} \right), \partial_y \right\rangle_{g(\varphi)} + \frac{1}{2|\partial_x|_{g(\varphi)}} \partial_y \left(|\partial_x|^2_{g(\varphi)} \right) \\ &= -|\partial_y|_{g(\varphi)} |\partial_x|_{g(\varphi)} k_\gamma + \frac{1}{2|\partial_x|_{g(\varphi)}} \partial_y \left(\sin^2 \left(\frac{\omega}{2} \right) \right). \end{aligned}$$

Moreover, $\langle \partial_x, \partial_y \rangle_{g(\varphi)} = 0$, $|\partial_x|_{g(\varphi)} = \sin(\frac{\omega}{2})$ and $|\partial_y|_{g(\varphi)} = \cos(\frac{\omega}{2})$ due to (2.4), so that (2.11) holds. ■

Proof. (Hazzidakis' formula): Let $(u_0, v_0) = D^{-1}(x_0, y_0)$. Let Γ^+ be the triangle delimited by the dual curve joining A to B and the two primal curves joining B to C and C to A (see Figure 2.1):

$$\begin{aligned} \Gamma^+ &= \varphi \left(\left\{ (x, y) \in \mathbb{R} \mid x_0 \leq x \leq x_0 + h, y_0 \leq y \leq y_0 + \frac{h}{2} - |x - x_0 - \frac{h}{2}| \right\} \right) \\ &= \Phi \left(\left\{ (u, v) \in \mathbb{R} \mid u \leq u_0 + \frac{h}{2}, v \leq v_0, u + v \geq u_0 + v_0 \right\} \right). \end{aligned}$$

Integrating (2.10) on Γ^+ leads to

$$\begin{aligned}
 -\int_{\Gamma^+} K &= \int_{u_0}^{u_0 + \frac{h}{2}} \int_{u_0 + v_0 - u}^{v_0} \partial_{uv}^2 \Omega(u, v) dv du \\
 &= \int_{u_0}^{u_0 + \frac{h}{2}} (\partial_u \Omega(u, v_0) - \partial_u \Omega(u, u_0 + v_0 - u)) du \\
 &= \Omega(u_0 + \frac{h}{2}, v_0) - \Omega(u_0, v_0) \\
 &\quad - \frac{1}{2} \int_{u_0}^{u_0 + \frac{h}{2}} (\partial_u - \partial_v) \Omega(u, u_0 + v_0 - u) du \\
 &\quad - \frac{1}{2} \int_{u_0}^{u_0 + \frac{h}{2}} (\partial_u + \partial_v) \Omega(u, u_0 + v_0 - u) du \\
 &= \Omega(u_0 + \frac{h}{2}, v_0) - \Omega(u_0, v_0) - \frac{1}{2} [\Omega(u_0 + \frac{h}{2}, v_0 - \frac{h}{2}) - \Omega(u_0, v_0)] \\
 &\quad - \frac{1}{2} \int_{x_0 + y_0}^{x_0 + y_0 + h} \partial_y \omega(-y_0 + x, y_0) dx \\
 &= \Omega(u_0 + \frac{h}{2}, v_0) - \frac{1}{2} \Omega(u_0, v_0) - \frac{1}{2} \Omega(u_0 + \frac{h}{2}, v_0 - \frac{h}{2}) - \int_{AB} \frac{\partial_y \omega}{2 \sin(\frac{\omega}{2})} \\
 &= \omega(x_0 + \frac{h}{2}, y_0 + \frac{h}{2}) - \frac{1}{2} \omega(x_0, y_0) - \frac{1}{2} \omega(x_0 + h, y_0) - \int_{AB} k_\gamma.
 \end{aligned}$$

This completes the proof. ■

Angle distribution along the dual curve

Lemma 2.7. *Let γ be a geodesic of M which splits this surface into two connected components M_1 and M_2 . If*

$$\max_{i=1,2} \int_{M_i} K^+ + \max_{i=1,2} \int_{M_i} K^- < \pi, \quad (2.12)$$

then there exists a distribution $\bar{\omega}: \mathbb{R} \rightarrow (0; \pi)$ such that the solution of Servant's equations (2.5) given by the Cauchy boundary conditions γ and $\bar{\omega}$ in (2.8) is a C^∞ -diffeomorphism.

Proof. Lemma 2.5 applied with $x_0 = x^1 - x^2$, $y_0 = 0$ and $h = 2x^2$ leads to the following estimate:

$$\forall (x^1, x^2) \in \mathbb{R}, \quad \inf_{s \in \mathbb{R}} \bar{\omega}(s) - \max_{i=1,2} \int_{M_i} K^+ \leq \omega(x^1, x^2) \leq \max_{i=1,2} \int_{M_i} K^- + \sup_{s \in \mathbb{R}} \bar{\omega}(s).$$

Hence, choosing for instance the constant distribution of angles along γ such that

$$\bar{\omega}(x) = \frac{\pi}{2} + \frac{1}{2} \max_{i=1,2} \int_{M_i} K^+ - \frac{1}{2} \max_{i=1,2} \int_{M_i} K^-$$

gives a global Chebyshev net owing to Lemma 2.4. ■

Proof of the main theorem

Let γ be a geodesic splitting M into two connected components M_1 and M_2 , as resulting from Proposition 2.2. Then the hypotheses of Lemma 2.7 are satisfied upon choosing the geodesic γ and the constant distribution of angles $\bar{\omega} = \frac{\pi}{2} + \frac{1}{4} \int_M K$ as Cauchy boundary conditions in (2.8). This proves the main theorem.

Chapter 3

Conical singularities

The main issue addressed in this thesis is to construct Chebyshev coordinates on a given surface M . These coordinates and the main difficulties regarding their construction are introduced in Section 3.1. As will be shown, the existence of Chebyshev coordinates is constrained by the total Gaussian curvature of M . Hence, we then introduce a new paradigm of Chebyshev nets with conical singularities to improve the conditions ensuring their existence. Next, we take a global view on parametrization and singularities in Section 3.2. We primarily consider the globalization of coordinate systems and we then define singularities of coordinate systems. We focus in Section 3.3 on Chebyshev nets with conical singularities and we justify the construction presented in Section 3.1. We finally present in Section 3.4 the proof of some properties concerning coordinate systems stated in Section 3.2.

Chebyshev coordinates

Introduction

We now introduce the main issues related to the construction of Chebyshev nets with singularities. Before this, we fix some notation and some definitions used in the sequel. We call surface a connected, smooth two-dimensional oriented manifold, denoted M , endowed with a metric, denoted g . Unless explicitly mentioned, the considered surfaces are supposed to be homeomorphic to the plane. We denote (Ω, φ) the coordinate system $\varphi: U \subset \mathbb{R}^2 \rightarrow \Omega \subset M$, with Ω an open set of M , U an open set of \mathbb{R}^2 and φ a diffeomorphism.

Definition 3.1 (Chebyshev nets). *We call Chebyshev net any coordinate system (Ω, φ) , with $\varphi: U \subset \mathbb{R}^2 \rightarrow \Omega \subset M$ a diffeomorphism satisfying*

$$|\partial_u \varphi|_g(u, v) = |\partial_v \varphi|_g(u, v) = 1, \quad (3.1)$$

for all $(u, v) \in U$.

While local existence of a Chebyshev net on any surface M is always satisfied [25], the existence of a global Chebyshev net (M, φ) , with $\varphi: U \subset \mathbb{R}^2 \rightarrow M$, is constrained by the total Gaussian curvature of M . The source of these constraints lies in the following Hazzidakis formula [28].

Property 3.2 (Hazzidakis formula). Let $U = [0, L_1] \times [0, L_2]$, with $L_1, L_2 > 0$. Let $\varphi: U \rightarrow \Omega \subset M$, with $\Omega = \varphi(U)$, be a Chebyshev net. We define the following points:

$$A = \varphi(0, 0), \quad B = \varphi(L_1, 0), \quad D = \varphi(0, L_2), \quad C = \varphi(L_1, L_2).$$

The angles between the coordinate curves at these points are respectively denoted

$$\omega_A = \omega(0, 0), \quad \omega_B = \omega(L_1, 0), \quad \omega_D = \omega(0, L_2), \quad \omega_C = \omega(L_1, L_2).$$

Then, these angles satisfy the Hazzidakis formula

$$\omega_A + \omega_C = \omega_B + \omega_D - \int_{\Omega} K dA, \quad (3.2)$$

where K is the Gaussian curvature of M .

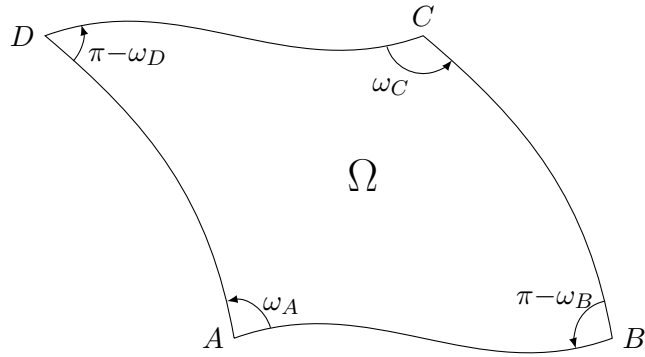


Fig. 3.1 Illustration of the angles between the coordinate curves of a Chebyshev net on Ω

From [14], there exists a Chebyshev net on any complete surface homeomorphic to the plane satisfying

$$\int_M K^{\pm} < 2\pi, \quad (3.3)$$

with K the Gaussian curvature of the surface, $K^+ = \max(K, 0)$ and $K^- = \max(-K, 0)$. Then, using the Hazzidakis formula (3.2), we emphasize that this result is optimal whenever the curvature of the surface has constant sign. However, let us mention that optimization methods have been introduced in [23, 13] to construct Chebyshev nets in practical cases where (3.3) is not satisfied. To consider a set of surfaces less restricted than surfaces satisfying (3.3), we introduce in the sequel singularities of Chebyshev nets. Indeed, as will be seen, the introduction of singularities permits to go beyond the constraint formulated by the Hazzidakis formula. Therefore, we consider the two following generalizations of (3.3):

1. The surface has a dominantly negative curvature: $\int_M K^+ < 2\pi$ and $\int_M K^- > 2\pi$.
2. The surface has a dominantly positive curvature: $\int_M K^+ > 2\pi$ and $\int_M K^- < 2\pi$.

In this manuscript, we focus on the case of surfaces with dominantly negative curvature (case 1). Concerning case 2, we mention that a global parametrization of the sphere minus two segments is presented in [25]. This parametrization has four cusp singularities. We also mention that

another parametrization of the sphere by a Chebyshev net can be obtained with two so-called rosette singularities (see Figure 1.9 of Chapter 1).

Then, in the case 1, Burago *et al* pointed out in [14] that so-called generalized Chebyshev nets can be constructed on every complete surface homeomorphic to the plane satisfying

$$\int_M K^+ < 2\pi, \quad \int_M K^- < \infty. \quad (3.4)$$

To construct Chebyshev nets on surfaces satisfying (3.4), we introduce Chebyshev nets with conical singularities in Section 3.1.2. We present in Chapter 5 a constructive proof of the existence of a piecewise smooth Chebyshev net with conical singularities on any complete surface homeomorphic to the plane.

Construction of Chebyshev nets with conical singularities

O-polyhedral surfaces

We define particular polyhedral surfaces obtained by junctions of $(\mathbb{R}^+)^2$ sets along their vertices located in $\mathbb{R}^+ \times \{0\} \cup \{0\} \times \mathbb{R}^+$. These surfaces are called O-polyhedral surfaces, as an abbreviation of orthogonal polyhedral surfaces. O-polyhedral surfaces are defined by a set of polygons whose boundaries are isometrically identified [7, Subsec 1.1.3]. These identifications are encoded in the so-called equivalence table.

Definition 3.3 (O-polyhedral surface). *Let $N_{\text{pol}} \geq 1$ be an integer and, for all $i \in \{1, \dots, N_{\text{pol}}\}$, let $\{\gamma_e^{i,\alpha}\}_{1 \leq \alpha \leq N_i}$, with $N_i \geq 2$, be a partition of $\mathbb{R}^+ \times \{0\} \cup \{0\} \times \mathbb{R}^+$. The polygon $(\mathbb{R}^+)^2$ delimited by the edges $\{\gamma_e^{i,\alpha}\}_{1 \leq \alpha \leq N_i}$ is denoted B_e^i , for all $i \in \{1, \dots, N_{\text{pol}}\}$. Assume that $T: \{1, \dots, N_{\text{pol}}\}^2 \rightarrow \mathbb{N}$ is a mapping satisfying the following: for all $i, j \in \{1, \dots, N_{\text{pol}}\}$ such that $i \neq j$,*

- $T(i, i) = T(j, j) = 0$;
- $T(i, j) = \alpha \in \{1, \dots, N_i\}$ and $T(j, i) = \beta \in \{1, \dots, N_j\}$ whenever the two edges $\gamma_e^{i,\alpha}$ and $\gamma_e^{j,\beta}$ are identified.
- $T(i, j) = T(j, i) = 0$ whenever no identification is made between edges belonging to the boundaries of B_e^i and B_e^j .

The mapping T is called an equivalence table and the pair $\mathcal{S} = (\{B_e^i\}_{1 \leq i \leq N_{\text{pol}}}, T)$ is called an O-polyhedral surface. The set of vertices of \mathcal{S} is denoted $\{p_e^i\}_{1 \leq i \leq N_{\text{ver}}}$. The set of edges of \mathcal{S} is denoted $\{\gamma_e^i\}_{1 \leq i \leq N_{\text{ed}}}$.

A simple O-polyhedral surface is presented in Figure 3.2 and an illustration of a portion of an O-surface is presented in Figure 3.3. Let us notice that each vertex of an O-polyhedral surface is either at a corner of a polygon containing this vertex or in the interior of some edge in the boundary of this polygon (see Figure 3.4).

Definition 3.4 (Interior angle of vertices). *Let \mathcal{S} be an O-polyhedral surface and let $\{p_e^i\}_{1 \leq i \leq N_{\text{ver}}}$ be its set of vertices. Let $i \in \{1, \dots, N_{\text{ver}}\}$. We denote $I_i \subset \{1, \dots, N_{\text{pol}}\}$ the indices of the polygons containing p_e^i . We denote $\theta_{i,\alpha} \in \{\frac{\pi}{2}, \pi\}$ the interior angle of B_e^α at p_e^i , for all $\alpha \in I_i$, and we set $\lambda_i := \sum_{\alpha \in I_i} \theta_{i,\alpha}$. We call interior angle of p_e^i the positive real number $\lambda_i = k_i \frac{\pi}{2}$, with $k_i \geq 1$ an integer.*

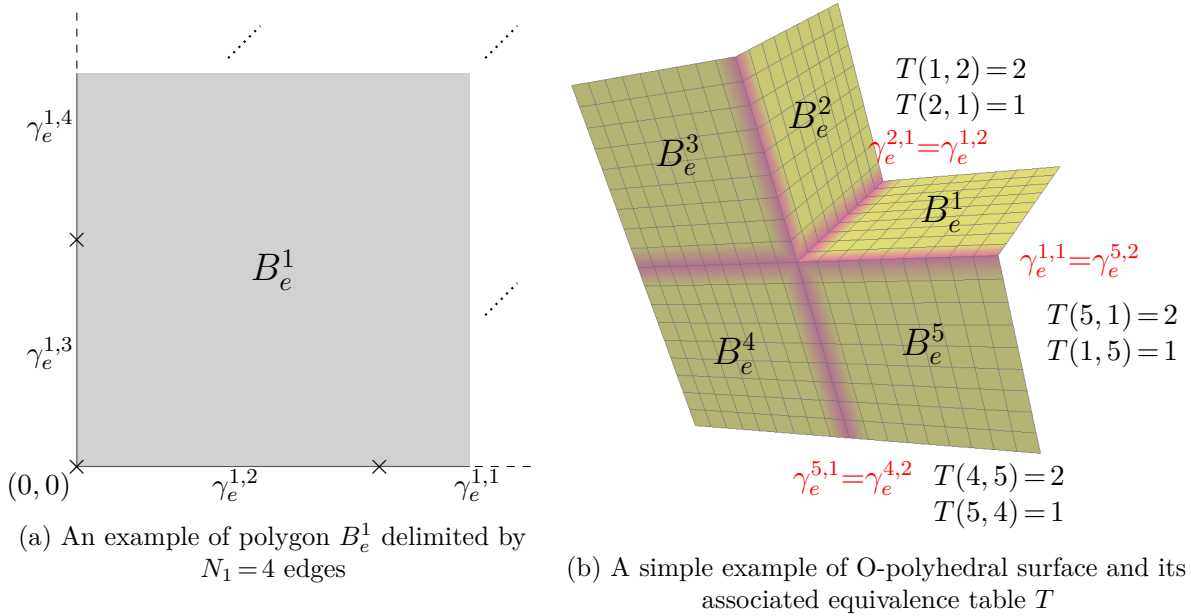


Fig. 3.2 Illustration of an O-polyhedral surface

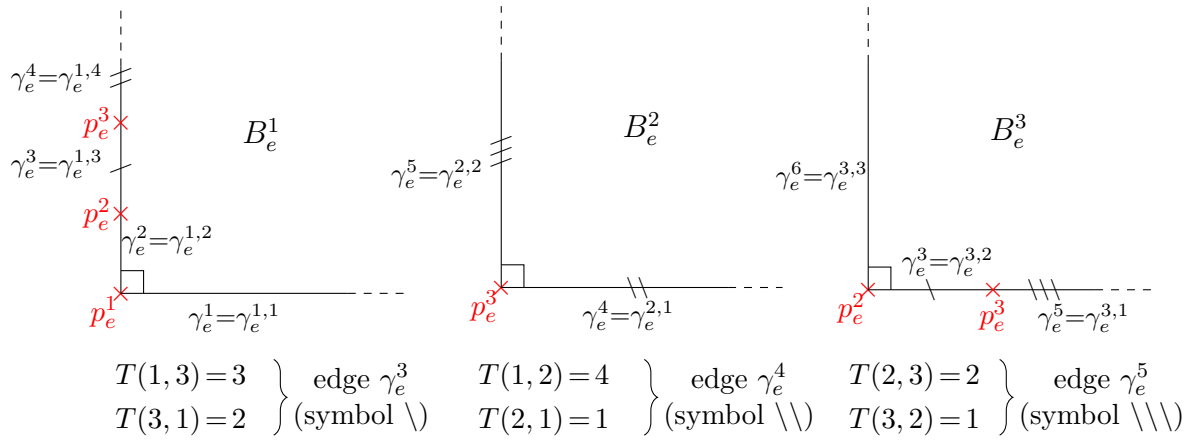
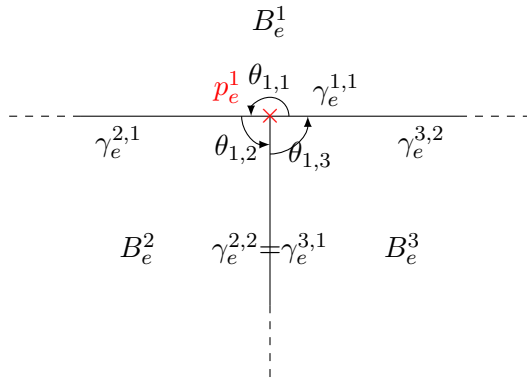


Fig. 3.3 Three polygons of an O-surface


 Fig. 3.4 A vertex p_e^1 of an O-polyhedral surface ($\lambda_1 = \theta_{1,1} + \theta_{1,2} + \theta_{1,3} = 2\pi$)

Junction of pieces of Chebyshev nets

Now, we outline the construction of Chebyshev nets with conical singularities, defined as the junction of Chebyshev nets $\varphi: B_e = (\mathbb{R}^+)^2 \rightarrow B_c \subset M$, with $B_c = \varphi(B_e)$, on a surface M .

Definition 3.5 (Chebyshev nets with conical singularities). *Let M be a surface and let $N_{\text{pol}} \geq 1$ be an integer. For all $i \in \{1, \dots, N_{\text{pol}}\}$, let $\{\gamma_e^{i,\alpha}\}_{1 \leq \alpha \leq N_i}$, with $N_i \geq 2$, be a partition of $\mathbb{R}^+ \times \{0\} \cup \{0\} \times \mathbb{R}^+$. The polygon $(\mathbb{R}^+)^2$ delimited by the edges $\{\gamma_e^{i,\alpha}\}_{1 \leq \alpha \leq N_i}$ is denoted B_e^i , for all $i \in \{1, \dots, N_{\text{pol}}\}$. Assume that $\{\varphi_i\}_{1 \leq i \leq N_{\text{pol}}}$ is a set of Chebyshev nets $\varphi_i: B_e^i \rightarrow B_c^i \subset M$, with $B_c^i = \varphi_i(B_e^i)$ for all $i \in \{1, \dots, N_{\text{pol}}\}$, and assume that $T: \{1, \dots, N_{\text{pol}}\}^2 \rightarrow \mathbb{N}$ is an array such that: for all $i, j \in \{1, \dots, N_{\text{pol}}\}$,*

- if $i = j$, then $T(i, j) = 0$;
- if $i \neq j$ and $T(i, j) \neq 0$, then:
 - $T(i, j) = \alpha \in \{1, \dots, N_i\}$, $T(j, i) = \beta \in \{1, \dots, N_j\}$;
 - $\varphi_i|_{\gamma_e^{i,\alpha}} = \varphi_j|_{\gamma_e^{j,\beta}}$ and $B_c^i \cap B_c^j = \varphi_i(\gamma_e^{i,\alpha}) = \varphi_j(\gamma_e^{j,\beta})$;
- if $i \neq j$ and $T(i, j) = 0$, then $T(j, i) = 0$ and $B_c^i \cap B_c^j = \emptyset$.

The array T is called an equivalence table and the triple $\mathcal{C} = (\{B_e^i\}_{1 \leq i \leq N_{\text{pol}}}, \{\varphi_i\}_{1 \leq i \leq N_{\text{pol}}}, T)$ is called a Chebyshev net with conical singularities.

Definition 3.6 (Piecewise smooth Chebyshev nets with conical singularities). *Let $\mathcal{C} = (\{B_e^i\}_{1 \leq i \leq N_{\text{pol}}}, \{\varphi_i\}_{1 \leq i \leq N_{\text{pol}}}, T)$ be a Chebyshev net with conical singularities. We say that \mathcal{C} is piecewise smooth if the mapping φ_i is piecewise smooth, for all $i \in \{1, \dots, N_{\text{pol}}\}$.*

We illustrate in Figure 3.5 the construction of the equivalence table associated with a Chebyshev net with one conical singularity. We present a second example of Chebyshev net with one conical singularity in Figure 3.6.

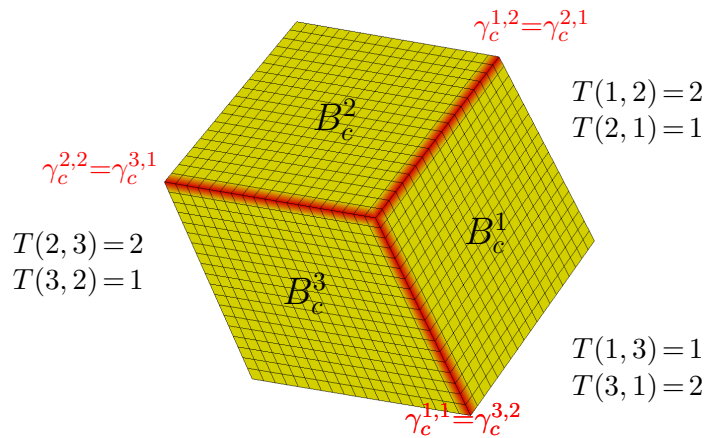


Fig. 3.5 Illustration of the equivalence table T of a Chebyshev net with one conical singularity on the plane

Remark 3.7 (Chebyshev nets with conical singularities and O-polyhedral surfaces). *Let $\mathcal{C} = (\{B_e^i\}_{1 \leq i \leq N_{\text{pol}}}, \{\varphi_i\}_{1 \leq i \leq N_{\text{pol}}}, T)$ be a Chebyshev net with conical singularities. Then, one easily verify that the pair $\mathcal{S} = (\{B_e^i\}_{1 \leq i \leq N_{\text{pol}}}, T)$ is an O-polyhedral surface. Two examples of Chebyshev*

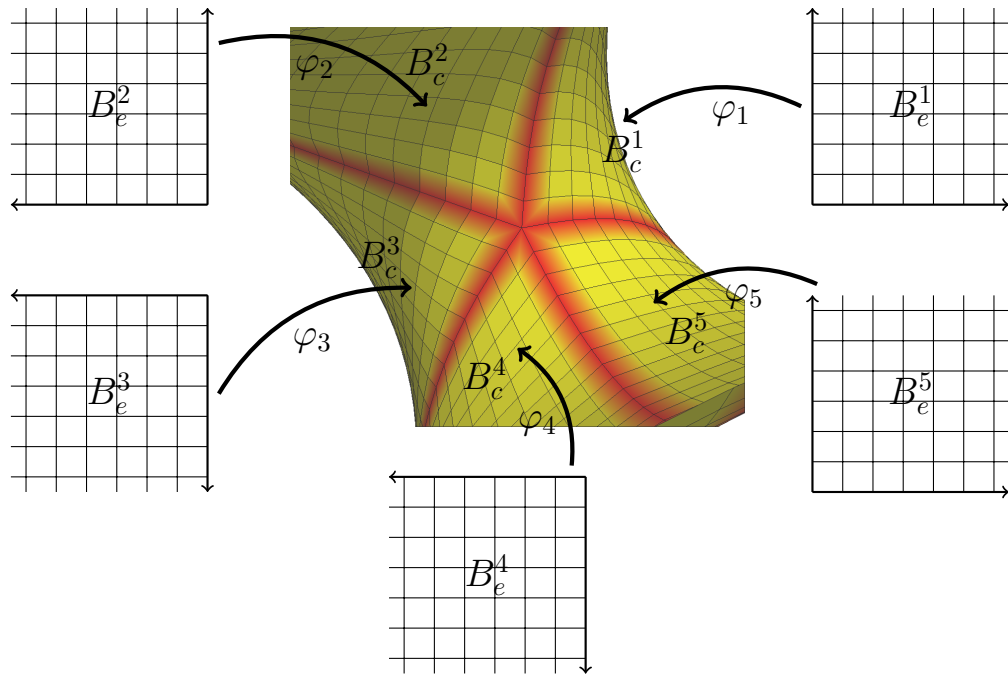


Fig. 3.6 A Chebyshev net with one conical singularity on Enneper's surface

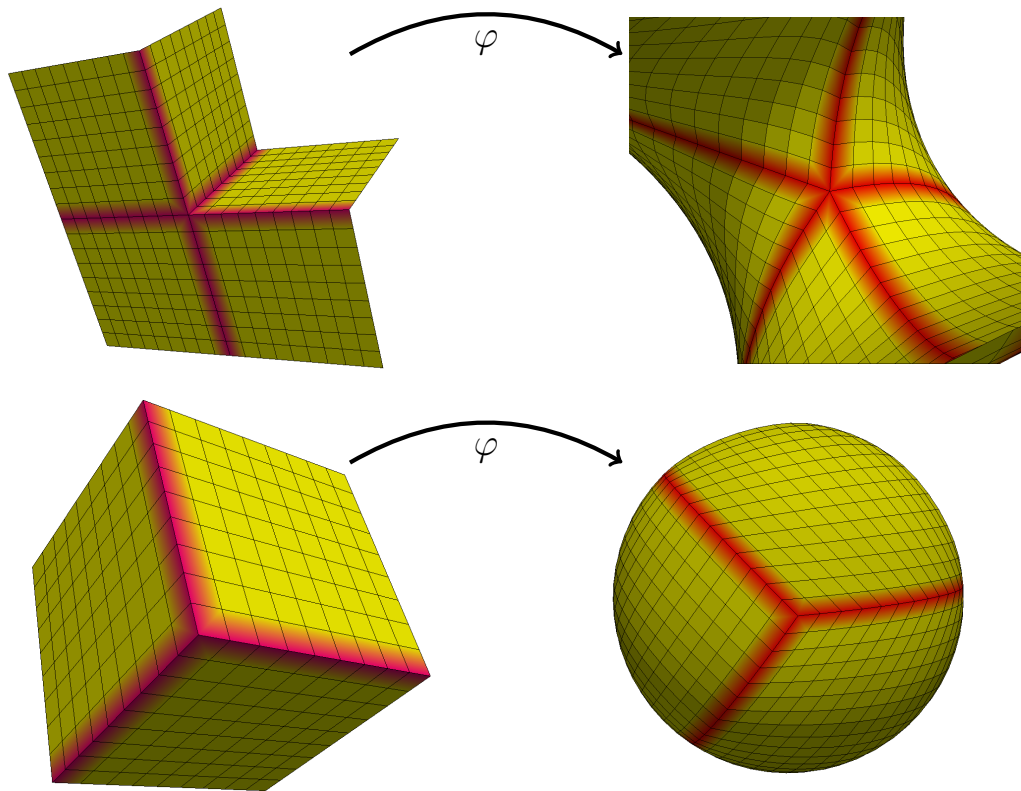


Fig. 3.7 Chebyshev nets with singularities: junction of 5 mappings on Enneper's surface (top) and junction of 3 mappings on the sphere (bottom)

nets with one conical singularity and their associated O-polyhedral surfaces embedded in \mathbb{R}^3 are presented in Figure 3.7.

By Remark 3.7, Chebyshev nets with conical singularities can be equivalently defined as follows.

Definition 3.8 (Chebyshev nets with conical singularities). *Let M be a surface and let \mathcal{S} be an O -polyhedral surface. Then, any homeomorphic mapping $\varphi: \mathcal{S} \rightarrow M$ inducing the metric*

$$ds^2 = du^2 + 2 \cos(\omega(u, v)) dudv + dv^2, \quad (3.5)$$

with $\omega: \mathcal{S} \rightarrow (0, \pi)$ the angle distribution between the coordinate curves, on \mathcal{S} is called a Chebyshev net with conical singularities. The mapping φ is said to be piecewise smooth whenever it is piecewise smooth on each polygon $B_e^i = (\mathbb{R}^+)^2$ of \mathcal{S} . Let $\{p_e^i\}_{1 \leq i \leq N_{\text{ver}}}$ be the set of vertices of \mathcal{S} and let $i \in \{1, \dots, N_{\text{pol}}\}$. Suppose that the interior angle $\lambda_i = k_i \frac{\pi}{2}$, with $k_i \geq 1$ an integer, of p_e^i is different from 2π . Then, the point $\varphi(p_e^i)$ is called a conical singularity of valence k_i of φ . The set of singularity points of φ is denoted \mathcal{P} .

For example, the Chebyshev nets with one conical singularities of Figure 3.7 have valence 5 (Enneper's surface) and 3 (sphere).

Remark 3.9 (Generalization to polygons of interior angle $\frac{\pi}{2}$). Chebyshev nets with conical singularities can be generalized to the junction of Chebyshev nets $\tilde{\varphi}: \tilde{B}_e \rightarrow \tilde{B}_c = \tilde{\varphi}(\tilde{B}_e) \subset M$, with \tilde{B}_e an orthogonal polygon of \mathbb{R}^2 . See Figure 3.8 for an illustration of the different types of orthogonal polygons of \mathbb{R}^2 . We present an example of Chebyshev nets with two conical singularities, in this generalized sense, on the sphere in Figure 3.9.

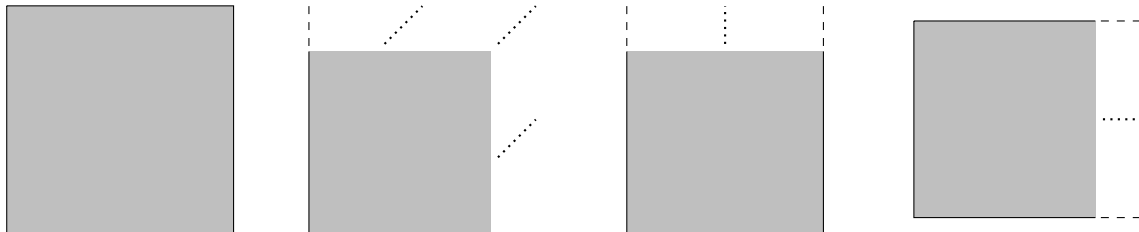


Fig. 3.8 Illustration of the four types of orthogonal polygons in \mathbb{R}^2

Let M be a surface and let \mathcal{C} be a Chebyshev net with conical singularities \mathcal{P} . Then, any point $p \in M \setminus \mathcal{P}$ has a Chebyshev net (Ω_0, φ_0) defined by \mathcal{C} in its neighborhood. On the other hand, the points in \mathcal{P} have a particular coordinate system on their neighborhood called conical net in what follows. We take a global view on these singularity points in the next section.

Global surface parametrization and conical singularities

We set in this section the theoretical basis to tackle the main problem addressed in this thesis: the construction of global Chebyshev nets on a given surface. The transition from local to global coordinate systems is considered in Section 3.2.1. This leads us to the introduction of globally compatible (GC) coordinate systems, defined to be a set of coordinate systems on the surface such that the coordinate curves are uniquely defined. Then, we consider in Section 3.2.2 GC coordinate systems on a surface minus a finite set of isolated points called singularity points. Next, we focus on singularities with one more property: at their neighborhood, coordinate systems are distortions of conical surfaces. These singularities are called conical singularities.

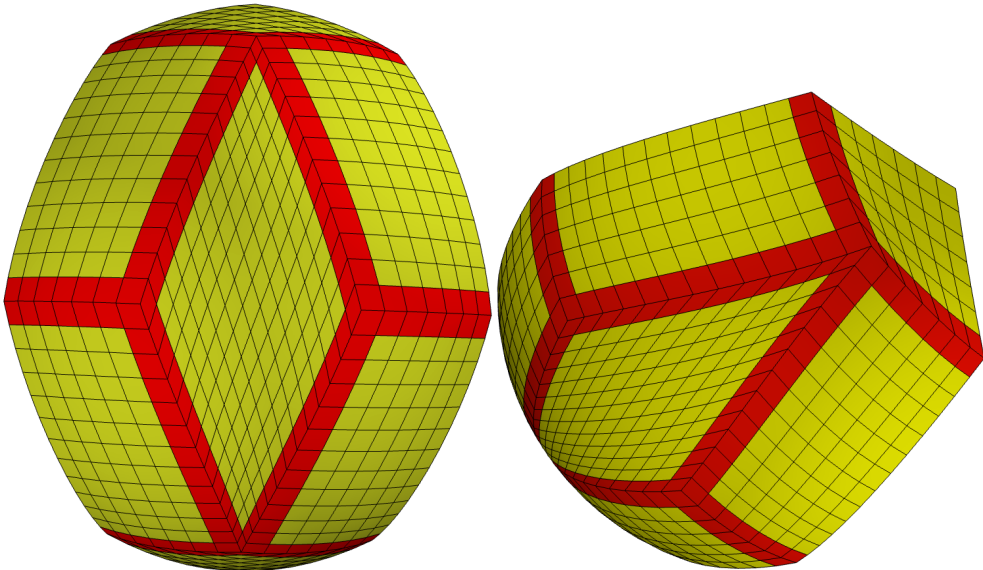


Fig. 3.9 A Chebyshev net with two conical singularities on the sphere: the image by φ of the orthogonal polygons are delimited by the red curves

From local to global coordinate systems

In this section, we introduce global “meshings”, that is, globally defined coordinate curves. We call these global “meshings” GC coordinate systems. With this purpose in mind, we emphasize that although global coordinate systems (M, φ) may exist in particular cases, in all generality coordinate systems are only defined locally. Hence, in order to consider surfaces non-homeomorphic to the plane or to consider singularity points, we define the coordinate curves on the surface with multiple coordinate systems $\mathcal{A} = \{(\Omega_i, \varphi_i)\}_{i \in E}$. Then, to have uniquely defined coordinate curves, the transition mappings between the nets in \mathcal{A} must satisfy compatibility conditions. Indeed, to define globally some notion on the surface, it is necessary to reduce the set of coordinate systems in order to have a definition independent of the coordinate system in which it is expressed. An example is given by the Riemann surfaces [7]: transition mappings are restricted to holomorphic mappings which permits to define oriented angles. In the same manner, whenever the transition mappings are restricted to affine transformations, the atlas is called an affine structure. In order to have a unique definition of the coordinate curves (and their parametrization) at each point of the surface, we restrict the transition mappings to grid automorphisms [38], which are isometric mappings of \mathbb{R}^2 defined as follows:

Definition 3.10 (Grid automorphism of translation vector V and flip k). *Let $v \in \mathbb{R}^2$ and let $k \in \{0, 1, 2, 3\}$. We call grid automorphism of translation vector V and flip k the isometry $L: \mathbb{R}^2 \rightarrow \mathbb{R}^2$ defined by*

$$L(x) = R_{k\frac{\pi}{2}}(x) + V, \quad (3.6)$$

for all $x \in \mathbb{R}^2$, with $R_{k\frac{\pi}{2}}$ the rotation of angle $k\frac{\pi}{2}$.

Two coordinate systems on M such that the transition mapping is a piecewise grid automorphism are said to be compatible.

Definition 3.11 (Compatibility of coordinate systems). *Let M be a surface and let (Ω_i, φ_i) and (Ω_j, φ_j) be two coordinate systems of M such that $\Omega_i \cap \Omega_j \neq \emptyset$. Let $L_{i,j} = \varphi_j^{-1} \circ \varphi_i: \varphi_i^{-1}(\Omega_i \cap \Omega_j) \rightarrow$*

$\varphi_j^{-1}(\Omega_i \cap \Omega_j)$ be the transition mapping between these two nets. Then, the coordinate systems (Ω_i, φ_i) and (Ω_j, φ_j) are said to be compatible whenever for all connected open set $U \subset \varphi_i^{-1}(\Omega_i \cap \Omega_j)$, the mapping $L_{i,j}|_U : U \rightarrow L_{i,j}(U)$ is the restriction to U of a grid automorphism.

We present in Figure 3.10 an illustration of two compatible nets (Ω_i, φ_i) and (Ω_j, φ_j) .

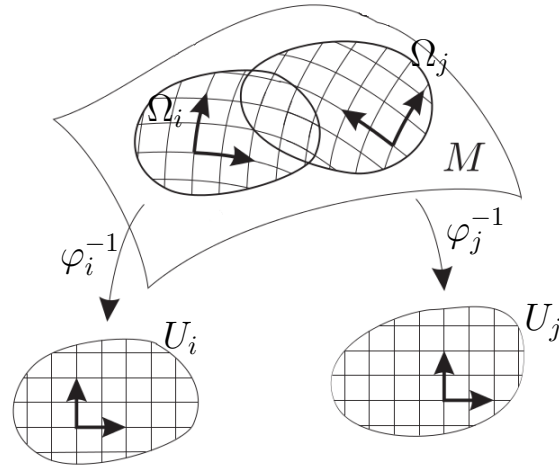


Fig. 3.10 Illustration of two compatible nets on M [31, p.3]

Definition 3.12 (Globally compatible (GC) atlases). *Let M be a surface and let \mathcal{A} be an atlas on M . The atlas \mathcal{A} is said to be globally compatible on M whenever all the coordinate systems in \mathcal{A} are compatible. In what follows, GC atlases are assumed to be maximal for the inclusion.*

Definition 3.13 (Grid automorphism associated with $\varphi_j^{-1} \circ \varphi_i$ at p). *Let \mathcal{A} be a GC atlas and let $(\Omega_i, \varphi_i) \in \mathcal{A}$ and $(\Omega_j, \varphi_j) \in \mathcal{A}$ be such that $\Omega_i \cap \Omega_j \neq \emptyset$. For all $p \in \Omega_i \cap \Omega_j$, we call grid automorphism associated with the transition mapping $\varphi_j^{-1} \circ \varphi_i$ at p , the grid automorphism of the connected component of $\varphi_i^{-1}(p)$ in $\varphi_i^{-1}(\Omega_i \cap \Omega_j)$.*

The GC atlases, as well as affine structures, are (G, H) -structures. We refer to [26] for a definition and study of these geometric structures. Moreover, we note that in the literature on mesh generation, grid automorphisms are used for defining so-called globally continuous meshes [42, 31]. We remark that for quadrangle mesh generation a stronger constraint is required for the discrete coordinate grid (image of $(\mathbb{Z} \times \mathbb{R} \cup \mathbb{R} \times \mathbb{Z}) \cap U$ for the coordinate system (Ω, φ) , with $U = \varphi^{-1}(\Omega)$) to be well defined. Coordinate systems satisfying this constraint are called Integer-Grid Maps [10].

Remark 3.14 (Construction of GC atlases). Let M be a surface and let $\cup_{i \in I} \Omega_i$ be an open cover of M . Assume that $\{(\Omega_i, \varphi_i)\}_{i \in I}$ is a set of compatible coordinate systems. Then, there exists a GC atlas on M containing these coordinate systems. This GC atlas is said to be induced by $\{(\Omega_i, \varphi_i)\}_{i \in I}$ in what follows.

We make explicit in the following proposition, proved in Section 3.4.3, the relations between GC atlases and homeomorphisms in the particular case of simply connected complete surfaces.

Proposition 3.15 (Existence of a global coordinate system). *Let M be a complete, simply connected surface and let \mathcal{A} be a GC atlas on M . Suppose that there exists $C > 0$ such that for all $(\Omega, \varphi) \in \mathcal{A}$,*

$$\sup_{y \in \varphi^{-1}(\Omega)} |\mathrm{d}\varphi_y(X)|_g^2 \leq C|X|^2, \quad \forall X \in \mathbb{R}^2,$$

with $d\varphi_y : \mathbb{R}^2 \rightarrow T_{\varphi(y)} M$ the differential of φ at y . Then, there exists a global coordinate system $(M, \tilde{\varphi}) \in \mathcal{A}$.

An example of GC atlas on a simply connected surface that does not contain a global coordinate system is presented in Figure 3.11.

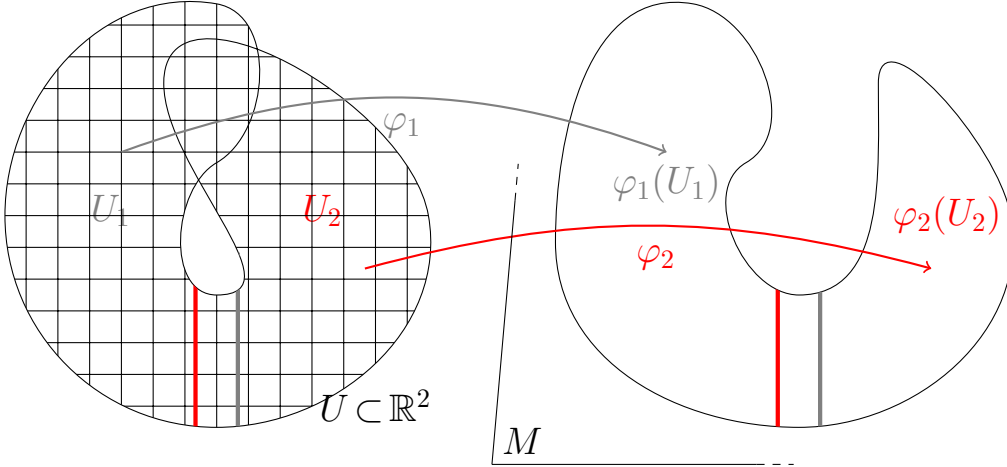


Fig. 3.11 Illustration of a GC atlas that does not contain a global coordinate system

Remark 3.16 (Coordinate curve parametrization in GC atlases). The coordinate curves and their parametrizations are preserved by transition mappings whenever these mappings are grid automorphisms. Hence, these items are defined in a unique manner everywhere on the surface. Whenever it is not necessary to have a unique definition of the coordinate curves parametrization, this constraint on the transition mappings $\varphi_j^{-1} \circ \varphi_i$ can be relaxed as follows:

$$\varphi_j^{-1} \circ \varphi_i(x) = \alpha \circ R_{k\frac{\pi}{2}}(x) + v, \quad \forall x \in \varphi_i^{-1}(\Omega_i \cap \Omega_j), \quad (3.7)$$

with $v \in \mathbb{R}^2$, $k \in \{0, \dots, 3\}$, $R_{k\frac{\pi}{2}}$ the rotation of angle $k\frac{\pi}{2}$ and $\alpha(\tilde{x}, \tilde{y}) = (\alpha_1(\tilde{x}), \alpha_2(\tilde{y}))$, $\alpha_1, \alpha_2 : \mathbb{R} \rightarrow \mathbb{R}$ being two diffeomorphisms.

In order to give some non-trivial (homeomorphisms) examples, we consider covering mappings, defined below.

Definition 3.17 (Covering mapping). Let N, M be two surfaces. The mapping $\tau : N \rightarrow M$ is called a smooth covering mapping whenever it is surjective, smooth and satisfies the following property: for all $m \in M$, there exists a neighborhood $V_m \subset M$ of m and a disjoint open cover $\cup_{i \in J} \tilde{V}_i$ of $\tau^{-1}(V_m) \subset N$ such that $\tau|_{\tilde{V}_i} : \tilde{V}_i \rightarrow V_m$ is a diffeomorphism for all $i \in J$.

Example 3.18 (GC atlases from covering mappings). Let $\tau : \mathbb{R}^2 \rightarrow M$ be a covering mapping and let $m \in M$. Let $V_m \subset M$ and $\cup_{i \in J} \tilde{V}_{m,i}$ be respectively the neighborhood of m in M and the disjoint open cover of $\tau^{-1}(V_m) \subset \mathbb{R}^2$ obtained using Definition 3.17. Suppose moreover that, for all $i, j \in J$, $\tau|_{\tilde{V}_{m,j}}^{-1} \circ \tau|_{\tilde{V}_{m,i}} : \tilde{V}_{m,i} \rightarrow \tilde{V}_{m,j}$ is a translation of the plane. Then, the coordinate systems $(V_m, \tau|_{\tilde{V}_{m,i}})$, defined for all $m \in M$ and $i \in J$, are compatible and cover M . Hence, these coordinate systems induce a GC atlas on M . We present two examples of GC atlases defined by covering mappings:

- Let $M = \{(x, y, z) \in \mathbb{R}^3 \mid x^2 + y^2 = 1\}$ be a cylinder of revolution and let $\tau : \mathbb{R}^2 \rightarrow M$ be the mapping defined by $\tau(u, v) = (\cos(u), \sin(u), v)$. Then, τ is a covering mapping defining a GC atlas on the surface M . This GC atlas is presented in Figure 3.12.

- Let $R, r \in \mathbb{R}_*^+$ be such that $R > r > 0$ and let $M = \{(x, y, z) \in \mathbb{R}^3 \mid (x^2 + y^2 + z^2 + R^2 - r^2)^2 = 4R^2(x^2 + y^2)\}$ be a torus. Let $\tau: \mathbb{R}^2 \rightarrow M$ be the mapping defined by

$$\tau(u, v) = ((R + r \cos(v)) \cos(u), (R + r \cos(v)) \sin(u), \sin(v)).$$

Then, τ is a covering mapping and it defines a GC atlas on the surface M . This GC atlas is presented in Figure 3.13.

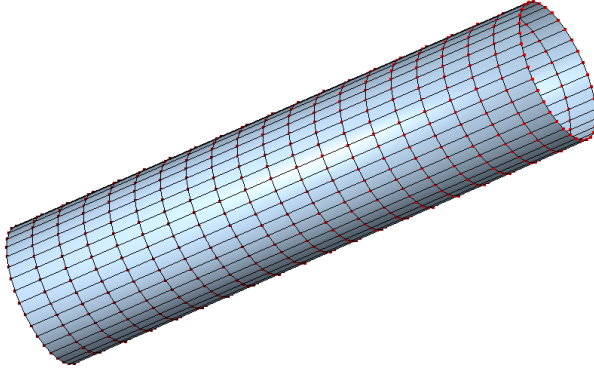


Fig. 3.12 A GC atlas on the cylinder of revolution

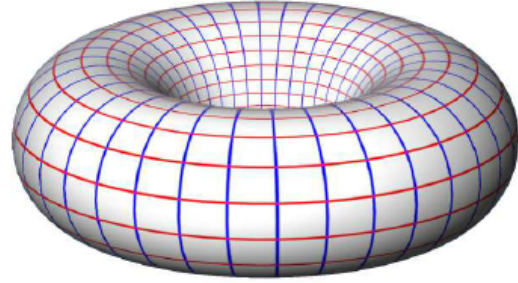


Fig. 3.13 A GC atlas on the torus

Singularities of globally compatible coordinate systems

We introduce in this section singularities of GC atlases and we then highlight a particular type of singularities called conical. First, in Subsection 3.2.2.1, we emphasize the importance of singularities in the search for GC atlases on surfaces and we introduce these objects in an informal setting. Then, we introduce these particular points of GC atlases in Subsection 3.2.2.2.

On the terminology

The existence of a GC atlas on a given surface M is constrained by the topology of the aforesaid surface, as can be seen by the Poincaré–Hopf formula. Then, whenever a particular type of parametrization is required on M , this constraint on the type of expected GC atlas can also be an obstacle to the existence of this structure on M . This lack of global existence often materialises itself with the appearance of singularities. In order to overcome these singularities or simply to permit a larger choice in the accessible parametrizations, an approach consists in constructing GC atlases with singularities. With this paradigm, the singularities are chosen beforehand. This point of view is often adopted in the literature on mesh generation, as can be seen in [32, 33, 42].

Usually, in the case of coordinate systems, the term singularity refers to a singularity of the mapping $\varphi: U \subset \mathbb{R}^2 \rightarrow \Omega \subset M$ that defines the coordinate system (Ω, φ) . For instance, let \bar{U} be an open set of \mathbb{R}^2 , $\bar{\Omega}$ be an open set of M and let $\bar{\varphi}: \bar{U} \rightarrow \bar{\Omega}$ be a smooth mapping. The singularity points of $\bar{\varphi}$ are the points $\bar{\varphi}(x) \in \bar{\Omega}$, with $x = (u, v) \in \bar{U}$, such that $(\partial_u \varphi(x), \partial_v \varphi(x))$ is not an independent family of vectors. We denote $\{x_i\}_{i \in I} \subset \bar{\Omega}$ this set. We refer to [25] for an analysis of this set in the generic case, where the singularity points of $\bar{\varphi}$ can be of two different types: cusps and folds. In the particular case of Chebyshev nets, an example of these singularities is presented in the Figure 3.14.

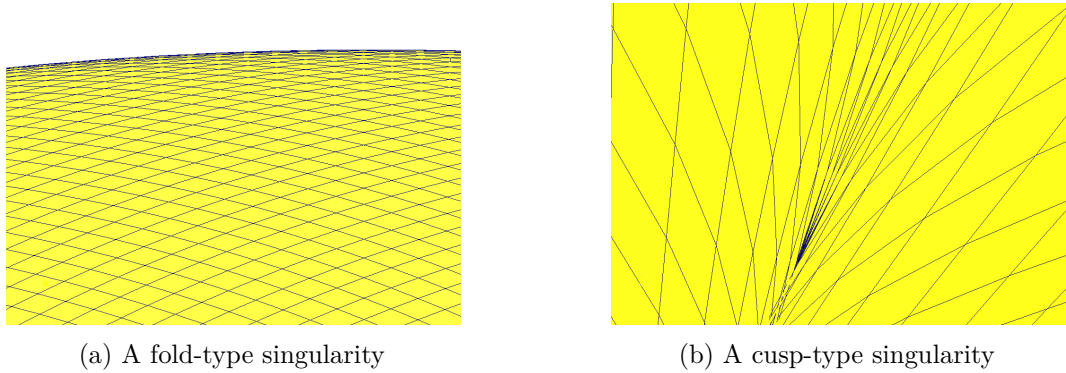
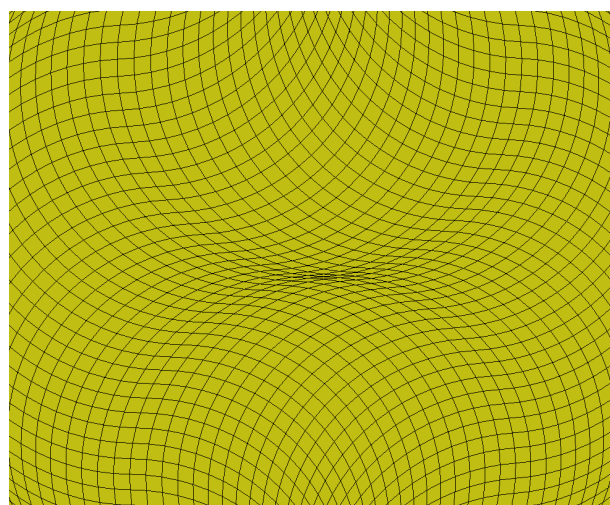


Fig. 3.14 Generic singularities of Chebyshev nets

In this manuscript, we consider a slightly different notion of singularity. Hence, we define a GC atlas on $M \setminus D$, where $D \subset M$ is a finite set of isolated points called singularity points. A usual singularity is also a singularity in the present meaning if it is restricted to a point. To illustrate this remark, we now suppose that the mapping $\bar{\varphi}: \bar{U} \subset \mathbb{R}^2 \rightarrow \bar{\Omega} \subset M$ is a diffeomorphism in $\bar{U} \setminus \{x_0\}$, where $x_0 \in \bar{U}$ is such that $(\partial_u \bar{\varphi}(x_0), \partial_v \bar{\varphi}(x_0))$ is not an independent family of vectors. We set $p = \bar{\varphi}(x_0)$. Then, the coordinate system $(\bar{\Omega} \setminus \{p\}, \bar{\varphi}|_{\bar{\Omega} \setminus \{p\}})$ cannot be extended in the neighborhood of p . The point p is called a singularity point of the GC atlas induced by this net. An example of this type of singularities defined by a Chebyshev net $\bar{\varphi}$ is presented in Figure 3.15. Let us notice that the generic singularities in the usual sense (cusp-type and fold-type) are one-dimensional submanifolds. Hence, these points do not define a GC atlas with singularities (D is not a finite set of isolated points in this case). Finally, a singularity in the present meaning is not necessarily a usual singularity. The most important examples are the conical singularities that we introduce below. **We note that another definition could have been given to singularities in order to take into account other types of generalized Chebyshev nets such as the parametrization of the sphere obtained by Ghys [25].** In this parametrization, the generalized Chebyshev nets contains four cusp-type singularities.


 Fig. 3.15 An example of singularity at once in the usual sense and in the present meaning on a Chebyshev net $\bar{\varphi}$

GC atlases with conical singularities

The singularities of GC atlases that are not usual singularities (see paragraph above), can be informally considered as the set of isolated points of M such that the “number of coordinate curves” at this point is different from two. The conical singularities are particular singularity points such that the “number of coordinate curves” at this point is finite. In order to define more precisely the conical singularities, we first fix some notation in Subsection 3.2.2.1. We then present a simple example of conical singularity in Subsection 3.2.2.2. We finally introduce in Subsection 3.2.2.3 the conical singularities.

3.2.2.1 Conical surfaces We first define the conical surface C_λ of interior angle $\lambda > 0$ [46]. See Figure 3.16 for a representation of this conical surface.

Definition 3.19 (Conical surface (or cone) of interior angle λ). *Let $\lambda > 0$ and let \sim be the equivalence relation on $\mathbb{R}^+ \times \mathbb{R}$ defined by*

$$(r, \theta) \sim (r', \theta') \quad \text{if and only if} \quad (r = r' \text{ and } \theta - \theta' \in \lambda\mathbb{Z}) \text{ or } (r = r' = 0),$$

for all $\theta, \theta' \in \mathbb{R}$, $r, r' \in \mathbb{R}^+$. The quotient set $C_\lambda := (\mathbb{R}^+ \times \mathbb{R}) / \sim$ endowed with the metric $ds^2 = dr^2 + r^2 d\theta^2$ is called a conical surface of interior angle λ .

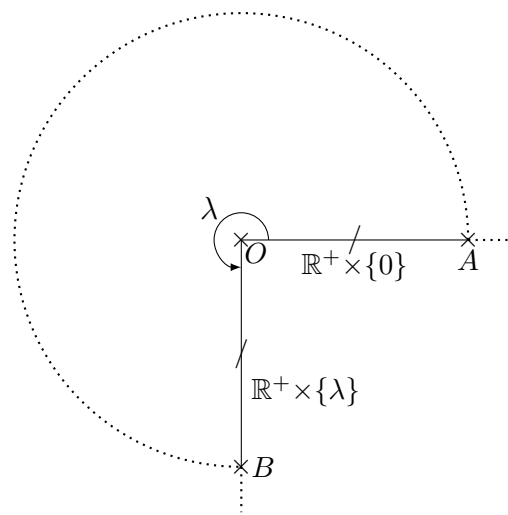
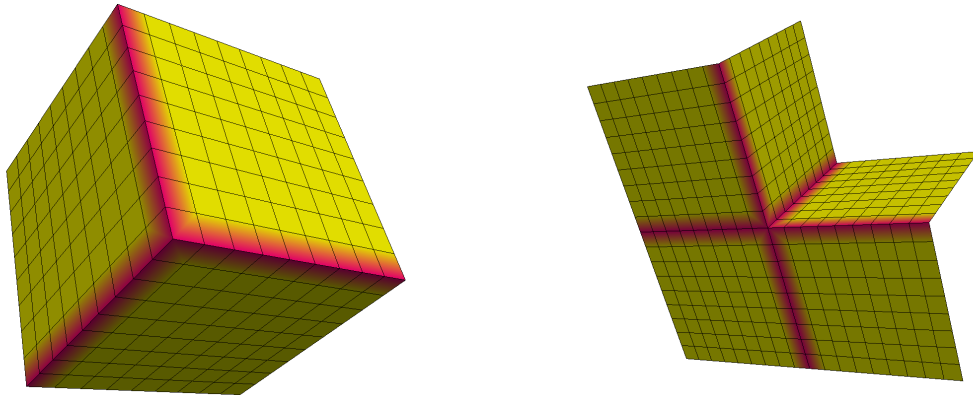


Fig. 3.16 A representation of the cone of interior angle λ : the rays (OA) and (OB) are isometrically identified as a single line

Remark 3.20 (Conical surface with interior angle $k\frac{\pi}{2}$). The conical surfaces we encounter in what follows have interior angle $k\frac{\pi}{2}$ for some integer $k \geq 1$. Embeddings in \mathbb{R}^3 of the cones of interior angles $3\frac{\pi}{2}$ and $5\frac{\pi}{2}$ are presented in Figure 3.17.

We call global isometry any mapping which is a bijective local isometry. Let us remark that conical surfaces are defined in polar coordinates. Hence, we point out in what follows subsets of cones, called branch-cut domains, that can be isometrically identified with the plane. In other words, we endow locally the conical surfaces with cartesian coordinates.

Definition 3.21 (Branch-cut domain). *Let C_λ be the conical surface of interior angle $\lambda > 0$. Let $\bar{V} \subset C_\lambda$ be a connected set and suppose that there exists $\eta_1 \in [0, \lambda)$ and $\delta \in (0, 2\pi] \cap (0, \lambda]$ such that $\theta > \eta_1$ or $\theta < \eta_2$, for all $(r, \theta) \in \bar{V}$, with $\eta_2 = (\eta_1 + \delta) \bmod \lambda$. We say that the domain $\bar{V} \subset C_\lambda$ is a*



(a) A conical surface with interior angle $3\frac{\pi}{2}$ (b) A conical surface with interior angle $5\frac{\pi}{2}$

Fig. 3.17 Illustrations of conical surfaces isometrically embedded in \mathbb{R}^3

branch-cut domain and we denote $\text{Is}(C_\lambda, \bar{V}): \bar{V} \rightarrow \text{Pl}(C_\lambda, \bar{V}) \subset \mathbb{R}^2$, with $\text{Pl}(C_\lambda, \bar{V}) = \text{Is}(C_\lambda, \bar{V})(\bar{V})$, the global isometry defined by

$$\text{Is}(C_\lambda, \bar{V})(r, \theta) = \begin{cases} (r \cos(\theta), r \sin(\theta)), & \text{if } \theta \geq \eta_1, \\ (r \cos[\theta + \lambda], r \sin[\theta + \lambda]), & \text{otherwise.} \end{cases}$$

We illustrate different types of branch-cut domains in a cone C_λ , with $\lambda > 0$, and their associated global isometry in Figure 3.18.

Definition 3.22 (Smoothness of mappings defined on cones). *Let M be a surface, let $p \geq 1$ be an integer and let C_λ be the conical surface of interior angle $\lambda > 0$. Let $\bar{U} \subset C_\lambda$ be a set with non-empty interior and let $\psi: \bar{U} \rightarrow M$ be a mapping. For all $\theta_0 \in [0, \lambda)$ and $\delta \in (0, \lambda)$, we define the set*

$$\bar{V}_{\theta_0, \delta} = \{(r, \theta_0 + \theta) \in C_\lambda \mid 0 \leq \theta \leq \delta\} \cap \bar{U},$$

with $\theta_0 + \theta$ the addition modulo λ . We say that ψ has regularity C^p whenever, for all $\theta_0 \in [0, \lambda)$ and $\delta \in (0, \lambda)$ such that $\bar{V}_{\theta_0, \delta}$ is a branch-cut domain, the mapping $\psi \circ \text{Is}(C_\lambda, \bar{V}_{\theta_0, \delta})^{-1}: \text{Pl}(C_\lambda, \bar{V}_{\theta_0, \delta}) \rightarrow M$ has regularity C^p .

The set $\bar{V}_{\theta_0, \delta}$, with $\theta_0 \in [0, \lambda)$ and $\delta \in (0, \lambda)$, introduced in the definition is depicted in Figure 3.19.

3.2.2.2.2 A simple example Let us present the example of the d^{th} -root mapping that highlights the peculiarities of conical singularities.

Example 3.23 (d^{th} -root mapping). Let $\tau: \mathbb{C} \rightarrow \mathbb{C}$ be the mapping defined by $\tau(z) = z^d$, with $d \geq 2$ an integer. In order to avoid any confusion, we denote this mapping $\tau: M \rightarrow \mathbb{C}$, with $M = \mathbb{C}$ and $M^* = \mathbb{C}^*$. Then, the mapping $\tau|_{M^*}: M^* \rightarrow \mathbb{C}^*$ defines a GC atlas \mathcal{A} on M^* that we make explicit as follows. First, we denote $\arg(p) \in [0, 2\pi)$ the argument of $p \in \mathbb{C}^*$ and we denote $\xi_0: \mathbb{C}^* \setminus \mathbb{R}^+ \rightarrow \xi_0(\mathbb{C}^* \setminus \mathbb{R}^+) \subset \mathbb{C}^*$ the mapping defined by

$$\xi_0(z) = z^{1/d} = r^{1/d} e^{\frac{i\theta}{d}}, \quad \text{for all } z = r e^{i\theta} \in \mathbb{C}^* \setminus \mathbb{R}^+,$$

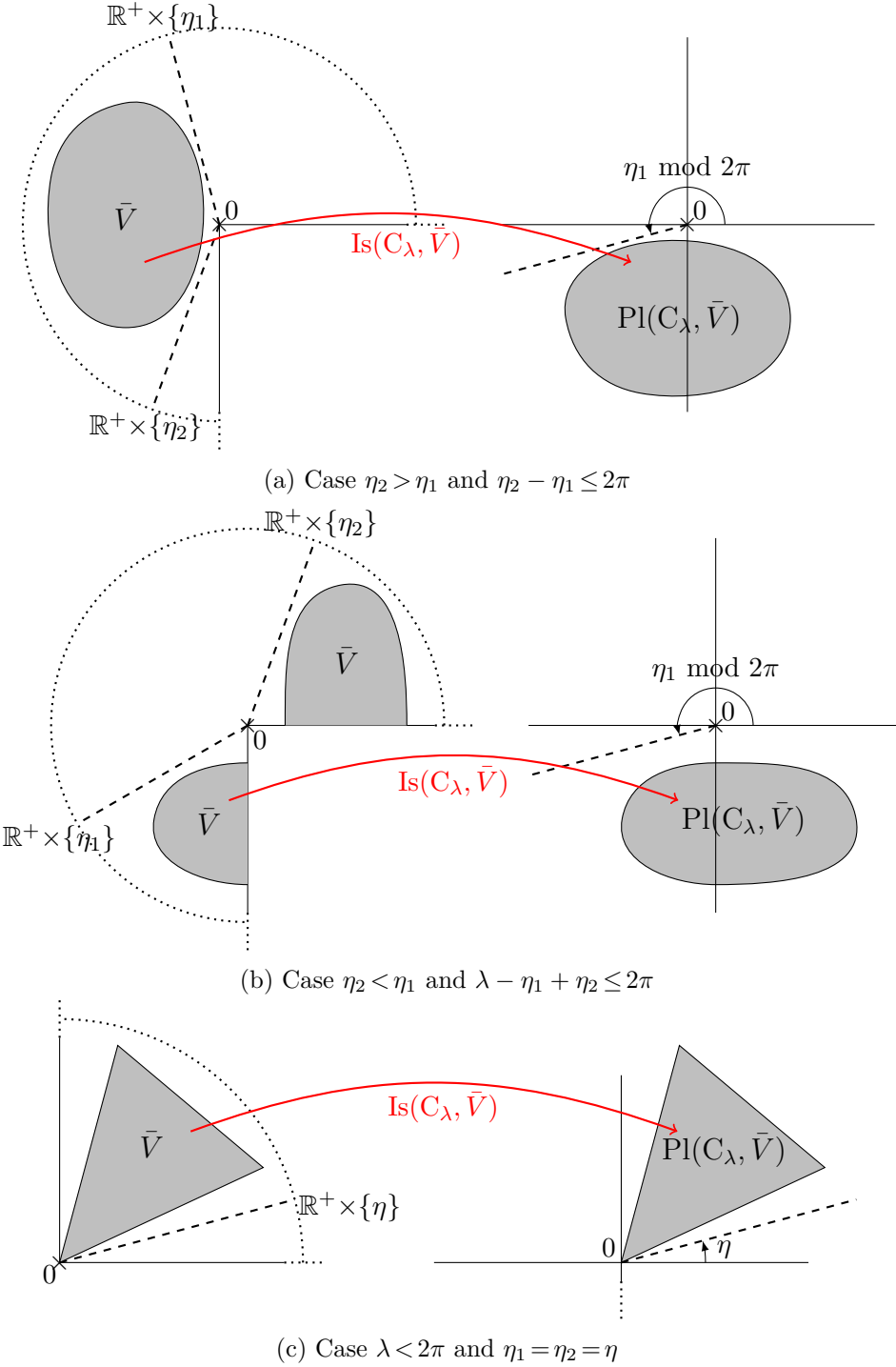


Fig. 3.18 Representation of the branch-cut domain $\bar{V} \subset C_\lambda$ with its associated global isometry $Is(C_\lambda, \bar{V})$ in principal subcases

with $r \in \mathbb{R}_*$ and $\theta \in [0, 2\pi)$. Moreover, for every $\eta \in [0, 2\pi)$, we define the set

$$U_\eta = \{z \in \mathbb{C}^* \mid \arg(z) \in [0, 2\pi) \setminus \{\eta\}\}$$

and we denote $\xi_\eta : U_\eta \rightarrow \xi_\eta(U_\eta) \subset \mathbb{C}^*$ the mapping defined by $\xi_\eta(z) = e^{\frac{i\eta}{d}} \xi_0(e^{-i\eta} z)$, for all $z \in U_\eta$. Finally, let $R_{\frac{2\pi}{d}} = \exp(\frac{2\pi i}{d})$ and, for all $\eta \in [0, 2\pi)$ and $\beta \in \{0, \dots, d-1\}$, we denote $\varphi_{\eta, \beta} : U_\eta \rightarrow$

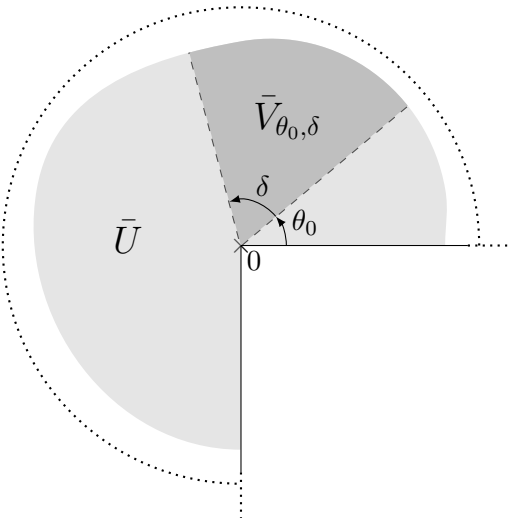


Fig. 3.19 Illustration of the set $\bar{V}_{\theta_0, \delta}$
introduced in Definition 3.22

$\varphi_{\eta, \beta}(U_\eta) \subset M^*$ the mapping defined by

$$\varphi_{\eta, \beta}(z) = (R_{\frac{2\pi}{d}})^\beta \xi_\eta(z), \text{ for all } z \in U_\eta.$$

Then, for all $\eta \in [0, 2\pi)$ and $\beta \in \{0, \dots, d-1\}$, the mapping $\varphi_{\eta, \beta}$ is a diffeomorphism and satisfy $\tau[\varphi_{\eta, \beta}(z)] = z$ for all $z \in U_\eta$. Then, the set of coordinate systems $(\varphi_{\eta, \beta}(U_\eta), \varphi_{\eta, \beta})$, with $\eta \in [0, 2\pi)$ and $\beta \in \{0, \dots, d-1\}$, is compatible and covers M^* . Hence, these coordinate systems induce a GC atlas. We present this atlas in Figure 3.20 in the case $d=2$.

We now prove that the GC atlas of the above example can be obtained by a homeomorphism defined on a cone and with image in $M = \mathbb{C}$.

Example 3.24 (Definition of the d^{th} -root mapping on a cone $C_{2\pi d}$). Let $d \geq 2$ and let $C_{2\pi d}$ be the cone of interior angle $2\pi d$. We denote $\bar{\varphi}: C_{2\pi d} \rightarrow \mathbb{C}$ the mapping defined by

$$\bar{\varphi}(r, \theta) = r^{1/d} \exp\left(\frac{i\theta}{d}\right),$$

for all $(r, \theta) \in C_{2\pi d}$. Then, the mapping $\bar{\varphi}$ is a homeomorphism [46]. Let $\beta \in \{0, \dots, d-1\}$ and let $\bar{U}_\beta \subset C_{2\pi d}$ be an open set such that, for all $(r, \theta) \in \bar{U}_\beta$, we have $\theta = 2\pi\beta + \tilde{\theta}$ with $r \in \mathbb{R}_*^+$ and $\tilde{\theta} \in [0, 2\pi)$. Hence, the set \bar{U}_β is a branch-cut domain and we set $U_0 := \text{Pl}(C_{2\pi d}, \bar{U}_\beta) \subset \mathbb{C}$ and $\Pi := \text{Is}(C_{2\pi d}, \bar{U}_\beta): \bar{U}_\beta \rightarrow U_0$. Then, the mapping $\bar{\varphi} \circ \Pi^{-1}: U_0 \rightarrow \bar{\varphi}(\bar{U}_\beta) \subset \mathbb{C}^*$ is a diffeomorphism defined by

$$\begin{aligned} \bar{\varphi} \circ \Pi^{-1}(z) &= \bar{\varphi}|_{\bar{U}_\beta}(r, \theta) = r^{1/d} \exp\left(\frac{i(2\pi\beta + \tilde{\theta})}{d}\right) \\ &= \exp\left(\frac{2\pi\beta i}{d}\right) (re^{i\tilde{\theta}})^{1/d} = \exp\left(\frac{2\pi\beta i}{d}\right) z^{1/d}, \end{aligned}$$

for all $z = re^{i\tilde{\theta}} \in U_0$, with $\tilde{\theta} \in [0, 2\pi)$. We infer that the mapping $\bar{\varphi} \circ \Pi^{-1}$ is compatible with the GC atlas \mathcal{A} defined in the Example 3.23. Finally, we observe that, since the mapping $\bar{\varphi} \circ \Pi^{-1}$ has no derivative at 0, the mapping $\bar{\varphi}$ does not have a C^1 -regularity (see Definition 3.22). However,

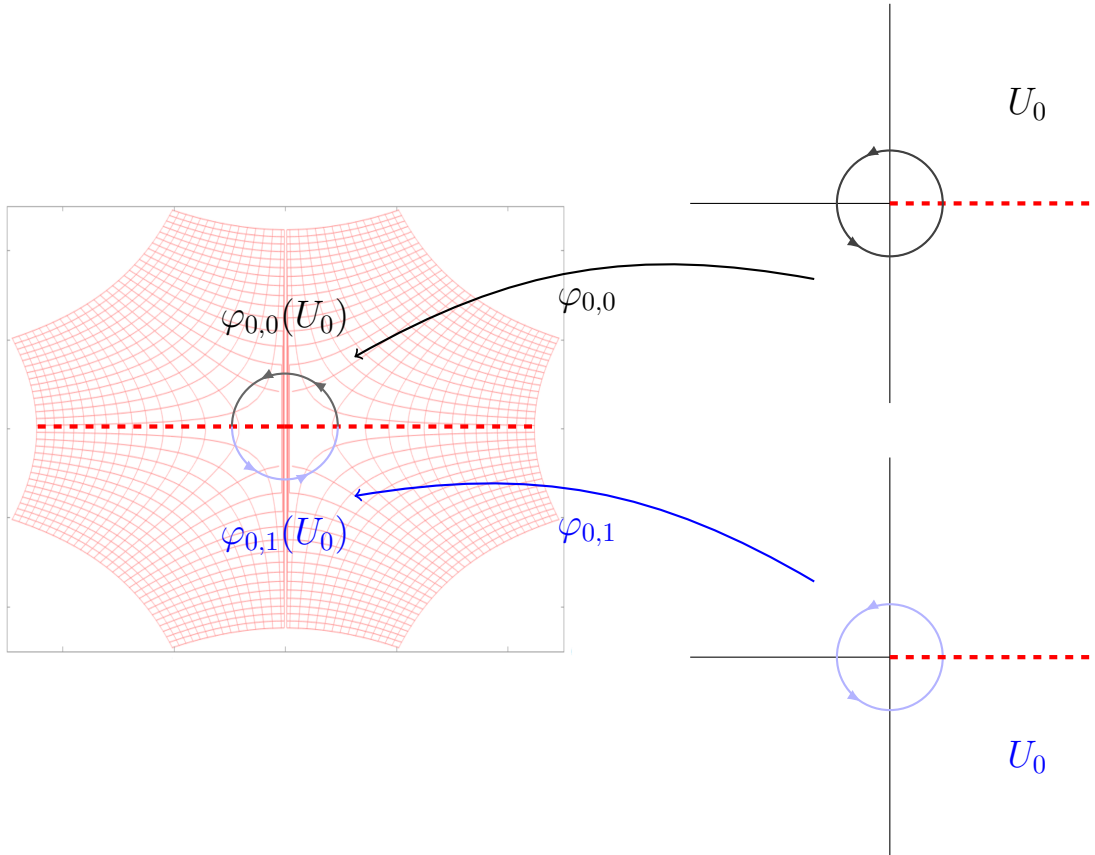


Fig. 3.20 Illustration of the GC atlas induced by the complex square root

the mapping $\bar{\varphi}|_{C_{2\pi d}\setminus\{0\}}$ has a C^∞ -regularity. We present in Figure 3.21 an illustration of the cone in the case $d=2$.

3.2.2.2.3 Definition and properties Now, we define the singularities of GC atlases. The definitions presented here are motivated by conical singularities of Euclidean surfaces [46].

Definition 3.25 (GC atlases with singularities). *Let M be a surface. The set of coordinate systems \mathcal{A} is called a GC atlas with singularities \mathcal{P} on M , with \mathcal{P} a finite set of isolated points, whenever \mathcal{A} is a GC atlas on $M \setminus \mathcal{P}$. The point $p \in \mathcal{P}$ is called a singularity point of \mathcal{A} whenever there is no local coordinate system $(\tilde{\Omega}, \tilde{\varphi})$ on M compatible with \mathcal{A} such that $p \in \tilde{\Omega}$. The GC atlases with singularities are also called generalized GC atlases.*

Let \mathcal{A} be a GC atlas with singularities \mathcal{P} on M . Let us remark from the definition that all the points in $M \setminus \mathcal{P}$ have a local coordinate system in \mathcal{A} in their neighborhood. We introduce in what follows a more restrictive definition which allows the coordinate systems of \mathcal{A} to be extended into a homeomorphism in the neighborhood of the singularity points. To fix a definition for these singularities, that will be called conical, we first make explicit the form of the coordinate systems in their neighborhood. This is the purpose of the following definitions.

Definition 3.26 (Conical net of valence n). *Let M be a surface, let $n \geq 1$ be an integer, and let \mathcal{A} be a GC atlas with singularity points \mathcal{P} on M . Let $\tilde{\Omega} \subset M$ be a neighborhood of $p \in \mathcal{P}$ and let $\bar{U} \subset C_\lambda$, with $\lambda = n\frac{\pi}{2}$, be a neighborhood of 0 in the cone C_λ . Assume that $\bar{\varphi}: \bar{U} \rightarrow \tilde{\Omega}$ is a homeomorphism such that $\bar{\varphi}(0) = p$. Then, the couple $(\tilde{\Omega}, \bar{\varphi})$ is called a conical coordinate system (or conical net) of valence n .*

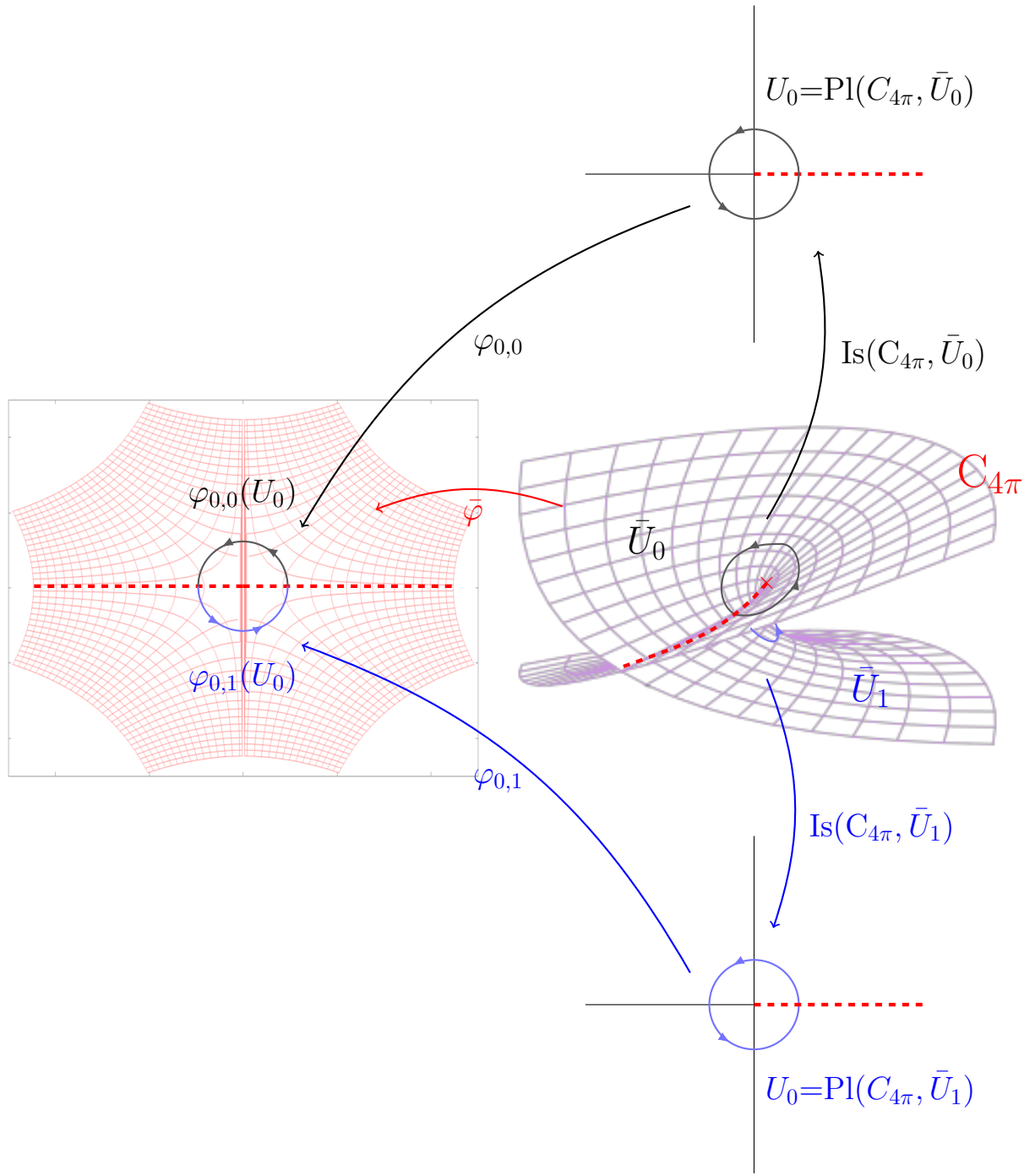


Fig. 3.21 Illustration of the mapping $\bar{\varphi}: C_{4\pi} \rightarrow \mathbb{C}$ defined from the square root

Definition 3.27 (Compatibility of conical nets). Let M be a surface and let \mathcal{A} be a GC atlas with singularity points \mathcal{P} . Let $\bar{\Omega} \subset M$ be a neighborhood of $p \in \mathcal{P}$ and let $(\bar{\Omega}, \bar{\varphi})$, with $\bar{\varphi}: \bar{U} \subset C_\lambda \rightarrow \bar{\Omega}$, be a conical net of valence $n \geq 1$, where $\lambda = n\frac{\pi}{2}$. For every branch-cut domain $\bar{V} \subset \bar{U}$, we denote $\Phi(\bar{\varphi}, \bar{V}): \text{Pl}(C_\lambda, \bar{V}) \rightarrow \bar{\varphi}(\bar{V})$ the mapping defined by

$$\Phi(\bar{\varphi}, \bar{V}) = \bar{\varphi} \circ \text{Is}(C_\lambda, \bar{V})^{-1}. \quad (3.8)$$

Let $(\Omega_i, \varphi_i) \in \mathcal{A}$ be such that $\bar{\Omega} \cap \Omega_i \neq \emptyset$ and such that $\bar{V}_i := \bar{\varphi}^{-1}(\bar{\Omega} \cap \Omega_i) \subset C_\lambda$ is a branch-cut domain. Then, the conical net $(\bar{\Omega}, \bar{\varphi})$ is said to be compatible with (Ω_i, φ_i) whenever the mapping

$\Phi(\bar{\varphi}, \bar{V}_i) : \text{Pl}(\mathbf{C}_\lambda, \bar{V}_i) \rightarrow \bar{\Omega} \cap \Omega_i$ is a diffeomorphism compatible with (Ω_i, φ_i) . The conical net $(\bar{\Omega}, \bar{\varphi})$ is said to be compatible with \mathcal{A} whenever it is compatible with all the coordinate systems in \mathcal{A} .

We present in Figure 3.21 a conical net $\bar{\varphi}$ of valence 8 compatible with two non-conical nets $\varphi_{0,0} := \Phi(\bar{\varphi}, \bar{U}_0)$, with $\bar{U}_0 \subset \mathbf{C}_{4\pi}$, and $\varphi_{0,1} := \Phi(\bar{\varphi}, \bar{U}_1)$, with $\bar{U}_1 \subset \mathbf{C}_{4\pi}$.

Remark 3.28 (Coordinate systems from branch-cut domains). Let \mathcal{A} be a GC atlas with singularities \mathcal{P} . Let $\bar{\Omega} \subset M$ be a neighborhood of $p \in \mathcal{P}$. Assume that $(\bar{\Omega}, \bar{\varphi})$ is a conical net of valence $n \geq 1$ compatible with \mathcal{A} . We set $\lambda = n\frac{\pi}{2}$ and $\bar{U} := \bar{\varphi}^{-1}(\bar{\Omega}) \subset \mathbf{C}_\lambda$. Let $\bar{V} \subset \bar{U}$ be a branch-cut domain of \mathbf{C}_λ . Then, we obtain from Definition 3.27 that $(\bar{\varphi}(\bar{V}), \Phi(\bar{\varphi}, \bar{V})) \in \mathcal{A}$ is a non-conical net.

In order to define in a unique manner the valence of a singularity point, we need the following justification:

Proposition 3.29 (Uniqueness of the valence of a singularity point). *Let M be a surface and let \mathcal{A} be a GC atlas with singularities \mathcal{P} . Assume that $(\bar{\Omega}_1, \bar{\varphi}_1)$ and $(\bar{\Omega}_2, \bar{\varphi}_2)$ are two conical nets of respective valence $n_1 \geq 1$ and $n_2 \geq 1$ in the neighborhood of $p \in \mathcal{P}$. Suppose moreover that the two conical nets are compatible with \mathcal{A} . Then, we have $n_1 = n_2$.*

Proof. We denote $\bar{\Omega} = \bar{\Omega}_1 \cap \bar{\Omega}_2$ and $\lambda_j = n_j \frac{\pi}{2}$, for all $j \in \{1, 2\}$. First, we obtain from Definition 3.26 that the conical net $\bar{\varphi}_j : \bar{U}_j \subset \mathbf{C}_{\lambda_j} \rightarrow \bar{\Omega}_j$ is a homeomorphism for all $j \in \{1, 2\}$. To prove the proposition, we show that the transition mapping

$$T := \bar{\varphi}_2^{-1} \circ \bar{\varphi}_1 : \bar{\varphi}_1^{-1}(\bar{\Omega}) \subset \mathbf{C}_{\lambda_1} \rightarrow \bar{\varphi}_2^{-1}(\bar{\Omega}) \subset \mathbf{C}_{\lambda_2} \quad (3.9)$$

is a global isometry. First, we have that T is an homeomorphism (composition of homeomorphisms). Then, let $(\Omega_\alpha, \varphi_\alpha) \in \mathcal{A}$ be a coordinate system such that $\Omega_\alpha \cap \bar{\Omega} \neq \emptyset$. Up to reducing Ω_α , we suppose that $\Omega_\alpha \cap \bar{\Omega}$ is connected and we suppose that $\bar{V}_j = \bar{\varphi}_j^{-1}(\bar{\Omega} \cap \Omega_\alpha)$ is a branch-cut domain, for all $j \in \{1, 2\}$. Let $j \in \{1, 2\}$. We denote $\Pi_j := \text{Is}(\mathbf{C}_{\lambda_j}, \bar{V}_j) : \bar{V}_j \rightarrow \text{Pl}(\mathbf{C}_{\lambda_j}, \bar{V}_j)$. Then, using the compatibility of $(\bar{\Omega}_j, \bar{\varphi}_j)$ with $(\Omega_\alpha, \varphi_\alpha)$, we have that $\Phi(\bar{\varphi}_j, \bar{V}_j) : \text{Pl}(\mathbf{C}_{\lambda_j}, \bar{V}_j) \rightarrow \bar{\varphi}_j(\bar{V}_j)$ satisfies

$$\Phi(\bar{\varphi}_j, \bar{V}_j) = \varphi_\alpha \circ L_j,$$

with $L_j : \mathbb{R}^2 \rightarrow \mathbb{R}^2$ a grid automorphism. Then, we infer that

$$\Phi(\bar{\varphi}_1, \bar{V}_1) = \varphi_\alpha \circ L_2 \circ L_2^{-1} \circ L_1 = \Phi(\bar{\varphi}_2, \bar{V}_2) \circ L_2^{-1} \circ L_1.$$

Using moreover (3.8), we obtain that

$$\bar{\varphi}_1 \circ \Pi_1^{-1} = \bar{\varphi}_2 \circ \Pi_2^{-1} \circ L_2^{-1} \circ L_1.$$

We conclude that the mapping $T|_{\bar{V}_1} : \bar{V}_1 \rightarrow \bar{V}_2$ satisfies

$$T|_{\bar{V}_1} = \Pi_2^{-1} \circ L_2^{-1} \circ L_1 \circ \Pi_1.$$

Therefore, the mapping $T|_{\bar{V}_1}$ is a global isometry (composition of global isometries). Using the definition of GC atlases with singularities, we obtain that there exists an open cover $\cup_{\alpha \in E} \Omega_\alpha$ of $\bar{\Omega}^* := \bar{\Omega} \setminus \{0\}$ such that there exists a coordinate system $(\Omega_\alpha, \varphi_\alpha) \in \mathcal{A}$ for all $\alpha \in E$. Hence, using that T is a homeomorphism, we obtain that the mapping $T|_{\bar{\varphi}_1^{-1}(\bar{\Omega}^*)} : \bar{\varphi}_1^{-1}(\bar{\Omega}^*) \rightarrow \bar{\varphi}_2^{-1}(\bar{\Omega}^*)$ is a global isometry. We conclude that T is a global isometry and the result follows. ■

Definition 3.30 (GC atlases with conical singularities). *Let M be a surface and let \mathcal{A}_1 be a GC atlas with singularities \mathcal{P} on M . A singularity point $p \in \mathcal{P}$ is called a conical singularity of valence $n \geq 1$ whenever there exists a neighborhood $\bar{\Omega} \subset M$ of p and a conical net $(\bar{\Omega}, \bar{\varphi})$ of valence n compatible with \mathcal{A}_1 . We call index of the conical singularity p the number*

$$\text{Ind}(p) = 1 - \frac{n}{4} = \frac{\delta}{2\pi},$$

where δ is the curvature at 0 of the cone $C_{n\frac{\pi}{2}}$ on which is defined the conical net $(\bar{\Omega}, \bar{\varphi})$. Moreover, supposing that all the points in \mathcal{P} are conical singularities, the set of coordinate systems $\mathcal{A} = \mathcal{A}_1 \cup \mathcal{A}_2$, with \mathcal{A}_2 the set of conical nets on the surface, is called a GC atlas with conical singularities. The GC atlases with conical singularities are supposed to be maximal for the inclusion.

Note that conical singularities are also called poles and saddle in the literature [4, 45]. Finally, we have that, whenever a GC atlas \mathcal{A}_1 with singularities can be extended at a singularity point, this point is a conical singularity of \mathcal{A}_1 . This result is stated in the following proposition proved in Section 3.4.3.

Proposition 3.31 (Extension into conical singularities). *Let M be a surface and let \mathcal{A}_1 be a GC atlas with singularities \mathcal{P} . Assume that, for all $p \in \mathcal{P}$, there exists a neighborhood $\bar{\Omega}_p$ of p and a finite open cover $\cup_{i=1}^N \Omega_i$ of $\bar{\Omega}_p^* := \bar{\Omega}_p \setminus \{p\}$. Moreover, for all $i \in \{1, \dots, N\}$, we suppose that Ω_i is geodesically convex and we suppose that there exists $(\Omega_i, \varphi_i) \in \mathcal{A}_1$ such that $\varphi_i^{-1} : \Omega_i \rightarrow U_i \subset \mathbb{R}^2$ is uniformly continuous. Then, there exists a GC atlas \mathcal{A} with conical singularities \mathcal{P} on M containing \mathcal{A}_1 .*

In the case where hypotheses of Proposition 3.31 are not satisfied, the main counter-example to this result is the following rosette singularity.

Example 3.32 (A rosette singularity). Let $\tau : \mathbb{R}^+ \times \mathbb{R} \rightarrow \mathbb{R}^2$ be the mapping defined by $\tau(u, v) = (u \cos(v), u \sin(v))$ and denote $N = \mathbb{R}^+ \times \mathbb{R}$, $N^* = \mathbb{R}_*^+ \times \mathbb{R}$, $M = \mathbb{R}^2$ and $M^* = \mathbb{R}_*^2$. Let $U_1 = \mathbb{R}_*^+ \times (-\pi, \frac{\pi}{2})$ and $U_2 = \mathbb{R}_*^+ \times (0, \frac{3\pi}{2})$. The two compatible coordinate systems $(\tau(U_1), \tau|_{U_1})$ and $(\tau(U_2), \tau|_{U_2})$ cover M^* . Hence, they induce a GC atlas on M^* denoted \mathcal{A} . Equivalently, \mathcal{A} is a GC atlas on M with one singularity at 0 (see Figure 3.22). Let D_h be the open disk of radius $h > 0$ centered at 0 and set $D_h^* := D_h \setminus \{0\}$. Then, we have

$$\tau|_{U_1}^{-1}(D_h^*) = (0, h) \times (-\pi, \frac{\pi}{2}), \quad \tau|_{U_2}^{-1}(D_h^*) = (0, h) \times (0, \frac{3\pi}{2}),$$

for all $h > 0$. We infer that the mapping $\tau|_{U_l}^{-1}$ is not uniformly continuous on U_l , for all $l \in \{1, 2\}$. Therefore, these mappings cannot be extended continuously at 0, so that the singularity point 0 is not a conical singularity. The GC atlas \mathcal{A} is presented in Figure 3.22.

Properties of Chebyshev globally compatible atlases with conical singularities

Let us first define Chebyshev GC atlases with conical singularities.

Definition 3.33 (Chebyshev GC atlases with conical singularities). *Let M be a surface. We call a Chebyshev GC atlas with conical singularities a GC atlas \mathcal{A} with conical singularities such*

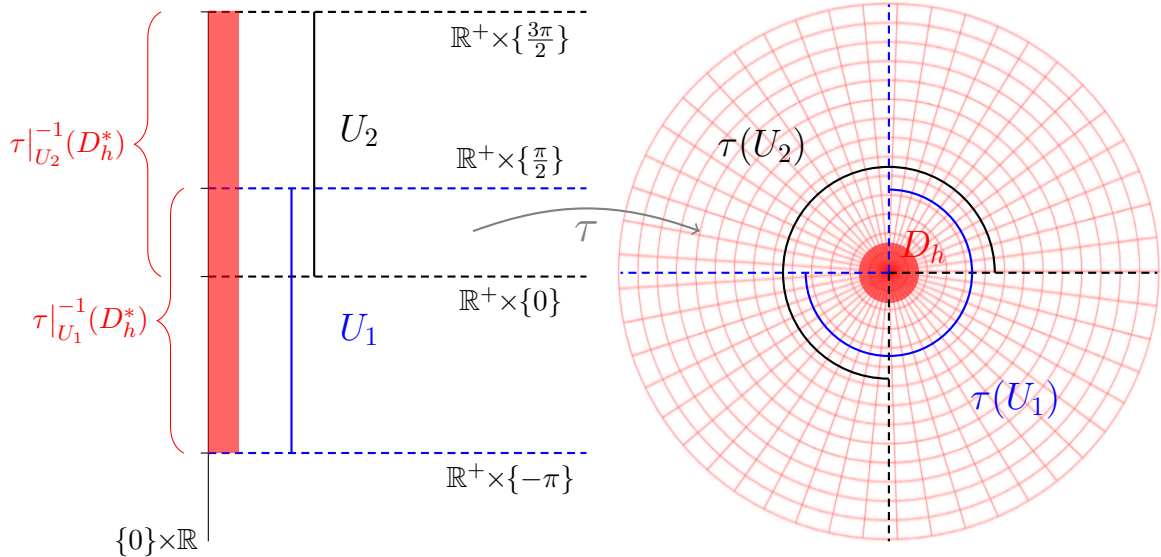


Fig. 3.22 A GC atlas with one singularity defined on \mathbb{R}^2
by the mapping τ of Example 3.32

that, for all non-conical net $(\Omega_i, \varphi_i) \in \mathcal{A}$, we have

$$|\partial_u \varphi|_g(u, v) = |\partial_v \varphi|_g(u, v) = 1,$$

for all $(u, v) \in \varphi_i^{-1}(\Omega_i)$.

In order to state properties of Chebyshev GC atlases, we need the following theorem proved in Chapter 4.

Theorem 3.34 (Existence of a unique solution to integrability condition). *Let M be a smooth, open, complete, and simply connected surface. Let $\eta_1 : [-L_1, 0] \rightarrow M$, with $L_1 \in \mathbb{R}_+^* \cup \{\infty\}$, and $\eta_2 : [0, L_2] \rightarrow M$, with $L_2 \in \mathbb{R}_+^* \cup \{\infty\}$, be two smooth curves with respective geodesic curvatures $\kappa_1 : [-L_1, 0] \rightarrow \mathbb{R}$ and $\kappa_2 : [0, L_2] \rightarrow \mathbb{R}$, and such that $\eta_1(0) = \eta_2(0)$. Suppose that $\psi := \angle(\eta'_1(0), \eta'_2(0)) \in (0, \pi)$. Then, there exists a unique angle distribution $\omega : D \rightarrow \mathbb{R}/2\pi\mathbb{Z}$, with $D = [0, L_2] \times [0, L_1]$, satisfying the Hazzidakis formula*

$$\omega(u, v) = \pi - \psi - \int_0^u \kappa_2 - \int_{-v}^0 \kappa_1 - \int_{\varphi([0, u] \times [0, v])} K, \quad (3.10)$$

with $\varphi : D \rightarrow M$ the unique smooth mapping satisfying the boundary conditions

$$\begin{aligned} \varphi(u, 0) &= \eta_2(u), & \forall u \in [0, L_2], \\ \varphi(0, v) &= \eta_1(-v), & \forall v \in [0, L_1], \end{aligned} \quad (3.11)$$

and such that its v -coordinate curves are arc-length parametrized curves with a geodesic curvature $\kappa_2^{\text{map}} : D \rightarrow \mathbb{R}$ satisfying $\kappa_2^{\text{map}}(u, v) = \partial_v \omega(u, v)$ for all $(u, v) \in D$.

Suppose moreover that there exists $\tilde{D} = [0, \tilde{L}_2] \times [0, \tilde{L}_1]$, with $\tilde{L}_1 \in (0, L_1]$ and $\tilde{L}_2 \in (0, L_2]$, such that $0 < \omega(u, v) < \pi$, for all $(u, v) \in \tilde{D}$. Then, the mapping φ satisfies

$$|\partial_u \varphi|_g(u, v) = |\partial_v \varphi|_g(u, v) = 1, \quad (3.12)$$

for all $(u, v) \in \tilde{D}$.

The Hazzidakis formula is illustrated in Figure 3.23. We deduce from Theorem 3.34 the following property satisfied by conical singularities of Chebyshev GC atlases.

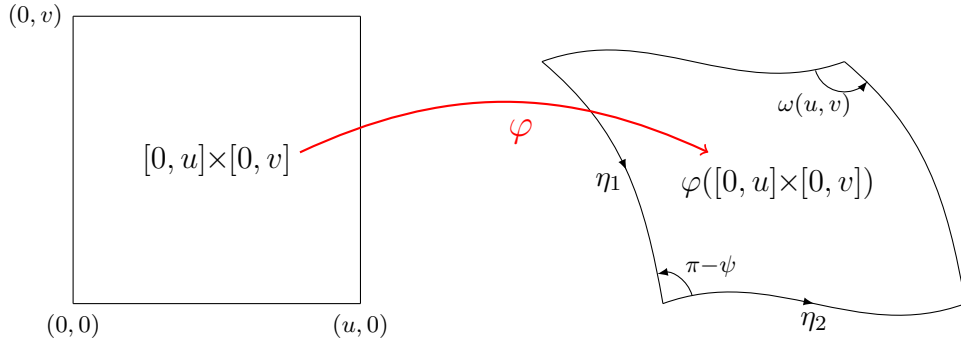


Fig. 3.23 Illustration of the Hazzidakis formula

Proposition 3.35 (Piecewise smoothness of conical singularities of Chebyshev GC atlases). *Let M be a surface and let \mathcal{A} be a Chebyshev GC atlas with conical singularities \mathcal{P} . Let $(\bar{\Omega}, \bar{\varphi}) \in \mathcal{A}$ be a conical net of valence $n \geq 1$ in the neighborhood of $p \in \mathcal{P}$. We set $\lambda = n\frac{\pi}{2}$ and $\bar{V} = \bar{\varphi}^{-1}(\bar{\Omega}) \subset C_\lambda$, with C_λ the cone of interior angle λ . Let $m \in \{0, \dots, n-1\}$. We define the set*

$$\bar{V}_{m,1} = \left\{ (r, \theta + m\frac{\pi}{2}) \in C_\lambda \mid 0 \leq r < h, 0 \leq \theta \leq \frac{\pi}{2} \right\}, \quad (3.13)$$

with $\theta + m\frac{\pi}{2}$ the addition modulo λ and $h > 0$ such that $\bar{V}_{m,1} \subset \bar{V}$. We set $\bar{V}_{m,1}^* := \bar{V}_{m,1} \setminus \{0\}$ and we suppose that $\bar{\varphi}|_{\bar{V}_{m,1}^*} : \bar{V}_{m,1}^* \rightarrow \bar{\varphi}(\bar{V}_{m,1}^*) \subset \bar{\Omega}$ is smooth. Then, the mapping $\bar{\varphi}|_{\bar{V}_{m,1}} : \bar{V}_{m,1} \rightarrow \bar{\varphi}(\bar{V}_{m,1}) \subset \bar{\Omega}$ is smooth.

We present in Figure 3.24 a conical net $\bar{\varphi} : \bar{V} \subset C_{4\pi} \rightarrow \bar{\varphi}(\bar{V}) \subset M$ of valence 8. The image by $\bar{\varphi}$ of the domains $\bar{V}_{m,1}$, with $m \in \{0, \dots, 7\}$, defined by (3.13) are delimited by the red curves in this figure.

Proof. Since $\bar{V}_{m,1}$ is not necessarily a branch-cut domain of C_λ (case $n=1$), we first define

$$\bar{\mathcal{O}}_{m,1} = \left\{ (r, \theta + m\frac{\pi}{2}) \in C_\lambda \mid 0 < r < h, 0 < \theta < \frac{\pi}{2} \right\} \subset \bar{V}_{m,1}.$$

Then, $\bar{\mathcal{O}}_{m,1}$ is a branch-cut domain and we set $\mathcal{O}_{m,1} := \text{Pl}(C_\lambda, \bar{\mathcal{O}}_{m,1}) \subset \mathbb{R}^2$ and, for the clarity of the proof, we suppose that $\mathcal{O}_{m,1} \subset (\mathbb{R}^+)^2$. Otherwise, the general case is reduced to that case by an application of the rotation of angle $-m\frac{\pi}{2}$ to $\mathcal{O}_{m,1}$. Then, we set $\varphi_{m,1} := \Phi(\bar{\varphi}, \bar{\mathcal{O}}_{m,1}) : \mathcal{O}_{m,1} \rightarrow \bar{\varphi}(\bar{\mathcal{O}}_{m,1})$. Let $L_1, L_2 > 0$ be such that $(0, L_2] \times (0, L_1] \subset \mathcal{O}_{m,1}$. We set $D = [0, L_2] \times [0, L_1]$ and we denote $\eta_1 : (-L_1, 0] \rightarrow M$ and $\eta_2 : [0, L_2) \rightarrow M$ the two smooth curves respectively defined by

$$\begin{aligned} \eta_1(v) &= \varphi_{m,1}(L_2, L_1 + v), & \text{for all } v \in (-L_1, 0], \\ \eta_2(u) &= \varphi_{m,1}(L_2 - u, L_1), & \text{for all } u \in [0, L_2]. \end{aligned} \quad (3.14)$$

See Figure 3.25a for an illustration of these curves. Using the smoothness of $\bar{\varphi}$ on $\bar{V}_{m,1}^*$, we extend smoothly η_1 at $-L_1$ and η_2 at L_2 , so that $\eta_1 : [-L_1, 0] \rightarrow M$ and $\eta_2 : [0, L_2] \rightarrow M$ are two smooth curves. Then, owing to Theorem 3.34, there exists a unique angle distribution

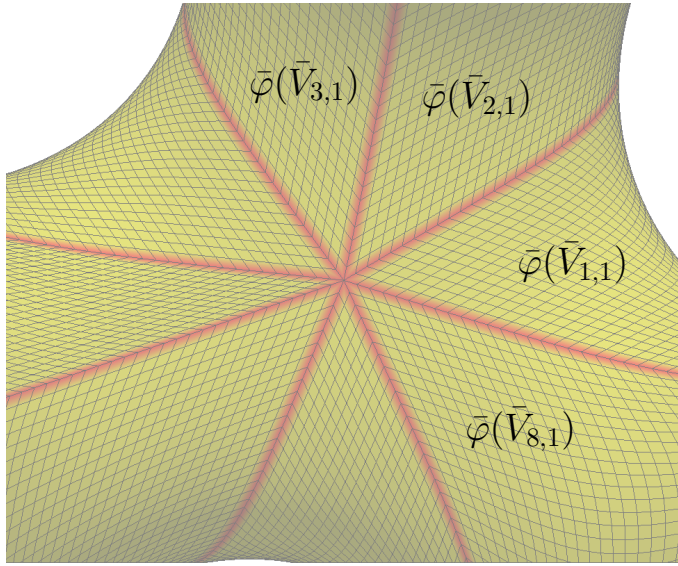


Fig. 3.24 A Chebyshev GC atlas with a conical singularity of valence 8 on Enneper's surface

$\omega: D \rightarrow \mathbb{R}/2\pi\mathbb{Z}$ satisfying the Hazzidakis formula (3.10), with $\varphi_0: D \rightarrow \varphi_0(D) \subset M$ the unique mapping satisfying the boundary conditions (3.11) and the properties presented in the theorem (see Figure 3.25b). Moreover, we remark that, since $\varphi_{m,1}$ is a Chebyshev net, the angle distribution $\omega|_{(0,L_2] \times (0,L_1]}: (0, L_2] \times (0, L_1] \rightarrow (0, \pi)$ defined by the angle between the coordinate curves of $\varphi_{m,1}$ on $(0, L_2] \times (0, L_1]$ satisfies the Hazzidakis formula. Hence, by uniqueness of the solution (Theorem 3.34), we obtain that $\varphi_0(L_2-u, L_1-v) = \varphi_{m,1}(u, v)$, for all $(u, v) \in (0, L_2] \times (0, L_1]$. We conclude that the mapping $\varphi_{m,1}$ has a smooth extension to D . Hence, the mapping $\bar{\varphi}|_{\bar{V}_{m,1}}$ is smooth. ■

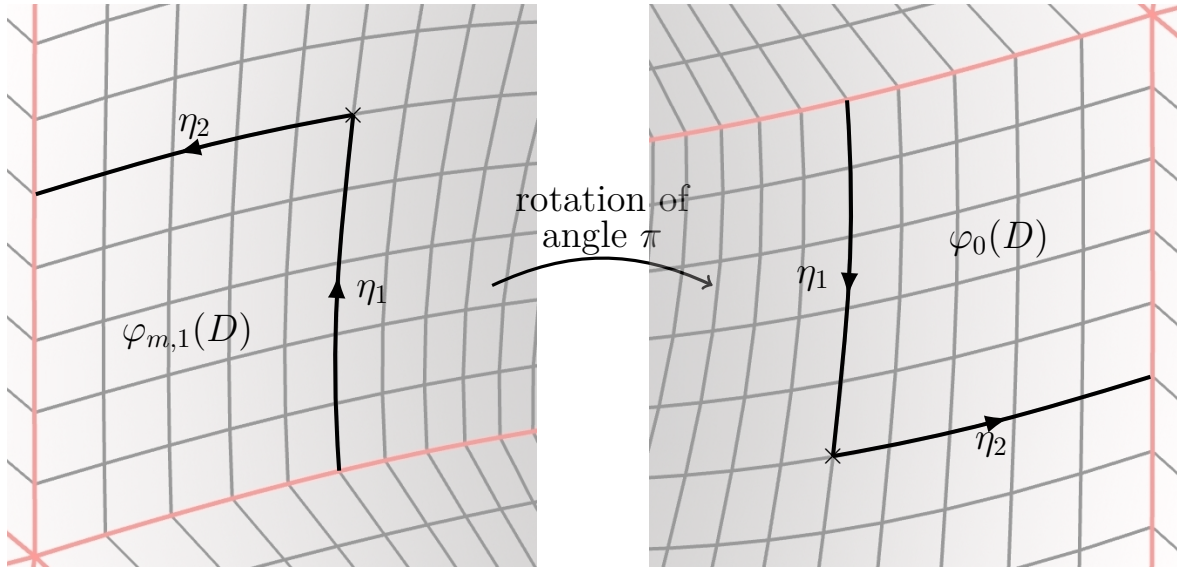


Fig. 3.25 Illustration of the proof of the smoothness of $\bar{\varphi}|_{\bar{V}_{m,1}}$ at 0

Remark 3.36 (Junction of smooth nets). Proposition 3.35 indicates that conical singularities of Chebyshev GC atlases can be obtained by junction of smooth Chebyshev nets $\varphi: B_e \rightarrow B_c \subset M$, where B_e is a polygon of \mathbb{R}^2 with right angles and $B_c = \varphi(B_e)$. This explains the construction outlined in Section 3.1.2.

We infer from Proposition 3.35 that Chebyshev nets with conical singularities are not smooth outside of the singularity points. This is stated in the following proposition:

Proposition 3.37 (Non-smoothness of Chebyshev GC atlases with conical singularities). *Let M be a surface and let \mathcal{A} be a Chebyshev GC atlas with conical singularities $\mathcal{P} \neq \emptyset$ on M . Then, there exists a non-conical net $(\Omega, \psi) \in \mathcal{A}$ such that ψ is not smooth.*

Proof. We prove the claim by contradiction. Thus, we suppose that all the non-conical nets are smooth. Let $p \in \mathcal{P}$ be a conical singularity of valence $n \neq 4$. Let $\lambda = n\frac{\pi}{2}$ and let $(\bar{\Omega}, \bar{\varphi}) \in \mathcal{A}$, with $\bar{\varphi}: \bar{U} \subset C_\lambda \rightarrow \bar{\Omega} \subset M$, be a conical net in the neighborhood of p . We infer from the smoothness of non-conical nets that $\bar{\varphi}$ is smooth on $\bar{U}^* := \bar{U} \setminus \{0\}$ (see Remark 3.28). Let $\alpha \in \{0, \dots, n-1\}$ and let $\bar{V}_{\alpha,1} \subset \bar{U}$ be the set defined by (3.13), with $h > 0$ small enough for the inclusion to hold true. Then, owing to Proposition 3.35, the mapping $\bar{\varphi}$ is smooth on $\bar{V}_{\alpha,1}$. Therefore, we define the two unit vectors

$$X_\alpha(x) = \frac{d}{dr} \bar{\varphi}(r, \alpha \frac{\pi}{2})|_{r=x}, \quad Y_\alpha(x) = \frac{d}{dr} \bar{\varphi}(r, \tilde{\alpha} \frac{\pi}{2})|_{r=x},$$

for all $x \in [0, h]$, with $\tilde{\alpha} = (\alpha + 1) \bmod n$ (see Figure 3.26a). Moreover, using the definition of

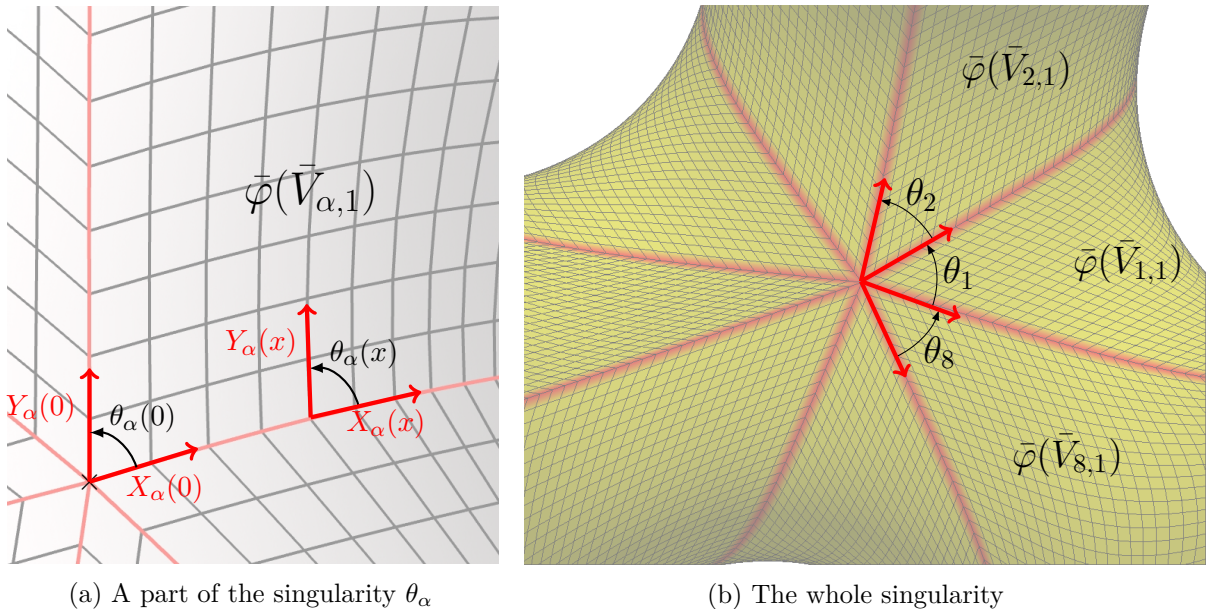


Fig. 3.26 Illustration of the angles $\{\theta_\alpha\}_{1 \leq \alpha \leq n}$ of a conical singularity (proof of Proposition 3.37)

compatible conical nets, we have that $\bar{\varphi}|_{\bar{U}^*}: \bar{U}^* \rightarrow \bar{\Omega}^*$ is a local diffeomorphism. We infer that we have $\angle(X_\alpha(x), Y_\alpha(x)) \in (0, \pi)$, for all $x \in (0, h)$. Hence, using the smoothness of $\bar{\varphi}|_{\bar{V}_{\alpha,1}}$ at 0, we define the smooth mapping $\theta_\alpha: [0, h] \rightarrow [0, \pi]$ by $\theta_\alpha(x) = \angle(X_\alpha(x), Y_\alpha(x))$ for all $x \in [0, h]$. Then, we have $\sum_{\alpha=0}^{n-1} \theta_\alpha(0) = 2\pi$ (see Figure 3.26b). Let us notice that the case $n=1$ yields a contradiction with $\theta_\alpha(0) \in [0, \pi]$, for all $\alpha \in \{0, \dots, n-1\}$. Hence, we can suppose that $n > 1$ in what follows. Moreover, since $n \neq 4$, there exists two consecutive integers $\alpha_0, \alpha_1 \in \{0, \dots, n-1\}$ (with the convention that 0 is after $n-1$ modulo n) such that

$$\theta_{\alpha_0}(0) + \theta_{\alpha_1}(0) \neq \pi. \tag{3.15}$$

Now, we define the open set

$$\bar{\mathcal{O}}_{\alpha_0,2} = \left\{ (r, \theta + \alpha_0 \frac{\pi}{2}) \in C_\lambda \mid 0 < r < h, 0 < \theta < \pi \right\} \subset \bar{U},$$

where $\theta + \alpha_0 \frac{\pi}{2}$ is the addition modulo λ and $h > 0$ is small enough for the inclusion to hold true. Using that $n > 1$, we infer that the open set $\bar{\mathcal{O}}_{\alpha_0,2}$ is a branch-cut domain of C_λ . Therefore, we set $\mathcal{O}_{\alpha_0,2} := P(C_\lambda, \bar{\mathcal{O}}_{\alpha_0,2})$ and $\varphi := \Phi(C_\lambda, \bar{\mathcal{O}}_{\alpha_0,2}) : \mathcal{O}_{\alpha_0,2} \rightarrow \bar{\varphi}(\bar{\mathcal{O}}_{\alpha_0,2}) \subset \bar{\Omega}$. For the clarity of the proof, we suppose that $\mathcal{O}_{\alpha_0,2} \subset \mathbb{R} \times \mathbb{R}^+$. Otherwise, the general case is reduced to that case by an application of the rotation of angle $-\alpha_0 \frac{\pi}{2}$ to $\mathcal{O}_{\alpha_0,2}$. Then, by hypothesis, φ is smooth and we have

$$\begin{aligned}\theta_{\alpha_0}(v) + \theta_{\alpha_1}(v) &= \angle(\partial_u \varphi, \partial_v \varphi)(0, v) + \angle(\partial_v \varphi, -\partial_u \varphi)(0, v) \\ &= \angle(\partial_u \varphi, -\partial_u \varphi)(0, v) = \pi,\end{aligned}$$

for all $v \in (0, h)$. Using the smoothness of θ_{α_0} and θ_{α_1} on $[0, h]$, we conclude that $\theta_{\alpha_0}(0) + \theta_{\alpha_1}(0) = \pi$. This contradicts (3.15), so that the claim follows. ■

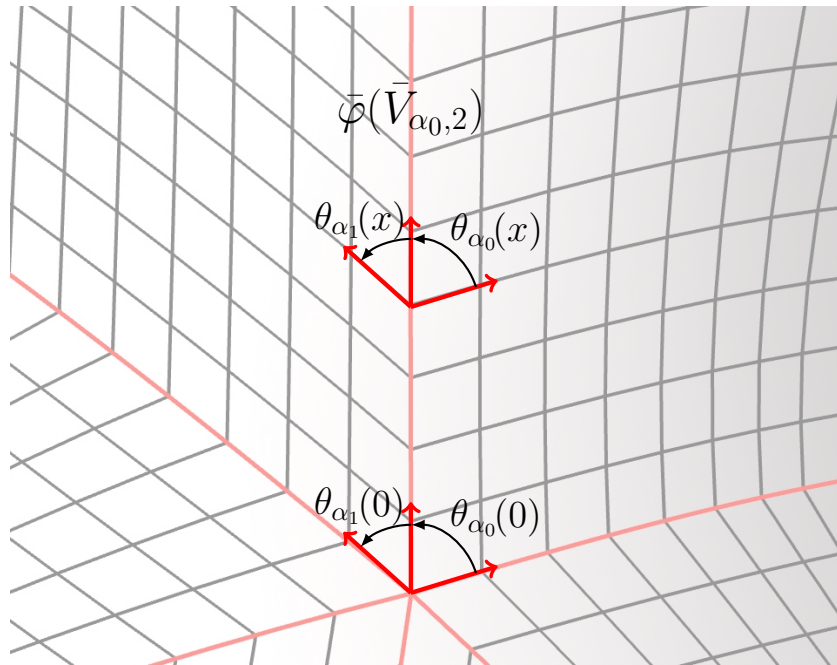


Fig. 3.27 Illustration of $\bar{\varphi}(\bar{V}_{\alpha_0,2})$ (proof of Proposition 3.37)

Some technical results

From globally compatible atlases to local homeomorphisms

We construct in this section a local homeomorphism $\psi : M \rightarrow \psi(M) \subset \mathbb{R}^2$ on any simply connected surface M equipped with a GC atlas \mathcal{A} . Before this, we define homotopies of curves.

Definition 3.38 (Homotopic curves). *Let $\Omega \subset M$ and let $\gamma_1 : [0, 1] \rightarrow \Omega$ and $\gamma_2 : [0, 1] \rightarrow \Omega$ be two continuous curves such that $\gamma_1(0) = \gamma_2(0)$ and $\gamma_1(1) = \gamma_2(1)$. A continuous mapping $H : [0, 1]^2 \rightarrow \Omega$ is called a homotopy whenever it satisfies*

$$\begin{aligned}H(0, t) &= \gamma_1(t), & H(1, t) &= \gamma_2(t), \\ H(t, 0) &= \gamma_1(0) = \gamma_2(0), & H(t, 1) &= \gamma_1(1) = \gamma_2(1),\end{aligned}$$

for all $t \in [0, 1]$, and the curves γ_1 and γ_2 are said to be homotopic in Ω .

To construct the mapping ψ , we join the domains in \mathbb{R}^2 associated with all the coordinate systems in \mathcal{A} . To this purpose, we define the total transition mapping as follows:

Definition 3.39 (Total transition mapping along γ). *Let M be a surface, let \mathcal{A} be a GC atlas on M and let $\gamma:[0, 1] \rightarrow M$ be a continuous curve. Let $0=t_0 < \dots < t_N=1$ and $\{\Omega_i\}_{1 \leq i \leq N}$, with $N \geq 2$, be such that $\gamma_i := \gamma|_{[t_{i-1}, t_i]} : [t_{i-1}, t_i] \rightarrow \Omega_i$, for all $i \in \{1, \dots, N\}$, and such that there exist coordinate systems $\{(\Omega_i, \varphi_i)\}_{1 \leq i \leq N} \subset \mathcal{A}$. We denote $U_i = \varphi_i^{-1}(\Omega_i)$, for all $i \in \{1, \dots, N\}$, and we denote $T_j : \mathbb{R}^2 \rightarrow \mathbb{R}^2$ the grid automorphism associated with the transition mapping $\varphi_{j+1}^{-1} \circ \varphi_j$ at $\gamma(t_j)$, for all $j \in \{1, \dots, N-1\}$. We call total transition mapping along γ and we denote $F_{\Omega_N, \gamma} : \mathbb{R}^2 \rightarrow \mathbb{R}^2$ the mapping defined by*

$$F_{\Omega_N, \gamma} := T_{N-1} \circ \dots \circ T_1 : U_1 \rightarrow U_N. \quad (3.16)$$

The construction of the total transition mapping along a curve $\gamma : [0, 1] \rightarrow M$ is illustrated in Figure 3.28.

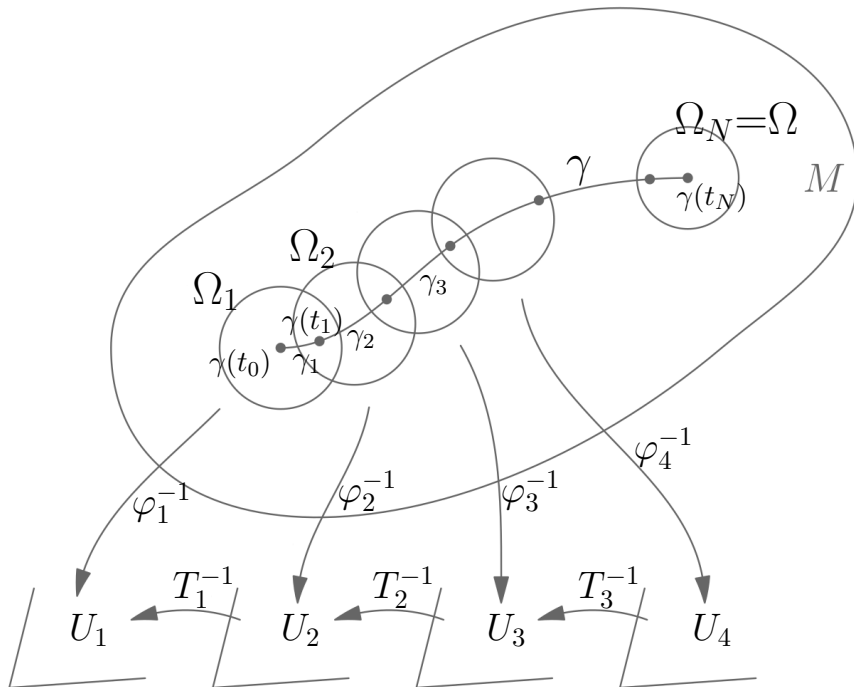


Fig. 3.28 Illustration of the total transition mapping [47]

Remark 3.40 (Notation of the total transition mapping). We state in the following lemma that the total transition mapping only depends on γ and on the first and the last coordinate systems of the cover of γ , denoted respectively $(\Omega_1, \varphi_1) \in \mathcal{A}$ and $(\Omega_N, \varphi_N) \in \mathcal{A}$, with $N \geq 2$, in the definition. Moreover, we fix in the sequel the coordinate system (Ω_1, φ_1) , so that this mapping only depends on γ and on (Ω_N, φ_N) . To simplify the notation, we only mention γ and Ω_N , its associated coordinate system being implicit, so that the total transition mapping along γ is denoted $F_{\Omega_N, \gamma}$.

Lemma 3.41 (Total transition mapping). *Let M be a surface, let \mathcal{A} be a GC atlas on M and let $\gamma : [0, 1] \rightarrow M$ be a continuous curve. Let $0=t_0 < \dots < t_N=1$ and $\{\Omega_i\}_{1 \leq i \leq N}$, with $N \geq 2$, be such that $\gamma_i := \gamma|_{[t_{i-1}, t_i]} : [t_{i-1}, t_i] \rightarrow \Omega_i$, for all $i \in \{1, \dots, N\}$, and such that there exist coordinate systems $\{(\Omega_i, \varphi_i)\}_{1 \leq i \leq N} \subset \mathcal{A}$. We denote $U_i = \varphi_i^{-1}(\Omega_i)$, for all $i \in \{1, \dots, N\}$, and we denote*

$T_j : \mathbb{R}^2 \rightarrow \mathbb{R}^2$ the grid automorphism associated with the transition mapping $\varphi_{j+1}^{-1} \circ \varphi_j$ at $\gamma(t_j)$, for all $j \in \{1, \dots, N-1\}$. Then, whenever $N > 2$, the total transition mapping $F_{\Omega_N, \gamma}$ defined by (3.16) is independent of the open cover $\{\Omega_i\}_{2 \leq i \leq N-1}$ of γ . Moreover, $F_{\Omega_N, \gamma}$ is invariant by homotopy in M with respect to γ .

Proof. Let $\{\tilde{\Omega}_\alpha\}_{1 \leq \alpha \leq \tilde{N}}$, with $\tilde{N} \geq 2$, be another open cover of γ such that $\{\tilde{\Omega}_\alpha, \tilde{\varphi}_\alpha\}_{1 \leq \alpha \leq \tilde{N}} \subset \mathcal{A}$, $(\tilde{\Omega}_1, \tilde{\varphi}_1) = (\Omega_1, \varphi_1)$ and $(\tilde{\Omega}_{\tilde{N}}, \tilde{\varphi}_{\tilde{N}}) = (\Omega_N, \varphi_N)$. Then, there exist $0 = s_0 < \dots < s_{\tilde{N}} = 1$ such that

$$\eta_\alpha := \gamma|_{[s_{\alpha-1}, s_\alpha]} : [s_{\alpha-1}, s_\alpha] \rightarrow \tilde{\Omega}_\alpha.$$

To avoid technicalities, whenever $N > 2$ and $\tilde{N} > 2$, we suppose that $s_\alpha \neq t_i$ for all $i \in \{2, \dots, N-1\}$ and $\alpha \in \{2, \dots, \tilde{N}-1\}$. Then, for all $\alpha \in \{1, \dots, \tilde{N}-1\}$, we denote $\tilde{T}_\alpha : \mathbb{R}^2 \rightarrow \mathbb{R}^2$ the grid automorphism associated with the transition mapping $\tilde{\varphi}_{\alpha+1}^{-1} \circ \tilde{\varphi}_\alpha$ at $\gamma(s_\alpha)$. Moreover, we define the mapping $\tilde{F}_{\Omega_N, \gamma} := \tilde{T}_{\tilde{N}-1} \circ \dots \circ \tilde{T}_1 : \mathbb{R}^2 \rightarrow \mathbb{R}^2$. We notice that there exists $1 = n_1 \leq \dots \leq n_{\tilde{N}+1} = N$ such that we have, for all $\alpha \in \{1, \dots, \tilde{N}\}$,

$$\eta_\alpha([s_{\alpha-1}, s_\alpha]) = \bigcup_{l=n_\alpha}^{n_{\alpha+1}} \eta_{\alpha,l}([0, 1]),$$

with $\eta_{\alpha,l} : [0, 1] \rightarrow \gamma_l([t_{l-1}, t_l])$ a portion of the curve γ_l , for all $l \in \{n_\alpha, \dots, n_{\alpha+1}\}$. We depict the notation in Figure 3.29. For all $\alpha \in \{1, \dots, \tilde{N}\}$ and $l \in \{n_\alpha, \dots, n_{\alpha+1}\}$, we denote $\tilde{T}_{l,\alpha} : \mathbb{R}^2 \rightarrow \mathbb{R}^2$ and $T_{\alpha,l} : \mathbb{R}^2 \rightarrow \mathbb{R}^2$ the grid automorphisms respectively associated with the transition mappings $\tilde{\varphi}_\alpha^{-1} \circ \varphi_l$ and $\varphi_l^{-1} \circ \tilde{\varphi}_\alpha$ at $\eta_{\alpha,l}(0)$. It is clear that all these mappings satisfy $T_{l,\alpha}^{-1} = T_{\alpha,l}$.

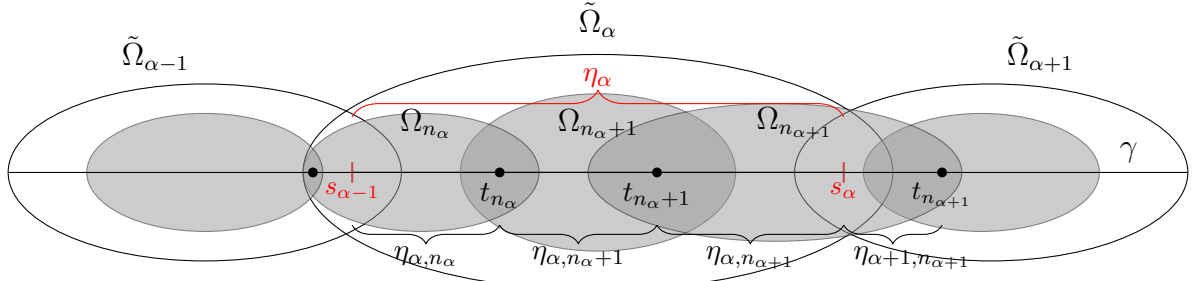


Fig. 3.29 Illustration of the open covers $\{\Omega_i\}_{1 \leq i \leq N}$ and $\{\tilde{\Omega}_\alpha\}_{1 \leq \alpha \leq \tilde{N}}$
($n_{\alpha+1} = n_\alpha + 2$)

Let $\alpha \in \{1, \dots, \tilde{N}\}$ and suppose first that $n_\alpha < n_{\alpha+1}$. Let $l \in \{n_\alpha, \dots, n_{\alpha+1}-1\}$. Since $\eta_{\alpha,l}([0, 1]) \subset \tilde{\Omega}_\alpha \cap \Omega_l$, we have that $\eta_{\alpha,l}(0)$ and $\eta_{\alpha,l}(1)$ are in the same connected component of $\tilde{\Omega}_\alpha \cap \Omega_l$ denoted \mathcal{U} . For all x in the connected component of $\varphi_l^{-1}(\eta_{\alpha,l}(1))$ in $\varphi_l^{-1}(\mathcal{U} \cap \Omega_{l+1})$, we have

$$T_l(x) = \varphi_{l+1}^{-1} \circ \varphi_l(x) = \varphi_{l+1}^{-1} \circ \tilde{\varphi}_\alpha \circ \tilde{\varphi}_\alpha^{-1} \circ \varphi_l(x) = T_{\alpha,l+1} \circ \tilde{T}_{l,\alpha}(x).$$

Hence, we obtain that

$$\begin{aligned} T_{n_{\alpha+1}-1} \circ \dots \circ T_{n_\alpha} &= (T_{\alpha,n_{\alpha+1}} \circ \tilde{T}_{n_{\alpha+1}-1,\alpha}) \circ \dots \circ (T_{\alpha,n_{\alpha+1}} \circ \tilde{T}_{n_\alpha,\alpha}) \\ &= T_{\alpha,n_{\alpha+1}} \circ \tilde{T}_{n_\alpha,\alpha}. \end{aligned} \tag{3.17}$$

Moreover, in the case where $\alpha \in \{1, \dots, \tilde{N}\}$ is such that $n_\alpha = n_{\alpha+1}$, we denote $T_{n_{\alpha+1}-1} \circ \dots \circ T_{n_\alpha}$ the identity and (3.17) is trivially satisfied.

Now, we suppose that $\alpha \in \{1, \dots, \tilde{N}-1\}$. As above, we notice that $\eta_{\alpha, n_{\alpha+1}}(0)$ and $\eta_{\alpha, n_{\alpha+1}}(1) = \gamma(s_\alpha)$ are in the same connected component of $\tilde{\Omega}_\alpha \cap \Omega_{n_{\alpha+1}}$ that we denote \mathcal{O} . Hence, for all x in the connected component of $\tilde{\varphi}_\alpha^{-1}(\gamma(s_\alpha))$ in $\tilde{\varphi}_\alpha^{-1}(\tilde{\Omega}_{\alpha+1} \cap \mathcal{O})$, we have

$$\begin{aligned}\tilde{T}_{n_{\alpha+1}, \alpha+1} \circ T_{\alpha, n_{\alpha+1}}(x) &= \tilde{\varphi}_{\alpha+1}^{-1} \circ \varphi_{n_{\alpha+1}} \circ \varphi_{n_{\alpha+1}}^{-1} \circ \tilde{\varphi}_\alpha(x) \\ &= \tilde{\varphi}_{\alpha+1}^{-1} \circ \tilde{\varphi}_\alpha(x) = \tilde{T}_\alpha(x).\end{aligned}\quad (3.18)$$

From (3.17), we infer that

$$\begin{aligned}F_{\Omega_N, \gamma} &= T_{N-1} \circ \dots \circ T_1 = (T_{n_{\tilde{N}+1}-1} \circ \dots \circ T_{n_{\tilde{N}}}) \circ \dots \circ (T_{n_2-1} \circ \dots \circ T_{n_1}) \\ &= (T_{\tilde{N}, n_{\tilde{N}+1}} \circ \tilde{T}_{n_{\tilde{N}}, \tilde{N}}) \circ \dots \circ (T_{1, n_2} \circ \tilde{T}_{n_1, 1}) \\ &= T_{\tilde{N}, n_{\tilde{N}+1}} \circ (\tilde{T}_{n_{\tilde{N}}, \tilde{N}} \circ T_{\tilde{N}-1, n_{\tilde{N}}}) \circ \dots \circ (\tilde{T}_{n_2, 2} \circ T_{1, n_2}) \circ \tilde{T}_{n_1, 1}.\end{aligned}\quad (3.19)$$

Hence, from (3.18) and (3.19), we obtain that

$$F_{\Omega_N, \gamma} = T_{\tilde{N}, n_{\tilde{N}+1}} \circ \tilde{T}_{\tilde{N}-1} \circ \dots \circ \tilde{T}_1 \circ \tilde{T}_{n_1, 1} = T_{\tilde{N}, n_{\tilde{N}+1}} \circ \tilde{F}_{\Omega_{\tilde{N}}, \gamma} \circ \tilde{T}_{n_1, 1}.$$

Using that $(\Omega_1, \varphi_1) = (\tilde{\Omega}_1, \tilde{\varphi}_1)$ and $(\Omega_N, \varphi_N) = (\tilde{\Omega}_{\tilde{N}}, \tilde{\varphi}_{\tilde{N}})$, we conclude that $F_{\Omega_N, \gamma} = \tilde{F}_{\Omega_N, \gamma}$. Therefore, $F_{\Omega_N, \gamma}$ is independent of the cover $\{\Omega_i\}_{2 \leq i \leq N-1}$ of γ . Finally, since $\{\Omega_i\}_{1 \leq i \leq N}$ are open sets, we obtain that there exists an open set $\Gamma \subset M$ in the neighborhood of γ such that $F_{\Omega_N, \gamma}$ is invariant by homotopy in Γ . Since \mathcal{A} covers M , we conclude that $F_{\Omega_N, \gamma}$ is invariant by homotopy in M . ■

Let $(\Omega_1, \varphi_1) \in \mathcal{A}$. Using the simple connectedness of M , we associate with every coordinate system $(\Omega_\alpha, \varphi_\alpha) \in \mathcal{A}$, such that Ω_α is an arcwise connected open set, the total transition mapping $F_{\Omega_\alpha, \gamma_\alpha}: \mathbb{R}^2 \rightarrow \mathbb{R}^2$, where $\gamma_\alpha: [0, 1] \rightarrow M$ is a curve such that $\gamma_\alpha(0) = g \in \Omega_1$ and $\gamma_\alpha(1) = q \in \Omega_\alpha$. This mapping, independent of the curve γ_α and of $q \in \Omega_\alpha$, is denoted F_{Ω_α} in what follows.

Proposition 3.42 (Existence of a local homeomorphism). *Let M be a simply connected surface and let \mathcal{A} be a GC atlas on M . Then, there exists a local homeomorphism $\psi: M \rightarrow \psi(M) \subset \mathbb{R}^2$ such that, for all $(\Omega_\alpha, \varphi_\alpha) \in \mathcal{A}$ with $\Omega_\alpha \subset M$ an arcwise connected open set, the mapping $\psi|_{\Omega_\alpha}: \Omega_\alpha \rightarrow \psi(\Omega_\alpha)$ is a homeomorphism and $(\Omega_\alpha, \psi|_{\Omega_\alpha}^{-1}) \in \mathcal{A}$.*

Proof. Let $(\Omega_\alpha, \varphi_\alpha) \in \mathcal{A}$ and $(\Omega_\beta, \varphi_\beta) \in \mathcal{A}$ be such that $\Omega_\alpha \cap \Omega_\beta \neq \emptyset$ and let $\bar{q} \in \Omega_\alpha \cap \Omega_\beta$. Let $\gamma: [0, 1] \rightarrow M$ be a curve such that $\gamma(0) = g \in \Omega_1$ and $\gamma(1) = \bar{q}$. We denote $T: \mathbb{R}^2 \rightarrow \mathbb{R}^2$ the grid automorphism associated with the transition mapping $\varphi_\beta^{-1} \circ \varphi_\alpha$ at \bar{q} . Then, we infer from (3.16) that $F_{\Omega_\beta, \gamma} = T \circ F_{\Omega_\alpha, \gamma}$ and we conclude that $F_{\Omega_\beta} = T \circ F_{\Omega_\alpha}$. Hence, we have

$$\begin{aligned}F_{\Omega_\beta}^{-1} \circ \varphi_\beta^{-1}(\bar{q}) &= F_{\Omega_\alpha}^{-1} \circ T^{-1} \circ \varphi_\beta^{-1}(\bar{q}) = F_{\Omega_\alpha}^{-1} \circ \varphi_\alpha^{-1} \circ \varphi_\beta \circ \varphi_\beta^{-1}(\bar{q}) \\ &= F_{\Omega_\alpha}^{-1} \circ \varphi_\alpha^{-1}(\bar{q}).\end{aligned}$$

We denote $\psi: M \rightarrow \psi(M) \subset \mathbb{R}^2$ the mapping defined by

$$\psi(q) = F_{\Omega_\alpha}^{-1} \circ \varphi_\alpha^{-1}(q), \text{ whenever } q \in \Omega_\alpha \text{ for } (\Omega_\alpha, \varphi_\alpha) \in \mathcal{A},$$

for all $q \in M$. Then, assume that $(\Omega_\alpha, \varphi_\alpha) \in \mathcal{A}$ is such that $\Omega_\alpha \subset M$ is an arcwise connected open set. The mapping $\psi|_{\Omega_\alpha}: \Omega_\alpha \rightarrow \psi(\Omega_\alpha) \subset \mathbb{R}^2$ is clearly a homeomorphism and, since F_{Ω_α} is a grid

automorphism, the mapping $\psi|_{\Omega_\alpha}^{-1}: \psi(\Omega_\alpha) \rightarrow \Omega_\alpha$ is compatible with \mathcal{A} . Since \mathcal{A} is maximal, the claim follows. ■

Proof of Proposition 3.15

Now, we present conditions ensuring that the local homeomorphism $\psi: M \rightarrow \psi(M) \subset \mathbb{R}^2$ constructed in Section 3.4.1 is a homeomorphism. The aim of the following proposition is to rule out the counter-example presented in Figure 3.11 by ensuring that $\psi(M) = \mathbb{R}^2$.

Proposition 3.43 (Existence of a global coordinate system). *Let M be a complete, simply connected surface and let \mathcal{A} be a GC atlas on M . Suppose that there exists $C > 0$ such that for all $(\Omega, \varphi) \in \mathcal{A}$,*

$$\sup_{y \in \varphi^{-1}(\Omega)} |\mathrm{d}\varphi_y(X)|_g^2 \leq C|X|^2, \quad \forall X \in \mathbb{R}^2, \quad (3.20)$$

with $\mathrm{d}\varphi_y: \mathbb{R}^2 \rightarrow T_{\varphi(y)}M$ the differential of φ at $y \in \varphi^{-1}(\Omega)$. Then, there exists a global coordinate system $(M, \tilde{\varphi}) \in \mathcal{A}$.

Proof. Owing to Proposition 3.42, there exists a local homeomorphism $\psi: M \rightarrow \psi(M) \subset \mathbb{R}^2$. Moreover, supposing that ψ is a homeomorphism, we have that the mapping ψ^{-1} is compatible with \mathcal{A} . Hence, we only have to show that ψ is a homeomorphism to prove the claim. We pullback by ψ the Euclidean metric g_E to obtain a flat metric on M denoted $\tilde{g} := \psi^*g_E$. In order to show that ψ is a covering mapping (see Definition 3.17), we prove that the surface (M, \tilde{g}) is a geodesically complete surface. Let $q \in M$, let $Y \in T_q M$ and let $(\Omega, \varphi) \in \mathcal{A}$, with $\Omega \subset M$ a connected open set, be a coordinate system in the neighborhood of q . We set $X := \mathrm{d}(\varphi^{-1})_q(Y) \in \mathbb{R}^2$. Then, using hypothesis (3.20), we obtain that

$$|X|^2 \geq \frac{1}{C} |\mathrm{d}\varphi_{\varphi^{-1}(q)}(X)|_g^2 = \frac{1}{C} |Y|_g^2. \quad (3.21)$$

Moreover, owing to Proposition 3.42, the mapping $\psi|_{\Omega}: \Omega \rightarrow \psi(\Omega) \subset \mathbb{R}^2$ is a homeomorphism and $(\Omega, \psi|_{\Omega}^{-1})$ is compatible with (Ω, φ) . Hence, we have that $F := \psi \circ \varphi: \varphi^{-1}(\Omega) \rightarrow \psi(\Omega)$ is an isometry of \mathbb{R}^2 . We infer that

$$|\mathrm{d}\psi_q(Y)|^2 = |\mathrm{d}\psi_q \circ \mathrm{d}\varphi_{\varphi^{-1}(q)}(X)|^2 = |\mathrm{d}F_{\varphi^{-1}(q)}(X)|^2 = |X|^2. \quad (3.22)$$

Using (3.21) and (3.22), we obtain that

$$|Y|_{\tilde{g}}^2 = |\mathrm{d}\psi_q(Y)|^2 \geq \frac{1}{C} |Y|_g^2.$$

Since (M, g) is a geodesically complete surface, we conclude that (M, \tilde{g}) is also geodesically complete.

The metric \tilde{g} has been constructed such that the mapping $\psi: (M, \tilde{g}) \rightarrow (\psi(M), g_E)$ is a local isometry. Then, using [22, prop. 2.106], we conclude that the mapping ψ is a covering mapping. Moreover, $\psi(M)$ is clearly a complete subset of \mathbb{R}^2 , and, since ψ is an open mapping, $\psi(M)$ is open. Hence, we have $\psi(M) = \mathbb{R}^2$ and, since \mathbb{R}^2 is simply connected, we infer that ψ is a homeomorphism [36, cor. 11.33]. This concludes the proof. ■

Proof of Proposition 3.31

Let M be a surface and let \mathcal{A}_1 be a GC atlas on M with singularities \mathcal{P} . Under the conditions of Proposition 3.31, we construct in the sequel a conical net compatible with \mathcal{A}_1 in some neighborhood $\bar{\mathcal{B}}_p$ of a singularity point $p \in \mathcal{P}$. First, let us fix some notation. We denote d_M the distance in M and d_E the Euclidean distance in \mathbb{R}^2 . We denote $B_M(p, h) \subset M$ the open ball centered at p with radius $h > 0$ and $B_\lambda(0, h) \subset C_\lambda$, with $\lambda > 0$, the open ball centered at the origin with radius h . For any set $\Omega \subset M$, we denote $\text{cl}_M(\Omega)$ its closure in M .

Lemma 3.44 (Construction of a mapping from $\bar{\mathcal{B}}_p$ to a cone). *Let M be a surface, let \mathcal{A}_1 be a GC atlas on M with singularities \mathcal{P} and let $p \in \mathcal{P}$. Assume that there exists a neighborhood $\bar{\Omega}_p \subset M$ of p such that there exists a finite open cover $\cup_{i=1}^N \Omega_i$ of $\bar{\Omega}_p^* := \bar{\Omega}_p \setminus \{p\}$. Moreover, for all $i \in \{1, \dots, N\}$, we suppose that Ω_i is geodesically convex and we suppose that there exists $(\Omega_i, \varphi_i) \in \mathcal{A}_1$ such that $\varphi_i^{-1} : \Omega_i \rightarrow U_i \subset \mathbb{R}^2$ is uniformly continuous. Then, there exists $\lambda = k \frac{\pi}{2}$, with $k \geq 1$ an integer, an open ball $\bar{\mathcal{B}}_p := B_M(p, h_0) \subset \bar{\Omega}_p$, with $h_0 > 0$, and a continuous mapping $\psi_{\text{cone}} : \bar{\mathcal{B}}_p \rightarrow \psi_{\text{cone}}(\bar{\mathcal{B}}_p) \subset C_\lambda$ such that $\psi_{\text{cone}}(p) = 0$ and such that:*

1. the mapping $\psi_{\text{cone}}|_{\bar{\mathcal{B}}_p^*} : \bar{\mathcal{B}}_p^* \rightarrow \psi_{\text{cone}}(\bar{\mathcal{B}}_p^*) \subset C_\lambda$, with $\bar{\mathcal{B}}_p^* := \bar{\mathcal{B}}_p \setminus \{p\}$, is a local homeomorphism;
2. for all $h \in (0, h_0]$, there exists $l > 0$ such that

$$\psi_{\text{cone}}^{-1}(B_\lambda(0, l)) \subset B_M(p, h); \quad (3.23)$$

3. for all $(\Omega_i, \varphi_i) \in \mathcal{A}_1$ such that $\Omega_i \subset \bar{\mathcal{B}}_p^*$ is arcwise connected and such that $\psi_{\text{cone}}(\Omega_i) \subset C_\lambda$ is a branch-cut domain, the mapping $\psi_{\text{cone}}|_{\Omega_i} : \Omega_i \rightarrow \psi_{\text{cone}}(\Omega_i) \subset C_\lambda$ is a homeomorphism and the inverse of the homeomorphism $\zeta_i := \text{Is}(C_\lambda, \psi_{\text{cone}}(\Omega_i)) \circ \psi_{\text{cone}}|_{\Omega_i} : \Omega_i \rightarrow \zeta_i(\Omega_i) \subset \mathbb{R}^2$ is compatible with \mathcal{A}_1 , i.e., $(\Omega_i, \zeta_i^{-1}) \in \mathcal{A}_1$.
4. the image of a closed curve homotopic to a circle around p in $\bar{\mathcal{B}}_p^*$ is a closed curve homotopic to a circle around 0 in $C_\lambda \setminus \{0\}$.

Proof. We prove the claims in two parts that we summarize as follows:

- Part 1: we proceed as in the proof of Proposition 3.42, i.e., we first construct the total transition mapping between a fixed coordinate system $(\Omega_\alpha, \varphi_\alpha) \in \mathcal{A}_1$, with $\Omega_\alpha \subset \bar{\Omega}_p^*$, and the other coordinate systems of \mathcal{A}_1 included in $\bar{\Omega}_p^*$. To overcome the difficulty of non-simple connectedness of $\bar{\Omega}_p^*$, we remove a geodesic curve η from $\bar{\Omega}_p^*$. Hence, as in Proposition 3.42, we obtain a mapping $\psi_1 : \bar{\Omega}_p^* \rightarrow \psi_1(\bar{\Omega}_p^*) \subset \mathbb{R}^2$ that is a local homeomorphism on $\bar{\Omega}_p^*$ minus the curve η . We construct the mapping ψ_1 in Step 1 and we prove that ψ_1 can be extended continuously at p in Step 2. We then show in Step 3 that p is the unique preimage of $\psi_1(p)$ by ψ_1 . We finally prove that, up to a rotation of angle $n \frac{\pi}{2}$, with $n \in \{0, \dots, 3\}$, the mapping ψ_1 is a local homeomorphism (Steps 4 and 5).
- Part 2: we construct the mapping ψ_{cone} in Step 6 by lifting the image of the mapping ψ_1 to the cone C_λ , where $\lambda = |2\pi\mathbf{N} - n \frac{\pi}{2}|$ and $\mathbf{N} \in \mathbb{Z}$. We finally prove Statements 1-4 in Step 7.

Part 1: mapping from $\bar{\Omega}_p^*$ to the plane

Step 1 (*Construction of the mapping ψ_1*). Let $g \in \bar{\Omega}_p^*$ and let $\eta : [0, 1] \rightarrow \text{cl}_M(\bar{\Omega}_p)$ be a geodesic curve starting from p , passing by g , and such that $\eta(1) \in \partial \bar{\Omega}_p$. We set $\eta_{\text{set}} := \eta([0, 1])$ and

$\eta_{\text{set}}^* := \eta_{\text{set}} \setminus \{p\}$. We denote \mathcal{O} the open and simply connected set defined by $\mathcal{O} := \bar{\Omega}_p \setminus \eta_{\text{set}}$ (see Figure 3.30). Let $q \in \bar{\Omega}_p^*$ and let $(\Omega_i, \varphi_i) \in \mathcal{A}_1$ be such that $q \in \Omega_i$. We fix in the sequel a path $\gamma : [0, 1] \rightarrow \bar{\Omega}_p^*$ from g to q to define the total transition mapping $F_{\Omega_i, \gamma}$ along γ (see Definition 3.39). Let us consider the two following subcases:

1. case $q \in \mathcal{O}$: let $\gamma_{gq} : [0, 1] \rightarrow \bar{\Omega}_p^*$ be a curve such that $\gamma(0) = g$, $\gamma(1) = q$ and $\gamma|_{(0,1]} : (0, 1] \rightarrow \mathcal{O}$. We moreover suppose that the oriented angle between η' at g and $\gamma'_{gq}(0)$ is in $(0, \pi)$ so that the curve γ_{gq} , up to homotopy, always turns in the positive sense.
2. case $q \in \eta_{\text{set}}^*$: let $\gamma_{gq} : [0, 1] \rightarrow \eta_{\text{set}}^*$ be a curve such that $\gamma(0) = g$ and $\gamma(1) = q$.

We show the notation in Figure 3.30. It is clear that, for a fixed $q \in \bar{\Omega}_p^*$, all the curves γ_{gq} satisfying these properties are homotopic to each other. Now, as in Proposition 3.42, we define the mapping $\psi_1 : \bar{\Omega}_p^* \rightarrow \psi_1(\bar{\Omega}_p^*) \subset \mathbb{R}^2$ by

$$\psi_1(w) = F_{\Omega_\alpha, \gamma_{gw}}^{-1} \circ \varphi_\alpha^{-1}(w), \text{ whenever } w \in \Omega_\alpha \text{ for } (\Omega_\alpha, \varphi_\alpha) \in \mathcal{A}_1, \quad (3.24)$$

for all $w \in \bar{\Omega}_p^*$. We easily obtain, in the same manner as in the proof of Proposition 3.42, that ψ_1 is well-defined. Then, assume that $(\Omega_i, \varphi_i) \in \mathcal{A}_1$ is such that $\Omega_i \subset \mathcal{O}$ and such that Ω_i is an arcwise connected set. Since Ω_i is arcwise connected, we infer that the total transition mapping $F_{\Omega_i, \gamma_{gq}}$ is independent of $q \in \Omega_i$. Hence, the mapping $\psi_1|_{\Omega_i} : \Omega_i \rightarrow \psi_1(\Omega_i) \subset \mathbb{R}^2$ is a homeomorphism (composition of homeomorphisms). Therefore, $\psi_1|_{\mathcal{O}}$ is a local homeomorphism and, using that $F_{\Omega_i, \gamma_{gq}}$, with $q \in \Omega_i$, is a grid automorphism, we conclude that the mapping $\psi_1|_{\Omega_i}^{-1}$ is compatible with \mathcal{A}_1 . Although, let us finally remark that ψ_1 may be discontinuous along η_{set}^* . Indeed, assume that $q \in \eta_{\text{set}}^* \cap \Omega_i$, with $(\Omega_i, \varphi_i) \in \mathcal{A}_1$. Then, $F_{\Omega_i, \gamma_{gq}}$ is not independent of $q \in \Omega_i$, so that this may materialise itself with a jump along η_{set}^* that we make explicit in Step 5.

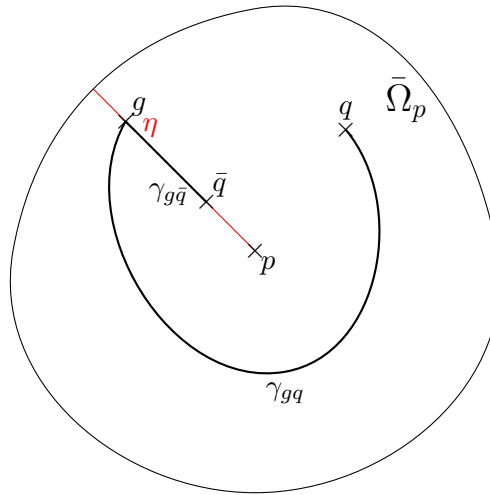


Fig. 3.30 Illustration of the branch-cut

Step 2 (Continuous extension of ψ_1 at p). Let $\varepsilon > 0$ and $I = \{1, \dots, N\}$. For all $i \in I$, using the uniform continuity of φ_i^{-1} , there exists $d_i > 0$ such that for all $q_1^i, q_2^i \in \Omega_i$,

$$d_M(q_1^i, q_2^i) < 2d_i \Rightarrow d_E[\varphi_i^{-1}(q_1^i), \varphi_i^{-1}(q_2^i)] < \frac{\varepsilon}{2N}. \quad (3.25)$$

We denote $\bar{d} = \inf_{i \in I} d_i$ and we set $B_M^*(p, \bar{d}) := B_M(p, \bar{d}) \setminus \{p\}$. We prove in what follows that

$$d_E[\psi_1(q), \psi_1(\bar{q})] < \varepsilon, \quad \text{for all } q, \bar{q} \in B_M^*(p, \bar{d}). \quad (3.26)$$

This clearly implies that ψ_1 admits a continuous extension at p . Let $q, \bar{q} \in B_M^*(p, \bar{d})$ and let $\gamma_{q\bar{q}} : [0, 1] \rightarrow B_M^*(p, \bar{d})$ be a curve such that $\gamma_{q\bar{q}}(0) = q$ and $\gamma_{q\bar{q}}(1) = \bar{q}$, and satisfying:

1. $\gamma_{q\bar{q}} : [0, 1] \rightarrow \mathcal{O}$, if $q, \bar{q} \in \mathcal{O}$;
2. $\gamma_{q\bar{q}} : [0, 1] \rightarrow \eta_{\text{set}}^*$, if $q, \bar{q} \in \eta_{\text{set}}^*$;
3. $\gamma_{q\bar{q}} : [0, 1] \rightarrow \mathcal{O}$, if $q \in \eta_{\text{set}}^*$ and $\bar{q} \in \mathcal{O}$. We also suppose in this case that, as above, $\gamma_{q\bar{q}}$ turns in the positive sense up to homotopy.

We emphasize that the subcase $\bar{q} \in \eta_{\text{set}}^*$ and $q \in \mathcal{O}$ is equivalent to Subcase 3 by symmetry. Moreover, we note that the curve $\gamma_{q\bar{q}}$ is defined such that the mapping $\psi_1 \circ \gamma_{q\bar{q}} : [0, 1] \rightarrow \mathbb{R}^2$ is continuous. Let $j \in I$ and suppose first that $\Omega_j \cap \eta_{\text{set}} \neq \emptyset$. Then, since Ω_j is geodesically convex, we obtain that the set $\Omega_j \setminus \eta_{\text{set}}^*$ has two arcwise connected components denoted $\tilde{\mathcal{U}}_{j,1}$ and $\tilde{\mathcal{U}}_{j,2}$. We suppose that they are indexed such that ψ_1 is continuous on $\mathcal{U}_{j,1} := \tilde{\mathcal{U}}_{j,1} \cup (\Omega_j \cap \eta_{\text{set}}^*)$ and we set $\mathcal{U}_{j,2} = \tilde{\mathcal{U}}_{j,2}$. For ease of notation, we set $\mathcal{U}_{j,1} = \Omega_j$ and $\mathcal{U}_{j,2} = \emptyset$ whenever $\Omega_j \cap \eta_{\text{set}}^* = \emptyset$.

Then, there exists an integer $A \in \{1, \dots, 2N\}$ and an injection $\xi : \{0, \dots, A-1\} \rightarrow I \times \{1, 2\}$, with $\xi = (\xi_1, \xi_2)$. Moreover, there exists $0 = t_0 < \dots < t_A = 1$, such that $\gamma_{q\bar{q}}(t_i), \gamma_{q\bar{q}}(t_{i+1}) \in \mathcal{U}_{\xi(i)}$ for all $i \in \{0, \dots, A-1\}$. Then, for all $i \in \{0, \dots, A-1\}$, using that $d_M[\gamma_{q\bar{q}}(t_i), \gamma_{q\bar{q}}(t_{i+1})] < 2\bar{d} < 2d_i$ and using (3.25), we obtain that

$$d_E[\varphi_{\xi_1(i)}^{-1}(\gamma_{q\bar{q}}(t_i)), \varphi_{\xi_1(i)}^{-1}(\gamma_{q\bar{q}}(t_{i+1}))] < \frac{\varepsilon}{2N}. \quad (3.27)$$

Furthermore, for all $j \in I$ and $l \in \{1, 2\}$ such that $\mathcal{U}_{j,l} \neq \emptyset$, we obtain from the construction of $\mathcal{U}_{j,l}$ that $F_{\Omega_j, \gamma_{gw}} = F_{\Omega_j, \gamma_{g\bar{w}}}$, for all $w, \bar{w} \in \mathcal{U}_{j,l}$. Then, using that grid automorphisms are isometries, we infer from the definition of ψ_1 , i.e., (3.24), and (3.27) that $d_E[\psi_1(\gamma_{q\bar{q}}(t_i)), \psi_1(\gamma_{q\bar{q}}(t_{i+1}))] < \frac{\varepsilon}{2N}$ for all $i \in \{0, \dots, A-1\}$. Using the triangle inequality, we conclude that (3.26) is satisfied.

Step 3 (Unique preimage of 0). We denote $T : \mathbb{R}^2 \rightarrow \mathbb{R}^2$ the translation of \mathbb{R}^2 such that $T \circ \psi_1(p) = 0$ and we define the mapping $\psi_2 := T \circ \psi_1 : \bar{\Omega}_p \rightarrow \psi_2(\bar{\Omega}_p) \subset \mathbb{R}^2$. We now prove the following:

There exists $h_0 > 0$ such that any sequence $(q_n)_{n \in \mathbb{N}} \subset B_M(p, h_0)$ satisfying $\lim_{n \rightarrow \infty} \psi_2(q_n) = \psi_2(p) = 0$ converges to p .

Let us first recall from Step 2 that $\bar{\Omega}_p^*$ is covered by the arcwise connected sets $\mathcal{U}_{j,l}$, with $j \in I$ and $l \in \{1, 2\}$, defined such that $\mathcal{U}_{i,1} \cup \mathcal{U}_{i,2} = \Omega_i$, for all $i \in I$. For all $h > 0$, we denote $\{\mathcal{U}_i^h\}_{i \in E}$ the sets $\mathcal{U}_{j,l}$, with $j \in I$ and $l \in \{1, 2\}$, such that $\mathcal{U}_{j,l} \cap B_M(p, h) \neq \emptyset$. Since $F_{\Omega_i, \gamma_{gw}} = F_{\Omega_i, \gamma_{g\bar{w}}}$, for all $w, \bar{w} \in \mathcal{U}_i^h$, we have that $\psi_2|_{\mathcal{U}_i^h}$ is a homeomorphism, for all $i \in E$ and $h > 0$. We moreover notice that, since the cover of $B_M(p, h) \setminus \{p\}$ by $\{\mathcal{U}_i^h\}_{i \in E}$ is finite, for all $h > 0$, there exists $h_0 > 0$ such that $B_M(p, 2h_0) \subset \bar{\Omega}_p$, and $p \in \text{cl}_M(\mathcal{U}_i^{2h_0})$ for all $i \in E$.

Now, let $(q_n)_{n \in \mathbb{N}} \subset B_M(p, h_0)$ be a sequence such that $\lim_{n \rightarrow \infty} \psi_2(q_n) = 0$. We prove that $(q_n)_{n \in \mathbb{N}}$ converges to p by a contradiction argument. First, using the compactness of $\text{cl}_M(B_M(p, h_0)) \subset B_M(p, 2h_0)$, there exists a subsequence of $(q_n)_{n \in \mathbb{N}}$ converging in $B_M(p, 2h_0)$. We denote $q_\infty \in B_M(p, 2h_0)$ this limit and we suppose that $q_\infty \neq p$. Then, $\psi_2(q_\infty) = 0$ and, for some $i \in E$, we have $q_\infty \in \mathcal{U}_i^{2h_0}$. Now, since $p \in \text{cl}_M(\mathcal{U}_i^{2h_0})$, there exists a sequence $(\tilde{q}_n)_{n \in \mathbb{N}} \subset \mathcal{U}_i^{2h_0}$ converging

to p and, due to the continuity of ψ_2 on $\mathcal{U}_i^{2h_0}$ and at p , we have

$$\lim_{n \rightarrow \infty} \psi_2(\tilde{q}_n) = 0. \quad (3.28)$$

Let $\Gamma_\infty \subset \mathcal{U}_i^{2h_0}$ be a neighborhood of q_∞ such that $p \notin \text{cl}_M(\Gamma_\infty)$. Since $\psi_2|_{\mathcal{U}_i^{2h_0}}$ is a homeomorphism, there exists a neighborhood U_∞ of $\psi_2(q_\infty) = 0$ such that $\psi_2|_{\mathcal{U}_i^{2h_0}}^{-1}(U_\infty) = \Gamma_\infty$. This is in contradiction with (3.28). We conclude that $q_\infty = p$ and we have the expected result.

Step 4 (A mapping $\tilde{\psi}_2$ in the neighborhood of η_{set}^*). To make explicit the jump of ψ_2 whenever we cross the curve η , let $\Gamma \subset \bar{\Omega}_p^*$ be a simply connected open set in the neighborhood of η_{set}^* such that $\Gamma \setminus \eta_{\text{set}} = \mathcal{O}_1 \cup \mathcal{O}_2$, with $\mathcal{O}_1, \mathcal{O}_2 \subset \mathcal{O}$ two simply connected open sets (see Figure 3.31). We suppose that \mathcal{O}_1 and \mathcal{O}_2 are indexed such that $\psi_2|_{\mathcal{O}_1 \cup \eta_{\text{set}}^*} : \mathcal{O}_1 \cup \eta_{\text{set}}^* \rightarrow \psi_2(\mathcal{O}_1 \cup \eta_{\text{set}}^*) \subset \mathbb{R}^2$ is a continuous mapping. Then, for all $q \in \Gamma$, let $\tilde{\gamma}_{gq} : [0, 1] \rightarrow \Gamma$ be a curve such that $\tilde{\gamma}_{gq}(0) = g$ and $\tilde{\gamma}_{gq}(1) = q$. In the same manner as for the mapping ψ_2 , we define the smooth mapping $\tilde{\psi}_2 : \Gamma \rightarrow \tilde{\psi}_2(\Gamma) \subset \mathbb{R}^2$ by

$$\tilde{\psi}_2(q) = T \circ F_{\Omega_\alpha, \tilde{\gamma}_{gq}}^{-1} \circ \varphi_\alpha^{-1}(q), \text{ where } q \in \Omega_\alpha \text{ with } (\Omega_\alpha, \varphi_\alpha) \in \mathcal{A}_1,$$

for all $q \in \Gamma$. Let us remark that, in the same manner as in Step 2, we obtain that $\tilde{\psi}_2$ has a continuous extension at p . Moreover, for all $(\Omega_i, \varphi_i) \in \mathcal{A}_1$ with Ω_i an arcwise connected set in Γ , the mapping $\tilde{\psi}_2|_{\Omega_i} : \Omega_i \rightarrow \tilde{\psi}_2(\Omega_i) \subset \mathbb{R}^2$ is an homeomorphism and $\tilde{\psi}_2|_{\Omega_i}^{-1}$ is compatible with \mathcal{A}_1 .

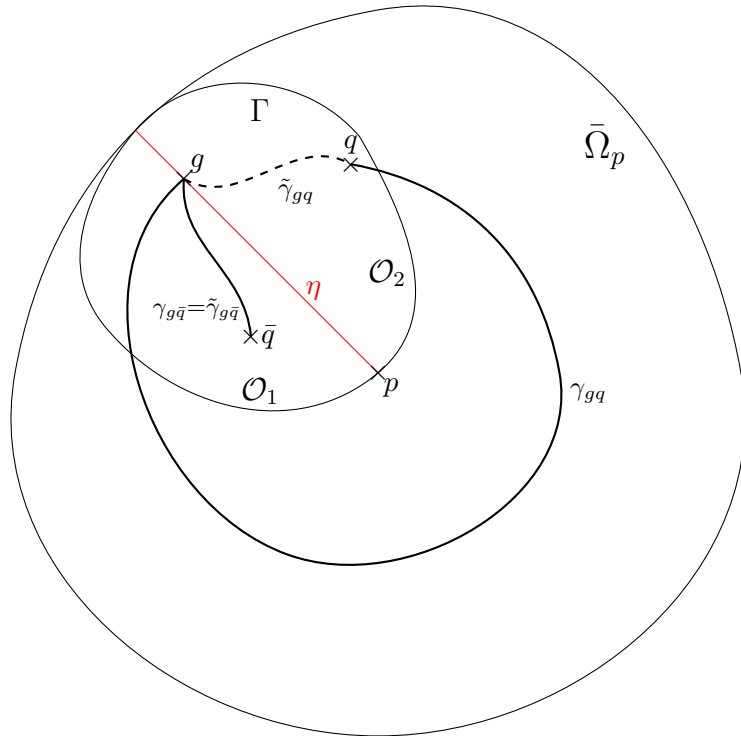


Fig. 3.31 Illustration of the construction of the mapping $\tilde{\psi}_2$

Step 5 (Local homeomorphism up to a rotation). We prove the following:

There exists $\mathbf{n} \in \{0, 1, 2, 3\}$ such that for all $q \in \Gamma$,

$$\tilde{\psi}_2(q) = \begin{cases} \psi_2(q), & \text{if } q \in \mathcal{O}_1 \cup \eta_{\text{set}}^*, \\ R_{\mathbf{n}\frac{\pi}{2}} \circ \psi_2(q), & \text{if } q \in \mathcal{O}_2. \end{cases} \quad (3.29)$$

By construction, for all $q \in \mathcal{O}_1 \cup \eta_{\text{set}}^*$, we have $\psi_2(q) = \tilde{\psi}_2(q)$. We denote $J \subset I$ the set of indices $i \in I$ such that $\Omega_i \cap \mathcal{O}_2 \neq \emptyset$. Then, for all $i \in J$ and $q \in \Omega_i \cap \mathcal{O}_2$, we have

$$\begin{aligned} \tilde{\psi}_2(q) &= T \circ F_{\Omega_i, \tilde{\gamma}_{gq}}^{-1} \circ \varphi_i^{-1}(q) = T \circ F_{\Omega_i, \tilde{\gamma}_{gq}}^{-1} \circ F_{\Omega_i, \gamma_{gq}} \circ T^{-1} \circ T \circ F_{\Omega_i, \gamma_{gq}}^{-1} \circ \varphi_i^{-1}(q) \\ &= T \circ F_{\Omega_i, \tilde{\gamma}_{gq}}^{-1} \circ F_{\Omega_i, \gamma_{gq}} \circ T^{-1} \circ \psi_2(q). \end{aligned} \quad (3.30)$$

Hence, we have $\tilde{\psi}_2(q) = G_{i,q} \circ \psi_2(q)$, with $G_{i,q}: \mathbb{R}^2 \rightarrow \mathbb{R}^2$ the grid automorphism defined by

$$G_{i,q} = T \circ F_{\Omega_i, \tilde{\gamma}_{gq}}^{-1} \circ F_{\Omega_i, \gamma_{gq}} \circ T^{-1},$$

for all $i \in J$ and $q \in \Omega_i \cap \mathcal{O}_2$. Therefore, due to the continuity of ψ_2 and $\tilde{\psi}_2$ on \mathcal{O}_2 , we have that $G_{i,q}$ is independent of $i \in J$ and $q \in \mathcal{O}_2$ and we denote this mapping $G: \mathbb{R}^2 \rightarrow \mathbb{R}^2$. Furthermore, since $\tilde{\psi}_2$ has a continuous extension at p , we infer from $\tilde{\psi}_2|_{\mathcal{O}_1 \cup \eta_{\text{set}}^*} = \psi_2|_{\mathcal{O}_1 \cup \eta_{\text{set}}^*}$ that $\tilde{\psi}_2(p) = \psi_2(p) = 0$. We conclude that 0 is a fixed-point of the grid automorphism G , so that there exists $\mathbf{n} \in \{0, 1, 2, 3\}$ such that $G = R_{\mathbf{n}\frac{\pi}{2}}$.

Part 2: mapping from $\bar{\Omega}_p^*$ to the cone C_λ

Step 6 (*Construction of the mapping ψ_{cone}*). We first lift the image of ψ_2 to the cylinder. We denote $\tau_{\text{cyl}}: \mathbb{R}_*^+ \times \mathbb{R} \rightarrow \mathbb{R}_*^2$ the mapping defined by $\tau_{\text{cyl}}(u, v) = (u \cos(v), u \sin(v))$. We fix $q_0 \in \mathcal{O}_1$ and, using that the mapping τ_{cyl} is a covering mapping and [36, Cor. 11.19], we obtain that there exists a unique lifting $\psi_{\text{cyl}}: \mathcal{O} \rightarrow \psi_{\text{cyl}}(\mathcal{O}) \subset \mathbb{R}_*^+ \times \mathbb{R}$ of the mapping $\psi_2|_{\mathcal{O}}: \mathcal{O} \rightarrow \psi_2(\mathcal{O}) \subset \mathbb{R}_*^2$ such that $\psi_{\text{cyl}}(q_0) = (|\psi_2(q_0)|, \arg(\psi_2(q_0))) \in \mathbb{R}_*^+ \times [0, 2\pi]$. By construction, the mapping ψ_{cyl} satisfies $\tau_{\text{cyl}} \circ \psi_{\text{cyl}} = \psi_2$. Moreover, the mapping $\psi_{\text{cyl}}|_{\mathcal{O}_1}: \mathcal{O}_1 \rightarrow \psi_{\text{cyl}}(\mathcal{O}_1) \subset \mathbb{R}_*^+ \times \mathbb{R}$ can be extended continuously on η_{set}^* . With this extension, we obtain a mapping $\psi_{\text{cyl}}: \bar{\Omega}_p^* \rightarrow \psi_{\text{cyl}}(\bar{\Omega}_p^*) \subset \mathbb{R}_*^+ \times \mathbb{R}$. We illustrate the lifting of the mapping ψ_2 in Figure 3.32. Owing to Step 5, there exists an integer $\mathbf{N} \in \mathbb{Z}$ such that, for all sequence $(q_n)_{n \in \mathbb{N}} \subset \mathcal{O}_2$ converging to $q_\infty \in \eta_{\text{set}}^*$, the following is satisfied:

$$\lim_{n \rightarrow \infty} \psi_{\text{cyl}}(q_n) = \psi_{\text{cyl}}(q_\infty) + \left(0, 2\pi\mathbf{N} - \mathbf{n}\frac{\pi}{2}\right). \quad (3.31)$$

We set $\lambda = |2\pi\mathbf{N} - \mathbf{n}\frac{\pi}{2}|$ and we denote C_λ the cone of interior angle λ . Let $\tau_\lambda: \mathbb{R}_*^+ \times \mathbb{R} \rightarrow C_\lambda \setminus \{0\}$ be the quotient mapping defined by $\tau_\lambda(u, v) = (u, \tilde{v})$, with $\tilde{v} = v \bmod \lambda$. Then, we define the mapping $\psi_{\text{cone}}: \bar{\Omega}_p \rightarrow C_\lambda$ by

$$\psi_{\text{cone}}(q) = \begin{cases} \tau_\lambda \circ \psi_{\text{cyl}}(q), & \text{if } q \in \bar{\Omega}_p^*, \\ 0, & \text{if } q = p, \end{cases}$$

for all $q \in \bar{\Omega}_p$. Now, in the same manner as above, we lift to the cylinder the image of the mapping $\tilde{\psi}_2$. We denote this mapping $\tilde{\psi}_{\text{cyl}}: \Gamma \rightarrow \tilde{\psi}_{\text{cyl}}(\Gamma) \subset \mathbb{R}_*^+ \times \mathbb{R}$. Then, using Step 5 and (3.31), we

obtain that

$$\tilde{\psi}_{\text{cyl}}(q) = \begin{cases} \psi_{\text{cyl}}(q), & \text{if } q \in \mathcal{O}_1 \cup \eta_{\text{set}}^*, \\ \psi_{\text{cyl}}(q) + (0, 2\pi\mathbf{N} - \mathbf{n}\frac{\pi}{2}), & \text{if } q \in \mathcal{O}_2, \end{cases}$$

for all $q \in \Gamma$. Hence, we have

$$\tau_\lambda \circ \tilde{\psi}_{\text{cyl}}(q) = \tau_\lambda \circ \psi_{\text{cyl}}(q) = \psi_{\text{cone}}(q), \quad (3.32)$$

for all $q \in \Gamma$.

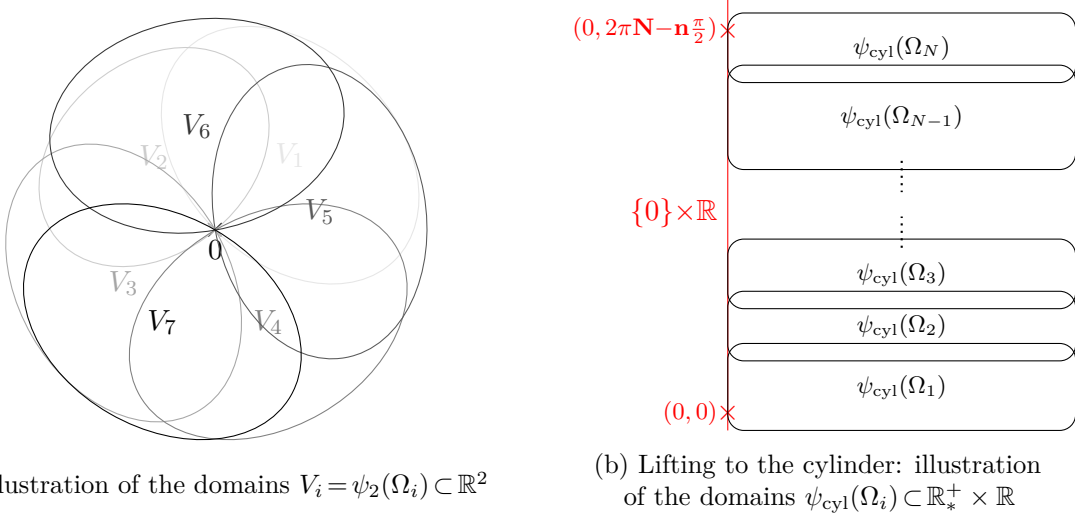


Fig. 3.32 Construction of the mapping ψ_{cyl}
(proof of Lemma 3.44)

Step 7 (Proof of Statements 1-4). First, since $\psi_2|_{\mathcal{O}}$ is a local homeomorphism, we infer that the mapping $\psi_{\text{cone}}|_{\mathcal{O}}$ is a local homeomorphism. Then, we easily conclude from (3.32) that the mapping $\psi_{\text{cone}}|_{\bar{\Omega}_p^*}$ is a local homeomorphism and Statement 1 follows. Moreover, Statement 4 is a direct consequence of (3.31). For Statement 2 to hold true, we restrict in what follows ψ_2 and ψ_{cone} to $\bar{\mathcal{B}}_p := B_M(p, h_0)$, with $h_0 > 0$ defined in Step 3. Then, owing to Step 3, for all $h \in (0, h_0]$, there exists $l > 0$ such that

$$d_E(\psi_2(q), 0) < l \Rightarrow d_M(q, p) < h,$$

for all $q \in \bar{\mathcal{B}}_p$. Equivalently, we have

$$\psi_2^{-1}(B_E(0, l)) \subset B_M(p, h),$$

and we conclude that

$$\psi_{\text{cone}}^{-1}(B_\lambda(0, l)) \subset B_M(p, h). \quad (3.33)$$

This yields Statement 2 and we prove Statement 3 as follows. Let $(\Omega_i, \varphi_i) \in \mathcal{A}_1$ be such that Ω_i is an arcwise connected set in $\bar{\mathcal{B}}_p^*$, with $\bar{\mathcal{B}}_p^* := \bar{\mathcal{B}}_p \setminus \{p\}$, and such that $\psi_{\text{cone}}(\Omega_i) \subset C_\lambda$ is a branch-cut domain. We first suppose that $\Omega_i \cap \eta_{\text{set}}^* = \emptyset$. Then, owing to Step 1, we have that $\psi_2|_{\Omega_i}$ is a homeomorphism and that $\psi_2|_{\Omega_i}^{-1}$ is compatible with (Ω_i, φ_i) . Hence, the mapping $F_i := \psi_2 \circ \varphi_i : \varphi_i^{-1}(\Omega_i) \rightarrow \psi_2(\Omega_i)$ is a grid automorphism. Let $(u, v) \in \varphi_i^{-1}(\Omega_i)$ and let $(r, \theta) \in \mathbb{R}_*^+ \times [0, 2\pi)$ be the polar coordinates of $F_i(u, v)$. Then, there exists $\bar{N}_i \in \mathbb{Z}$ such that $\psi_{\text{cyl}} \circ \varphi_i(u, v) = (r, \theta + 2\pi\bar{N}_i)$.

We infer that

$$\psi_{\text{cone}} \circ \varphi_i(u, v) = \tau_\lambda(r, \theta + 2\pi\bar{N}_i).$$

Then, setting $\Pi := \text{Is}(C_\lambda, \psi_{\text{cone}}(\Omega_i)) : \psi_{\text{cone}}(\Omega_i) \rightarrow \text{Pl}(C_\lambda, \psi_{\text{cone}}(\Omega_i))$, we obtain that there exists $n_i \in \mathbb{Z}$ such that

$$\Pi \circ \psi_{\text{cone}} \circ \varphi_i(u, v) = R_{n_i \frac{\pi}{2}} \circ F_i(u, v). \quad (3.34)$$

Since Π , ψ_{cone} , φ_i and F_i are continuous, we infer that n_i is independent of $(u, v) \in \varphi_i^{-1}(\Omega_i)$ and we deduce that $\psi_{\text{cone}}|_{\Omega_i}$ is a homeomorphism. Moreover, setting $\zeta_i := \Pi \circ \psi_{\text{cone}}|_{\Omega_i} : \Omega_i \rightarrow \zeta_i(\Omega_i) \subset \mathbb{R}^2$, we have that (3.34) is equivalent to

$$\zeta_i \circ \varphi_i(u, v) = R_{n_i \frac{\pi}{2}} \circ F_i(u, v). \quad (3.35)$$

We conclude that (Ω_i, ζ_i^{-1}) is compatible with (Ω_i, φ_i) . Finally, in the case where $\Omega_i \cap \eta_{\text{set}}^* \neq \emptyset$, we emphasize that the result (3.35) is obtained in the same manner using $\tilde{\psi}_{\text{cyl}}$ instead of ψ_{cyl} . This yields Statement 3. ■

Now, we can prove Proposition 3.31 restated as follows.

Proposition 3.45 (Extension into conical singularities). *Let M be a surface and let \mathcal{A}_1 be a GC atlas with singularities \mathcal{P} . Assume that, for all $p \in \mathcal{P}$, there exists a neighborhood $\bar{\Omega}_p$ of p and a finite open cover $\cup_{i=1}^N \Omega_i$ of $\bar{\Omega}_p^* := \bar{\Omega}_p \setminus \{p\}$. Moreover, for all $i \in \{1, \dots, N\}$, we suppose that Ω_i is geodesically convex and we suppose that there exists $(\Omega_i, \varphi_i) \in \mathcal{A}_1$ such that $\varphi_i^{-1} : \Omega_i \rightarrow U_i \subset \mathbb{R}^2$ is uniformly continuous. Then, there exists a GC atlas \mathcal{A} with conical singularities \mathcal{P} on M containing \mathcal{A}_1 .*

Proof.

Step 1 (Preliminaries). Let $p \in \mathcal{P}$ and let $\bar{\Omega}_p \subset M$ be a neighborhood of p satisfying the assumptions of the proposition. Owing to Lemma 3.44, there exists $\lambda = k\frac{\pi}{2}$, with $k \geq 1$ an integer, an open ball $\bar{\mathcal{B}}_p := B_M(p, h_0)$, with $h_0 > 0$, and a continuous mapping $\psi_{\text{cone}} : \bar{\mathcal{B}}_p \rightarrow \psi_{\text{cone}}(\bar{\mathcal{B}}_p) \subset C_\lambda$ satisfying Statements 1-4 of Lemma 3.44. To prove the claim, we only need to show that there exists $\bar{h} \in (0, h_0]$ such that $\psi_{\text{cone}}|_{B_M(p, \bar{h})} : B_M(p, \bar{h}) \rightarrow \psi_{\text{cone}}(B_M(p, \bar{h})) \subset C_\lambda$ is a homeomorphism. Indeed, supposing that $\psi_{\text{cone}}|_{B_M(p, \bar{h})}$ is a homeomorphism, Statement 3 (of Lemma 3.44) ensures the compatibility of the conical net $\psi_{\text{cone}}|_{B_M(p, \bar{h})}^{-1}$ with \mathcal{A}_1 . Then, noting that $\psi_{\text{cone}}|_{\bar{\mathcal{B}}_p^*}$, with $\bar{\mathcal{B}}_p^* := \bar{\mathcal{B}}_p \setminus \{p\}$, is a local homeomorphism (Statement 1), we first prove that for some neighborhood $\bar{\Omega}_0 \subset \bar{\mathcal{B}}_p$ of p , the mapping $\psi_{\text{cone}}|_{\bar{\Omega}_0^*} : \bar{\Omega}_0^* \rightarrow \psi_{\text{cone}}(\bar{\Omega}_0^*) \subset C_\lambda \setminus \{0\}$, with $\bar{\Omega}_0^* := \bar{\Omega}_0 \setminus \{p\}$, is a covering mapping. To this purpose, we prove that this mapping is proper, i.e., that the preimage by $\psi_{\text{cone}}|_{\bar{\Omega}_0^*}$ of a compact set in $\psi_{\text{cone}}(\bar{\Omega}_0^*)$ is a compact set. In Step 2, we ensure that $\psi_{\text{cone}}|_{\bar{\Omega}_0^*}$ is proper by showing that we can keep away the preimage of compact sets in $\psi_{\text{cone}}(\bar{\Omega}_0^*)$ from the boundary of $\bar{\mathcal{B}}_p^*$, that is, from p and from the boundary of $\bar{\mathcal{B}}_p$. We finally prove in Step 3 that $\psi_{\text{cone}}|_{B_M(p, \bar{h})}$ is a homeomorphism.

Step 2 (Proof that ψ_{cone} is a covering mapping). Let $h_{\max} > 0$ be such that $\text{cl}_M(B_M(p, h_{\max})) \subset \bar{\mathcal{B}}_p$. Owing to Statement 2, there exists $l > 0$ such that

$$\psi_{\text{cone}}^{-1}(B_\lambda(0, l)) \subset B_M(p, h_{\max}). \quad (3.36)$$

Moreover, using the continuity of ψ_{cone} at p and $\psi_{\text{cone}}(p)=0$, there exists $\bar{h}>0$ such that

$$B_M(p, \bar{h}) \subset \psi_{\text{cone}}^{-1}(B_\lambda(0, l)). \quad (3.37)$$

We set $\bar{\Omega}_0 := \psi_{\text{cone}}^{-1}[\psi_{\text{cone}}(B_M(p, \bar{h}))]$ and $\bar{\Omega}_0^* := \bar{\Omega}_0 \setminus \{p\}$. Then, using (3.37), we obtain that

$$\bar{\Omega}_0 \subset \psi_{\text{cone}}^{-1}\left[\psi_{\text{cone}}\left(\psi_{\text{cone}}^{-1}(B_\lambda(0, l))\right)\right] \subset \psi_{\text{cone}}^{-1}(B_\lambda(0, l)).$$

We deduce from (3.36) that

$$\bar{\Omega}_0 \subset B_M(p, h_{\max}). \quad (3.38)$$

Furthermore, using that $\psi_{\text{cone}}|_{\bar{\mathcal{B}}_p^*}$ is an open mapping (as a local homeomorphism), we obtain that the set $\psi_{\text{cone}}[B_M(p, \bar{h})]$ is open. Hence, $\bar{\Omega}_0^*$ is an open set. We conclude that the mapping $\psi_{\text{cone}}|_{\bar{\Omega}_0^*} : \bar{\Omega}_0^* \rightarrow \psi_{\text{cone}}(\bar{\Omega}_0^*)$ is a local homeomorphism (restriction to an open set of a local homeomorphism). Moreover, since $p \notin \bar{\Omega}_0^*$, we have $0 \notin \psi_{\text{cone}}(\bar{\Omega}_0^*)$ by Statement 2.

Let $D \subset \psi_{\text{cone}}(\bar{\Omega}_0^*)$ be a compact set. Since $0 \notin D$, we denote $L_0 = d_\lambda(0, D) > 0$ the distance from 0 to the compact set D in C_λ . Then, using the continuity of ψ_{cone} at p , we obtain that there exists $h_{\min} > 0$ such that $B_M(p, h_{\min}) \subset \psi_{\text{cone}}^{-1}(B_\lambda(0, \frac{L_0}{2}))$ (see Figure 3.33). Moreover, using (3.38), we have $\psi_{\text{cone}}^{-1}(D) \subset \bar{\Omega}_0 \subset B_M(p, h_{\max})$. Therefore, since ψ_{cone} is continuous, $\psi_{\text{cone}}^{-1}(D)$ is a closed subset of the compact set $\text{cl}_M(B_M(p, h_{\max})) \setminus B_M(p, h_{\min})$ in $\bar{\mathcal{B}}_p$. We conclude that $\psi_{\text{cone}}^{-1}(D)$ is a compact set. Hence, $\psi_{\text{cone}}|_{\bar{\Omega}_0^*}$ is a proper mapping, so that, owing to [36, Exercise 11.9], this mapping is a covering.

Step 3 (Proof that ψ_{cone} is a homeomorphism). First, using that $\psi_{\text{cone}}|_{\bar{\Omega}_0^*}$ is a covering mapping and using Statement 2, we easily obtain that there exists $l_0 > 0$ such that $B_\lambda(0, l_0) \subset \psi_{\text{cone}}(\bar{\Omega}_0)$. Then, owing to Statement 4 the image of a closed curve around p homotopic to a circle in $\bar{\Omega}_0^*$ is a closed curve around 0 homotopic to a circle in $\psi_{\text{cone}}(\bar{\Omega}_0^*) \subset C_\lambda \setminus \{0\}$. To prove that $\psi_{\text{cone}}|_{\bar{\Omega}_0^*}$ is a homeomorphism, suppose that $x \in \psi_{\text{cone}}(\bar{\Omega}_0)$ has two distincts preimages q_1 and q_2 in $\bar{\Omega}_0^*$. Let \tilde{C} be a closed curve passing by q_1 and q_2 , and homotopic to a circle around p in $\bar{\Omega}_0^*$. Then, $\psi_{\text{cone}}(\tilde{C})$ is composed by two closed curves and is homotopic to a circle around 0 in $\psi_{\text{cone}}(\bar{\Omega}_0^*)$. Therefore, one of these closed curves is contractible in $\psi_{\text{cone}}(\bar{\Omega}_0^*)$, which contradicts that $q_1 \neq q_2$. We conclude that the covering mapping $\psi_{\text{cone}}|_{\bar{\Omega}_0^*} : \bar{\Omega}_0^* \rightarrow \psi_{\text{cone}}(\bar{\Omega}_0^*)$ is a homeomorphism. Therefore, we have $\bar{\Omega}_0 = B_M(p, \bar{h})$ and we conclude that $\psi_{\text{cone}}|_{B_M(p, \bar{h})} : B_M(p, \bar{h}) \rightarrow \psi_{\text{cone}}(B_M(p, \bar{h}))$ is a homeomorphism using Statement 2. The claim follows. ■

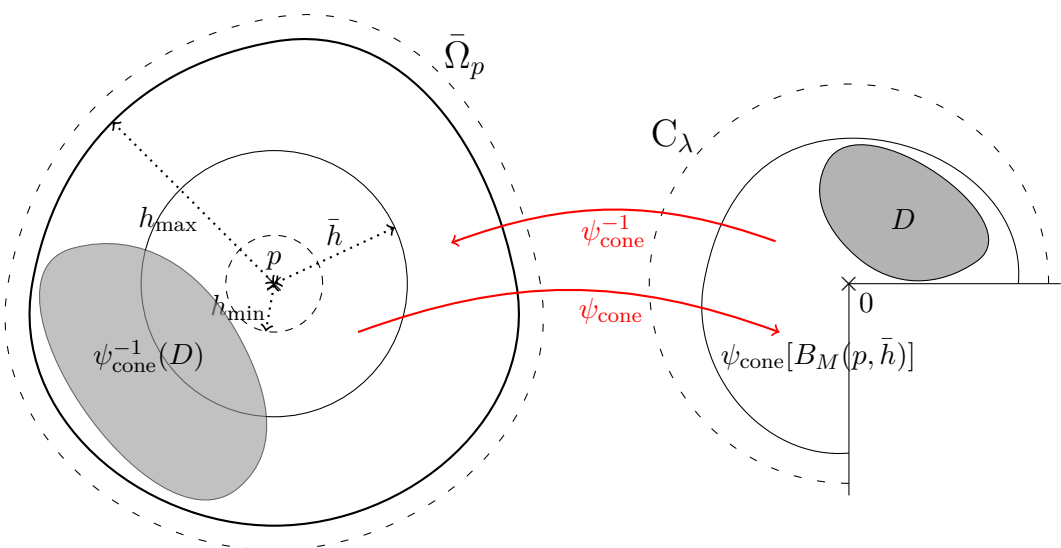


Fig. 3.33 Illustration of the sets $\bar{\Omega}_0$ and D

Chapter 4

Smooth Chebyshev nets defined by primal boundary conditions

We prove in this chapter the existence and the uniqueness of a Chebyshev net delimited by two smooth curves called boundary conditions. We outline the main ideas of the proof as follows. Following [25], we consider the angle distribution defined by the angle between the coordinate curves of the candidate Chebyshev net. We prove that one can construct a unique mapping from this angle distribution such that the v -coordinate curves are arc-length parametrized curves with the proper geodesic curvature defined by this angle distribution. Note that the choice of the direction is arbitrary, so that the u -coordinate curves could have been chosen. This construction entails a loss of symmetry between these two coordinates which materializes itself by a differentiation between the regularity of the two directions of coordinates curves. The aim is now to view the Hazzidakis formula as a fixed-point equation on the angle distribution, using that the candidate Chebyshev net depends (Lipschitz) continuously on this angle distribution.

We then show that, supposing that the Hazzidakis formula is satisfied by the angle distribution, we obtain a regularity pick-up by the use of this identity, and therefore we recover the symmetry between the two directions. Furthermore, we prove that, under suitable regularity conditions, the candidate mapping constructed from the angle distribution is indeed a Chebyshev net, i.e., the u -coordinate curves are also arc-length parametrized. The last step of the proof is to show the existence of a unique solution to the equation associated with Hazzidakis formula. This is obtained in the spirit of the Cauchy–Lipschitz theorem: we first prove this existence and uniqueness for a small interval in the v -coordinate, and we then extend this result to the whole domain.

Preliminaries

Informal statement of the main result

Let

$$D = [0, L_u] \times [0, L_v], \quad \text{with } L_u, L_v \in \mathbb{R}_*^+,$$

and let $\gamma_u : [0, L_u] \rightarrow M$ and $\gamma_v : [0, L_v] \rightarrow M$ be two curves such that $\gamma_u(0) = \gamma_v(0)$, and forming an interior angle $\angle(\gamma'_u(0), \gamma'_v(0)) \in (0, \pi)$ at their intersection. For clarity of exposition, throughout this chapter, we consider a slightly different notion of Chebyshev net which will refer to mappings

(not necessarily homeomorphisms) $\varphi: D \rightarrow M$ satisfying

$$|\partial_u \varphi|_g(u, v) = 1, \quad (4.1a)$$

$$|\partial_v \varphi|_g(u, v) = 1, \quad (4.1b)$$

for all $(u, v) \in D$. Furthermore, note that the orientation of the boundary curve γ_v is reversed in this chapter to simplify the exposition. We prove in the sequel the existence and the uniqueness of a Chebyshev net $\varphi: D \rightarrow M$ verifying the primal boundary conditions

$$\begin{aligned} \varphi(u, 0) &= \gamma_u(u), \quad \forall u \in [0, L_u], \\ \varphi(0, v) &= \gamma_v(v), \quad \forall v \in [0, L_v]. \end{aligned} \quad (4.2)$$

Moreover, we show that the solution depends continuously on these boundary curves, in a sense that will be made precise later on. The considered surface M is supposed to be smooth, open, complete, and simply connected and we denote K its Gaussian curvature. Due to the above assumptions, the surface M is homeomorphic to the plane so that we suppose in what follows that $M = (\mathbb{R}^2, g)$. We moreover suppose that the metric g satisfies the following property: for all compact set $W \subset M$, there exists $C_{\text{surf}} > 1$ such that

$$|X|_{g(p)} \leq C_{\text{surf}} |X|, \quad (4.3)$$

for all $p \in W$ and $X \in \mathbb{R}^2$. Unless explicitly mentioned, all the considered curves are assumed to be arc-length parametrized. Then, the geodesic curvature $\kappa_\sigma: I \subset \mathbb{R} \rightarrow \mathbb{R}$ of a curve $\sigma: I \rightarrow M$ is defined by

$$\kappa_\sigma = \langle \sigma'', \sigma'^\perp \rangle_g, \quad (4.4)$$

where σ'^\perp is the direct $\frac{\pi}{2}$ -rotation of σ' . In the sequel, C and \tilde{C} are two generic constants whose values can change at each occurrence and we will often explicit their dependence.

Following [25], we reformulate the problem of finding a Chebyshev net $\varphi: D \rightarrow M$ as the problem of finding the angle distribution $\omega: D \rightarrow \mathbb{R}/2\pi\mathbb{Z}$ between the coordinate curves defined by $\omega(u, v) = \angle(\partial_u \varphi, \partial_v \varphi)(u, v)$. With this purpose in mind, we observe that ω satisfies the following integrability condition (in the form of a modified Sine-Gordon equation) [25]

$$\partial_{uv} \omega = -K(\varphi) \sin(\omega). \quad (4.5)$$

Equivalently, ω satisfies the integrated form of (4.5) called the Hazzidakis formula

$$\begin{aligned} \omega(u, v) &= \angle(\gamma'_u(0), \gamma'_v(0)) - \int_0^u \kappa_u(s) ds + \int_0^v \kappa_v(s) ds \\ &\quad - \int_0^u \int_0^v K(\varphi(s, t)) \sin[\omega(s, t)] ds dt, \end{aligned} \quad (4.6)$$

for all $(u, v) \in D$, with $\kappa_u: [0, L_u] \rightarrow \mathbb{R}$ and $\kappa_v: [0, L_v] \rightarrow \mathbb{R}$ the geodesic curvatures of γ_u and γ_v respectively (see Figure 4.1). We moreover remark that, since φ is a Chebyshev net, it satisfies the following property:

$$\kappa_u^{\text{map}}(u, v) = -\partial_u \omega(u, v), \quad (4.7a)$$

$$\kappa_v^{\text{map}}(u, v) = \partial_v \omega(u, v), \quad (4.7b)$$

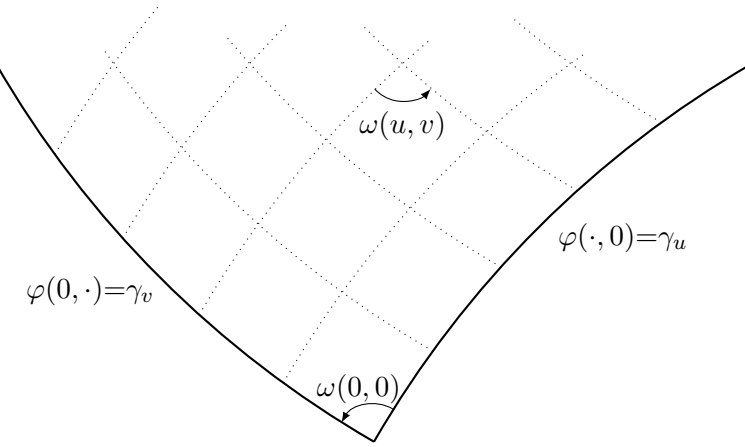


Fig. 4.1 Illustration of the coordinate curves of a Chebyshev net φ

for all $(u, v) \in D$, where $\kappa_u^{\text{map}} : D \rightarrow \mathbb{R}$ and $\kappa_v^{\text{map}} : D \rightarrow \mathbb{R}$ are respectively the geodesic curvatures of the u -coordinate curves and of the v -coordinate curves of φ . We obtain by combining (4.2) and (4.7) that the angle distribution ω satisfies the boundary conditions

$$\omega(u, 0) = \angle(\gamma'_u(0), \gamma'_v(0)) - \int_0^u \kappa_u(s) ds, \quad \forall u \in [0, L_u], \quad (4.8a)$$

$$\omega(0, v) = \angle(\gamma'_u(0), \gamma'_v(0)) + \int_0^v \kappa_v(s) ds, \quad \forall v \in [0, L_v]. \quad (4.8b)$$

We will first show that we can associate with any angle distribution $\omega : D \rightarrow \mathbb{R}/2\pi\mathbb{Z}$ satisfying (4.8) a unique mapping $\varphi := \mathcal{I}(\gamma, \omega) : D \rightarrow M$ satisfying (4.1b), (4.2), and (4.7b), and then we will show that this mapping also satisfies (4.1a) and (4.7a) whenever ω satisfies the integrability condition (4.5). This section aims at proving the following result:

Theorem 4.1 (Existence and uniqueness of Chebyshev nets). *Let M be a smooth, open, complete, and simply connected surface. Let $\gamma_u : [0, L_u] \rightarrow M$, with $L_u \in \mathbb{R}_*^+$, and $\gamma_v : [0, L_v] \rightarrow M$, with $L_v \in \mathbb{R}_*^+$, be two curves with respective geodesic curvatures $\kappa_u : [0, L_u] \rightarrow \mathbb{R}$ and $\kappa_v : [0, L_v] \rightarrow \mathbb{R}$, and such that $\gamma_u(0) = \gamma_v(0)$. Suppose that $\angle(\gamma'_u(0), \gamma'_v(0)) \in (0, \pi)$. Then, there exists a unique angle distribution $\omega : D \rightarrow \mathbb{R}/2\pi\mathbb{Z}$, with $D = [0, L_u] \times [0, L_v]$, verifying the boundary conditions (4.8) and satisfying the Hazzidakis formula (4.6), with $\varphi := \mathcal{I}(\gamma, \omega) : D \rightarrow M$ the unique mapping satisfying (4.1b), (4.2) and (4.7b).*

Suppose moreover that we have $0 < \omega(u, v) < \pi$, for all $(u, v) \in D$. Then, φ is a Chebyshev net, i.e., it also satisfies (4.1a) and (4.7a), and the dependency of ω and φ is continuous with respect to the boundary conditions γ_u and γ_v .

In the previous statement, we have not defined precisely the regularity of the objects or the norms on the considered vector spaces. These are defined in Section 4.1.2, and a more accurate statement of Theorem 4.1 is given by Theorem 4.3. A direct consequence of Theorem 4.3 is the following theorem:

Theorem 4.2 (Existence of a unique solution to integrability condition). *Let M be a smooth, open, complete, and simply connected surface. Let $\gamma_u : [0, L_u] \rightarrow M$, with $L_u \in \mathbb{R}_*^+ \cup \{\infty\}$, and $\gamma_v : [0, L_v] \rightarrow M$, with $L_v \in \mathbb{R}_*^+ \cup \{\infty\}$, be two smooth curves with respective geodesic curvatures $\kappa_u : [0, L_u] \rightarrow \mathbb{R}$ and $\kappa_v : [0, L_v] \rightarrow \mathbb{R}$, and such that $\gamma_u(0) = \gamma_v(0)$. Suppose that $\angle(\gamma'_u(0), \gamma'_v(0)) \in (0, \pi)$. Then, there exists a unique angle distribution $\omega : D \rightarrow \mathbb{R}/2\pi\mathbb{Z}$, with $D = [0, L_u] \times [0, L_v]$, verifying the*

boundary conditions (4.8) and satisfying the Hazzidakis formula (4.6), with $\varphi := \mathcal{I}(\gamma, \omega) : D \rightarrow M$ the unique mapping satisfying (4.1b), (4.2) and (4.7b).

Suppose moreover that there exists $\tilde{D} = [0, \tilde{L}_u] \times [0, \tilde{L}_v]$, with $\tilde{L}_u \in (0, L_u]$ and $\tilde{L}_v \in (0, L_v]$, such that $0 < \omega(u, v) < \pi$, for all $(u, v) \in \tilde{D}$. Then, the mapping $\varphi|_{\tilde{D}}$ is a Chebyshev nets, that is, it satisfies (4.1) for all $(u, v) \in \tilde{D}$.

In order to prove Theorem 4.3, we proceed along the following plan. In Section 4.2, given the two curves γ_u and γ_v on M and the angle distribution $\omega : D \rightarrow \mathbb{R}/2\pi\mathbb{Z}$ between the coordinate curves, we first construct the candidate Chebyshev net $\varphi = \mathcal{I}(\gamma, \omega) : D \rightarrow M$. We then show that whenever φ satisfies the integrability condition (4.5), this mapping also satisfies (4.1) under suitable regularity conditions. In Section 4.3, we view the Hazzidakis formula (4.6), with $\varphi := \mathcal{I}(\gamma, \omega)$, as a fixed-point problem on ω . We show existence and uniqueness of the solution to this fixed-point equation for the curves γ_u and $\gamma_v|_{[0, L_0]} : [0, L_0] \rightarrow M$, where $L_0 \in (0, L_v]$ is a constant depending on the C^0 -norm of the geodesic curvatures of γ_u and γ_v . This result is called “local existence” in what follows. We finally extend this result to the curves γ_u and γ_v of arbitrary length, in the spirit of the Cauchy–Lipschitz theorem.

Functional spaces and statement of the main result

We now turn to the regularity required on the curves γ_u and γ_v and on the angle distribution ω . In what follows, we define the spaces in which the curves, parametrizations and angles are constructed. Recall that

$$D = [0, L_u] \times [0, L_v], \quad \text{with } L_u, L_v \in \mathbb{R}_*^+.$$

Let $k \in \mathbb{N}$ and $L \in (0, L_v]$. We consider the space $C^{k+2}([0, L], M)$ of curves γ with general parametrizations on M and such that the geodesic curvature of γ has C^k -regularity. We define $\Gamma^{k+2}([0, L])$ to be the closed subset of $C^{k+2}([0, L], M)$ formed by arc-length parametrized curves:

$$\Gamma^{k+2}([0, L]) = \left\{ \gamma \in C^{k+2}([0, L], M) \text{ s.t. } \forall s \in [0, L], |\gamma'(s)|_{g(\gamma(s))} = 1 \right\},$$

equipped with the norm $\|\cdot\|_{C^{k+2}([0, L])}$. Note that the norms involved in the Sobolev spaces are the Euclidean norms. Let $r \in \mathbb{N}$. We define the space $\Theta^{r,k}(D)$ of angle distributions on D :

$$\Theta^{r,k}(D) = C^r([0, L_u], C^k([0, L_v], \mathbb{R}/2\pi\mathbb{Z})),$$

equipped with the norm

$$\|\omega\|_{\Theta^{r,k}(D)} = \|\omega\|_{C^r([0, L_u], C^k([0, L_v]))}.$$

In the case where $k = r$, the notation of $\Theta^{k,k}(D)$ is simplified to $\Theta^k(D)$. We denote $\Phi^{r,k+2}(D)$ the closed subset of the Banach space $C^r([0, L_u], C^{k+2}([0, L_v], M))$ formed by arc-length parametrized curves with C^{k+2} -regularity depending on a parameter of regularity C^r :

$$\Phi^{r,k+2}(D) := C^r([0, L_u], \Gamma^{k+2}([0, L_v])) \subset C^r([0, L_u], C^{k+2}([0, L_v], M)).$$

This space is equipped with the norm

$$\|\varphi\|_{\Phi^{r,k+2}(D)} = \|\varphi\|_{C^r([0, L_u], \Gamma^{k+2}([0, L_v]))}.$$

Note that we do not require the regularity on the first variable to be the same as the regularity on the second variable. This will be made visible in the construction of the candidate Chebyshev net φ : the first coordinate denotes the initial conditions of an ordinary differential equation in the second coordinate, which does not entail the same regularity.

Let $\gamma = (\gamma_u, \gamma_v) \in \Gamma^{r+2}([0, L_u]) \times \Gamma^{k+2}([0, L_v])$ be two curves with respective geodesic curvatures $\kappa_u : [0, L_u] \rightarrow \mathbb{R}$ and $\kappa_v : [0, L_v] \rightarrow \mathbb{R}$, and such that $\gamma_u(0) = \gamma_v(0)$. We define the affine subspace composed of the angle distributions satisfying the boundary conditions (4.8):

$$\Theta_{\gamma}^{r,k}(D) = \left\{ \omega \in \Theta^{r,k}(D), \text{ s.t. } \omega \text{ satisfies (4.8)} \right\}.$$

The subspace $\Theta_{\gamma}^{r,k}$ is a closed subset of the Banach space $\Theta^{r,k}$. Again, in the case where $r=k$, we set $\Theta_{\gamma}^k = \Theta_{\gamma}^{k,k}$.

We can now restate Theorem 4.1 with the correct regularity.

Theorem 4.3 (Existence and uniqueness of Chebyshev nets). *Let M be a smooth, open, complete, and simply connected surface and let $k \in \mathbb{N}$. Let $\gamma = (\gamma_u, \gamma_v) \in \Gamma^{k+2}([0, L_u]) \times \Gamma^{k+2}([0, L_v])$, with $L_u, L_v \in \mathbb{R}_*^+$, be two curves with respective geodesic curvatures $\kappa_u \in C^k([0, L_u])$ and $\kappa_v \in C^k([0, L_v])$, and such that $\gamma_u(0) = \gamma_v(0)$. Suppose that $\angle(\gamma'_u(0), \gamma'_v(0)) \in (0, \pi)$. Then, there exists a unique angle distribution $\omega := \mathcal{J}(\gamma) \in \Theta_{\gamma}^{k+1}(D)$, with $D = [0, L_u] \times [0, L_v]$, verifying the boundary conditions (4.8) and satisfying the Hazzidakis formula (4.6), with $\varphi := \mathcal{I}(\gamma, \omega) \in \Phi^{k+2}(D)$ the unique mapping satisfying (4.1b), (4.2) and (4.7b).*

Suppose moreover that we have $0 < \omega(u, v) < \pi$, for all $(u, v) \in D$. Then, φ is a Chebyshev net, i.e., it also satisfies (4.1a) and (4.7a), and the mappings

$$\begin{aligned} \mathcal{J} : \quad \Gamma^{k+2}([0, L_u]) \times \Gamma^{k+2}([0, L_v]) &\rightarrow \Theta^{k+1}(D), \\ \mathcal{I} : \quad \Gamma^{k+2}([0, L_u]) \times \Gamma^{k+2}([0, L_v]) \times \Theta^{k+1}(D) &\rightarrow \Phi^{k+2}(D) \end{aligned}$$

are continuous.

Construction of a Chebyshev net from its angle distribution

We now prove that a Chebyshev net can be constructed uniquely from its angle distribution. We start by showing in Subsection 4.2.1 that the construction of curves from their geodesic curvature, initial point and initial tangent vector is a well-posed problem. We then define, following [25], the mapping $\mathcal{I}(\gamma, \omega)$ which, for given boundary curves γ_u and γ_v , associates with any angle distribution ω satisfying the boundary conditions (4.8) the candidate Chebyshev net φ , with angle distribution ω , satisfying the boundary conditions (4.2) (Subsection 4.2.2). The parametrization φ is constructed in such a way that the v -coordinate curves are arc-length parametrized curves with geodesic curvatures satisfying (4.7b). We moreover show the continuity of the mapping \mathcal{I} with respect to the angle distribution and to the delimiting curves γ_u and γ_v . In Subsection 4.2.3, we show that the candidate Chebyshev net φ has improved regularity in the u -coordinate whenever ω satisfies the integrability condition (4.5). Finally, in Subsection 4.2.4, we prove that φ is indeed a Chebyshev net if ω satisfies the integrability condition and has a sufficient regularity.

Construction of curves from their geodesic curvature

Proposition 4.4 (Construction of curves from their geodesic curvature). *Let M be a smooth, open, complete, and simply connected surface. Let $L_{\max} \in \mathbb{R}_*^+$, $L \in (0, L_{\max})$ and $k, r \in \mathbb{N}$. Let $x \in M$, let $V \in T_x M$ be a unit vector, i.e., a vector such that $|V|_g = 1$, and let $\kappa \in C^k([0, L], \mathbb{R})$. Then, there exists a unique (arc-length parametrized) curve $\sigma(x, V, \kappa) := \sigma \in \Gamma^{k+2}([0, L])$ such that $\sigma(0) = x$, $\sigma'(0) = V$, and with geodesic curvature κ .*

Moreover, let $L_1, L_2 \in (0, L_{\max})$, let $x_1, x_2 \in C^r([0, L_1], M)$ be initial position distributions and let $V_1, V_2 \in C^r([0, L_1], TM)$, with $|V_1|_g = |V_2|_g = 1$, be initial derivatives distribution. Let $D_{1,2} = [0, L_1] \times [0, L_2]$ and let $\kappa_1, \kappa_2 \in C^r([0, L_1], C^k([0, L_2], \mathbb{R}))$ be geodesic curvatures. We denote $\sigma_1, \sigma_2 : [0, L_1] \rightarrow \Gamma^{k+2}([0, L_2])$ the two families of curves defined by $\sigma_m(\eta, \cdot) := \sigma(x_m(\eta), V_m(\eta), \kappa_m(\eta, \cdot))$, for all $\eta \in [0, L_1]$ and $m \in \{1, 2\}$. Then, we have

$$\sigma_1, \sigma_2 \in \Phi^{r, k+2}(D_{1,2}) = C^r([0, L_1], \Gamma^{k+2}([0, L_2])),$$

and, for all $m \in \{1, 2\}$,

$$\|\sigma_m\|_{\Phi^{r, k+2}(D_{1,2})} \leq C, \quad (4.9)$$

where the constant C depends on L_{\max} , $\|x_m\|_{C^r([0, L_1])}$, $\|V_m\|_{C^r([0, L_1])}$, and $\|\kappa_m\|_{C^r([0, L_1], C^k([0, L_2]))}$. Finally, we have

$$\begin{aligned} \|\sigma_1 - \sigma_2\|_{\Phi^0(D_{1,2})} &\leq C \left(L_2 \|\kappa_1 - \kappa_2\|_{C^0(D_{1,2})} \right. \\ &\quad \left. + \|x_1 - x_2\|_{C^0([0, L_1])} + \|V_1 - V_2\|_{C^0([0, L_1])} \right), \end{aligned} \quad \text{if } k=0 \text{ and } r=0, \quad (4.10a)$$

$$\begin{aligned} \|\sigma_1 - \sigma_2\|_{\Phi^{r, k+2}(D_{1,2})} &\leq \tilde{C} \left(\|\kappa_1 - \kappa_2\|_{C^r([0, L_1], C^k([0, L_2]))} \right. \\ &\quad \left. + \|x_1 - x_2\|_{C^r([0, L_1])} + \|V_1 - V_2\|_{C^r([0, L_1])} \right), \end{aligned} \quad (4.10b)$$

where the constants C and \tilde{C} depend on L_{\max} , $\|x_m\|_{C^r([0, L_1])}$, $\|V_m\|_{C^r([0, L_1])}$, and $\|\kappa_m\|_{C^r([0, L_1], C^k([0, L_2]))}$, with $m \in \{1, 2\}$.

We illustrate the family of curves σ_1 introduced in Proposition 4.4 in Figure 4.2.

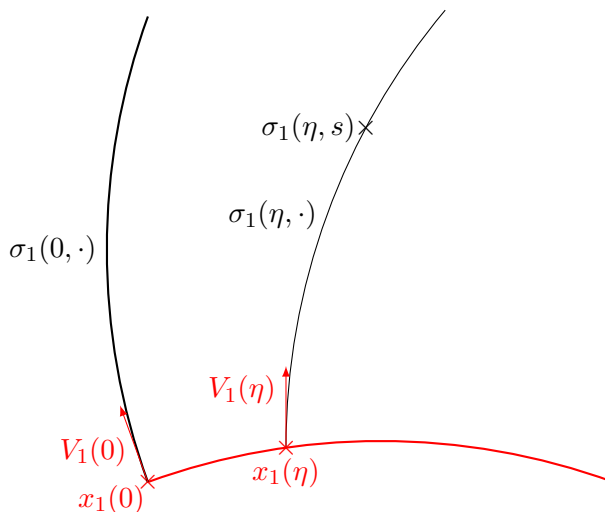


Fig. 4.2 Illustration of the construction of the family of curves σ_1

Proof. To prove the claim, we proceed as follows. We first introduce in Step 1 the geodesic curvature equation that permits to define uniquely a curve from its geodesic curvature. The existence and the uniqueness of the curve is proved in Step 2 using Cauchy–Lipschitz theorem. Then, in order to apply an induction argument, we prove (4.9) and (4.10) in the case $k=0$ and $r=0$ using Grönwall’s inequality. The equation satisfied by the derivatives of the solution is presented in a generic form to facilitate the end of the proof in Step 3. Finally, we prove (4.9) and (4.10b) in Steps 4 and 5 using induction arguments. Whenever there is no ambiguity, the domain of the variables will be omitted.

Step 1 (*Formulation of the geodesic curvature equation*). Let (σ^1, σ^2) , with $\sigma^1, \sigma^2 : [0, L] \rightarrow \mathbb{R}$, be the coordinates of the candidate curve $\sigma : [0, L] \rightarrow M$ with geodesic curvature κ . We denote $\frac{D}{dt}$ the covariant derivative along the curve σ . The geodesic curvature equation for arc-length parametrized curves gives

$$\frac{D}{dt} \sigma' = \kappa \sigma'^\perp, \quad (4.11)$$

which can be written, in coordinates,

$$\dot{X} = G(X) + \kappa f(X), \quad (4.12)$$

with $X(0) = (x^1, x^2, V^1, V^2)$. Here, we have denoted

$$X = \begin{pmatrix} \sigma^1 \\ \sigma^2 \\ \sigma'^1 \\ \sigma'^2 \end{pmatrix}, \quad f(X) = \begin{pmatrix} 0 \\ 0 \\ N^1 \\ N^2 \end{pmatrix}, \quad G(X) = \begin{pmatrix} X^3 \\ X^4 \\ - \sum_{1 \leq i, j \leq 2} \Gamma_{i,j}^1(X^1, X^2) X^{2+i} X^{2+j} \\ - \sum_{1 \leq i, j \leq 2} \Gamma_{i,j}^2(X^1, X^2) X^{2+i} X^{2+j} \end{pmatrix},$$

Γ_{ij}^k being the smooth Christoffel symbols, G the smooth geodesic function and N the normal vector defined by

$$N = \begin{pmatrix} N^1 \\ N^2 \end{pmatrix} = \sqrt{\det g(X^1, X^2)} g^{-1}(X^1, X^2) \begin{pmatrix} -X^4 \\ X^3 \end{pmatrix}.$$

Step 2 (*Proof for $k=0$ and $r=0$*). As $G + \kappa f$ is continuous and locally Lipschitz continuous with respect to X , owing to Cauchy–Lipschitz theorem, there exists a local solution to (4.12). Moreover, since σ is by construction arc-length parametrized, we have $|\sigma'|_g = 1$ and we infer from (4.3) that $|\sigma'| \leq C_{\text{surf}}$. Hence, the image of X is included in a ball \mathcal{B} whose radius depends only on L_{\max} and C_{surf} . We deduce that the solution is defined on $[0, L]$. Moreover, G and f are Lipschitz continuous with respect to X on \mathcal{B} . Hence, $G + \kappa f$ is Lipschitz continuous with respect to X on \mathcal{B} , so that the uniqueness of the solution follows. Moreover, we infer from (4.12) that $\sigma \in \Gamma^2([0, L])$.

Let $m \in \{1, 2\}$ and let $X_m = (\sigma_m^1, \sigma_m^2, \sigma_m'^1, \sigma_m'^2)^t : D_{1,2} \rightarrow \mathbb{R}^4$ be such that $X_m(\eta, \cdot)$ is the unique solution to (4.12) with $\kappa = \kappa_m(\eta, \cdot)$, for all $\eta \in [0, L_1]$. First, owing to [27, Chap. V, Th. 2.1], we have $X_m \in C^0([0, L_1], C^1([0, L_2]))$, so that $\sigma_m \in \Phi^{0,2}(D_{1,2})$. Then, since $|\sigma'| \leq C_{\text{surf}}$, we infer that $\|\sigma_m\|_{\Phi^{0,2}(D_{1,2})} \leq C$, where the constant C depends on $\|\sigma_m(\cdot, 0)\|_{C^0([0, L_1])}$ and $\|X'_m\|_{C^0(D_{1,2})}$. Moreover, due to $|f(X_m)|_g = |\sigma'_m|_g = 1$, we have

$$|f(X_m)| \leq C_{\text{surf}}. \quad (4.13)$$

Furthermore, since $X_m(\{\eta\} \times [0, L_2]) \subset \mathcal{B}$, we infer that $G(X_m)$ is bounded and that this bound only depends on \mathcal{B} , so that it only depends on $X_m(\eta, 0)$, L_{\max} and C_{surf} , for all $\eta \in [0, L_1]$. We conclude that

$$\|\sigma_m\|_{\Phi^{0,2}(D_{1,2})} \leq C,$$

where the constant C depends on $\|x_m\|_{C^0([0, L_1])}$ and $\|\kappa_m\|_{C^0(D_{1,2})}$, and (4.9) holds with $k=r=0$. Then, since the restriction of G and f to \mathcal{B} are Lipschitz continuous in the variable X with coefficients denoted respectively C_G and C_f , we have

$$|\dot{X}_1 - \dot{X}_2| \leq (C_G + |\kappa_1| C_f) |X_2 - X_1| + |\kappa_2 - \kappa_1| \|f(X_2)\|_{C^0(D_{1,2})}.$$

Therefore, using Grönwall's inequality and (4.13), we infer that

$$|X_1(t) - X_2(t)| \leq \exp \left[t(C_G + C_f \|\kappa_1\|_{C^0(D_{1,2})}) \right] \left(|X_2(0) - X_1(0)| + C_{\text{surf}} \int_0^t |\kappa_2 - \kappa_1| \right), \quad (4.14)$$

for all $t \in [0, L]$. We deduce that (4.10a) and (4.10b) are satisfied for $k=r=0$.

Step 3 (*Differential equation on the derivatives of X*). Let $m \in \{1, 2\}$. Owing to [27, Chap. V, Th. 4.1], we have that $\sigma \in \Gamma^{k+2}([0, L])$ and $\sigma_m \in \Phi^{r,k+2}(D_{1,2})$. We use the following notation: for $I = (i_1, i_2) \in \mathbb{N}^2$, we set $\partial^I f(\eta, t) = \partial_\eta^{i_1} \partial_t^{i_2} f(\eta, t)$. We denote $(\mathcal{H}_{r,k})$, with $r, k \in \mathbb{N}^*$, the following induction hypothesis:

for all $I = (i_1, i_2) \in \{0, \dots, r\} \times \{0, \dots, k\}$ such that $I \neq (0, 0)$, we have

$$\begin{aligned} \partial_t \partial^I X_m &= (\nabla G(X_m) + \kappa_m \nabla f(X_m)) \partial^I X_m \\ &+ \sum_{0 \leq \alpha \leq i_1} \sum_{0 \leq \beta \leq i_2} F_{\alpha,\beta}^I \left[(\partial^{(p,q)} X_m)_{0 \leq p+\alpha \leq i_1, 0 \leq q+\beta \leq i_2, p+q < i_1+i_2} \right] \partial^{(\alpha,\beta)} \kappa_m, \end{aligned} \quad (4.15)$$

where $F_{\alpha,\beta}^I : \mathbb{R}^{4n_0} \rightarrow \mathbb{R}^4$, with

$$n_0 = \begin{cases} (i_1 - \alpha + 1)(i_2 - \beta + 1), & \text{if } \alpha + \beta \neq 0, \\ (i_1 + 1)(i_2 + 1) - 1, & \text{otherwise,} \end{cases}$$

are C^∞ functions, for all $(\alpha, \beta) \in \{0, \dots, i_1\} \times \{0, \dots, i_2\}$.

We denote ∂_1 and ∂_2 the derivatives with respect to η and t respectively. We first obtain from (4.12) that, for all $m \in \{1, 2\}$ and $i \in \{1, 2\}$,

$$\partial_t \partial_i X_m = \nabla G(X_m) \partial_i X_m + \partial_i \kappa_m f(X_m) + \kappa_m \nabla f(X_m) \partial_i X_m.$$

Hence, (4.15) is satisfied for $I = (0, 1)$ and $I = (1, 0)$, so that $(\mathcal{H}_{1,1})$ holds. We now suppose that $(\mathcal{H}_{r,k})$ holds for $r, k \in \mathbb{N}^*$. Then, for $I = (i_1, i_2)$ with $i_1 = r$ and $i_2 = k$, we have

$$\begin{aligned} \partial_t \partial_i \partial^I X_m &= (\nabla G(X_m) + \kappa_m \nabla f(X_m)) \partial_i \partial^I X_m + \partial_i [\nabla G(X_m) + \kappa_m \nabla f(X_m)] \partial^I X_m \\ &+ \sum_{0 \leq \alpha \leq i_1} \sum_{0 \leq \beta \leq i_2} \left[\partial_i \left(F_{\alpha,\beta}^I \left[(\partial^{(p,q)} X_m)_{0 \leq p+\alpha \leq i_1, 0 \leq q+\beta \leq i_2, p+q < i_1+i_2} \right] \right) \partial^{(\alpha,\beta)} \kappa_m \right. \\ &\quad \left. + F_{\alpha,\beta}^I \partial_i \partial^{(\alpha,\beta)} \kappa_m \right]. \end{aligned}$$

The first term is in the form of the first term on the right-hand side of (4.15) and the last two terms can be put in the form of the second term on the right-hand side of (4.15). Equation (4.15) is then satisfied for $I = (r+1, k)$ and $I = (r, k+1)$, so that $(\mathcal{H}_{r+1,k})$ and $(\mathcal{H}_{r,k+1})$ hold. The claim follows.

Step 4 (*Proof of (4.9)*). Let $m \in \{1, 2\}$. First note that we have by definition

$$\|\sigma_m\|_{\Phi^{r,k+2}(D_{1,2})} \leq \sum_{i_1=0}^r \sum_{i_2=0}^{k+1} \|\partial_\eta^{i_1} \partial_t^{i_2} X_m\|_{C^0(D_{1,2})}.$$

Then, to obtain (4.9), we only need to prove that

$$\|\partial^I X_m\|_{C^0(D_{1,2})} \leq C, \quad (4.16)$$

where the constant C depends on L_{\max} , $\|x_m\|_{C^{i_1}([0, L_1])}$, $\|V_m\|_{C^{i_1}([0, L_1])}$, and $\|\kappa_m\|_{C^{i_1}([0, L_1], C^{i_2}([0, L_2]))}$, for all $I = (i_1, i_2) \in \{0, \dots, r\} \times \{0, \dots, k+1\}$. We prove (4.16) by induction on $I \in \{0, \dots, r\} \times \{0, \dots, k+1\}$. Hence, we first consider the case $i_2 = 0$, in which case we have, using (4.15) and Grönwall's inequality,

$$\begin{aligned} |\partial_\eta^{i_1} X_m(t)| &\leq \exp [\|\nabla G(X_m) + \kappa_{\sigma_m} \nabla f(X_m)\|_{C^0(D_{1,2})} t] \\ &\times \left(|\partial_\eta^{i_1} X_m(0)| + \sum_{\alpha=0}^{i_1} \int_0^t \left| F_{\alpha,0}^{(i_1,0)} [X_m, \dots, \partial_\eta^{i_1-1} X_m] \partial^{(\alpha,0)} \kappa_{\sigma_m} \right| dt \right), \end{aligned}$$

for all $i_1 \in \{1, \dots, r\}$. Moreover, from Step 2, we have that (4.16) holds in the case where $I = (0, 0)$. Then, since the functions $F_{\alpha,0}^{(i_1,0)}$ have C^∞ -regularity with respect to $(X_m, \dots, \partial_\eta^{i_1-1} X_m)$, for all $\alpha \in \{0, \dots, i_1\}$ and $i_1 \in \{1, \dots, r\}$, an induction argument on $i_1 \in \{0, \dots, r\}$ permits to prove that (4.16) holds for all $I \in \{0, \dots, r\} \times \{0\}$.

Now, noting that $\partial_t \partial^I X_m = \partial_\eta^{i_1} \partial_t^{i_2+1} X_m$, we infer from (4.15) that

$$\begin{aligned} \|\partial_t \partial^I X_m\|_{C^0(D_{1,2})} &\leq \|\nabla G(X_m) + \kappa \nabla f(X_m)\|_{C^0(D_{1,2})} \|\partial^I X_m\|_{C^0(D_{1,2})} \\ &+ \sum_{0 \leq \alpha \leq i_1} \sum_{0 \leq \beta \leq i_2} \left\| F_{\alpha,\beta}^I [(\partial^{(p,q)} X_m)_{0 \leq p+\alpha \leq i_1, 0 \leq q+\beta \leq i_2, p+q < i_1+i_2}] \right\|_{C^0(D_{1,2})} \|\partial^{(\alpha,\beta)} \kappa_m\|_{C^0(D_{1,2})}, \end{aligned}$$

for all $I = (i_1, i_2) \in \{0, \dots, r\} \times \{0, \dots, k\}$ such that $I \neq (0, 0)$. Finally, since (4.16) holds for all $I = (i_1, 0) \in \{0, \dots, r\} \times \{0\}$ and for $I = (0, 1)$ by step 2, and since all the functions $F_{\alpha,\beta}^I$ have C^∞ -regularity, the induction argument on I to prove that (4.16) holds for all $I \in \{0, \dots, r\} \times \{0, \dots, k+1\}$ is straightforward. We conclude that (4.9) holds.

Step 5 (*Proof of (4.10b)*). Let $I = (i_1, i_2) \in \{0, \dots, r\} \times \{0, \dots, k\}$ be such that $I \neq (0, 0)$ and let $m \in \{1, 2\}$. Owing to (4.9), $\partial^I X_m$ is bounded by a constant depending only on $\|\kappa_m\|_{C^r([0, L_1], C^k([0, L_2]))}$, $\|x_m\|_{C^r([0, L_1])}$, and $\|V_m\|_{C^r([0, L_1])}$, for all $\tilde{I} \in \{0, \dots, r\} \times \{0, \dots, k\}$. Hence, the smooth functions $F_{\alpha,\beta}^I$ are Lipschitz continuous on the compact set defined by the image of the derivatives of X_m , for all $(\alpha, \beta) \in \{0, \dots, i_1\} \times \{0, \dots, i_2\}$. We denote $C_{F_{\alpha,\beta}^I}$ their respective Lipschitz coefficients in

this compact set and we set $W_m = \partial^I X_m$. Using (4.15), we easily obtain that

$$\begin{aligned} |\partial_t W_2 - \partial_t W_1| &\leq (\|\nabla G(X_1)\|_{C^0} + |\kappa_1| \|\nabla f(X_1)\|_{C^0}) |W_2 - W_1| \\ &\quad + \left(|\kappa_1 \nabla f(X_1) - \kappa_2 \nabla f(X_2)| + |\nabla G(X_1) - \nabla G(X_2)| \right) \|W_2\|_{C^0} \\ &\quad + \sum_{\alpha=0}^{i_1} \sum_{\beta=0}^{i_2} C_{F_{\alpha,\beta}^I} \sum_{\substack{p \in \{0, \dots, i_1\}, q \in \{0, \dots, i_2\} \\ p+q < i_1+i_2}} |\partial^{(p,q)} X_2 - \partial^{(p,q)} X_1| \|\partial^{(\alpha,\beta)} \kappa_1\|_{C^0} \\ &\quad + \sum_{\alpha=0}^{i_1} \sum_{\beta=0}^{i_2} \left\| F_{\alpha,\beta}^I [(\partial^{(p,q)} X_2)_{0 \leq p+\alpha \leq i_1, 0 \leq q+\beta \leq i_2, p+q < i_1+i_2}] \right\|_{C^0} |\partial^{(\alpha,\beta)} \kappa_1 - \partial^{(\alpha,\beta)} \kappa_2|, \end{aligned}$$

where C^0 refers to the norm $C^0(D_{1,2})$. Using Grönwall's inequality, we infer that

$$\begin{aligned} |W_1 - W_2|(\eta, t) &\leq \exp [\|\nabla G(X_1) + \kappa_1 \nabla f(X_1)\|_{C^0} t] \times \\ &\quad \left(|W_1 - W_2|(\eta, 0) + \|W_2\|_{C^0} \max_{i \in \{1, 2\}} \max (\|\kappa_i\|_{C^0}, \|\nabla f(X_i)\|_{C^0}, 1) \int_0^t [|\kappa_2 - \kappa_1| + (C_{\nabla f} + C_{\nabla G}) |X_2 - X_1|] \right. \\ &\quad + \sum_{\alpha=0}^{i_1} \sum_{\beta=0}^{i_2} C_{F_{\alpha,\beta}^I} \|\partial^{(\alpha,\beta)} \kappa_1\|_{C^0} \sum_{\substack{p \in \{0, \dots, i_1\}, q \in \{0, \dots, i_2\} \\ p+q < i_1+i_2}} \int_0^t |\partial^{(p,q)} X_2 - \partial^{(p,q)} X_1| \\ &\quad \left. + \sum_{\alpha=0}^{i_1} \sum_{\beta=0}^{i_2} \left\| F_{\alpha,\beta}^I [(\partial^{(p,q)} X_2)_{0 \leq p+\alpha \leq i_1, 0 \leq q+\beta \leq i_2, p+q < i_1+i_2}] \right\|_{C^0} \int_0^t |\partial^{(\alpha,\beta)} \kappa_1 - \partial^{(\alpha,\beta)} \kappa_2| \right), \end{aligned}$$

where C^0 refers to the norm $C^0(D_{1,2})$, and $C_{\nabla f}$ and $C_{\nabla G}$ are the Lipschitz constants of ∇f and ∇G , respectively. Then, we obtain using (4.9) that

$$\begin{aligned} \|\sigma_1 - \sigma_2\|_{\Phi^{i_1, i_2+1}(D_{1,2})} &\leq C \left(\|\kappa_1 - \kappa_2\|_{C^{i_1}([0, L_1], C^{i_2}([0, L_2]))} + \|x_1 - x_2\|_{C^{i_1}([0, L_1])} \right. \\ &\quad \left. + \|V_1 - V_2\|_{C^{i_1}([0, L_1])} + \Sigma_1 + \Sigma_2 \right), \end{aligned}$$

where the constant C depends on L_{\max} , $\|x_l\|_{C^{i_1}([0, L_1])}$, $\|V_l\|_{C^{i_1}([0, L_1])}$, and $\|\kappa_l\|_{C^{i_1}([0, L_1], C^{i_2}([0, L_2]))}$, with $l \in \{1, 2\}$, and

$$\Sigma_1 = \begin{cases} \|\sigma_1 - \sigma_2\|_{\Phi^{i_1-1, i_2+1}(D_{1,2})}, & \text{if } i_1 > 0, \\ 0, & \text{otherwise,} \end{cases} \quad \Sigma_2 = \begin{cases} \|\sigma_1 - \sigma_2\|_{\Phi^{i_1, i_2}(D_{1,2})}, & \text{if } i_2 > 0, \\ 0, & \text{otherwise.} \end{cases}$$

Hence, using (4.15), we obtain in the same manner that

$$\begin{aligned} \|\sigma_1 - \sigma_2\|_{\Phi^{i_1, i_2+2}(D_{1,2})} &\leq C \left(\|\kappa_1 - \kappa_2\|_{C^{i_1}([0, L_1], C^{i_2}([0, L_2]))} + \|x_1 - x_2\|_{C^{i_1}([0, L_1])} \right. \\ &\quad \left. + \|V_1 - V_2\|_{C^{i_1}([0, L_1])} + \Sigma_1 + \Sigma_2 \right), \end{aligned}$$

where the constant C depends on L_{\max} , $\|x_l\|_{C^r([0, L_1])}$, $\|V_l\|_{C^r([0, L_1])}$, and $\|\kappa_l\|_{C^r([0, L_1], C^k([0, L_2]))}$, with $l \in \{1, 2\}$. We then obtain (4.10) by a straightforward induction argument on $I = (i_1, i_2) \in \{0, \dots, r\} \times \{0, \dots, k\}$, recalling that the case $I = (0, 0)$ was proved in Step 2. This concludes the proof of the proposition. ■

Construction of the parametrization

Let $\mathcal{R}_x(\theta)$ be the rotation of angle θ in the tangent plane $T_x M$ at $x \in M$ and let $D = [0, L_u] \times [0, L_v]$, with $L_u, L_v \in \mathbb{R}_*^+$. Let $r, k \in \mathbb{N}$. Using the notation of Proposition 4.4, given an angle distribution $\omega \in \Theta_\gamma^{r+1, k+1}(D)$ satisfying the boundary conditions (4.8) given by the two curves $\gamma = (\gamma_u, \gamma_v) \in \Gamma^{r+2}([0, L_u]) \times \Gamma^{k+2}([0, L_v])$, we set

$$x(\eta) = \gamma_u(\eta) \in M, \quad V(\eta) = \mathcal{R}_{\gamma_u(\eta)}(\omega(\eta, 0)) \gamma'_u(\eta) \in T_{\gamma_u(\eta)} M, \quad (4.17)$$

and $\kappa(\eta, s) = \partial_v \omega(\eta, s)$, for all $(\eta, s) \in D$. Let $\varphi_\omega : D \rightarrow M$ be the family of curves such that the curve $\varphi_\omega(\eta, \cdot) \in \Gamma^{k+2}([0, L_v])$ has initial position $\varphi_\omega(\eta, 0) = x(\eta)$, initial tangent vector $\partial_v \varphi_\omega(\eta, 0) = V(\eta)$, and geodesic curvature $\kappa(\eta, \cdot)$, for all $\eta \in [0, L_u]$ (see Figure 4.3). Note that the mapping φ_ω also depends on the curves $\gamma = (\gamma_u, \gamma_v)$ but since these curves are kept fixed in what follows, we do not mention them explicitly. We denote

$$\begin{aligned} \mathcal{I}(\gamma, \cdot) : \Theta_\gamma^{r+1, k+1}(D) &\rightarrow \Phi^{r+1, k+2}(D), \\ \omega &\mapsto \varphi_\omega, \end{aligned}$$

the mapping that associates with each angle distribution ω with $\Theta^{r+1, k+1}$ -regularity and satisfying the boundary conditions (4.8), the mapping $\varphi_\omega : D \rightarrow M$.

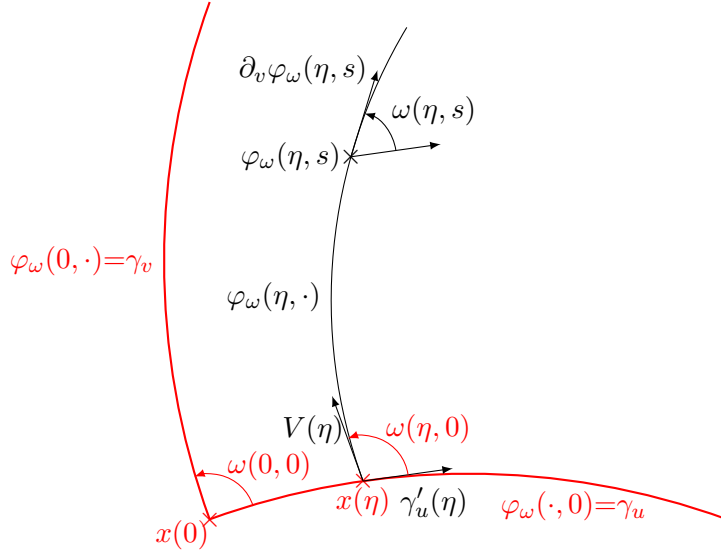


Fig. 4.3 Illustration of the construction of the parametrization φ_ω

Proposition 4.5 (Continuity of the construction). *Let M be a smooth, open, complete, and simply connected surface, let $k, r \in \mathbb{N}$, and let $D = [0, L_u] \times [0, L_v]$, with $L_u, L_v \in \mathbb{R}_*^+$. For all $\gamma = (\gamma_u, \gamma_v) \in \Gamma^{r+2}([0, L_u]) \times \Gamma^{k+2}([0, L_v])$, the mapping $\mathcal{I}(\gamma, \cdot)$ is well defined. Moreover, let $\gamma_1, \gamma_2 \in \Gamma^{r+2}([0, L_u]) \times \Gamma^{k+2}([0, L_v])$, with $\gamma_1 = (\gamma_{u,1}, \gamma_{v,1})$ and $\gamma_2 = (\gamma_{u,2}, \gamma_{v,2})$, be such that $\gamma_{u,1}(0) = \gamma_{u,2}(0) = \gamma_{v,1}(0) = \gamma_{v,2}(0)$ and such that $\gamma'_{u,1}(0) = \gamma'_{u,2}(0)$ and $\gamma'_{v,1}(0) = \gamma'_{v,2}(0)$. Consider the two angle distributions $\omega_m \in \Theta_{\gamma_m}^{r+1, k+1}(D)$, for $m \in \{1, 2\}$. Then, we have*

$$\|\mathcal{I}(\gamma_m, \omega_m)\|_{\Phi^{r+1, k+2}(D)} \leq C \quad (4.18)$$

where the constant C depends on L_u , L_v , $\|\gamma_{u,m}\|_{\Gamma^s([0,L_u])}$, and $\|\omega_m\|_{\Theta^{r+1,k+1}(D)}$, with $s = \max(r+1, 2)$. Moreover, for all $L \in (0, L_v]$, setting $D_L = [0, L_u] \times [0, L]$, we have

$$\begin{aligned} \|\mathcal{I}(\gamma_1, \omega_1) - \mathcal{I}(\gamma_2, \omega_2)\|_{\Phi^0(D_L)} &\leq C \left(L \|\omega_1 - \omega_2\|_{\Theta^1(D_L)} \right. \\ &\quad \left. + \|\gamma_{u,2} - \gamma_{u,1}\|_{\Gamma^2([0, L_u])} \right), \end{aligned} \quad (4.19a)$$

$$\begin{aligned} \|\mathcal{I}(\gamma_1, \omega_1) - \mathcal{I}(\gamma_2, \omega_2)\|_{\Phi^{1,k+2}(D_L)} &\leq C \left(\|\omega_1 - \omega_2\|_{\Theta^{1,k+1}(D_L)} \right. \\ &\quad \left. + \|\gamma_{u,2} - \gamma_{u,1}\|_{\Gamma^2([0, L_u])} \right), \end{aligned} \quad (4.19b)$$

$$\begin{aligned} \|\mathcal{I}(\gamma_1, \omega_1) - \mathcal{I}(\gamma_2, \omega_2)\|_{\Phi^{r+1,k+2}(D_L)} &\leq C \left(\|\omega_1 - \omega_2\|_{\Theta^{r+1,k+1}(D_L)} \right. \\ &\quad \left. + \|\gamma_{u,2} - \gamma_{u,1}\|_{\Gamma^{r+1}([0, L_u])} \right), \end{aligned} \quad (4.19c)$$

where the constant C depends on L_u , L_v , $\|\gamma_{u,i}\|_{\Gamma^s([0, L_u])}$, and $\|\omega_i\|_{\Theta^{r+1,k+1}(D)}$, with $i \in \{1, 2\}$ and $s = \max(r+1, 2)$.

Proof. Since the construction of the mapping φ_ω is the same as that in the construction of Proposition 4.4, we only need to prove that the boundary conditions used in the construction of φ_ω are smooth enough. We denote $\kappa_{u,1} : [0, L_u] \rightarrow \mathbb{R}$ and $\kappa_{u,2} : [0, L_v] \rightarrow \mathbb{R}$ the geodesic curvatures of the curves $\gamma_{u,1}$ and $\gamma_{u,2}$ respectively. Using the notation of Proposition 4.4, for all $m \in \{1, 2\}$ and $u \in [0, L_u]$, we set $x_m(u) = \gamma_{u,m}(u)$ and

$$V_m(u) = \mathcal{R}_{\gamma_{u,m}(u)}(\omega_m(u, 0))\gamma'_{u,m}(u) = \cos(\omega_m(u, 0))\gamma'_{u,m}(u) + \sin(\omega_m(u, 0))\gamma'^\perp_{u,m}(u), \quad (4.20)$$

where $\gamma'^\perp_{u,m}$ is the direct $\frac{\pi}{2}$ -rotation of $\gamma'_{u,m}$. Since $|V_m|_g = 1$, we infer from (4.3) that $\|V_m\|_{C^0([0, L_u])} \leq C_{\text{surf}}$, for all $m \in \{1, 2\}$. Furthermore, using that $\omega_1 \in \Theta_{\gamma_1}^{r+1,k+1}(D)$ and $\omega_2 \in \Theta_{\gamma_2}^{r+1,k+1}(D)$ both satisfy the boundary conditions (4.8), we obtain

$$|\omega_2 - \omega_1|(u, 0) = \left| \int_0^u \kappa_{u,2} - \int_0^u \kappa_{u,1} \right| \leq \int_0^u |\kappa_{u,2} - \kappa_{u,1}|.$$

Hence, using (4.20), we obtain by a straightforward computation that

$$\|V_2 - V_1\|_{C^0([0, L_u])} \leq C \left(\|\kappa_{u,2} - \kappa_{u,1}\|_{C^0([0, L_u])} + \|\gamma'_2 - \gamma'_1\|_{C^0([0, L_u])} \right). \quad (4.21)$$

Let $m \in \{1, 2\}$. Since ω_m satisfies the boundary conditions (4.8) given by the arc-length parametrized curve $\gamma_{u,m}$, we infer from the definition of geodesic curvature (4.4) that

$$\begin{aligned} \frac{D}{du} \gamma'_{u,m} &= \kappa_{u,m} \gamma'^\perp_{u,m} = -\partial_u \omega_m(\cdot, 0) \gamma'^\perp_{u,m}, \\ \frac{D}{du} \gamma'^\perp_{u,m} &= -\kappa_{u,m} \gamma'_{u,m} = \partial_u \omega_m(\cdot, 0) \gamma'_{u,m}, \end{aligned}$$

where $\frac{D}{du}$ is the covariant derivative along the curve $\gamma_{u,m}$. Hence, we deduce from (4.20) that

$$\begin{aligned} \frac{D}{du} V_m(u) &= \partial_u \omega_m(u, 0) \left(\cos(\omega_m(u, 0))\gamma'^\perp_{u,m} - \sin(\omega_m(u, 0))\gamma'_{u,m} \right) \\ &\quad + \cos(\omega_m(u, 0)) \frac{D}{du} \gamma'_{u,m} + \sin(\omega_m(u, 0)) \frac{D}{du} \gamma'^\perp_{u,m} = 0, \end{aligned} \quad (4.22)$$

for all $u \in [0, L_u]$. Therefore, in the same manner as in Proposition 4.4, using that V_m is bounded, (4.21) and (4.22), we obtain

$$\|V_m\|_{C^{r+1}([0, L_u])} \leq C, \quad \|V_1 - V_2\|_{C^{r+1}([0, L_u])} \leq \tilde{C} \|\gamma_{u,1} - \gamma_{u,2}\|_{\Gamma^s([0, L_u])}, \quad (4.23)$$

where $s = \max(r+1, 2)$, the constant C depends on L_u , L_v , and $\|\gamma_{u,m}\|_{\Gamma^s([0, L_u])}$, and the constant \tilde{C} depends on L_u , L_v , and $\|\gamma_{u,l}\|_{\Gamma^s([0, L_u])}$, with $l \in \{1, 2\}$. Moreover, since $x_m = \gamma_{u,m}$, we have

$$\|x_m\|_{C^{r+1}([0, L_u])} = \|\gamma_{u,m}\|_{\Gamma^{r+1}([0, L_u])}, \quad \|x_1 - x_2\|_{C^{r+1}([0, L_u])} = \|\gamma_{u,1} - \gamma_{u,2}\|_{\Gamma^{r+1}([0, L_u])}. \quad (4.24)$$

We set $\kappa_{v,m}^{\text{map}}(u, \cdot) := \partial_v \omega_m(u, \cdot) : [0, L_v] \rightarrow \mathbb{R}$, for all $u \in [0, L_u]$. We conclude the proof using (4.23), (4.24) and Proposition 4.4 with regularity $(r+1, k)$, i.e., with $x_1, x_2 \in C^{r+1}([0, L_u])$, $V_1, V_2 \in C^{r+1}([0, L_u])$ and $\kappa_{v,1}^{\text{map}}, \kappa_{v,2}^{\text{map}} \in C^{r+1}([0, L_u], C^k([0, L_v]))$. \blacksquare

Regularity of the candidate Chebyshev nets

Let us now consider the case where we have the same regularity in both coordinates in the data permitting the construction of φ_ω , i.e., $r = k$. Then, taking $r = k$ in Proposition 4.5 gives an optimal estimate in the second coordinate regularity but a suboptimal estimate in the first coordinate, since we expect C^{k+2} -regularity in both directions. We show in this section that, whenever the mapping constructed satisfies the integrability equation (4.5), it has indeed the expected regularity in the first variable as well.

Proposition 4.6 (Regularity of mappings satisfying the integrability condition). *Keeping the assumptions of Proposition 4.5 with $k = r \in \mathbb{N}$, we moreover suppose that $\omega_m \in \Theta^{k+1}(D)$ satisfies the Hazzidakis formula (4.6) with $\varphi_m := \mathcal{I}(\gamma_m, \omega_m)$, i.e.,*

$$\begin{aligned} \omega_m(u, v) &= \angle(\gamma'_{u,m}(0), \gamma'_{v,m}(0)) - \int_0^u \kappa_{u,m} + \int_0^v \kappa_{v,m} \\ &\quad - \int_0^u \int_0^v K[\mathcal{I}(\gamma_m, \omega_m)(t, s)] \sin(\omega_m(t, s)) dt ds, \end{aligned} \quad (4.25)$$

for all $m \in \{1, 2\}$. Then, we have $\varphi_m \in \Phi^{k+2}(D)$ and

$$\|\mathcal{I}(\gamma_m, \omega_m)\|_{\Phi^{k+2}(D)} \leq C, \quad (4.26)$$

where the constant C depends on L_u , L_v , $\|\gamma_{u,m}\|_{\Gamma^{k+2}([0, L_u])}$, and $\|\omega_m\|_{\Theta^{k+1}(D)}$, for all $m \in \{1, 2\}$. Moreover, we have

$$\begin{aligned} \|\mathcal{I}(\gamma_1, \omega_1) - \mathcal{I}(\gamma_2, \omega_2)\|_{\Phi^{k+2}(D)} &\leq C \left(\|\omega_1 - \omega_2\|_{\Theta^{k+1}(D)} \right. \\ &\quad \left. + \|\gamma_{2,u} - \gamma_{1,u}\|_{\Gamma^{k+2}([0, L_u])} \right) \end{aligned} \quad (4.27)$$

where the constant C depends on L_u , L_v , $\|\gamma_{u,i}\|_{\Gamma^{k+2}([0, L_u])}$ and $\|\omega_i\|_{\Theta^{k+1}(D)}$, for $i \in \{1, 2\}$.

Proof. Let $m \in \{1, 2\}$. First, owing to Proposition 4.5, we have $\varphi_m = \mathcal{I}(\gamma_m, \omega_m) \in \Phi^{k+1, k+2}(D)$. We denote $\kappa_{v,m}^{\text{map}} = \partial_v \omega_m \in C^{k+1}([0, L_u], C^k([0, L_v]))$ the geodesic curvatures of the v -coordinate curves of φ_m . Let us remark that, since $\omega_m \in \Theta^1(D)$ satisfies the Hazzidakis formula (4.25), ω_m satisfies the integrability condition (4.5), i.e.,

$$\partial_{uv} \omega_m = -K(\varphi_m) \sin(\omega_m). \quad (4.28)$$

Then, the claim is obtained by remarking that (4.28) implies that the geodesic curvatures $\kappa_{v,m}^{\text{map}}$ of the v -coordinate curves satisfy

$$\kappa_{v,m}^{\text{map}} \in C^{k+2}([0, L_u], C^k([0, L_v])). \quad (4.29)$$

Indeed, for all $i, j \in \{0, \dots, k\}$, we have

$$\partial_u^{i+1} \partial_v^j \kappa_{v,m}^{\text{map}} = \partial_u^i \partial_v^j (\partial_u \partial_v \omega_m) = \partial_u^i \partial_v^j (-K(\varphi_m) \sin(\omega_m)). \quad (4.30)$$

Hence, since $\omega_m \in \Theta_{\gamma_m}^{k+1}(D)$ and $\varphi_m \in \Phi^{k+1,k+2}(D)$ and since K is smooth, we infer that (4.29) holds and that (4.30) is satisfied for all $i \in \{0, \dots, k+1\}$ and $j \in \{0, \dots, k\}$. Furthermore, we have

$$\partial_u^2 \kappa_{v,m}^{\text{map}} = \partial_u (-K(\varphi_m) \sin(\omega_m)) = -\sin(\omega_m) \nabla K(\varphi_m) \partial_u \varphi_m - K(\varphi_m) \cos(\omega_m) \partial_u \omega_m, \quad (4.31)$$

so that we easily obtain $\|\partial_u^2 \kappa_{v,m}^{\text{map}}\|_{C^k([0, L_u], C^k([0, L_v]))} \leq C$, where the constant C depends on L_u , L_v , $\|\omega_m\|_{\Theta^{k+1}(D)}$, and $\|\varphi_m\|_{\Phi^{k+1}(D)}$. Using moreover (4.18), we conclude that the constant C only depends on L_u , L_v , $\|\omega_m\|_{\Theta^{k+1}(D)}$, and $\|\gamma_{u,m}\|_{\Gamma^s([0, L_u])}$, with $s = \max(k+1, 2)$. We infer that

$$\|\kappa_{v,m}^{\text{map}}\|_{C^{k+2}([0, L_u], C^k([0, L_v]))} \leq C, \quad (4.32)$$

where the constant C depends on L_u , L_v , $\|\omega_m\|_{\Theta^{k+1}(D)}$, and $\|\gamma_{u,m}\|_{\Gamma^s([0, L_u])}$. Recalling that $s = \max(k+1, 2)$, we deduce from (4.31) and (4.19) that

$$\begin{aligned} \|\partial_u^2 \kappa_{v,2}^{\text{map}} - \partial_u^2 \kappa_{v,1}^{\text{map}}\|_{C^k([0, L_u], C^k([0, L_v]))} &\leq \tilde{C} (\|\omega_2 - \omega_1\|_{\Theta^{k+1}(D)} + \|\varphi_2 - \varphi_1\|_{\Phi^{k+1}(D)}) \\ &\leq C (\|\omega_2 - \omega_1\|_{\Theta^{k+1}(D)} + \|\gamma_{u,2} - \gamma_{u,1}\|_{\Gamma^s([0, L_u])}), \end{aligned}$$

where the constants C, \tilde{C} depend on L_u , L_v , $\|\gamma_{u,i}\|_{\Gamma^s([0, L_u])}$, and $\|\omega_i\|_{\Theta^{k+1}(D)}$, with $i \in \{1, 2\}$. We conclude that

$$\|\kappa_{v,2}^{\text{map}} - \kappa_{v,1}^{\text{map}}\|_{C^{k+2}([0, L_u], C^k([0, L_v]))} \leq C (\|\omega_2 - \omega_1\|_{\Theta^{k+1}(D)} + \|\gamma_{u,2} - \gamma_{u,1}\|_{\Gamma^s([0, L_u])}), \quad (4.33)$$

where the constant C depends on L_u , L_v , $\|\gamma_{u,i}\|_{\Gamma^s([0, L_u])}$, and $\|\omega_i\|_{\Theta^{k+1}(D)}$, with $i \in \{1, 2\}$. As in the proof of Proposition 4.5, for all $u \in [0, L_u]$, we set $x_m(u) = \gamma_{u,m}(u)$ and

$$V_m(u) = \mathcal{R}_{\gamma_{u,m}(u)}(\omega_m(u, 0)) \gamma'_{u,m}(u).$$

Before we apply Proposition 4.4 with regularity $(k+2, k)$, let us first note that, as in the proof of Proposition 4.5, the estimate on $x_1, x_2 \in C^{k+2}([0, L_u])$, $V_1, V_2 \in C^{k+2}([0, L_u])$ is given by (4.23), (4.24). Hence, the claim follows from the estimate on $\kappa_{v,1}^{\text{map}}, \kappa_{v,2}^{\text{map}} \in C^{k+2}([0, L_u], C^k([0, L_v]))$ given by (4.32) and (4.33), and Proposition 4.4 with regularity $(k+2, k)$. ■

From integrability conditions to Chebyshev nets

Proposition 4.7 (From integrability conditions to Chebyshev nets). *Let M be a smooth, open, complete, and simply connected surface, let $D = [0, L_u] \times [0, L_v]$, with $L_u, L_v \in \mathbb{R}_*^+$, and let $k \geq 1$. Let $\gamma = (\gamma_u, \gamma_v) \in \Gamma^{k+2}([0, L_u]) \times \Gamma^{k+2}([0, L_v])$. Assume that $\omega \in \Theta_\gamma^{k+1}(D)$ is an angle distribution satisfying the integrability condition (4.5), with $\varphi := \mathcal{I}(\gamma, \omega) \in \Phi^{k+2}(D)$. Suppose moreover that*

$0 < \omega(u, v) < \pi$, for all $(u, v) \in D$. Then, the mapping φ is a Chebyshev net in the sense that it satisfies (4.1).

Proof. First, owing to Proposition 4.6, we have that $\varphi \in \Phi^{k+2}(D)$, so that φ has C^3 -regularity. Since the v -coordinate curves are arc-length parametrized curves, we have by construction $|\partial_v \varphi|_g(u, v) = 1$, and we set $R(u, v) = |\partial_u \varphi|_g(u, v)$, for all $(u, v) \in D$. Then, since γ_u is an arc-length parametrized curve, we have $R(u, 0) = 1$, for all $u \in [0, L_u]$. The proof amounts to showing that

$$\exists L \in (0, L_v], \quad \partial_v R(u, v) = 0, \quad \forall (u, v) \in [0, L_u] \times [0, L]. \quad (4.34)$$

Indeed, suppose that (4.34) is satisfied and denote $I \subset [0, L_v]$ the maximal interval on which we have $R(u, v) = 1$, for all $(u, v) \in [0, L_u] \times I$. Owing to (4.34), we first have that $[0, L] \subset I$, so that I is nonempty. Moreover, suppose that $[0, \tilde{L}_0] \subset I$, for some $\tilde{L}_0 \in (0, L_v]$. Then, since the angle distribution $\omega|_{[0, L_u] \times [\tilde{L}_0, L_v]}$ and the mapping $\varphi|_{[0, L_u] \times [\tilde{L}_0, L_v]}$ satisfy the hypotheses of the proposition, we infer from (4.34) that there exists $\tilde{L}_1 \in (\tilde{L}_0, L_v]$ such that $[0, \tilde{L}_1] \subset I$. Hence, I is open in $[0, L_v]$, and we deduce from the continuity of R that I is closed. Therefore, (4.34) implies the claim.

We now suppose that $L \in (0, L_v]$ is small enough so that $R(u, v) > 0$, for all $(u, v) \in [0, L_u] \times [0, L]$, we set $D_L = [0, L_u] \times [0, L]$, and we set $X_1(u, v) := \langle \frac{\partial_u \varphi}{R}(u, v), \partial_v \varphi(u, v) \rangle_g$ and $X_2(u, v) := \langle \frac{\partial_u \varphi^\perp}{R}(u, v), \partial_v \varphi(u, v) \rangle_g$, for all $(u, v) \in D_L$. Note that by definition $X_1^2 + X_2^2 = 1$ in D_L . Recalling that $R(\cdot, 0) = 1$ by construction of φ , we have

$$X_1(u, 0) = \langle \partial_u \varphi, \partial_v \varphi \rangle_g(u, 0) = \cos(\omega(u, 0)), \quad (4.35a)$$

$$X_2(u, 0) = \langle \partial_u \varphi^\perp, \partial_v \varphi \rangle_g(u, 0) = \sin(\omega(u, 0)), \quad (4.35b)$$

for all $u \in [0, L_u]$. Hence, since X_2 is continuous, up to reducing L , we have $X_2 > 0$ due to the assumption that $0 < \omega < \pi$.

We prove (4.34) as follows. We show that an identification of the Gaussian curvature computed using the local coordinates φ with (4.5) leads to the following integro-differential equation on R in the v -coordinates:

$$\partial_{vv} R = \partial_v \omega \partial_v R T + \frac{(\partial_v R)^2}{R} T^2 - K(\varphi) X_2 \left(\sin \omega \int_0^v \frac{\partial_v R}{X_2} \sin \omega + \cos \omega \int_0^v \frac{\partial_v R}{X_2} \cos \omega \right), \quad (4.36)$$

with $T = \frac{X_1}{X_2}$. We show that $\partial_v R = 0$ is the unique solution to (4.36) to prove the claim (4.34). First, we compute in Step 1 the initial conditions satisfied by $\partial_v R$ necessary to obtain the uniqueness of the solution of (4.36), i.e., we prove that $\partial_v R(\cdot, 0) = 0$. Then, we compute in Steps 2-4 the Gaussian curvature K in terms of R , X_1 and X_2 . Using (4.5), we reduce the Gaussian curvature to (4.36) in Step 5 and we conclude in Step 6.

Step 1 (Initial conditions). We prove that $\partial_v R(u, 0) = 0$, for all $u \in [0, L_u]$.

We denote in what follows $D_{\partial_u} Y$ and $D_{\partial_v} Y$ the covariant derivative of the vector field Y in the directions $\partial_u \varphi$ and $\partial_v \varphi$, respectively. First, since $R(\cdot, 0) = 1$, we have that $\partial_u R(u, 0) = 0$, for all $u \in [0, L_u]$. Moreover, since ω satisfies the boundary conditions (4.8), we have that

$D_{\partial_u} \partial_u \varphi(u, 0) = -[\partial_u \omega \partial_u \varphi^\perp](u, 0)$. Combining these results with (4.35), we obtain

$$\begin{aligned} \frac{1}{2} \partial_v(R^2)(u, 0) &= \langle D_{\partial_v} \partial_u \varphi, \partial_u \varphi \rangle_g(u, 0) = \partial_u(RX_1)(u, 0) - \langle D_{\partial_u} \partial_u \varphi, \partial_v \varphi \rangle_g(u, 0) \\ &= R(u, 0) \partial_u X_1(u, 0) + \langle \partial_u \omega \partial_u \varphi^\perp, \partial_v \varphi \rangle_g(u, 0) \\ &= \frac{d}{du} [\cos(\omega(u, 0))] + \partial_u \omega(u, 0) \sin(\omega(u, 0)) = 0, \end{aligned}$$

for all $u \in [0, L_u]$. Therefore, we have $\partial_v R(u, 0) = 0$, for all $u \in [0, L_u]$.

Step 2 (*Computation of the Gaussian curvature (1st part)*). We prove the following relations on the parallel transport of vectors:

$$D_{\partial_u} \partial_u \varphi = \left(\frac{\partial_u R}{R} + \frac{X_1}{X_2^2} (\partial_v R - \partial_u X_1) \right) \partial_u \varphi + \left(\frac{R}{X_2^2} (\partial_u X_1 - \partial_v R) \right) \partial_v \varphi, \quad (4.37a)$$

$$D_{\partial_v} \partial_u \varphi = D_{\partial_u} \partial_v \varphi = \frac{\partial_v R}{RX_2^2} \partial_u \varphi - \frac{\partial_v RX_1}{X_2^2} \partial_v \varphi, \quad (4.37b)$$

$$D_{\partial_v} \partial_v \varphi = \partial_v \omega \partial_v \varphi^\perp. \quad (4.37c)$$

The results (4.37a) and (4.37b) easily follow from the identities

$$\begin{aligned} \langle D_{\partial_u} \partial_u \varphi, \partial_u \varphi \rangle_g &= R \partial_u R, \\ \langle D_{\partial_u} \partial_u \varphi, \partial_v \varphi \rangle_g &= \partial_u(RX_1) - \langle \partial_u \varphi, D_{\partial_v} \partial_u \varphi \rangle_g = \partial_u RX_1 + R \partial_u X_1 - R \partial_v R, \\ \langle D_{\partial_u} \partial_v \varphi, \partial_u \varphi \rangle_g &= R \partial_v R, \\ \langle D_{\partial_u} \partial_v \varphi, \partial_v \varphi \rangle_g &= 0, \end{aligned}$$

where we have used in the last equality the fact that $|\partial_v \varphi|_g = 1$. Equation (4.37c) is obtained using that the v -coordinate curves of φ are arc-length parametrized and have by construction a geodesic curvature given by $\partial_v \omega$.

Step 3 (*Computation of the Gaussian curvature (2nd part)*). We prove that X_1 and X_2 satisfy

$$\partial_v X_1 = -\partial_v \omega X_2 - \frac{\partial_v R}{R} X_1, \quad (4.38a)$$

$$\partial_v X_2 = \partial_v \omega X_1 + \frac{X_1}{X_2} \frac{\partial_v R}{R} X_1. \quad (4.38b)$$

First, using that $\langle D_{\partial_v} \partial_u \varphi, \partial_v \varphi \rangle = 0$ and (4.37c), we obtain

$$\begin{aligned} \partial_v X_1 &= \langle D_{\partial_v} \partial_v \varphi, \frac{\partial_u \varphi}{R} \rangle_g + \langle D_{\partial_v} \frac{\partial_u \varphi}{R}, \partial_v \varphi \rangle_g = \partial_v \omega \langle \partial_v \varphi^\perp, \frac{\partial_u \varphi}{R} \rangle_g + \langle -\frac{\partial_v R}{R^2} \partial_u \varphi + \frac{1}{R} D_{\partial_v} \partial_u \varphi, \partial_v \varphi \rangle_g \\ &= -\partial_v \omega X_2 - \frac{\partial_v R}{R} X_1, \end{aligned}$$

which proves (4.38a). Then, using that the geodesic curvatures of the v -coordinate curves of φ is $\partial_v \omega$, we obtain $D_{\partial_v} \partial_v \varphi^\perp = -\partial_v \omega \partial_v \varphi$. Moreover, a straightforward computation gives

$$\partial_v \varphi^\perp = -\frac{1}{RX_2} \partial_u \varphi + T \partial_v \varphi, \quad \langle \partial_u \varphi^\perp, \partial_v \varphi \rangle_g = -\langle \partial_u \varphi, \partial_v \varphi^\perp \rangle_g.$$

Combining these results, we infer that

$$\begin{aligned}
 \partial_v X_2 &= -\langle D_{\partial_v} \frac{\partial_u \varphi}{R}, \partial_v \varphi^\perp \rangle_g - \langle D_{\partial_v} \partial_v \varphi^\perp, \frac{\partial_u \varphi}{R} \rangle_g \\
 &= \frac{\partial_v R}{R^2} \langle \partial_u \varphi, \partial_v \varphi^\perp \rangle_g - \frac{1}{R} \langle D_{\partial_u} \partial_v \varphi, \partial_v \varphi^\perp \rangle_g + \partial_v \omega \langle \partial_v \varphi, \frac{\partial_u \varphi}{R} \rangle_g \\
 &= -\frac{\partial_v R}{R} X_2 - \frac{1}{R} \langle D_{\partial_u} \partial_v \varphi, -\frac{1}{R X_2} \partial_u \varphi + T \partial_v \varphi \rangle_g + \partial_v \omega X_1 \\
 &= -\frac{\partial_v R}{R} X_2 + \frac{\partial_v (R^2)}{2 R^2 X_2} + \partial_v \omega X_1 = \frac{\partial_v R}{R} \left(\frac{1}{X_2} - X_2 \right) + \partial_v \omega X_1 \\
 &= \partial_v \omega X_1 + \frac{X_1}{X_2} \frac{\partial_v R}{R} X_1.
 \end{aligned}$$

Step 4 (*Computation of the Gaussian curvature (3rd part)*). We now compute the expression of the Gaussian curvature K in the local parametrization φ . Note that the metric induced by φ is $\tilde{g} = R^2 du^2 + 2RX_1 dudv + dv^2$ giving $\det \tilde{g} = R^2 X_2^2$. Then, recall that, by definition, the Gaussian curvature K satisfies

$$K \det \tilde{g} = \langle D_{\partial_v} D_{\partial_u} \partial_u \varphi - D_{\partial_u} D_{\partial_v} \partial_u \varphi, \partial_v \varphi \rangle_g. \quad (4.39)$$

Using (4.37a), we first obtain that

$$\begin{aligned}
 \langle D_{\partial_v} D_{\partial_u} \partial_u \varphi, \partial_v \varphi \rangle_g &= \langle D_{\partial_v} (A \partial_u \varphi + B \partial_v \varphi), \partial_v \varphi \rangle_g \\
 &= A \langle D_{\partial_v} \partial_u \varphi, \partial_v \varphi \rangle_g + B \langle D_{\partial_v} \partial_v \varphi, \partial_v \varphi \rangle_g + RX_1 \partial_v A + \partial_v B,
 \end{aligned}$$

with $A = \frac{\partial_u R}{R} + \frac{X_1}{X_2^2} (\partial_v R - \partial_u X_1)$ and $B = \frac{R}{X_2^2} (\partial_u X_1 - \partial_v R)$. Then, we infer that

$$\begin{aligned}
 \langle D_{\partial_v} D_{\partial_u} \partial_u \varphi, \partial_v \varphi \rangle_g &= RX_1 \partial_v A + \partial_v B \\
 &= \partial_v \left(\frac{\partial_u R}{R} \right) RX_1 + RX_1^2 \partial_v \left(\frac{\partial_v R - \partial_u X_1}{X_2^2} \right) + RX_1 \partial_v X_1 \frac{\partial_v R - \partial_u X_1}{X_2^2} \\
 &\quad - \partial_v R \frac{\partial_v R - \partial_u X_1}{X_2^2} - R \partial_v \left(\frac{\partial_v R - \partial_u X_1}{X_2^2} \right) \\
 &= \partial_v \left(\frac{\partial_u R}{R} \right) RX_1 - RX_2^2 \partial_v \left(\frac{\partial_v R - \partial_u X_1}{X_2^2} \right) \\
 &\quad + RX_1 \partial_v X_1 \frac{\partial_v R - \partial_u X_1}{X_2^2} - \partial_v R \frac{\partial_v R - \partial_u X_1}{X_2^2}.
 \end{aligned} \quad (4.40)$$

Secondly, using (4.37b), we obtain that

$$\begin{aligned}
 \langle D_{\partial_u} D_{\partial_v} \partial_u \varphi, \partial_v \varphi \rangle_g &= \left\langle D_{\partial_u} \left[\frac{\partial_v R}{R X_2^2} \partial_u \varphi - \frac{\partial_v R X_1}{X_2^2} \partial_v \varphi \right], \partial_v \varphi \right\rangle_g \\
 &= \frac{\partial_v R}{R X_2^2} \langle D_{\partial_u} \partial_u \varphi, \partial_v \varphi \rangle_g - \frac{\partial_v R X_1}{X_2^2} \langle D_{\partial_u} \partial_v \varphi, \partial_v \varphi \rangle_g + RX_1 \partial_u \left(\frac{\partial_v R}{R X_2^2} \right) - \partial_u \left(\frac{\partial_v R X_1}{X_2^2} \right) \\
 &= \frac{\partial_v R}{R X_2^2} \langle D_{\partial_u} \partial_u \varphi, \partial_v \varphi \rangle_g - \frac{\partial_u R}{R^2} \frac{\partial_v R}{X_2^2} RX_1 + \partial_u \left(\frac{\partial_v R}{X_2^2} \right) X_1 - \partial_u \left(\frac{\partial_v R}{X_2^2} \right) X_1 - \frac{\partial_u X_1 \partial_v R}{X_2^2} \\
 &= \frac{\partial_v R}{X_2^2} \left(\frac{1}{R} \langle D_{\partial_u} \partial_u \varphi, \partial_v \varphi \rangle_g - \frac{X_1 \partial_u R}{R} - \partial_u X_1 \right).
 \end{aligned}$$

Since $\langle D_{\partial_u} \partial_u \varphi, \partial_v \varphi \rangle_g = \partial_u R X_1 + R \partial_u X_1 - R \partial_v R$, we infer that

$$\langle D_{\partial_v} D_{\partial_u} \partial_u \varphi, \partial_v \varphi \rangle_g = -\frac{(\partial_v R)^2}{X_2^2}. \quad (4.41)$$

Combining (4.39), (4.40) and (4.41) gives

$$\begin{aligned}
 K \det \tilde{g} &= -RX_2^2 \partial_v \left(\frac{\partial_v R - \partial_u X_1}{X_2^2} \right) + RX_1 \partial_v X_1 \frac{\partial_v R - \partial_u X_1}{X_2^2} + \frac{\partial_v R \partial_u X_1}{X_2^2} + \partial_v \left(\frac{\partial_u R}{R} \right) RX_1 \\
 &= \frac{1}{X_2^2} [RX_1 \partial_v X_1 (\partial_v R - \partial_u X_1) + \partial_v R \partial_u X_1] - R\partial_{vv}R + R\partial_{uv}X_1 \\
 &\quad + 2\partial_v X_2 \frac{R(\partial_v R - \partial_u X_1)}{X_2} + \partial_v \left(\frac{\partial_u R}{R} \right) RX_1 \\
 &= \frac{1}{X_2^2} \left[-RX_1 \left(\partial_v \omega X_2 + \frac{\partial_v R}{R} X_1 \right) (\partial_v R - \partial_u X_1) + \partial_v R \partial_u X_1 \right] - R\partial_{vv}R - R\partial_u \left[\partial_v \omega X_2 + \frac{\partial_v R}{R} X_1 \right] \\
 &\quad + 2 \left(\partial_v \omega X_1 + \frac{X_1^2 \partial_v R}{RX_2} \right) \frac{R(\partial_v R - \partial_u X_1)}{X_2} + \partial_v \left(\frac{\partial_u R}{R} \right) RX_1,
 \end{aligned}$$

using (4.38) for the last equality. Then, we split the computation in two parts. First, we have

$$\begin{aligned}
 C &:= \frac{1}{X_2^2} \left[-RX_1 \left(\partial_v \omega X_2 + \frac{\partial_v R}{R} X_1 \right) (\partial_v R - \partial_u X_1) + \partial_v R \partial_u X_1 \right] \\
 &= \frac{1}{X_2^2} \left[-R\partial_v \omega X_1 X_2 \partial_v R + RX_1 X_2 \partial_v \omega \partial_u X_1 - X_1^2 (\partial_v R)^2 + X_1^2 \partial_u X_1 \partial_v R + \partial_v R \partial_u X_1 \right] \\
 &= -R\partial_v R \partial_v \omega T + RT \partial_v \omega \partial_u X_1 - T^2 (\partial_v R)^2 + T^2 \partial_u X_1 \partial_v R + \frac{\partial_v R \partial_u X_1}{X_2^2}.
 \end{aligned} \tag{4.42}$$

Then, we obtain

$$\begin{aligned}
 E &:= -R\partial_{vv}R - R\partial_u \left[\partial_v \omega X_2 + \frac{\partial_v R}{R} X_1 \right] \\
 &\quad + 2 \left(\partial_v \omega X_1 + \frac{X_1^2 \partial_v R}{RX_2} \right) \frac{R(\partial_v R - \partial_u X_1)}{X_2} + \partial_v \left(\frac{\partial_u R}{R} \right) RX_1 \\
 &= -R\partial_{vv}R - R \left[\partial_{uv} \omega X_2 + \partial_v \omega \partial_u X_2 + \partial_v \left(\frac{\partial_u R}{R} \right) X_1 + \frac{\partial_v R}{R} \partial_u X_1 \right] \\
 &\quad + 2\partial_v \omega T R (\partial_v R - \partial_u X_1) + 2T^2 \partial_v R (\partial_v R - \partial_u X_1) + \partial_v \left(\frac{\partial_u R}{R} \right) RX_1 \\
 &= -R\partial_{vv}R - R\partial_{uv} \omega X_2 - R\partial_v \omega (\partial_u X_2 + T \partial_u X_1) - \partial_v R \partial_u X_1 (1 + T^2) \\
 &\quad - T \partial_u X_1 R \partial_v \omega - T^2 \partial_v R \partial_u X_1 + 2T \partial_v R \partial_v \omega R + 2T^2 (\partial_v R)^2.
 \end{aligned}$$

Moreover, since $X_1^2 + X_2^2 = 1$, we have $1 + T^2 = \frac{1}{X_2^2}$ and $T \partial_u X_1 + \partial_u X_2 = 0$. We infer that

$$\begin{aligned}
 E &= -R\partial_{vv}R - R\partial_{uv} \omega X_2 - \frac{\partial_v R \partial_u X_1}{X_2^2} - T \partial_u X_1 R \partial_v \omega \\
 &\quad - T^2 \partial_v R \partial_u X_1 + 2T \partial_v R \partial_v \omega R + 2T^2 (\partial_v R)^2.
 \end{aligned} \tag{4.43}$$

We obtain by combining (4.42) and (4.43) that

$$K \det \tilde{g} = C + E = T^2 (\partial_v R)^2 - R\partial_{uv} \omega X_2 - R\partial_{vv}R + TR \partial_v R \partial_v \omega. \tag{4.44}$$

Using that $\det \tilde{g} = X_2^2 R^2$ and dividing by R , we finally obtain

$$-\partial_v \omega \partial_v R T - \frac{(\partial_v R)^2}{R} T^2 + \partial_{vv}R = -X_2 (\partial_{uv} \omega + K X_2 R). \tag{4.45}$$

Step 5 (*Bound on the right-hand side of the equation (4.45)*). By (4.45) and the integrability condition (4.5), we have

$$\partial_{vv}R = \partial_v\omega\partial_vRT + \frac{(\partial_vR)^2}{R}T^2 + K(\varphi)X_2[\sin(\omega) - X_2R]. \quad (4.46)$$

The proof is now reduced to showing that $\partial_vR=0$ is the unique solution to (4.46) such that $\partial_vR(\cdot, 0)=0$. To this end, we bound the right-hand side of this equation. Let $F_1=\sin(\omega) - RX_2$ and $F_2=\cos(\omega) - RX_1$. We infer from (4.38b) that

$$\begin{aligned} \partial_vF_1 &= \partial_v\omega\cos(\omega) - \partial_vRX_2 - R\partial_vX_2 = \partial_v\omega(\cos(\omega) - RX_1) - \partial_vR(X_2 + TX_1) \\ &= \partial_v\omega F_2 - \frac{\partial_vR}{X_2}, \end{aligned}$$

using that $X_2 + TX_1 = X_2 + \frac{1-X_2^2}{X_2} = \frac{1}{X_2}$ in the last equality. In the same manner, we deduce from (4.38a) that $\partial_vF_2 = -\partial_v\omega F_1$, so that the couple (F_1, F_2) satisfies the system of differential equations

$$\begin{cases} \partial_vF_1 = \partial_v\omega F_2 - \frac{\partial_vR}{X_2}, \\ \partial_vF_2 = -\partial_v\omega F_1, \end{cases}$$

with $F_1(0) = F_2(0) = 0$, since $R(u, 0) = 1$, $X_1(u, 0) = \cos\omega(u, 0)$, and $X_2(u, 0) = \sin\omega(u, 0)$, for all $u \in [0, L_1]$. A straightforward computation shows that the unique solution to this linear ordinary differential equation is

$$\begin{aligned} (\sin\omega - X_2R)(u, v) &= F_1(u, v) = -\sin\omega(u, v) \int_0^v \frac{\partial_vR}{X_2}(u, s) \sin\omega(u, s) ds \\ &\quad - \cos\omega(u, v) \int_0^v \frac{\partial_vR}{X_2}(u, s) \cos\omega(u, s) ds, \end{aligned} \quad (4.47a)$$

$$\begin{aligned} (\cos\omega - X_1R)(u, v) &= F_2(u, v) = -\cos\omega(u, v) \int_0^v \frac{\partial_vR}{X_2}(u, s) \sin\omega(u, s) ds \\ &\quad + \sin\omega(u, v) \int_0^v \frac{\partial_vR}{X_2}(u, s) \cos\omega(u, s) ds, \end{aligned} \quad (4.47b)$$

since $\partial_vR(u, 0) = 0$, for all $u \in [0, L_u]$, by Step 1.

Step 6 (*Conclusion*). Finally, we infer from (4.46) and (4.47a) that

$$\partial_{vv}R = \partial_v\omega\partial_vRT + \frac{(\partial_vR)^2}{R}T^2 - K(\varphi)X_2\left(\sin\omega \int_0^v \frac{\partial_vR}{X_2} \sin\omega + \cos\omega \int_0^v \frac{\partial_vR}{X_2} \cos\omega\right). \quad (4.48)$$

Then, since $0 < \omega(u, v) < \pi$, for all $(u, v) \in D_L$, we have that T and $\frac{1}{X_2}$ are bounded. Using moreover that $\frac{1}{R}$, $\partial_v\omega$ and $K \circ \varphi$ are bounded, and using $\partial_vR(\cdot, 0) = 0$, we infer from (4.48) that

$$\begin{aligned} |\partial_vR(t)| &\leq \tilde{C}\left(\int_0^t |\partial_vR(s)| ds + \int_0^t |(\partial_vR)^2(s)| ds + \int_0^t \int_0^s |\partial_vR(l)| dl ds\right) \\ &\leq C \int_0^t |\partial_vR(s)| ds, \end{aligned}$$

for all $u \in [0, L_u]$ and $t \in [0, L]$. Using Grönwall's inequality, we conclude that $\partial_vR(u, v) = 0$, for all $(u, v) \in D_L$. The claim follows. ■

Existence and uniqueness of angle distribution

Let $k \in \mathbb{N}$, let $D = [0, L_u] \times [0, L_v]$, with $L_u, L_v \in \mathbb{R}_*^+$, and let $\gamma = (\gamma_u, \gamma_v) \in \Gamma^{k+2}([0, L_u]) \times \Gamma^{k+2}([0, L_v])$ be two curves of geodesic curvatures $\kappa_u \in C^k([0, L_u], \mathbb{R})$ and $\kappa_v \in C^k([0, L_v], \mathbb{R})$, respectively. In this section, we consider the Hazzidakis formula (4.6) as an equation on $\omega \in \Theta_\gamma^{k+1}(D)$, i.e., on angle distributions satisfying the boundary conditions (4.8). Hence, we define the mapping $F: \Theta_\gamma^{k+1}(D) \rightarrow \Theta_\gamma^{k+1}(D)$ by

$$F[\omega](u, v) = \angle(\gamma'_u(0), \gamma'_v(0)) - \int_0^u \kappa_u + \int_0^v \kappa_v - \int_0^u \int_0^v K[\mathcal{I}(\gamma, \omega)(t, s)] \sin(\omega(t, s)) dt ds,$$

and we prove in what follows that there exists a unique solution to

$$\omega(u, v) = F[\omega](u, v), \quad (4.49)$$

for all $(u, v) \in D$. We first show in Subsection 4.3.1 that there exists a unique $\omega^* \in \Theta_\gamma^{k+1}([0, L_u] \times [0, L_v])$, for $L_0 \in (0, L_v]$ small enough, satisfying (4.49). We also prove that this solution depends continuously on the curves γ_u and γ_v . Then, we extend this result to finite rectangles $D = [0, L_u] \times [0, L_v]$, with $L_u, L_v \in \mathbb{R}_*^+$, in Subsection 4.3.2. Finally, we prove by a density argument on the regularity of γ_u and γ_v that the associated parametrization $\mathcal{I}(\gamma, \omega^*)$ is indeed a Chebyshev net.

Local existence of a solution

We first suppose that $k=0$ and we state the local existence of the angle distribution ω in the following proposition.

Proposition 4.8 (Local existence of a solution). *Let M be a smooth, open, complete, and simply connected surface, let $L_u, L_v \in \mathbb{R}_*^+$, and let $\gamma = (\gamma_u, \gamma_v) \in \Gamma^2([0, L_u]) \times \Gamma^2([0, L_v])$ be such that $\gamma_u(0) = \gamma_v(0)$ and $\angle(\gamma'_u(0), \gamma'_v(0)) \in (0, \pi)$. Then, there exists $L_0 \in (0, L_v]$, depending only on $\|\gamma_u\|_{\Gamma^2([0, L_u])}$ and $\|\gamma_v\|_{\Gamma^2([0, L_v])}$, such that there exists a unique solution $\omega_\gamma^* \in \Theta_\gamma^1([0, L_u] \times [0, L_0])$ to (4.49). Moreover, we have*

$$\|\omega_\gamma^*\|_{\Theta_\gamma^1([0, L_u] \times [0, L_0])} \leq C, \quad (4.50)$$

where the constant C depends on $\|\gamma_u\|_{\Gamma^2([0, L_u])}$ and $\|\gamma_v\|_{\Gamma^2([0, L_v])}$.

Proof. Let $D = [0, L_u] \times [0, L_v]$ and let $D_L = [0, L_u] \times [0, L]$, with $L \in (0, L_v]$. We prove the claim by application of the Banach fixed-point theorem to the functional $F: \Theta_\gamma^1(D_L) \rightarrow \Theta_\gamma^1(D_L)$, supposing that L is small enough. Hence, we first prove that F is stable in some bounded closed subset of $\Theta_\gamma^1(D_L)$ (Step 1) and we then show that F^2 is a contraction mapping in this space (Step 2). We conclude using the Banach fixed-point theorem in Step 3.

Step 1 (Stability in a closed subset). We denote $\kappa_{u,1} \in C^0([0, L_u])$ and $\kappa_{v,1} \in C^0([0, L_v])$ the geodesic curvatures of γ_u and γ_v respectively. We set $\varphi_\gamma := \mathcal{I}(\gamma, \omega_\gamma) \in \Phi^{1,2}(D)$. Since φ_γ is bounded by (4.18), we have that $K \circ \varphi_\gamma$ is bounded. Moreover, a straightforward computation

gives

$$\begin{aligned} \|F(\omega_\gamma)\|_{C^0(D)} &\leq \pi + L_u \|\kappa_{u,1}\|_{C^0([0,L_u])} + L_v \|\kappa_{v,1}\|_{C^0([0,L_v])} + L_u L_v \|K \circ \varphi_\gamma\|_{C^0(D)}, \\ \|\partial_u F(\omega_\gamma)\|_{C^0(D)} &\leq \|\kappa_{u,1}\|_{C^0([0,L_u])} + L_v \|K \circ \varphi_\gamma\|_{C^0(D)}, \\ \|\partial_v F(\omega_\gamma)\|_{C^0(D)} &\leq \|\kappa_{v,1}\|_{C^0([0,L_v])} + L_u \|K \circ \varphi_\gamma\|_{C^0(D)}, \\ \|\partial_{uv} F(\omega_\gamma)\|_{C^0(D)} &\leq \|K \circ \varphi\|_{C^0(D)}, \end{aligned}$$

for all $\omega_\gamma \in \Theta_\gamma^1(D)$. Then, there exists $\mathcal{R}(\gamma) > 0$ such that $F : \mathcal{B}_{\Theta^1(D_L)}(\mathcal{R}(\gamma)) \rightarrow \mathcal{B}_{\Theta^1(D_L)}(\mathcal{R}(\gamma))$, where $\mathcal{B}_{\Theta^1(D_L)}(\mathcal{R}(\gamma))$ is the closed ball of radius $\mathcal{R}(\gamma)$ centered at the origin in $\Theta_\gamma^1(D_L)$. In what follows, we restrict F to this ball.

Step 2 (Contraction mapping). We now prove the following result:

Let $\sigma = (\sigma_u, \sigma_v) \in \Gamma^2([0, L_u]) \times \Gamma^2([0, L_v])$ be such that $\gamma_u(0) = \gamma_v(0) = \sigma_u(0) = \sigma_v(0)$, $\gamma'_u(0) = \sigma'_u(0)$ and $\gamma'_v(0) = \sigma'_v(0)$. Let $\omega_\gamma \in \mathcal{B}_{\Theta^1(D_L)}(\mathcal{R}(\gamma))$ and $\omega_\sigma \in \mathcal{B}_{\Theta^1(D_L)}(\mathcal{R}(\sigma))$. Then, we have

$$\begin{aligned} \|F^2(\omega_\gamma) - F^2(\omega_\sigma)\|_{\Theta^1(D_L)} &\leq C \left(\|\gamma_u - \sigma_u\|_{\Gamma^2([0, L_u])} + \|\gamma_v - \sigma_v\|_{\Gamma^2([0, L_v])} \right. \\ &\quad \left. + L \|\omega_\gamma - \omega_\sigma\|_{\Theta^1(D_L)} \right), \end{aligned} \quad (4.51)$$

where the constant C depends on $\mathcal{R}(\gamma)$ and $\mathcal{R}(\sigma)$. Note that (4.51) holds for all $L \in (0, L_v]$ and $\gamma, \sigma \in \Gamma^2([0, L_u]) \times \Gamma^2([0, L_v])$.

In this step, the domain of definition of the two-dimensional variables for the different norms is always $D_L = [0, L_u] \times [0, L]$ and will not be specified. In all the subsequent estimates, unless explicitly mentioned, the constants only depend on $\mathcal{R}(\gamma)$ and $\mathcal{R}(\sigma)$. We set $\varphi_\sigma := \mathcal{I}(\sigma, \omega_\sigma) \in \Phi^{1,2}$ and we denote $\kappa_{u,2} \in C^0([0, L_u])$ and $\kappa_{v,2} \in C^0([0, L_v])$ the geodesic curvatures of σ_u and σ_v , respectively. First, we prove that

$$\|F(\omega_\gamma) - F(\omega_\sigma)\|_{\Theta^0} \leq \tilde{C} \left(\|\gamma_u - \sigma_u\|_{\Gamma^2([0, L_u])} + \|\gamma_v - \sigma_v\|_{\Gamma^2([0, L_v])} + L \|\omega_\gamma - \omega_\sigma\|_{\Theta^1} \right), \quad (4.52a)$$

$$\begin{aligned} \|F(\omega_\gamma) - F(\omega_\sigma)\|_{\Theta^1} &\leq C \left(\|\gamma_u - \sigma_u\|_{\Gamma^2([0, L_u])} + \|\gamma_v - \sigma_v\|_{\Gamma^2([0, L_v])} + L \|\omega_\gamma - \omega_\sigma\|_{\Theta^1} \right. \\ &\quad \left. + \|\omega_\gamma - \omega_\sigma\|_{\Theta^0} \right). \end{aligned} \quad (4.52b)$$

To this end, first note that we have

$$\begin{aligned} |F(\omega_\gamma) - F(\omega_\sigma)|(u, v) &\leq \int_0^u |\kappa_{u,1} - \kappa_{u,2}| + \int_0^v |\kappa_{v,1} - \kappa_{v,2}| + |\angle(\gamma'_u(0), \gamma'_v(0)) - \angle(\sigma'_u(0), \sigma'_v(0))| \\ &\quad + \int_0^u \int_0^v |K(\varphi_\sigma) \sin(\omega_\sigma) - K(\varphi_\gamma) \sin(\omega_\gamma)| \\ &\leq C \left(\|\gamma_u - \sigma_u\|_{\Gamma^2([0, L_u])} + \|\gamma_v - \sigma_v\|_{\Gamma^2([0, L_v])} \right. \\ &\quad \left. + L \|K(\varphi_\sigma) \sin(\omega_\sigma) - K(\varphi_\gamma) \sin(\omega_\gamma)\|_{C^0} \right), \end{aligned}$$

for all $(u, v) \in D_L$. Doing the same for $\partial_u F(\omega)$, $\partial_v F(\omega)$ and $\partial_{uv} F(\omega) = -K(\varphi) \sin(\omega)$, we obtain

$$\begin{aligned}\|F(\omega_\gamma) - F(\omega_\sigma)\|_{\Theta^0} &\leq \tilde{C} \left(\|\gamma_u - \sigma_u\|_{\Gamma^2([0, L_u])} + \|\gamma_v - \sigma_v\|_{\Gamma^2([0, L_v])} \right. \\ &\quad \left. + L \|K(\varphi_\gamma) \sin(\omega_\gamma) - K(\varphi_\sigma) \sin(\omega_\sigma)\|_{C^0} \right), \\ \|F(\omega_\gamma) - F(\omega_\sigma)\|_{\Theta^1} &\leq C \left(\|\gamma_u - \sigma_u\|_{\Gamma^2([0, L_u])} + \|\gamma_v - \sigma_v\|_{\Gamma^2([0, L_v])} \right. \\ &\quad \left. + \|K(\varphi_\gamma) \sin(\omega_\gamma) - K(\varphi_\sigma) \sin(\omega_\sigma)\|_{C^0} \right).\end{aligned}$$

Moreover, since K is smooth and since φ_γ and φ_σ are bounded, we have

$$\|K(\varphi_\gamma) \sin(\omega_\gamma) - K(\varphi_\sigma) \sin(\omega_\sigma)\|_{C^0} \leq C \left(\|\omega_\gamma - \omega_\sigma\|_{\Theta^0} + \|\varphi_\gamma - \varphi_\sigma\|_{\Phi^0} \right),$$

and we conclude the proof of (4.52) with

$$\|\varphi_\gamma - \varphi_\sigma\|_{\Phi^0} \leq C \left(L \|\omega_\gamma - \omega_\sigma\|_{\Theta^1} + \|\gamma_u - \sigma_u\|_{\Gamma^2([0, L_u])} \right), \quad (4.53)$$

obtained using (4.19a) of Proposition 4.5. Finally, using (4.52), we obtain

$$\begin{aligned}\|F^2(\omega_\gamma) - F^2(\omega_\sigma)\|_{\Theta^1} &\leq \tilde{C} \left(\|\gamma_u - \sigma_u\|_{\Gamma^2([0, L_u])} + \|\gamma_v - \sigma_v\|_{\Gamma^2([0, L_v])} \right. \\ &\quad \left. + L \|F(\omega_\gamma) - F(\omega_\sigma)\|_{\Theta^1} + \|F(\omega_\gamma) - F(\omega_\sigma)\|_{\Theta^0} \right) \\ &\leq C \left(\|\gamma_u - \sigma_u\|_{\Gamma^2([0, L_u])} + \|\gamma_v - \sigma_v\|_{\Gamma^2([0, L_v])} + L \|\omega_\gamma - \omega_\sigma\|_{\Theta^1} \right).\end{aligned}$$

The inequality (4.51) follows.

Step 3 (Conclusion). We infer from (4.51) that there exists $L_0 \in (0, L_v]$ such that F^2 is a contraction mapping in $\mathcal{B}_{\Theta^1(D_{L_0})}(\mathcal{R}(\gamma))$ for the norm in $\Theta^1(D_{L_0})$. Hence, the claim follows from the Banach fixed-point theorem on the closed subset $\mathcal{B}_{\Theta^1(D_{L_0})}(\mathcal{R}(\gamma))$ of the Banach space $C^1([0, L_u], C^1([0, L_0]))$.

■

Let $R_0 \in \mathbb{R}_*^+$ and let $\mathcal{B}_{\Gamma^2 \times \Gamma^2}(R_0)$ be the closed ball of radius R_0 centered at the origin in $\Gamma^2([0, L_u]) \times \Gamma^2([0, L_v])$ (supposing R_0 is large enough for this set not to be empty). As the length of integration $L_0 \in (0, L_v]$ of the v -coordinate curves of φ defined in Proposition 4.8 only depends on the norm in $\Gamma^2([0, L_u]) \times \Gamma^2([0, L_v])$ of the initial conditions $\gamma = (\gamma_u, \gamma_v)$, we can define the mapping

$$\begin{aligned}\mathcal{J}_{0, R_0} : \mathcal{B}_{\Gamma^2 \times \Gamma^2}(R_0) &\rightarrow \Theta^1([0, L_u] \times [0, L_0(R_0)]), \\ \gamma = (\gamma_u, \gamma_v) &\mapsto \omega_\gamma = F(\omega_\gamma),\end{aligned} \quad (4.54)$$

which maps the boundary conditions γ to the solution ω_γ to (4.49). We then state the following proposition which asserts the continuity of the mapping \mathcal{J}_{0, R_0} with respect to these boundary conditions.

Proposition 4.9 (Continuity with respect to the boundary conditions). *Let M be a smooth, open, complete, and simply connected surface, let $R_0 \in \mathbb{R}_*^+$, and let $D = [0, L_u] \times [0, L_v]$, with $L_u, L_v \in \mathbb{R}_*^+$. We equip $\mathcal{B}_{\Gamma^2 \times \Gamma^2}(R_0)$ and $\Theta^1([0, L_u] \times [0, L_0(R_0)])$ with the norms in $\Gamma^2([0, L_u]) \times \Gamma^2([0, L_v])$ and*

$\Theta^1([0, L_u] \times [0, L_0(R_0)])$, respectively. Then, the mappings \mathcal{J}_{0,R_0} and

$$\begin{aligned} \mathcal{I} \circ (\text{Id}, \mathcal{J}_{0,R_0}) : \mathcal{B}_{\Gamma^2 \times \Gamma^2}(R_0) &\rightarrow \Phi^2([0, L_u] \times [0, L_0(R_0)]) \\ \gamma = (\gamma_u, \gamma_v) &\mapsto \varphi_\omega := \mathcal{I}(\gamma, \mathcal{J}_{0,R_0}(\gamma)) \end{aligned}$$

are Lipschitz continuous, with Id the identity operator in $\mathcal{B}_{\Gamma^2 \times \Gamma^2}(R_0)$.

Proof. Let $\gamma, \sigma \in \mathcal{B}_{\Gamma^2 \times \Gamma^2}(R_0)$, with $\gamma = (\gamma_u, \gamma_v)$ and $\sigma = (\sigma_u, \sigma_v)$, be such that $\gamma_u(0) = \gamma_v(0) = \sigma_u(0) = \sigma_v(0)$, $\gamma'_u(0) = \sigma'_u(0)$ and $\gamma'_v(0) = \sigma'_v(0)$. Suppose moreover that $\angle(\gamma'_u(0), \gamma'_v(0)) = \angle(\sigma'_u(0), \sigma'_v(0)) \in (0, \pi)$. We set $D_{L_0} = [0, L_u] \times [0, L_0(R_0)]$, $\omega_\gamma := \mathcal{J}_{0,R_0}(\gamma) \in \Theta_\gamma^1(D_{L_0})$, and $\omega_\sigma := \mathcal{J}_{0,R_0}(\sigma) \in \Theta_\sigma^1(D_{L_0})$. Let us recall from the proof of Proposition 4.8 that $F^2 : \mathcal{B}_{\Theta^1(D_{L_0})}(\mathcal{R}(\gamma)) \rightarrow \mathcal{B}_{\Theta^1(D_{L_0})}(\mathcal{R}(\gamma))$ is a contraction mapping, with $\mathcal{R}(\gamma) \in \mathbb{R}_*^+$ a constant depending only on R_0 , and $\mathcal{B}_{\Theta^1(D_{L_0})}(\mathcal{R}(\gamma))$ the ball centered at the origin with radius $\mathcal{R}(\gamma)$ in $\Theta^1(D_{L_0})$. Since ω_γ and ω_σ are both contained in this ball, we deduce from (4.51) that

$$\begin{aligned} \|F^2(\omega_\gamma) - F^2(\omega_\sigma)\|_{\Theta^1(D_{L_0})} &\leq C_1 \left[\|\gamma_u - \sigma_u\|_{\Gamma^2([0, L_u])} + \|\gamma_v - \sigma_v\|_{\Gamma^2([0, L_v])} \right] \\ &\quad + C_2 \|\omega_\gamma - \omega_\sigma\|_{\Theta^1(D_{L_0})}, \end{aligned}$$

with $C_1 \in \mathbb{R}_*^+$ and $C_2 \in (0, 1)$ two constants. As $F(\omega) = \omega$, we infer that

$$\|\omega_\gamma - \omega_\sigma\|_{\Theta^1(D_{L_0})} \leq \frac{C_1}{1 - C_2} \left[\|\gamma_u - \sigma_u\|_{\Gamma^2([0, L_u])} + \|\gamma_v - \sigma_v\|_{\Gamma^2([0, L_v])} \right],$$

which proves that \mathcal{J}_{0,R_0} is Lipschitz continuous. Finally, using additionally Proposition 4.6, we infer that $\mathcal{I} \circ (\text{Id}, \mathcal{J}_{0,R_0})$ is Lipschitz continuous. \blacksquare

We now prove that C^{k+2} -regularity for the boundary conditions γ implies Θ^{k+1} -regularity for the solution ω , for all $k \in \mathbb{N}$.

Proposition 4.10 (Regularity of the solution). *Let M be a smooth, open, complete, and simply connected surface, let $k \in \mathbb{N}$, and let $D = [0, L_u] \times [0, L_v]$, with $L_u, L_v \in \mathbb{R}_*^+$. Let $\gamma = (\gamma_u, \gamma_v) \in \Gamma^{k+2}([0, L_u]) \times \Gamma^{k+2}([0, L_v])$ be such that $\gamma_u(0) = \gamma_v(0)$ and $\angle(\gamma'_u(0), \gamma'_v(0)) \in (0, \pi)$. Then, there exists $L_0 \in (0, L_v]$, depending only on $\|\gamma_u\|_{\Gamma^2([0, L_u])}$ and $\|\gamma_v\|_{\Gamma^2([0, L_v])}$, such that there exists a unique solution $\omega_\gamma \in \Theta_\gamma^{k+1}([0, L_u] \times [0, L_0])$ to (4.49). Moreover, we have*

$$\|\omega_\gamma\|_{\Theta^{k+1}([0, L_u] \times [0, L_0])} \leq C, \quad (4.55)$$

where the constant C depends on $\|\gamma_u\|_{\Gamma^{k+2}([0, L_u])}$ and $\|\gamma_v\|_{\Gamma^{k+2}([0, L_v])}$.

Proof. Owing to Proposition 4.8, there exists $L_0 \in (0, L_v]$ such that there exists a unique solution $\omega_\gamma \in \Theta_\gamma^1(D_{L_0})$ to (4.49). We prove in what follows that $\omega_\gamma \in \Theta_\gamma^{k+1}(D_{L_0})$. In this proof, the domain of definition of the two-dimensional variables for the different spaces is always $D_{L_0} = [0, L_u] \times [0, L_0]$ and it will not be specified. Owing to Proposition 4.6, we have that $\varphi_\omega = \mathcal{I}(\gamma, \omega) \in \Phi^{r+2}$ whenever $\omega_\gamma \in \Theta_\gamma^{r+1}$, for all $r \in \{0, \dots, k\}$. Therefore, using that $\omega_\gamma = F(\omega_\gamma)$, we obtain by an induction argument on $r \in \{0, \dots, k\}$ that $\omega_\gamma \in \Theta_\gamma^{k+1}$ (the only limiting factor being the regularity of the

boundary curves γ). Hence, we have $\varphi_\omega \in \Phi^{k+2}$. Now, to prove (4.55), we note that

$$\partial^{(i_1,0)} F(\omega_\gamma)(u,v) = \partial_u^{i_1-1} \kappa_u + \int_0^v \partial_u^{i_1-1} [K(\varphi_\omega) \sin(\omega_\gamma)](u,t) dt, \quad (4.56a)$$

$$\partial^{(0,i_2)} F(\omega_\gamma)(u,v) = \partial_v^{i_2-1} \kappa_v + \int_0^u \partial_v^{i_2-1} [K(\varphi_\omega) \sin(\omega_\gamma)](s,v) ds, \quad (4.56b)$$

$$\partial^I F(\omega_\gamma)(u,v) = \partial^{(i_1-1, i_2-1)} [K(\varphi_\omega) \sin(\omega_\gamma)](u,v), \quad (4.56c)$$

for all $I = (i_1, i_2) \in \{1, \dots, k+1\}^2$. Furthermore, a straightforward computation gives

$$\|K(\varphi_\omega) \sin(\omega_\gamma)\|_{C^k([0, L_u], C^k([0, L_0]))} \leq C, \quad (4.57)$$

where the constant C depends on $\|\varphi_\omega\|_{\Phi^k}$ and $\|\omega_\gamma\|_{\Theta^k}$. Using moreover Proposition 4.6, we infer that the constant C only depends on $\|\gamma_u\|_{\Gamma^s([0, L_u])}$, with $s = \max(k, 2)$, and $\|\omega_\gamma\|_{\Theta^l}$, with $l = \max(k, 1)$. Then, if $k \geq 1$, we deduce from (4.56) and (4.57) that $\|\omega_\gamma\|_{\Theta^{k+1}} \leq C$, where the constant C depends on $\|\gamma_u\|_{\Gamma^{k+2}([0, L_u])}$, $\|\gamma_v\|_{\Gamma^{k+2}([0, L_v])}$, and $\|\omega_\gamma\|_{\Theta^k}$. Finally, since the case $k=0$ follows from (4.50), we obtain (4.55) by a straightforward induction argument on $k \geq 0$. The claim follows. ■

Let $\mathcal{B}_{\Gamma^{k+2} \times \Gamma^{k+2}}(R_k)$ be the closed ball of radius $R_k \in \mathbb{R}_*^+$ centered at the origin in $\Gamma^{k+2}([0, L_u]) \times \Gamma^{k+2}([0, L_v])$. We denote \mathcal{J}_{k,R_k} the restriction of the mapping (4.54) to this ball, i.e.,

$$\mathcal{J}_{k,R_k} : \mathcal{B}_{\Gamma^{k+2} \times \Gamma^{k+2}}(R_k) \rightarrow \Theta^{k+1}([0, L_u] \times [0, L_0(R_k)]).$$

We can now state the equivalent of Proposition 4.9 in $\Gamma^{k+2}([0, L_u]) \times \Gamma^{k+2}([0, L_v])$.

Proposition 4.11 (Continuity with respect to boundary conditions). *Let M be a smooth, open, complete, and simply connected surface and let $k \in \mathbb{N}$. Let $R_k \in \mathbb{R}_*^+$ and let $D = [0, L_u] \times [0, L_v]$, with $L_u, L_v \in \mathbb{R}_*^+$. We equip $\mathcal{B}_{\Gamma^{k+2} \times \Gamma^{k+2}}(R_k)$ and $\Theta^{k+1}([0, L_u] \times [0, L_0(R_k)])$ with the norms in $\Gamma^{k+2}([0, L_u]) \times \Gamma^{k+2}([0, L_v])$ and $\Theta^{k+1}(D)$, respectively. Then, the mappings \mathcal{J}_{k,R_k} and*

$$\begin{aligned} \mathcal{I} \circ (\text{Id}, \mathcal{J}_{k,R_k}) : \mathcal{B}_{\Gamma^{k+2} \times \Gamma^{k+2}}(R_k) &\rightarrow \Phi^{k+2}([0, L_u] \times [0, L_0(R_k)]), \\ \gamma = (\gamma_u, \gamma_v) &\mapsto \varphi_\omega := \mathcal{I}(\gamma, \mathcal{J}_{k,R_k}(\gamma)), \end{aligned}$$

are Lipschitz continuous, with Id the identity operator in $\mathcal{B}_{\Gamma^{k+2} \times \Gamma^{k+2}}(R_k)$.

Proof. Similarly to the previous proofs, the domain of definition of the two-dimensional variables for the different norms is always $D_{L_0} = [0, L_u] \times [0, L_0(R_k)]$ and it will not be specified. Let $\gamma = (\gamma_u, \gamma_v) \in \mathcal{B}_{\Gamma^{k+2} \times \Gamma^{k+2}}(R_k)$ be such that $\gamma_u(0) = \gamma_v(0)$ and $\angle(\gamma'_u(0), \gamma'_v(0)) \in (0, \pi)$. Then, let $\sigma = (\sigma_u, \sigma_v) \in \mathcal{B}_{\Gamma^{k+2} \times \Gamma^{k+2}}(R_k)$ be such that $\gamma_u(0) = \sigma_u(0) = \sigma_v(0)$, $\gamma'_u(0) = \sigma'_u(0)$ and $\gamma'_v(0) = \sigma'_v(0)$. We set $\omega_\gamma := \mathcal{J}_{k,R_k}(\gamma) \in \Theta_\gamma^{k+1}$, $\omega_\sigma := \mathcal{J}_{k,R_k}(\sigma) \in \Theta_\sigma^{k+1}$ and we set $\varphi_\gamma := \mathcal{I}(\gamma, \omega_\gamma) \in \Phi^{k+1}$ and $\varphi_\sigma := \mathcal{I}(\sigma, \omega_\sigma) \in \Phi^{k+1}$. Using (4.56), a straightforward computation gives

$$\begin{aligned} \|F(\omega_\gamma) - F(\omega_\sigma)\|_{\Theta^{k+1}} &\leq C \left(\|\gamma_u - \sigma_u\|_{\Gamma^{k+2}([0, L_u])} + \|\gamma_v - \sigma_v\|_{\Gamma^{k+2}([0, L_v])} \right. \\ &\quad \left. + \|K(\varphi_\gamma) \sin(\omega_\gamma) - K(\varphi_\sigma) \sin(\omega_\sigma)\|_{C^k([0, L_u], C^k([0, L_0]))} \right). \end{aligned}$$

Moreover, we deduce from Proposition 4.6 that

$$\begin{aligned} \|K(\varphi_\gamma) \sin(\omega_\gamma) - K(\varphi_\sigma) \sin(\omega_\sigma)\|_{C^k([0, L_u], C^k([0, L_0]))} &\leq \tilde{C} \left(\|\varphi_\gamma - \varphi_\sigma\|_{\Phi^k} + \|\omega_\gamma - \omega_\sigma\|_{\Theta^k} \right) \\ &\leq C \left(\|\gamma_u - \sigma_u\|_{\Gamma^s([0, L_u])} + \|\omega_\gamma - \omega_\sigma\|_{\Theta^l} \right), \end{aligned}$$

with $s = \max(k, 2)$ and $l = \max(k, 1)$. Hence, if $k \geq 1$, we have

$$\|\omega_\gamma - \omega_\sigma\|_{\Theta^{k+1}} \leq C \left(\|\gamma_u - \sigma_u\|_{\Gamma^{k+2}([0, L_u])} + \|\gamma_v - \sigma_v\|_{\Gamma^{k+2}([0, L_v])} + \|\omega_\gamma - \omega_\sigma\|_{\Theta^k} \right).$$

Since the Lipschitz continuity of \mathcal{J}_{k, R_k} in the case where $k=0$ follows from Proposition 4.9, we then obtain the Lipschitz continuity of \mathcal{J}_{k, R_k} in the general case by a straightforward induction argument on $k \geq 0$. Finally, the Lipschitz continuity of $\mathcal{I} \circ (\text{Id}, \mathcal{J}_{k, R_k})$ follows from Proposition 4.6. This concludes the proof. ■

In what follows, we will not make explicit the dependency of the mapping \mathcal{J}_{k, R_k} on R_k , so that it will be denoted \mathcal{J}_k .

Extension to rectangles

We now extend Propositions 4.8 and 4.10 on the existence and uniqueness of a solution to the fixed-point equation (4.49) and Propositions 4.9 and 4.11 on the continuity with respect to boundary conditions to the whole domain $D = [0, L_u] \times [0, L_v]$, with $L_u, L_v \in \mathbb{R}_*^+$. In the same manner as above, we start with the case where $k=0$.

Proposition 4.12 (Global existence of a solution). *Let M be a smooth, open, complete, and simply connected surface, let $D = [0, L_u] \times [0, L_v]$, with $L_u, L_v \in \mathbb{R}_*^+$, and let $\gamma = (\gamma_u, \gamma_v) \in \Gamma^2([0, L_u]) \times \Gamma^2([0, L_v])$ be such that $\gamma_u(0) = \gamma_v(0)$ and $\angle(\gamma'_u(0), \gamma'_v(0)) \in (0, \pi)$. Then, there exists a unique solution $\omega \in \Theta_\gamma^1(D)$ to (4.49).*

Proof.

Step 1 (Restriction of F to angle distributions coinciding with the local solution). First, owing to Proposition 4.8, there exists $L_0 \in (0, L_v]$ such that there exists a unique solution $\omega_\gamma = \mathcal{J}_0(\gamma) \in \Theta_\gamma^1(D_{L_0})$, with $D_{L_0} = [0, L_u] \times [0, L_0]$, to (4.49). Suppose that $L_0 < L_v$. Otherwise, we have the expected result. We set $\varphi_\gamma := \mathcal{I}(\gamma, \omega_\gamma) \in \Phi^1(D_{L_0})$. Since we cannot expect in the general setting that the u -coordinate curves of the mapping φ_γ are arc-length parametrized, we cannot construct an extension of φ_γ using the curves $\varphi_\gamma(\cdot, L_0)$ and γ_v as new boundary conditions. Therefore, we prove the claim using a fixed-point argument on the angle distributions $\tilde{\omega}_\gamma$ defined to be extensions of $\omega_\gamma: D_{L_0} \rightarrow \mathbb{R}$. Let $L_1 \in (L_0, L_v]$ be such that $L_1 \leq 2L_0$ and let $D_{L_1} = [0, L_u] \times [0, L_1]$. We define the set $S_{1,\gamma}(D_{L_1})$ composed of extensions of ω_γ as follows:

$$S_{1,\gamma}(D_{L_1}) = \left\{ \tilde{\omega}_\gamma \in \Theta_\gamma^1(D_{L_1}) \text{ s.t. } \tilde{\omega}_\gamma|_{D_{L_0}} = \omega_\gamma \right\}.$$

Note that $S_{1,\gamma}(D_{L_1})$ is clearly not empty and, to abbreviate the notation, we also denote ω_γ the generic elements of $S_{1,\gamma}$. We now adapt the proof of Proposition 4.8 to show that F^2 is a contraction mapping in some bounded subset of $S_{1,\gamma}(D_{L_1})$ that is stable by F . Recall from this proof that there exists $\mathcal{R}(\gamma) > 0$, depending only on $\|\gamma_u\|_{\Gamma^2([0, L_u])}$ and $\|\gamma_v\|_{\Gamma^2([0, L_v])}$, such that

$F : \mathcal{B}_{\Theta^1(D_{L_1})}(\mathcal{R}(\gamma)) \rightarrow \mathcal{B}_{\Theta^1(D_{L_1})}(\mathcal{R}(\gamma))$, where $\mathcal{B}_{\Theta^1(D_{L_1})}(\mathcal{R}(\gamma))$ is the closed ball of radius $\mathcal{R}(\gamma)$ centered at the origin in $\Theta_\gamma^1(D_{L_1})$.

Step 2 (Contraction mapping). Let $\sigma = (\sigma_u, \sigma_v) \in \Gamma^2([0, L_u]) \times \Gamma^2([0, L_v])$ be such that $\sigma_u(0) = \sigma_v(0) = \gamma_u(0)$, $\gamma'_u(0) = \sigma'_u(0)$, and $\gamma'_v(0) = \sigma'_v(0)$. Let $\omega_\sigma \in S_{1,\sigma}(D_{L_1})$. We now prove the following counterpart of (4.51):

$$\begin{aligned} \|F^2(\omega_\gamma) - F^2(\omega_\sigma)\|_{\Theta^1(D_{L_1})} &\leq C \left(\|\gamma_u - \sigma_u\|_{\Gamma^2([0, L_u])} + \|\gamma_v - \sigma_v\|_{\Gamma^2([0, L_v])} + L_0 \|\omega_\gamma - \omega_\sigma\|_{\Theta^1(D_{L_0})} \right. \\ &\quad \left. + (L_1 - L_0) \|\omega_\gamma - \omega_\sigma\|_{\Theta^1([0, L_u] \times [L_0, L_1])} \right), \end{aligned} \quad (4.58)$$

where the constant C is independent of L_0 and L_1 . A simple modification of the proof of (4.10a) implying (4.19a) gives the following counterpart of (4.53):

$$\begin{aligned} \|\mathcal{I}(\gamma, \omega_\gamma) - \mathcal{I}(\sigma, \omega_\sigma)\|_{\Phi^0(D_{L_1})} &\leq C \left((L_1 - L_0) \|\omega_\gamma - \omega_\sigma\|_{\Theta^1([0, L_u] \times [L_0, L_1])} \right. \\ &\quad \left. + L_0 \|\omega_\gamma - \omega_\sigma\|_{\Theta^1(D_{L_0})} + \|\gamma_u - \sigma_u\|_{\Gamma^2([0, L_u])} \right), \end{aligned}$$

where the constant C is independent of L_0 and L_1 . Hence, we obtain the following counterpart of (4.52):

$$\begin{aligned} \|F(\omega_\gamma) - F(\omega_\sigma)\|_{\Theta^0(D_{L_1})} &\leq C \left(\|\gamma_u - \sigma_u\|_{\Gamma^2([0, L_u])} + \|\gamma_v - \sigma_v\|_{\Gamma^2([0, L_v])} \right. \\ &\quad \left. + L_0 \|\omega_\gamma - \omega_\sigma\|_{\Theta^1(D_{L_0})} + (L_1 - L_0) \|\omega_\gamma - \omega_\sigma\|_{\Theta^1([0, L_u] \times [L_0, L_1])} \right), \end{aligned} \quad (4.59a)$$

$$\begin{aligned} \|F(\omega_\gamma) - F(\omega_\sigma)\|_{\Theta^1(D_{L_1})} &\leq C \left(\|\gamma_u - \sigma_u\|_{\Gamma^2([0, L_u])} + \|\gamma_v - \sigma_v\|_{\Gamma^2([0, L_v])} \right. \\ &\quad \left. + L_0 \|\omega_\gamma - \omega_\sigma\|_{\Theta^1(D_{L_0})} + (L_1 - L_0) \|\omega_\gamma - \omega_\sigma\|_{\Theta^1([0, L_u] \times [L_0, L_1])} \right. \\ &\quad \left. + \|\omega_\gamma - \omega_\sigma\|_{\Theta^0(D_{L_0})} + \|\omega_\gamma - \omega_\sigma\|_{\Theta^0([0, L_u] \times [L_0, L_1])} \right), \end{aligned} \quad (4.59b)$$

where the constant C is independent of L_0 and L_1 . Then, (4.58) follows from (4.59) in the same manner as in the proof of Proposition 4.8.

Step 3 (Conclusion). We set $\mathcal{B}_{S_{1,\gamma}(D_{L_1})}(\mathcal{R}(\gamma)) := \mathcal{B}_{\Theta^1(D_{L_1})}(\mathcal{R}(\gamma)) \cap S_{1,\gamma}(D_{L_1})$. We clearly have that F maps $\mathcal{B}_{S_{1,\gamma}(D_{L_1})}(\mathcal{R}(\gamma))$ onto itself, so that we now restrict F to this ball. We infer from (4.58) that there exists $L_1^* \in (L_0, L_v]$, with $L_1^* \leq 2L_0$, such that F^2 is a contraction mapping in $\mathcal{B}_{S_{1,\gamma}(D_{L_1^*})}(\mathcal{R}(\gamma))$. Hence, using the Banach fixed-point theorem, we obtain that there exists a unique solution $\omega_\gamma^* \in S_{1,\gamma}(D_{L_1^*})$. Moreover, since the constants in (4.58) are independent of L_0 , we infer that L_1^* is independent of L_0 , so that we can repeat (a finite number of times) the argument until we reach L_v . The claim follows. ■

Proposition 4.13 (Regularity of the global solution). *Let M be a smooth, open, complete, and simply connected surface, let $k \in \mathbb{N}$, and let $D = [0, L_u] \times [0, L_v]$, with $L_u, L_v \in \mathbb{R}_*^+$. Let $\gamma = (\gamma_u, \gamma_v) \in \Gamma^{k+2}([0, L_u]) \times \Gamma^{k+2}([0, L_v])$ be such that $\gamma_u(0) = \gamma_v(0)$ and $\angle(\gamma'_u(0), \gamma'_v(0)) \in (0, \pi)$. Then, there exists a unique solution $\omega \in \Theta_\gamma^{k+1}(D)$ to (4.49).*

Proof. The claim is obtained in the same manner as in Proposition 4.10. ■

For all $k \in \mathbb{N}$ and $R_k \in \mathbb{R}_*^+$, we now extend \mathcal{J}_{k,R_k} to the whole rectangle $D = [0, L_u] \times [0, L_v]$ as follows:

$$\mathcal{J}_{k,R_k} : \mathcal{B}_{\Gamma^{k+2} \times \Gamma^{k+2}}(R_k) \rightarrow \Theta_\gamma^{k+1}(D).$$

We prove in the following proposition that \mathcal{J}_{k,R_k} is Lipschitz continuous.

Proposition 4.14 (Continuity with respect to boundary conditions). *Let M be a smooth, open, complete, and simply connected surface, let $k \in \mathbb{N}$, let $R_k \in \mathbb{R}_*^+$, and let $D = [0, L_u] \times [0, L_v]$, with $L_u, L_v \in \mathbb{R}_*^+$. We equip $\mathcal{B}_{\Gamma^{k+2} \times \Gamma^{k+2}}(R_k)$ and $\Theta^{k+1}(D)$ with the norms in $\Gamma^{k+2}([0, L_u]) \times \Gamma^{k+2}([0, L_v])$ and $\Theta^{k+1}(D)$, respectively. Then, the mappings \mathcal{J}_{k,R_k} and*

$$\begin{aligned}\mathcal{I} \circ (\text{Id}, \mathcal{J}_{k,R_k}) : \mathcal{B}_{\Gamma^{k+2} \times \Gamma^{k+2}}(R_k) &\rightarrow \Phi^{k+2}(D) \\ \gamma = (\gamma_u, \gamma_v) &\mapsto \varphi_\omega := \mathcal{I}(\gamma, \mathcal{J}_{k,R_k}(\gamma))\end{aligned}$$

are Lipschitz continuous, with Id the identity operator in $\mathcal{B}_{\Gamma^{k+2} \times \Gamma^{k+2}}(R_k)$.

Proof. We first prove the claim in the case where $k=0$. Let $\gamma, \sigma \in \mathcal{B}_{\Gamma^{k+2} \times \Gamma^{k+2}}(R_k)$, with (γ_u, γ_v) and $\sigma = (\sigma_u, \sigma_v)$, be such that $\gamma_u(0) = \gamma_v(0) = \sigma_u(0) = \sigma_v(0)$, $\gamma'_u(0) = \sigma'_u(0)$ and $\gamma'_v(0) = \sigma'_v(0)$. We moreover suppose that $\angle(\gamma'_u(0), \gamma'_v(0)) = \angle(\sigma'_u(0), \sigma'_v(0)) \in (0, \pi)$. We denote $\omega_\gamma := \mathcal{J}_{0,R_0}(\gamma) \in \Theta_\gamma^1(D)$ and $\omega_\sigma := \mathcal{J}_{0,R_0}(\sigma) \in \Theta_\sigma^1(D)$. In the same manner as in the proof of Proposition 4.9, we infer from (4.58) that

$$\begin{aligned}\|\omega_\gamma - \omega_\sigma\|_{\Theta^1(D_{L_1})} &\leq \tilde{C} \left[\|\gamma_u - \sigma_u\|_{\Gamma^2([0, L_u])} + \|\gamma_v - \sigma_v\|_{\Gamma^2([0, L_v])} + L_0 \|\omega_\gamma - \omega_\sigma\|_{\Theta^1(D_{L_0})} \right] \\ &\leq C \left[\|\gamma_u - \sigma_u\|_{\Gamma^2([0, L_u])} + \|\gamma_v - \sigma_v\|_{\Gamma^2([0, L_v])} \right],\end{aligned}$$

using that the mapping (4.54) is Lipschitz continuous (Proposition 4.9) for the second inequality. Since the extension process is only operated a finite number of times, we easily obtain by repeating the above argument that the mapping \mathcal{J}_{0,R_0} is Lipschitz continuous. Then, the proof for the case $k > 0$ is obtained in the same manner as Proposition 4.11. Finally, the Lipschitz continuity of $\mathcal{I} \circ (\text{Id}, \mathcal{J}_{k,R_k})$ follows from Proposition 4.6. ■

Proof of the main result

Proof of Theorem 4.3. First, owing to Proposition 4.13, we obtain the existence of an angle distribution $\omega_\gamma := \mathcal{J}_k(\gamma) \in \Theta_\gamma^{k+1}(D)$ satisfying (4.49). Then, the continuity of \mathcal{J}_k and \mathcal{I} is a direct consequence of Proposition 4.14. Hence, to prove the claim, we suppose that $0 < \omega(u, v) < \pi$, for all $(u, v) \in D$, and we show that $\varphi := \mathcal{I}(\gamma, \omega_\gamma) \in \Theta_\gamma^{k+2}(D)$ satisfies (4.1). We suppose that $k=0$. Otherwise, this is a direct consequence of Proposition 4.7. Using the density of $\Gamma^3([0, L_u])$ and $\Gamma^3([0, L_v])$ in $\Gamma^2([0, L_u])$ and $\Gamma^2([0, L_v])$ respectively, let $(\gamma_{u,n})_{n \in \mathbb{N}} \subset \Gamma^3([0, L_u])$ and $(\gamma_{v,n})_{n \in \mathbb{N}} \subset \Gamma^3([0, L_v])$ be sequences satisfying $\gamma_{u,n}(0) = \gamma_u(0)$, $\gamma_{v,n}(0) = \gamma_v(0)$, $\gamma'_{u,n}(0) = \gamma'_u(0)$, $\gamma'_{v,n}(0) = \gamma'_v(0)$, for all $n \in \mathbb{N}$, and

$$\begin{aligned}\gamma_{u,n} &\xrightarrow[n \rightarrow \infty]{\Gamma^2} \gamma_u, \quad \text{and} \quad \|\gamma_{u,n}\|_{\Gamma^2([0, L_u])} \leq \|\gamma_u\|_{\Gamma^2([0, L_u])}, \quad \forall n \in \mathbb{N}, \\ \gamma_{v,n} &\xrightarrow[n \rightarrow \infty]{\Gamma^2} \gamma_v, \quad \text{and} \quad \|\gamma_{v,n}\|_{\Gamma^2([0, L_v])} \leq \|\gamma_v\|_{\Gamma^2([0, L_v])}, \quad \forall n \in \mathbb{N}.\end{aligned}$$

We set $\gamma_n = (\gamma_{u,n}, \gamma_{v,n}) \in \Gamma^3([0, L_u]) \times \Gamma^3([0, L_v])$, $\omega_n = \mathcal{J}_1(\gamma_n) \in \Theta_\gamma^2(D)$, and $\varphi_n = \mathcal{I}(\gamma_n, \omega_n) \in \Phi^3(D)$, for all $n \in \mathbb{N}$. Owing to Proposition 4.11, we infer that the sequence $(\omega_n)_{n \in \mathbb{N}}$ converges to ω in the $C^0(D)$ -norm. Hence, there exists $n_0 \in \mathbb{N}$ such that $0 < \omega_n(u, v) < \pi$, for all $(u, v) \in D$ and all $n \geq n_0$. Since $\omega_n \in \Theta_\gamma^2(D)$ and $\gamma_n \in \Gamma^3([0, L_u]) \times \Gamma^3([0, L_v])$, we obtain from Proposition 4.7 that φ_n is a Chebyshev net, for all $n \geq n_0$. Moreover, owing to Proposition 4.11,

we have that $\varphi_n \xrightarrow[n \rightarrow \infty]{\Phi^2(D)} \varphi$. Finally, since φ_n satisfies (4.1) for all $(u, v) \in D$ and all $n \geq n_0$, we conclude that φ satisfies (4.1) for all $(u, v) \in D$. The claim follows. \blacksquare

Chapter 5

Construction of Chebyshev nets with singularities

Introduction

We call *surface* a Riemannian 2-manifold, whose metric will be denoted g , and we consider complete, simply connected surfaces. A Chebyshev net $\varphi:U\subset\mathbb{R}^2\rightarrow\varphi(U)\subset M$, with U an open set, is a coordinate system satisfying

$$|\partial_u\varphi|_g(u,v)=|\partial_v\varphi|_g(u,v)=1, \quad (5.1)$$

for all $(u,v)\in U$. We construct in what follows Chebyshev nets with a finite set of conical singularities on surfaces with finite total negative curvature and total positive curvature lower than 2π . The main result of this chapter is the following theorem.

Theorem 5.1 (Existence of piecewise smooth Chebyshev nets with singularities). *Let M be a smooth, complete, simply connected surface satisfying*

$$\int_M K^+ < 2\pi \quad \text{and} \quad \int_M K^- < \infty, \quad (5.2)$$

where K is the Gaussian curvature of M , $K^+=\max(K,0)$ and $K^-=\max(-K,0)$. Then, there exists a piecewise smooth Chebyshev net with conical singularities $\mathcal{C}=(\{B_e^i\}_{1\leq i\leq N_{\text{pol}}}, \{\varphi_e^i\}_{1\leq i\leq N_{\text{pol}}}, T)$, with $N_{\text{pol}}\leq \frac{4}{\pi}\int_M K^- + 8$, on M .

We highlight that the proof of the theorem is constructive. The chapter is organized as follows. In Section 5.2, we first consider the construction of Chebyshev nets on broken half-surfaces, defined to be half-surfaces with polygonal boundaries. We prove the existence of Chebyshev nets on broken half-surfaces under some condition on their total curvature in Theorem 5.15. Then, we show in Section 5.3 that we can split surfaces satisfying (5.2) into broken half-surfaces (Theorem 5.20), each of them satisfying the conditions of Theorem 5.15. Finally, we combine these two results to construct the Chebyshev net with conical singularities in Section 5.4 and we show that this Chebyshev net is piecewise smooth.

Before this, let us introduce some notation. First, unless explicitly mentioned, any curve $\eta:I\subset\mathbb{R}\rightarrow M$ we consider in what follows is arc-length parametrized, continuous on I , and piecewise smooth according to the following definition:

Definition 5.2 (Piecewise smooth curves). Let $\eta: I \subset \mathbb{R} \rightarrow M$ be a continuous curve. We say that the curve η is piecewise smooth if there exists a partition of I in the form $\bigcup_{i=1}^{N+1} [a_{i-1}, a_i] = I$, with $a_0 < \dots < a_{N+1}$. Suppose moreover that η restricted to (a_{i-1}, a_i) is a smooth curve with all the derivatives having a finite limit from the right at a_{i-1} and from the left at a_i , for all $i \in \{1, \dots, N+1\}$. We say that the curve η is piecewise smooth.

We denote $\angle(X, Y) \in (-\pi, \pi]$ the oriented angle (using the orientation of M) between the vectors X and Y in the tangent plane $T_p M$ at any point $p \in M$. We define the total positive and negative turn angle of continuous piecewise smooth curves (see [14]):

Definition 5.3 (Positive and negative turn angle τ_{\pm}). Let $\eta: I \subset \mathbb{R} \rightarrow M$ be a continuous piecewise smooth curve on the partition of I defined by $a_0 < \dots < a_{N+1}$. Then, for all $i \in \{1, \dots, N+1\}$, let $\kappa_i: [a_{i-1}, a_i] \rightarrow \mathbb{R}$ be the geodesic curvature of $\eta|_{[a_{i-1}, a_i]}$ defined by

$$\kappa_i(s) = \langle \eta''(s), \eta'^{\perp}(s) \rangle_g,$$

with $\eta'^{\perp}(s) \in T_{\eta(s)} M$ the vector such that $\angle(\eta'(s), \eta'^{\perp}(s)) = \frac{\pi}{2}$, for all $s \in [a_{i-1}, a_i]$. Let $\psi_i = \angle(\eta'(a_i^-), \eta'(a_i^+))$, for all $i \in \{1, \dots, N\}$. We suppose that $-\pi < \psi_i < \pi$, for all $i \in \{1, \dots, N\}$. We define the total positive and negative turn angles $\tau(\eta)$ by

$$\tau_+(\eta) = \sum_{i=1}^{N+1} \int_{a_{i-1}}^{a_i} \kappa_i^+ + \sum_{i=1}^N \psi_i^+, \quad \tau_-(\eta) = \sum_{i=1}^{N+1} \int_{a_{i-1}}^{a_i} \kappa_i^- + \sum_{i=1}^N \psi_i^-, \quad (5.3)$$

and we define the total turn angle as $\tau(\eta) = \tau_+(\eta) - \tau_-(\eta)$. (Note that $\tau_{\pm}(\eta)$ are different from $(\tau(\eta))^{\pm}$.) We denote $\tau(\eta|_{[a, b]})$, with $a, b \in \mathbb{R}$ such that $a < b$, the restriction to $[a, b]$ of the total turn angle. Note that, if any, the pointwise turns at a and b are included.

An illustration of the turn angle is presented in Figure 5.1. Finally, we denote $\text{int}(D)$ the interior of any set D .

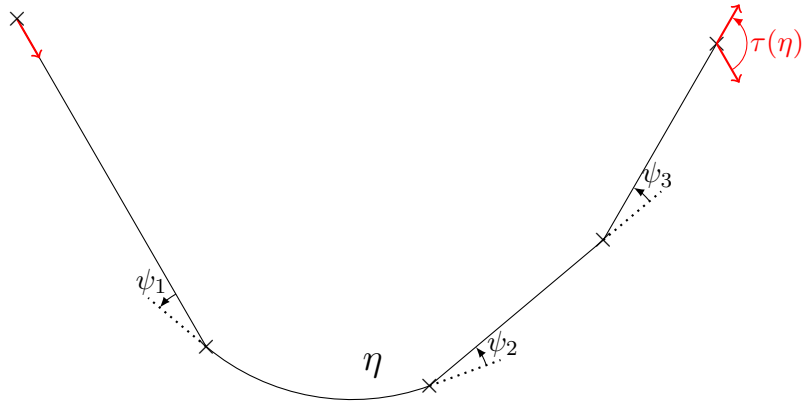


Fig. 5.1 Illustration of the total turn angle $\tau(\eta)$

Chebyshev nets on broken half-surfaces

In order to construct a Chebyshev net on broken half-surfaces with $N \geq 1$ vertices, we first restrict ourselves in Section 5.2.1 to the case of a sector, which corresponds to the case $N = 1$. Then, in Section 5.2.2, we show that broken half-surfaces admit a Chebyshev parametrization as a particular piecewise smooth sector, under conditions on their total Gaussian curvature.

Construction on a sector

We give in this section some existence results for Chebyshev nets on sectors.

Definition 5.4 ((Smooth) sector). *A sector Q of the surface M is an unbounded connected domain of M delimited by the two curves $\eta_1 : \mathbb{R}^- \rightarrow M$ and $\eta_2 : \mathbb{R}^+ \rightarrow M$ intersecting only at $p = \eta_1(0) = \eta_2(0)$. Sectors are said to be smooth whenever the two curves η_1 and η_2 are smooth. The angle $\psi = \angle(\eta'_1(0), \eta'_2(0))$ is supposed to be in $(0, \pi)$ and is called the exterior angle of the sector Q .*

A sector with the notation introduced above is presented in Figure 5.2. Now, we recall a theorem obtained by Bakelman [2] and stated in the present form in [14]:

Theorem 5.5 (I. Ya. Bakelman). *Let Q be a sector delimited by the two curves $\eta_1 : \mathbb{R}^- \rightarrow M$ and $\eta_2 : \mathbb{R}^+ \rightarrow M$ intersecting at $p \in M$. Suppose that Q satisfies the conditions*

$$\tau_+(\eta_1) + \tau_+(\eta_2) + \int_Q K^+ < \pi - \psi, \quad (5.4a)$$

$$\tau_-(\eta_1) + \tau_-(\eta_2) + \int_Q K^- < \psi, \quad (5.4b)$$

where $\psi > 0$ is the exterior angle of Q at the vertex p and $\tau_{\pm}(\eta_i)$, with $i \in \{1, 2\}$, are the total positive and negative turn angles of η_i defined by (5.3). Then, there exist global Chebyshev coordinates in Q such that η_1 and η_2 are coordinate curves. Furthermore, the angle between the coordinate curves is bounded away from 0 and π by the positive real number

$$\min \left(\pi - \psi - \int_Q K^+ - \tau_+(\eta_1) - \tau_+(\eta_2), \psi - \int_Q K^- - \tau_-(\eta_1) - \tau_-(\eta_2) \right).$$

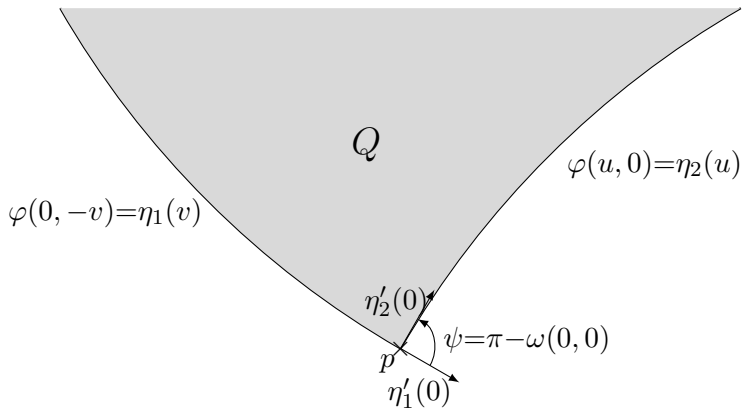


Fig. 5.2 Illustration of a Chebyshev net φ on a sector Q of exterior angle ψ

This theorem gives no information about the regularity of the Chebyshev net, even when the two delimiting curves of the sector are smooth curves. Our goal is now to sharpen Theorem 5.5 (see Proposition 5.9 below) to prove the existence of smooth Chebyshev nets on sectors delimited by smooth curves satisfying the counterpart of (5.4) for smooth curves, namely

$$\int_{\mathbb{R}^+} \kappa_2^+ + \int_{\mathbb{R}^-} \kappa_1^+ + \int_Q K^+ < \pi - \psi \text{ and } \int_{\mathbb{R}^+} \kappa_2^- + \int_{\mathbb{R}^-} \kappa_1^- + \int_Q K^- < \psi. \quad (5.5)$$

To this purpose, we state some preliminary results. First, we relate in Property 5.6 the geodesic curvatures of the coordinate curves of Chebyshev nets to the angle ω between these coordinate curves. Then, we present the Hazzidakis formula in Property 5.7. See [25] for a proof of these properties.

Property 5.6 (Geodesic curvature of coordinate curves). *Let $\varphi:U\subset\mathbb{R}^2\rightarrow\varphi(U)\subset M$ be a smooth mapping satisfying (5.1) and let $(u_1, v_1)\in\mathbb{R}^2$ and $(u_2, v_2)\in\mathbb{R}^2$. We denote $\omega:U\rightarrow\mathbb{R}/2\pi\mathbb{Z}$ the angle distribution defined by $\omega(u, v)=\angle(\partial_u\varphi, \partial_v\varphi)(u, v)$, for all $(u, v)\in U$. Then, supposing u_1 , v_1 and v_2 are such that $\{u_1\}\times[v_1, v_2]\subset U$, we have*

$$\omega(u_1, v_2)=\omega(u_1, v_1)-\int_{-v_2}^{-v_1}\kappa_v, \quad (5.6)$$

where $\kappa_v:[-v_2, -v_1]\rightarrow\mathbb{R}$ is the geodesic curvature of the curve $\eta_1:[-v_2, -v_1]\rightarrow M$ defined by $\eta_1(v)=\varphi(u_1, -v)$, for all $v\in[-v_2, -v_1]$. This property, illustrated in Figure 5.3, results from the parallel transport of the vector field $\partial_u\varphi$ along η_1 . Moreover, supposing u_1 , u_2 and v_1 are such that $[u_1, u_2]\times\{v_1\}\subset U$, we have

$$\omega(u_2, v_1)=\omega(u_1, v_1)-\int_{u_1}^{u_2}\kappa_u, \quad (5.7)$$

where $\kappa_u:[u_1, u_2]\rightarrow\mathbb{R}$ is the geodesic curvature of the curve $\eta_2:[u_1, u_2]\rightarrow M$ defined by $\eta_2(u)=\varphi(u, v_1)$, for all $u\in[u_1, u_2]$.

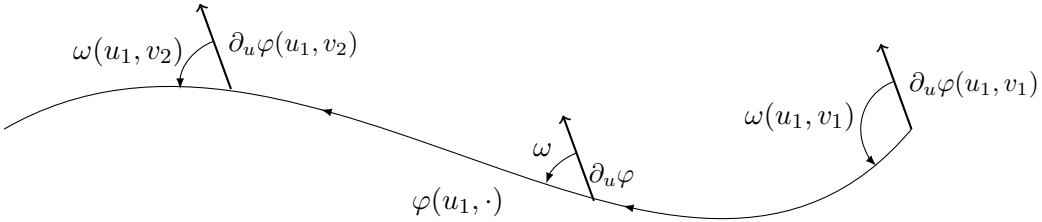


Fig. 5.3 Illustration of the parallel transport of $\partial_u\varphi$ along $\varphi(u_1, \cdot)$

Property 5.7 (Hazzidakis formula). *Let $U=[u_1, u_2]\times[v_1, v_2]$, with $(u_1, v_1)\in\mathbb{R}^2$ and $(u_2, v_2)\in\mathbb{R}^2$. Let $\varphi:U\rightarrow\Omega\subset M$, with $\Omega=\varphi(U)$, be a smooth Chebyshev net. We denote $\omega:U\rightarrow(0, \pi)$ the angle distribution defined by $\omega=\angle(\partial_u\varphi, \partial_v\varphi)$ and we denote $\eta_1:[-v_2, -v_1]\rightarrow M$ and $\eta_2:[u_1, u_2]\rightarrow M$ the two curves respectively defined by $\eta_1(v)=\varphi(u_1, -v)$, for all $v\in[-v_2, -v_1]$, and $\eta_2(u)=\varphi(u, v_1)$, for all $u\in[u_1, u_2]$. We denote $\kappa_u:[u_1, u_2]\rightarrow\mathbb{R}$ and $\kappa_v:[-v_2, -v_1]\rightarrow\mathbb{R}$ their respective geodesic curvature. Then, the angle distribution ω satisfies the following Hazzidakis formula*

$$\omega(u_2, v_2)=\omega(u_1, v_1)-\int_{u_1}^{u_2}\kappa_u-\int_{-v_2}^{-v_1}\kappa_v-\int_{\Omega}K. \quad (5.8)$$

Lemma 5.8 (Homeomorphism). *Let Q be a smooth sector delimited by the two smooth curves $\eta_1:\mathbb{R}^-\rightarrow M$ and $\eta_2:\mathbb{R}^+\rightarrow M$ intersecting at $p\in M$, and satisfying (5.5). Assume that $\varphi:(\mathbb{R}^+)^2\rightarrow\varphi[(\mathbb{R}^+)^2]\subset M$ is a smooth mapping satisfying (5.1), and such that $\varphi(u, 0)=\eta_2(u)$, $\varphi(0, v)=\eta_1(-v)$ for all $(u, v)\in(\mathbb{R}^+)^2$. Then, $\varphi:(\mathbb{R}^+)^2\rightarrow Q$ is a homeomorphism.*

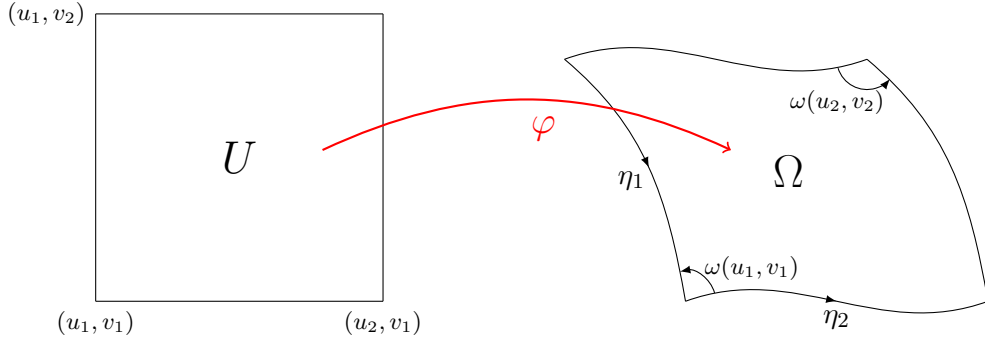


Fig. 5.4 Illustration of the Hazzidakis formula

Proof. The proof is obtained in the same manner as in [43]. We just recall here the principal ideas. We denote $\omega:(\mathbb{R}^+)^2 \rightarrow \mathbb{R}/2\pi\mathbb{Z}$ the angle distribution defined by $\omega(u, v) = \angle(\partial_u \varphi, \partial_v \varphi)(u, v)$, for all $(u, v) \in (\mathbb{R}^+)^2$. We denote $\kappa_1:\mathbb{R}^- \rightarrow \mathbb{R}$ and $\kappa_2:\mathbb{R}^+ \rightarrow \mathbb{R}$ the geodesic curvatures of η_1 and η_2 respectively. First, using (5.7), we obtain that

$$\omega(u, 0) = \omega(0, 0) - \int_0^u \kappa_2 = \pi - \psi - \int_0^u \kappa_2,$$

for all $u \in \mathbb{R}^+$. Then, using hypothesis (5.5), we deduce that $\omega(u, 0) \in (0, \pi)$, for all $u \in \mathbb{R}^+$. In the same manner, we obtain that $\omega(0, v) = \pi - \psi - \int_{-v}^0 \kappa_1 \in (0, \pi)$, for all $v \in \mathbb{R}^+$. Hence, using the continuity of ω , we infer that there exists $\tilde{D} = [0, l_1] \times [0, l_2] \subset (\mathbb{R}^+)^2$, with $l_1, l_2 \in \mathbb{R}_*^+$, such that $\omega(\tilde{D}) \subset (0, \pi)$. Since (5.1) is satisfied, we infer that $\varphi|_{\tilde{D}}:\tilde{D} \rightarrow \varphi(\tilde{D}) \subset M$ is a local homeomorphism, so that, up to reducing l_1 and l_2 , φ is a homeomorphism. Moreover, since $\omega(\tilde{D}) \subset (0, \pi)$, we deduce that $\angle(\eta'_2(u), \partial_v \varphi(u, 0)) \in (0, \pi)$, for all $u \in [0, l_1]$, and $\angle(\eta'_1(-v), \partial_v \varphi(0, v)) \in (0, \pi)$, for all $v \in [0, l_2]$. We conclude that, up to reducing l_1 and l_2 , we have $\varphi(\tilde{D}) \subset Q$.

Reasoning by contradiction, we first suppose that φ is not a homeomorphism. Let $U = [0, L_1] \times [0, L_2]$ and $U_{\text{cl}} = [0, L_1] \times [0, L_2]$, with $L_1, L_2 > 0$, be such that $\varphi|_U:U \rightarrow \varphi(U) \subset M$ is a homeomorphism and such that $\varphi|_{U_{\text{cl}}}:U_{\text{cl}} \rightarrow \varphi(U_{\text{cl}}) \subset M$ is not a homeomorphism. Using the Hazzidakis formula (5.8) and hypothesis (5.5), we easily obtain that $\omega(U_{\text{cl}}) \subset (0, \pi)$. Hence, the mapping $\varphi|_{U_{\text{cl}}}$ is a local homeomorphism. Now, suppose that there exist $(u_1, v_1), (u_2, v_2) \in (0, L_1] \times \{L_2\} \cup \{L_1\} \times (0, L_2]$ with $\varphi(u_1, v_1) = \varphi(u_2, v_2)$. Then, the two following cases are possible:

- case 1: $u_1 = u_2 = L_1$ or $v_1 = v_2 = L_2$. We only consider the first subcase, since the reasoning for the second subcase is similar. Then, assuming that $u_1 = u_2 = L_1$, one can see that the Gauss–Bonnet formula applied to the curve $\varphi(\{L_1\} \times [v_1, v_2])$ is in contradiction with (5.5).
- case 2: $u_1 \neq u_2$ and $v_1 \neq v_2$. In this case, we can suppose, without loss of generality, that $v_1 = L_2$ and $u_2 = L_1$. Then, the Gauss–Bonnet formula applied to the curve $\varphi([u_1, L_1] \times \{L_2\}) \cup \varphi(\{L_1\} \times [L_2, v_2])$ yields a contradiction with (5.5).

We finally suppose that $\varphi((\mathbb{R}^+)^2) \not\subset Q$. Then, let $\tilde{U} = [0, \tilde{L}_1] \times [0, \tilde{L}_2]$, with $\tilde{L}_1, \tilde{L}_2 > 0$, be such that $\varphi(\tilde{U}) \subset Q$ and such that there exists $(\tilde{u}, \tilde{v}) \in (0, \tilde{L}_1] \times \{\tilde{L}_2\} \cup \{\tilde{L}_1\} \times (0, \tilde{L}_2]$ with $\varphi(\tilde{u}, \tilde{v}) \in \partial Q$. Then, $\varphi(\tilde{u}, \tilde{v}) \in \eta_1(\mathbb{R}^-)$ or $\varphi(\tilde{u}, \tilde{v}) \in \eta_2(\mathbb{R}^+)$ and we obtain again a contradiction between the Gauss–Bonnet formula and (5.5). This concludes the proof. ■

Proposition 5.9 (Existence of smooth Chebyshev nets on sectors). *Let Q be a smooth sector delimited by the two smooth curves $\eta_1:\mathbb{R}^- \rightarrow M$ and $\eta_2:\mathbb{R}^+ \rightarrow M$, and with exterior angle $\psi \in$*

$(0, \pi)$. Suppose that the geodesic curvatures $\kappa_1 : \mathbb{R}^- \rightarrow \mathbb{R}$ and $\kappa_2 : \mathbb{R}^+ \rightarrow \mathbb{R}$ of η_1 and η_2 respectively and the Gaussian curvature K of Q satisfy (5.5). Then, there exists a unique Chebyshev net $\varphi : (\mathbb{R}^+)^2 \rightarrow Q$ such that

$$\begin{aligned}\varphi(u, 0) &= \eta_2(u), \quad \forall u \in \mathbb{R}^+, \\ \varphi(0, v) &= \eta_1(-v), \quad \forall v \in \mathbb{R}^+.\end{aligned}\tag{5.9}$$

Moreover, the angle $\omega = \angle(\partial_u \varphi, \partial_v \varphi) \in (0, \pi)$ of φ satisfies the Hazzidakis formula

$$\omega(u, v) = \pi - \psi - \int_0^u \kappa_2 - \int_{-v}^0 \kappa_1 - \int_{\varphi([0, u] \times [0, v])} K,\tag{5.10}$$

for all $(u, v) \in (\mathbb{R}^+)^2$.

The Hazzidakis formula in the sector Q is illustrated in Figure 5.5.

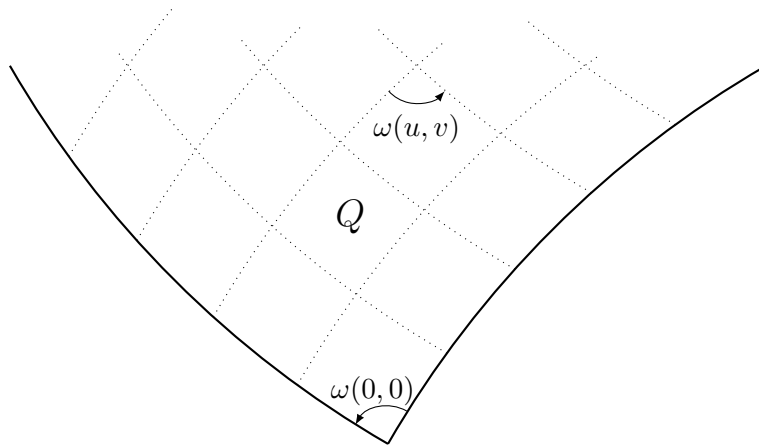


Fig. 5.5 Illustration of the Hazzidakis formula in the sector Q

Before proving this result, we recall a theorem proved in Chapter 4.

Theorem 5.10 (Existence of a unique solution to integrability condition). *Let M be a smooth, open, complete, and simply connected surface. Let $\eta_1 : \mathbb{R}^- \rightarrow M$ and $\eta_2 : \mathbb{R}^+ \rightarrow M$ be two smooth curves with respective geodesic curvatures $\kappa_1 : \mathbb{R}^- \rightarrow \mathbb{R}$ and $\kappa_2 : \mathbb{R}^+ \rightarrow \mathbb{R}$, and such that $\eta_1(0) = \eta_2(0)$. Suppose that $\psi := \angle(\eta'_1(0), \eta'_2(0)) \in (0, \pi)$. Then, there exists a unique angle distribution $\omega : (\mathbb{R}^+)^2 \rightarrow \mathbb{R}/2\pi\mathbb{Z}$ satisfying the Hazzidakis formula (5.10), with $\varphi : (\mathbb{R}^+)^2 \rightarrow M$ the unique smooth mapping satisfying the boundary conditions (5.9), and such that its v -coordinate curves are arc-length parametrized curves with a geodesic curvature $\kappa_2^{\text{map}} : D \rightarrow \mathbb{R}$ satisfying $\kappa_2^{\text{map}}(u, v) = \partial_v \omega(u, v)$, for all $(u, v) \in (\mathbb{R}^+)^2$.*

Suppose moreover that there exists $\tilde{D} = [0, \tilde{L}_2] \times [0, \tilde{L}_1]$, with $\tilde{L}_1, \tilde{L}_2 \in \mathbb{R}_*^+$, such that $0 < \omega(u, v) < \pi$, for all $(u, v) \in \tilde{D}$. Then, the mapping φ satisfies

$$|\partial_u \varphi|_g(u, v) = |\partial_v \varphi|_g(u, v) = 1,\tag{5.11}$$

for all $(u, v) \in \tilde{D}$.

Proof of Proposition 5.9. Using Theorem 5.10, we infer that there exists a unique angle distribution $\omega : (\mathbb{R}^+)^2 \rightarrow \mathbb{R}/2\pi\mathbb{Z}$ satisfying the Hazzidakis formula (5.10), with $\varphi : (\mathbb{R}^+)^2 \rightarrow M$ the unique mapping satisfying the boundary conditions (5.9) and the properties presented in the theorem.

Then, using the continuity of the angle distribution ω and $\omega(0, 0) = \pi - \psi \in (0, \pi)$, we infer that there exists $\tilde{L}_1, \tilde{L}_2 > 0$ such that $\omega(u, v) \in (0, \pi)$ for all $(u, v) \in [0, \tilde{L}_1] \times [0, \tilde{L}_2]$. Hence, by Theorem 5.10, the mapping φ satisfies (5.11) for all $(u, v) \in [0, \tilde{L}_1] \times [0, \tilde{L}_2]$. Then, in the same manner as in the proof of Lemma 5.8, we obtain that $\varphi: (\mathbb{R}^+)^2 \rightarrow Q$ is a Chebyshev net. Suppose finally that $\tilde{\varphi}: (\mathbb{R}^+)^2 \rightarrow M$ is a Chebyshev net satisfying the boundary conditions (5.9). Then, using Property 5.7, we obtain that the angle distribution $\tilde{\omega}: (\mathbb{R}^+)^2 \rightarrow (0, \pi)$ defined by $\tilde{\omega} = \angle(\partial_u \tilde{\varphi}, \partial_v \tilde{\varphi})(u, v)$, for all $(u, v) \in (\mathbb{R}^+)^2$, satisfies the Hazzidakis formula (5.10). We deduce from Theorem 5.10 that $\varphi = \tilde{\varphi}$. This concludes the proof. ■

Construction on a broken half-surface

We now introduce broken half-surfaces which are defined to be half-surfaces with polygonal boundaries:

Definition 5.11 ((Geodesic) broken half-surfaces). *Let $N \geq 1$ be an integer. We say that B_c is a broken half-surface if B_c is a half-surface delimited by a piecewise smooth curve $\gamma: \mathbb{R} \rightarrow M$ on the partition of \mathbb{R} defined by $-\infty = a_0 < \dots < a_{N+1} = \infty$. We denote $p_i = \gamma(a_i)$, for all $i \in \{1, \dots, N\}$, and we set $\gamma_i := \gamma|_{[a_{i-1}, a_i]}: [a_{i-1}, a_i] \rightarrow M$, for all $i \in \{1, \dots, N+1\}$. The points $\{p_i\}_{1 \leq i \leq N}$ are called the vertices of B_c . We suppose moreover that the exterior angle $\psi_i = \angle(\gamma'_i(a_i^-), \gamma'_{i+1}(a_i^+))$ at the vertex p_i satisfies $\psi_i \in (0, \pi)$, for all $i \in \{1, \dots, N\}$. Finally, we define*

$$|\psi|_{l^1} = \sum_{1 \leq i \leq N} \psi_i, \quad \text{and} \quad |\psi|_{l^\infty} = \max_{1 \leq i \leq N} \psi_i$$

and we suppose that $|\psi|_{l^1} < \pi$. Broken half-surfaces are called geodesic when the boundary curves are geodesic curves. Broken half-surfaces with N vertices are called N -half-surfaces.

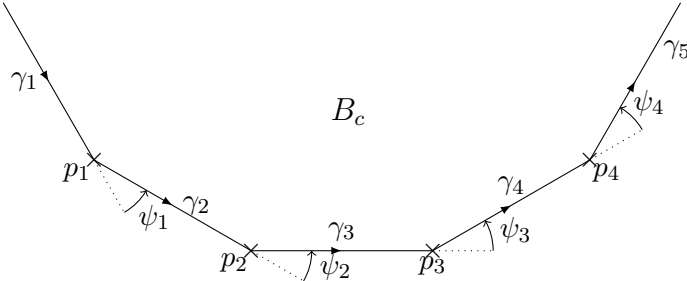


Fig. 5.6 Illustration of a geodesic N -half-surface B_c with $N=4$

We depict the notation introduced in Definition 5.11 in Figure 5.6. Note that the edges composing ∂B_c are depicted as straight edges in this figure although they are more generally curved edges. We observe that 1-half-surfaces are smooth sectors. Now, in order to find Chebyshev nets on broken half-surfaces, we view them as sectors delimited by two piecewise smooth curves. This process, called sectorization, is described in the following definition.

Definition 5.12 (Sectorization). *Let $N \geq 1$ and let B_c be a N -half-surface delimited by the curves $\{\gamma_i\}_{1 \leq i \leq N+1}$. We denote $\{p_i\}_{1 \leq i \leq N}$ the vertices of B_c . Let $m \in \{1, \dots, N\}$. We denote $Q(B_c, p_m)$ the piecewise smooth sector delimited by the curves $\eta_1^m: \mathbb{R}^- \rightarrow M$ and $\eta_2^m: \mathbb{R}^+ \rightarrow M$*

defined so that

$$\eta_1^m(\mathbb{R}^-) = \bigcup_{i=1}^m \gamma_i([a_{i-1}, a_i]) \quad \text{and} \quad \eta_2^m(\mathbb{R}^+) = \bigcup_{i=m+1}^{N+1} \gamma_i([a_{i-1}, a_i]). \quad (5.12)$$

The sectorization of a broken half-surface is depicted in Figure 5.7. We give in the following

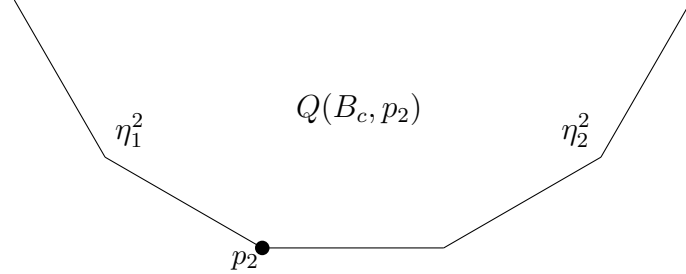


Fig. 5.7 Illustration of the sectorization $Q(B_c, p_2)$ of a N -half-surface B_c with $N=4$

proposition conditions on B_c for the existence of a sector $Q(B_c, p_m)$, for some $m \in \{1, \dots, N\}$, satisfying the conditions (5.4).

Proposition 5.13 (From N -half-surfaces to sectors). *Let $N \geq 1$ be an integer. Suppose that the N -half-surface B_c satisfies the conditions*

$$\tau_+(\partial B_c) + \int_{B_c} K^+ < \pi, \quad (5.13a)$$

$$\tau_-(\partial B_c) + \int_{B_c} K^- < |\psi|_{l^\infty}. \quad (5.13b)$$

Then, there exists $m \in \{1, \dots, N\}$ such that the piecewise smooth sector $Q(B_c, p_m)$ satisfies the conditions (5.4).

Proof. Let $m = \operatorname{argmax}_{1 \leq i \leq N} \psi_i$ and denote $Q_m = Q(B_c, p_m)$. Then, a straightforward computation gives

$$\begin{aligned} \int_{Q_m} K^+ + \tau_+(\eta_1) + \tau_+(\eta_2) &= \int_{Q_m} K^+ + |\psi|_{l^1} - \psi_m + \sum_{i=1}^{N+1} \int_{a_{i-1}}^{a_i} \kappa_i^+ = \tau_+(\partial B_c) + \int_{B_c} K^+ - \psi_m, \\ \int_{Q_m} K^- + \tau_-(\eta_1) + \tau_-(\eta_2) &= \int_{Q_m} K^- + \sum_{i=1}^{N+1} \int_{a_{i-1}}^{a_i} \kappa_i^- < \psi_m. \end{aligned}$$

Then, conditions (5.4) follow from (5.13). ■

Corollary 5.14 (Existence of Chebyshev nets on N -half-surfaces). *Let $N \geq 1$ be an integer. Let B_c be a N -half-surface delimited by the curves $(\gamma_i)_{1 \leq i \leq N+1}$. Suppose that B_c satisfies the conditions (5.13). Then, there exist Chebyshev coordinates on B_c such that $(\gamma_i)_{1 \leq i \leq N+1}$ are coordinate curves. Moreover, the angle of the net is bounded away from 0 and π by*

$$\varepsilon = \min \left(\pi - \tau_+(\partial B_c) - \int_{B_c} K^+, \quad |\psi|_{l^\infty} - \tau_-(\partial B_c) - \int_{B_c} K^- \right). \quad (5.14)$$

Proof. The proof follows by combining Proposition 5.13 and Theorem 5.5. ■

Finally, in the specific case of geodesic N -half-surfaces, we obtain the following theorem:

Theorem 5.15 (Existence of Chebyshev nets on geodesic N -half-surfaces). *Let $N \geq 1$. Let B_c be a geodesic N -half-surface delimited by the geodesic curves $\{\gamma_i\}_{1 \leq i \leq N+1}$. Suppose B_c satisfies the conditions*

$$\int_{B_c} K^+ < \pi - |\psi|_{l^1}, \quad (5.15a)$$

$$\int_{B_c} K^- < |\psi|_{l^\infty}. \quad (5.15b)$$

Then, there exist Chebyshev coordinates on B_c such that $\{\gamma_i\}_{1 \leq i \leq N+1}$ are coordinate curves. Moreover, the angle of the net is bounded away from 0 and π by the positive real number

$$\min \left(\pi - |\psi|_{l^1} - \int_{B_c} K^+, |\psi|_{l^\infty} - \int_{B_c} K^- \right). \quad (5.16)$$

Splitting of a surface into geodesic broken half-surfaces

In this section, we show how to split any surface M satisfying the curvature bound (5.2) into geodesic broken half-surfaces, each of them satisfying the conditions (5.15). This is the principal result of this section, stated in Theorem 5.20. This result is obtained in a similar manner to [14, Th. 4]: first, we split the surface into four sectors, all of them satisfying (5.15a) (see Theorem 5.18). Then, we split recursively each sector into broken half-surfaces, all of them satisfying (5.15a) (see Theorem 5.16). We finally prove that, after a finite number of splittings, all of the broken half-surfaces also satisfy the condition (5.15b).

Splitting of broken half-surfaces

We prove in this subsection the following theorem which extends the splitting of sectors, introduced in [14], to broken half-surfaces.

Theorem 5.16 (Splitting of N -half-surfaces). *Let $N \geq 1$ and let B_c be a N -half-surface with exterior angles $\{\psi_i^0\}_{1 \leq i \leq N}$ satisfying*

$$\int_{B_c} K^+ < \pi - |\psi^0|_{l^1} - 2\varepsilon \text{ and } \int_{B_c} K^- < C, \quad (5.17)$$

for positive C and ε . Then, there exist $N_1, N_2 \geq 1$ such that

$$N_1 + N_2 \in \{N + 1, N + 2\} \quad (5.18)$$

and a geodesic curve σ^ splitting B_c into a N_1 -half-surface B_c^1 with exterior angles $\{\psi_i^1\}_{1 \leq i \leq N_1}$ and a N_2 -half-surface B_c^2 with exterior angles $\{\psi_i^2\}_{1 \leq i \leq N_2}$ satisfying*

$$\int_{B_c^1} K^+ < \pi - |\psi^1|_{l^1} - \varepsilon, \quad \int_{B_c^1} K^- < \frac{C}{2}, \quad (5.19a)$$

$$\int_{B_c^2} K^+ < \pi - |\psi^2|_{l^1} - \varepsilon, \quad \int_{B_c^2} K^- < \frac{C}{2}, \quad (5.19b)$$

with $|\psi^1|_{l^1} = \sum_{i=1}^{N_1} \psi_i^1$, and $|\psi^2|_{l^1} = \sum_{i=1}^{N_2} \psi_i^2$.

Remark 5.17 (N_1 and N_2). Two different cases can happen for the splitting : either the geodesic curve σ^* intersects ∂B_c at some vertex and we have $N_1 + N_2 = N + 1$, or σ^* intersects ∂B_c in the interior of some edge and we have $N_1 + N_2 = N + 2$. See Figure 5.8 for an illustration of these two cases.

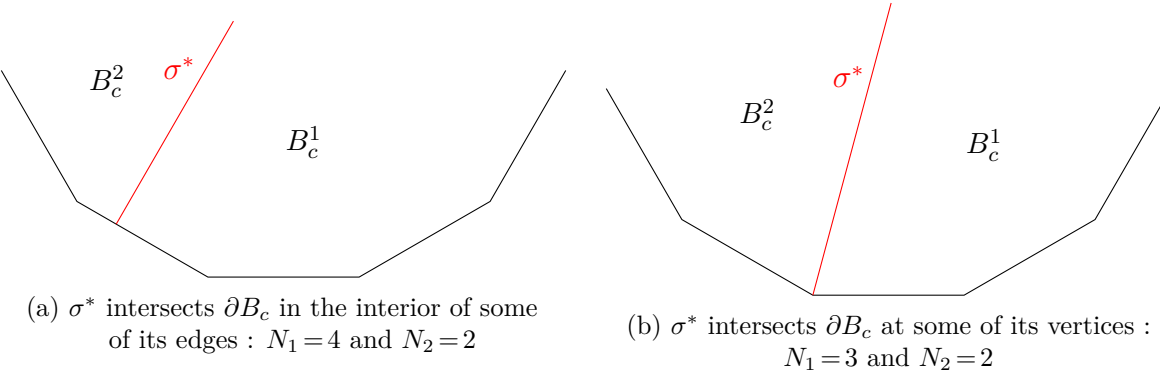


Fig. 5.8 Illustration of the two possible cases for the splitting in Theorem 5.16 ($N=4$)

Proof. We adapt the proof of [14, Thm.3] to N -half-surfaces. Let us first recall the setting of this proof. We can assume the metric to be flat outside a compact set $\tilde{D} \subset \text{int}(B_c)$ homeomorphic to the disk. Moreover, we can suppose that \tilde{D} is totally convex, i.e., all the geodesic curves joining two points $p, q \in \tilde{D}$ are included in \tilde{D} . Let $T_p \tilde{D}$ be the tangent plane at the point $p \in \tilde{D}$ and let

$$S\tilde{D} = \{(p, \theta), \text{ with } p \in \tilde{D}, \theta \in T_p \tilde{D}, |\theta|_g = 1\}$$

be the circle bundle over \tilde{D} . For any $v = (p, \theta) \in S\tilde{D}$, we denote $-v = (p, -\theta)$ and $\sigma(v) : \mathbb{R} \rightarrow M$ the unique geodesic curve passing through the point p orthogonally to v (the orientation of $\sigma(v)$ has no importance in what follows). Since \tilde{D} is totally convex, the geodesic $\sigma(v)$ splits \tilde{D} into two connected components. The vector v is directed inwards one of these components, which we denote by $U(v)$, and the other component is then denoted $U(-v)$. We now define a function α which plays a similar role to the angular function α in the original proof of [14, Thm.3]. The continuous function $\alpha : S\tilde{D} \rightarrow [0, \pi]$ should satisfy $\alpha(v) + \alpha(-v) = \pi - |\psi^0|_{l^1}$ for all $v \in S\tilde{D}$. For this definition, different cases, depicted in Figure 5.9, have to be considered:

1. $U(v)$ is a half-surface with boundary $\sigma(v)$;
2. $U(v)$ is a so-called polygonal strip;
3. $U(v)$ and $U(-v)$ are respectively a N_1 -half-surface and a N_2 -half-surface. We denote $\{\psi_i^1(v)\}_{1 \leq i \leq N_1}$ the exterior angles of B_c^1 and we set $|\psi^1|_{l^1} := \sum_{i=1}^{N_1} \psi_i^1(v)$;
4. $U(v)$ is a bounded polygonal domain with N_1 vertices. We denote $\{\psi_i^1\}_{1 \leq i \leq N_1}$ the exterior angles of $U(v)$ and we set $|\psi^1|_{l^1} := \sum_{i=1}^{N_1} \psi_i^1$;
5. $U(v)$ is the complementary of a bounded polygonal domain (so that $U(-v)$ is a bounded polygonal domain).

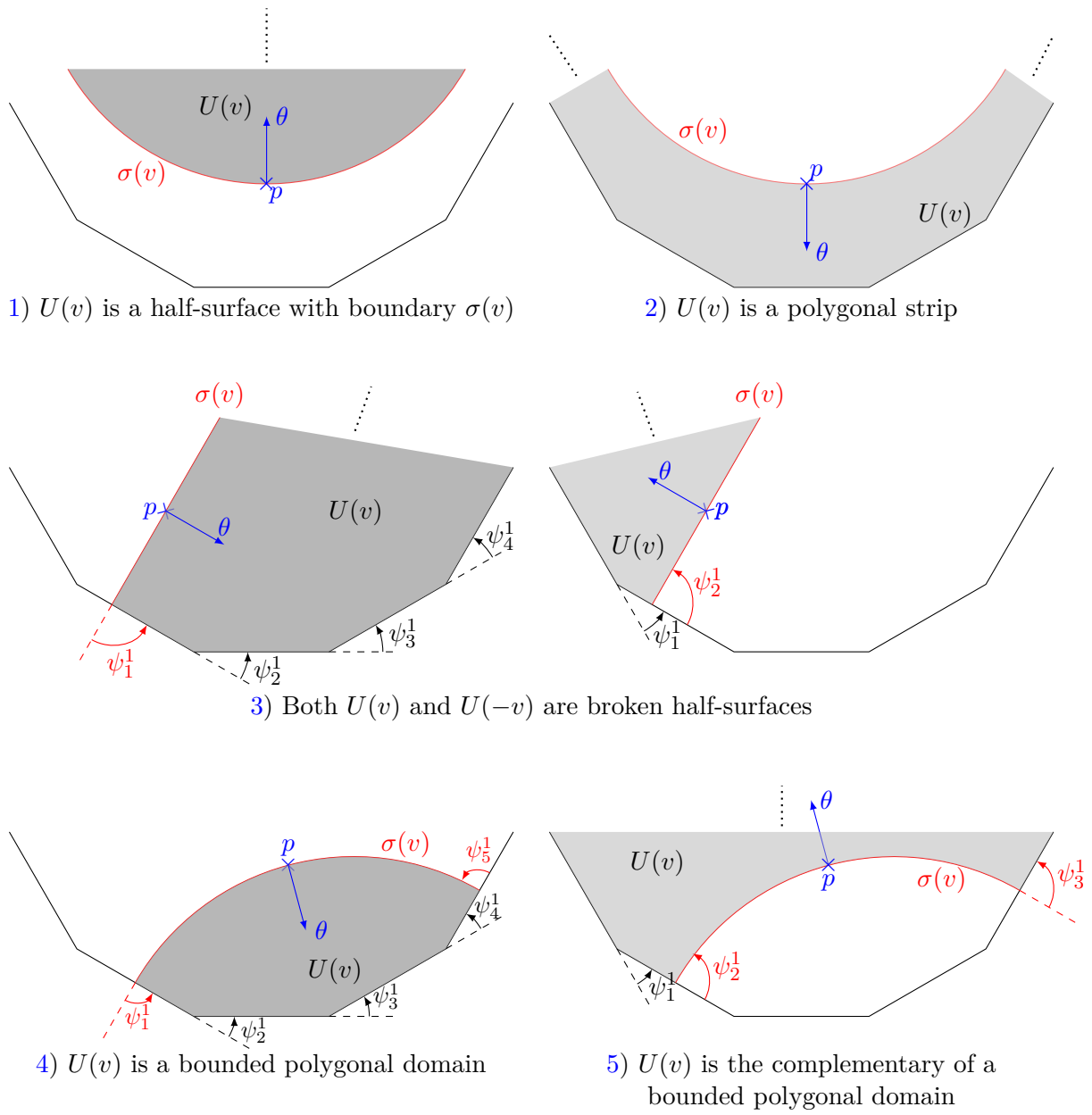


Fig. 5.9 Illustration of the possible splittings of a N -half-surface with $N=4$ (proof of Theorem 5.16)

We emphasize that, for all $v \in \tilde{D}$, $U(v)$ belongs to one of the above cases. Then, we define the function α in each of these cases as follows

$$\alpha(v) = \begin{cases} \pi - |\psi^0|_{l^1}, & \text{in case 1,} \\ 0, & \text{in case 2,} \\ \max [\min (\pi - |\psi^1|_{l^1}, \pi - |\psi^0|_{l^1}), 0], & \text{in case 3,} \\ \max [\min (2\pi - |\psi^1|_{l^1}, \pi - |\psi^0|_{l^1}), 0], & \text{in case 4,} \\ \pi - |\psi^0|_{l^1} - \alpha(-v), & \text{in case 5.} \end{cases} \quad (5.20)$$

Using the continuity of $|\psi^1|_{l^1}$ as $\sigma(v)$ crosses the vertices of B_c and the continuity of all the case transitions, one can check that $\alpha: S\tilde{D} \rightarrow [0, \pi]$ is a continuous function which satisfies

$\alpha(-v) + \alpha(v) = \pi - |\psi^0|_{l^1}$. Now, we introduce the mapping $\xi: S\tilde{D} \rightarrow \mathbb{R}^2$ defined by

$$\xi(v) = (\xi_1(v), \xi_2(v)) = \left((\pi - |\psi^0|_{l^1} - 2\varepsilon) \frac{\int_{U(v)} K^+}{\int_{\tilde{D}} K^+} - \alpha(v) + \varepsilon, \quad \frac{\int_{U(v)} K^-}{\int_{\tilde{D}} K^-} - \frac{1}{2} \right).$$

Then, ξ_1 satisfies

$$\begin{aligned} \xi_1(-v) &= (\pi - |\psi^0|_{l^1} - 2\varepsilon) \frac{\int_{\tilde{D}} K^+ - \int_{U(v)} K^+}{\int_{\tilde{D}} K^+} - \alpha(-v) + \varepsilon \\ &= \pi - |\psi^0|_{l^1} - 2\varepsilon - (\pi - |\psi^0|_{l^1} - 2\varepsilon) \frac{\int_{U(v)} K^+}{\int_{\tilde{D}} K^+} - (\pi - |\psi^0|_{l^1} - \alpha(v)) + \varepsilon \\ &= -\xi_1(v). \end{aligned}$$

In the same manner, we obtain that $\xi_2(-v) = -\xi_2(v)$, so that $\xi(-v) = -\xi(v)$. Therefore, using [14, Prop. 1], we can conclude that there exists $v_0 \in S\tilde{D}$ such that $\xi(v_0) = (0, 0)$, which corresponds to

$$\alpha(v_0) = (\pi - |\psi^0|_{l^1} - 2\varepsilon) \frac{\int_{U(v_0)} K^+}{\int_{\tilde{D}} K^+} + \varepsilon, \quad \int_{U(v_0)} K^- = \frac{1}{2} \int_{\tilde{D}} K^-. \quad (5.21)$$

We now prove that $U(v_0)$ necessarily matches case 3. First, by (5.21), we have

$$\alpha(v_0) \in [\varepsilon, \pi - |\psi^0|_{l^1} - \varepsilon], \quad (5.22)$$

which rules out cases 1 and 2. In order to rule out cases 4 and 5, suppose now that $U(v)$ is a bounded polygonal domain. Applying the Gauss–Bonnet formula on $U(v)$, we infer that

$$|\psi^1|_{l^1} + \int_{U(v)} K = 2\pi,$$

which gives $2\pi - |\psi^1|_{l^1} \leq \int_{U(v_0)} K^+$. Then, using the hypotheses (5.17) and (5.21), we obtain that

$$\int_{U(v_0)} K^+ + \varepsilon < \alpha(v_0). \quad (5.23)$$

Combining these two results and the definition of α in case 4, we obtain the following contradiction:

$$2\pi - |\psi^1|_{l^1} \leq \int_{U(v_0)} K^+ < \alpha(v_0) - \varepsilon \leq 2\pi - |\psi^1|_{l^1} - \varepsilon.$$

Finally, if $U(v_0)$ matches case 5, then $\xi(-v_0) = 0$. Hence, $U(-v_0)$ matches case 4 which leads, as above, to a contradiction. Therefore $U(v_0)$ necessarily matches case 3, i.e., both $U(v_0)$ and $U(-v_0)$ are broken half-surfaces. Moreover, (5.20) and (5.22) show that $\alpha(v_0) = \pi - |\psi^1|_{l^1}$. Then, using (5.21) and (5.23), we infer that (5.19) is satisfied by $U(v_0)$. Since $\xi(-v_0) = 0$, we obtain, by symmetry, the same result for $U(-v_0)$. Finally, recalling Remark 5.17, we have $N_1 + N_2 \in \{N + 1, N + 2\}$. This concludes the proof. ■

Recursive splitting

We first restate a result by Burago *et al* [14, Theorem 3] that allows one to split surfaces satisfying

$$\int_M K^+ < 2\pi - 4\varepsilon, \quad \text{and} \quad \int_M K^- < C - 4\varepsilon, \quad (5.24)$$

for positive C and ε , into four sectors delimited by geodesic curves, all of them satisfying the condition (5.15a). This result is stated in [14] with $C=2\pi$, but the proof is valid in the general setting.

Theorem 5.18 (Burago *et al.*). *Let M be a complete Riemannian 2-manifold homeomorphic to the plane and satisfying the conditions (5.24), for positive C and ε . Then, there exist four sectors $\{Q_i\}_{1 \leq i \leq 4}$ with exterior angles $\{\psi_i\}_{1 \leq i \leq 4}$ and delimited by geodesic curves such that $\text{int}(Q_i) \cap \text{int}(Q_j) = \emptyset$ for all $i \neq j$ and $\cup_{1 \leq i \leq 4} Q_i = M$, and such that, for all $i \in \{1, \dots, 4\}$, the sector Q_i satisfies the conditions*

$$\int_{Q_i} K^+ \leq \pi - \psi_i - \varepsilon, \quad \int_{Q_i} K^- \leq \frac{C}{2\pi} \psi_i - \varepsilon. \quad (5.25)$$

The four sectors obtained by this theorem are sketched in Figure 5.10. We also need the

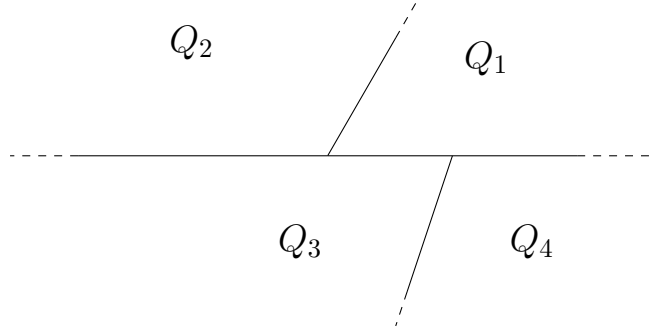


Fig. 5.10 Illustration of the splitting of Theorem 5.18

following lemma to bound from below the exterior angles of the broken half-surfaces resulting from splitting:

Lemma 5.19 (Bound on exterior angles). *Let $N \geq 1$ and let B_c be a N -half-surface satisfying the condition (5.15a). Let $\sigma : \mathbb{R}^+ \rightarrow B_c$ be a geodesic curve with $\sigma(0) \in \partial B_c$ and suppose that σ splits B_c into a N_1 -half-surface B_c^1 and a N_2 -half-surface B_c^2 , both of which satisfy the condition (5.15a). Then, denoting $\{\psi_k^0\}_{1 \leq k \leq N}$, $\{\psi_k^1\}_{1 \leq k \leq N_1}$, and $\{\psi_k^2\}_{1 \leq k \leq N_2}$, the positive exterior angles of B_c , B_c^1 , and B_c^2 , respectively, we have*

$$\forall i \in \{1, 2\}, \quad |\psi^i|_{l^\infty} \geq |\psi^0|_{l^\infty}. \quad (5.26)$$

Proof. We denote ψ_k^1 , with $k \in \{1, \dots, N_1\}$, and ψ_l^2 , with $l \in \{1, \dots, N_2\}$, the exterior angle of B_c^1 and B_c^2 respectively at the intersection of σ with ∂B_c . Two cases can occur: either the intersection point is not located at some vertex of ∂B_c , or σ intersects a vertex $p_n \in \partial B_c$, with $n \in \{1, \dots, N\}$, with exterior angle ψ_n^0 (see Remark 5.17 and Figure 5.8). In the first case, we have $\psi_k^1 + \psi_l^2 = \pi$. In the second case, since $\psi_n^0 \geq 0$, we have $\psi_k^1 + \psi_l^2 = \pi + \psi_n^0 \geq \pi$. In both cases, we infer that

$$\psi_k^1 + \psi_l^2 \geq \pi. \quad (5.27)$$

Note that all the angles of both B_c^1 and B_c^2 are angles of B_c , except for the angle newly created by the intersection of σ with ∂B_c . Let ψ_m^0 , with $m \in \{1, \dots, N\}$, be an exterior angle of B_c such that $\psi_m^0 = |\psi^0|_{l^\infty}$. Let p_m be the corresponding vertex of ∂B_c . We only prove that (5.26) is satisfied for $i = 1$, since the case $i = 2$ is treated similarly. We remark that three cases can occur:

1. If p_m is contained in B_c^1 , the result is straightforward;
2. If p_m is contained in B_c^2 , applying (5.27) and the condition (5.15a) in B_c^1 , we obtain that

$$\psi_k^1 \geq \pi - \psi_l^2 \geq |\psi^0|_{l^1} - \psi_l^2 + \int_{B_c^2} K^+ \geq \psi_m^0.$$

3. Finally, if σ intersects ∂B_c at p_m , we have $\psi_k^1 + \psi_l^2 = \pi + \psi_m^0$. Since $\psi_l^2 \leq \pi$, we infer that $\psi_k^1 \geq \psi_m^0$.

In all the cases, we obtain the expected result. This concludes the proof. \blacksquare

We can now prove the main result of this section.

Theorem 5.20 (Surface splitting into broken half-surfaces). *Let M be a smooth, complete, simply connected surface. Suppose that M satisfies the curvature bound (5.2), i.e.,*

$$\int_M K^+ < 2\pi \quad \text{and} \quad \int_M K^- < \infty,$$

with K the Gaussian curvature of M , $K^+ = \max(K, 0)$ and $K^- = \max(-K, 0)$. We set $n_{\max} := \log_2 \left(\frac{1}{\pi} \int_M K^- + 1 \right) + 2$. Then, there exist $N_{\text{pol}} \leq \frac{4}{\pi} \int_M K^- + 8$ geodesic N_α -half-surfaces $\{B_c^\alpha\}_{1 \leq \alpha \leq N_{\text{pol}}}$, with $N_\alpha \leq n_{\max}$ for all $\alpha \in \{1, \dots, N_{\text{pol}}\}$, satisfying the conditions (5.15) and such that $\text{int}(B_c^\alpha) \cap \text{int}(B_c^\beta) = \emptyset$ for all $\alpha \neq \beta$ and $M = \bigcup_{\alpha=1}^{N_{\text{pol}}} B_c^\alpha$.

Proof. Let $\bar{\varepsilon} = \frac{1}{5}(2\pi - \int_M K^+)$ and $\bar{C} = \int_M K^- + 5\bar{\varepsilon}$. Then, the hypotheses of Theorem 5.18 are satisfied by M with $\varepsilon = \bar{\varepsilon}$ and $C = \bar{C}$. We denote $\{S_{\alpha,0}\}_{1 \leq \alpha \leq 4}$ the four sectors satisfying (5.25) obtained by this theorem. As condition (5.15a) is satisfied by each 1-half-surface $S_{\alpha,0}$ the proof consists in applying multiple times Theorem 5.16 to all of them so as to split these 1-half-surfaces recursively until condition (5.15b) on the total negative curvature is satisfied. Since each broken half-surface is treated similarly, we only enumerate one broken half-surface in each sector $S_{\alpha,0}$ at each step of the subdivision. (Note that, otherwise, multi-indices should have been introduced.) See Figure 5.11 for an illustration of the resulting splitting. We denote, for all $\alpha \in \{1, \dots, 4\}$, $\psi_\alpha > 0$ the exterior angle of $S_{\alpha,0}$ and we set $C_\alpha = \frac{\bar{C}\psi_\alpha}{2\pi}$. Since $S_{\alpha,0}$ satisfies (5.25), the hypotheses of Theorem 5.16 are satisfied with $B_c = S_{\alpha,0}$, $\varepsilon = \frac{\bar{\varepsilon}}{3}$ and $C = C_\alpha$. Hence, there exists a splitting of $S_{\alpha,0}$ into two broken half-surfaces satisfying the conditions (5.19). By symmetry, we consider only one of them, denoted $S_{\alpha,1}$. In the same manner, we apply recursively Theorem 5.16 with $B_c = S_{\alpha,n-1}$, $\varepsilon = \frac{\bar{\varepsilon}}{3 \cdot 2^{n-1}}$ and $C = \frac{C_\alpha}{2^{n-1}}$. This yields a splitting of $S_{\alpha,n-1}$ into two broken half-surfaces satisfying the conditions (5.19). By symmetry, we consider only one of them, the N -half-surface denoted $S_{\alpha,n}$, whose exterior angles are denoted $\{\psi_k^n\}_{1 \leq k \leq N}$. Note that $N \leq n + 1$ by (5.18). Then, Lemma 5.19 ensures that $|\psi^n|_{l^\infty} \geq \psi_\alpha$ (with $|\psi^n|_{l^\infty} = \max_{1 \leq k \leq N} \psi_k^n$). Therefore, condition (5.15b) is satisfied by $S_{\alpha,n}$ whenever

$$\int_{S_{\alpha,n}} K^- < |\psi^n|_{l^\infty} \leq \psi_\alpha. \tag{5.28}$$

Since $\int_{S_{\alpha,n}} K^- \leq \frac{C_\alpha}{2^n}$, we infer that (5.28) is satisfied whenever $n = n_\alpha^{\max}$, where

$$n_\alpha^{\max} = \left\lceil \log_2 \left(\frac{C_\alpha}{\psi_\alpha} \right) \right\rceil = \left\lceil \log_2 \left(\frac{\bar{C}}{2\pi} \right) \right\rceil$$

and $\lceil \cdot \rceil$ is the ceiling function. Therefore, we have proved that there exist \mathcal{N}_α N_i -half-surfaces $\{B_c^{\alpha,i}\}_{1 \leq i \leq \mathcal{N}_\alpha}$, with $N_i \leq n_\alpha^{\max} + 1$, such that $\text{int}(B_c^{\alpha,i}) \cap \text{int}(B_c^{\alpha,j}) = \emptyset$ for all $i \neq j$. Moreover, we have $\mathcal{N}_\alpha \leq \mathcal{N}_\alpha^{\max}$, with:

$$\mathcal{N}_\alpha^{\max} = 2^{n_\alpha^{\max}} \leq \frac{\bar{C}}{\pi} \leq \frac{1}{\pi} \int_M K^- + 2. \quad (5.29)$$

We finally define $\mathcal{N}_{\text{pol}} = \sum_{\alpha=1}^4 \mathcal{N}_\alpha$ and the set of N_i -half-surfaces $\{B_c^i\}_{1 \leq i \leq \mathcal{N}_{\text{pol}}}$ as the union of the sets $\{B_c^{\alpha,i}\}_{1 \leq i \leq \mathcal{N}_\alpha}$, for $\alpha \in \{1, \dots, 4\}$. For all $i \in \{1, \dots, \mathcal{N}_{\text{pol}}\}$, the number N_i of vertices of B_c^i satisfies

$$\begin{aligned} N_i &\leq \max_{\alpha \in \{1, \dots, 4\}} n_\alpha^{\max} + 1 = \left\lceil \log_2 \left(\frac{\bar{C}}{2\pi} \right) \right\rceil + 1 \\ &\leq \log_2 \left(\frac{1}{2\pi} \int_M K^- + 1 \right) + 2 = n_{\max}. \end{aligned}$$

Moreover, using (5.29), we obtain that the number \mathcal{N}_{pol} of polygons satisfies

$$\mathcal{N}_{\text{pol}} = \sum_{\alpha=1}^4 \mathcal{N}_\alpha \leq \frac{4}{\pi} \int_M K^- + 8.$$

The claim follows. ■

Remark 5.21 (Tree representation). The construction can be seen as a binary tree of broken half-surfaces, each splitting being an edge, n_{\max} being the maximal depth of the tree, and \mathcal{N}_{pol} being the maximal number of leaves of the tree. Once the splitting is achieved, we renumber the broken half-surfaces to obtain the set $\{B_c^\alpha\}_{1 \leq \alpha \leq \mathcal{N}_{\text{pol}}}$.

Definition 5.22 (Skeleton). *The graph in the surface M defined by the vertices of the boundaries of the broken half-surfaces $\{B_c^\alpha\}_{1 \leq \alpha \leq \mathcal{N}_{\text{pol}}}$ obtained using Theorem 5.20 and the edges (geodesic curves) joining the vertices is called the skeleton. The vertices and the edges in the skeleton are respectively enumerated as $\{p_c^i\}_{1 \leq i \leq \mathcal{N}_{\text{ver}}}$ and $\{\gamma_c^i\}_{1 \leq i \leq \mathcal{N}_{\text{ed}}}$.*

An example of skeleton is then presented in Figure 5.12.

Proof of the main theorem

We prove in this section Theorem 5.1 on the existence of piecewise smooth Chebyshev nets with singularities on surfaces M satisfying the curvature bound (5.2). We first gather the results of Theorem 5.15 and Theorem 5.20 to construct a Chebyshev net with singularities on M (Theorem 5.23). Then, we show that the Chebyshev parametrization obtained on each broken half-surface by Theorem 5.15 is piecewise smooth (Theorem 5.28). The proof of Theorem 5.1 then follows from Theorem 5.23 and Theorem 5.28.

Existence of a Chebyshev net with conical singularities

Theorem 5.23 (Existence of Chebyshev nets with singularities). *Let M be a smooth, complete, simply connected surface satisfying the curvature bound (5.2). Then, there exists a Chebyshev net with conical singularities $\mathcal{C} = (\{B_c^i\}_{1 \leq i \leq \mathcal{N}_{\text{pol}}}, \{\varphi_c^i\}_{1 \leq i \leq \mathcal{N}_{\text{pol}}}, T)$, with $\mathcal{N}_{\text{pol}} \leq \frac{4}{\pi} \int_M K^- + 8$, on M .*

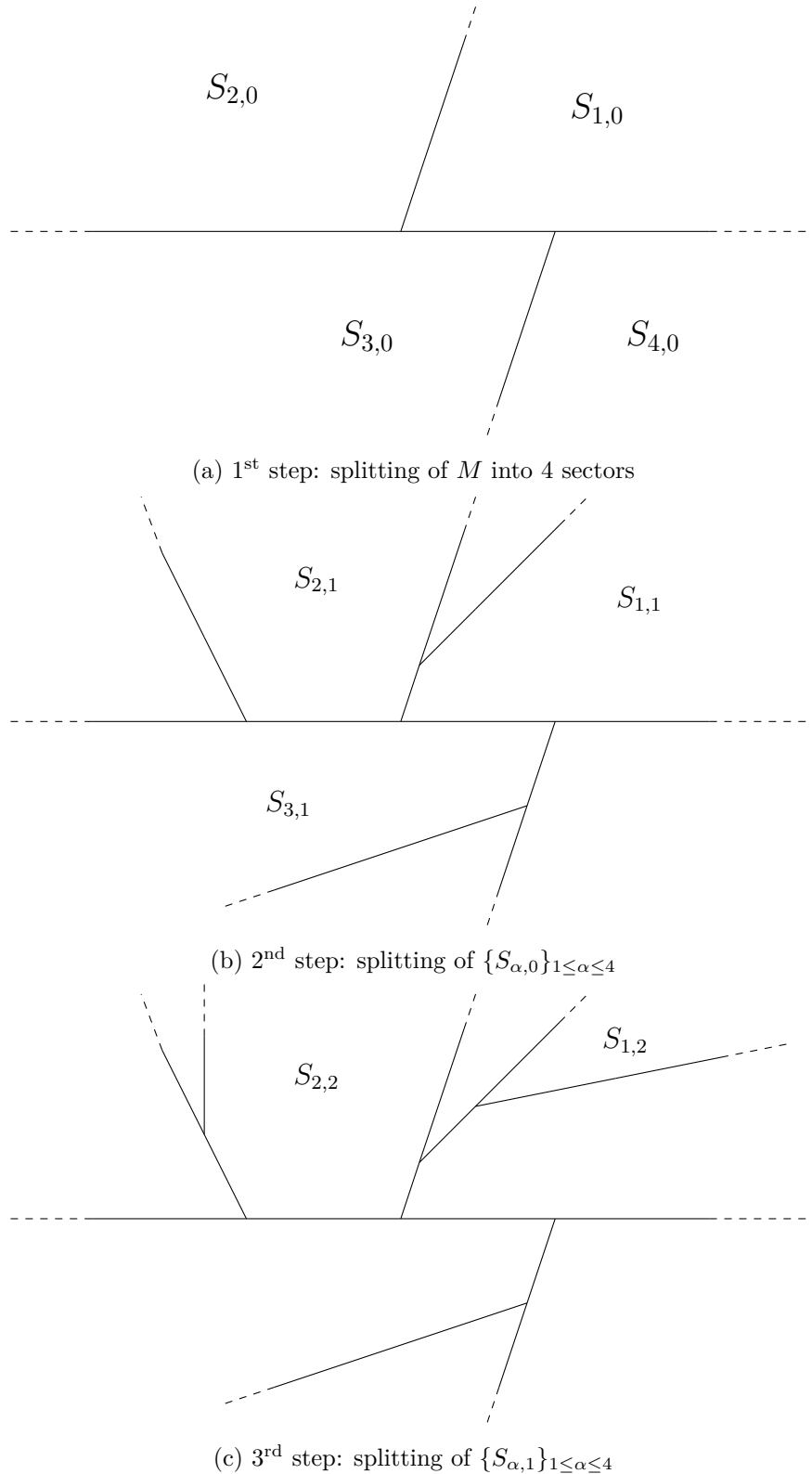


Fig. 5.11 Illustration of the recursive splitting used for the proof of Theorem 5.20

Proof. First, we apply Theorem 5.20 to obtain a splitting of M into broken half-surfaces $\{B_c^i\}_{1 \leq i \leq N_{\text{pol}}}$, with $N_{\text{pol}} \leq \frac{4}{\pi} \int_M K^- + 8$, all of them satisfying the conditions

$$\int_{B_c^i} K^+ < \pi - |\psi^i|_{l^1}, \quad \int_{B_c^i} K^- < |\psi^i|_{l^\infty}.$$

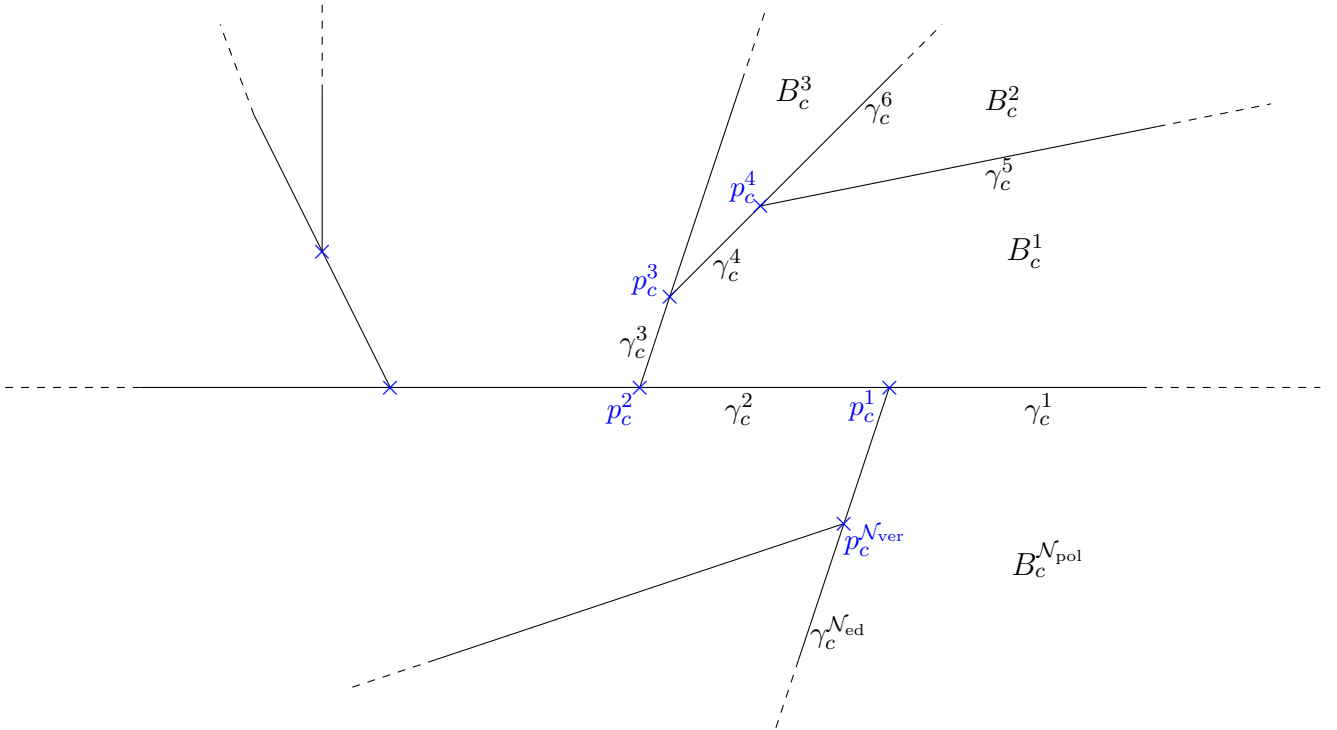


Fig. 5.12 An example of skeleton

Then, owing to Theorem 5.15, we infer that there exists a Chebyshev parametrization $\varphi_i : (\mathbb{R}^+)^2 \rightarrow B_c^i$, for all $i \in \{1, \dots, N_{\text{pol}}\}$. We set $B_e^i = (\mathbb{R}^+)^2$, for all $i \in \{1, \dots, N_{\text{pol}}\}$. We construct the equivalence table $T : \{1, \dots, N_{\text{pol}}\} \rightarrow \mathbb{N}$ as follows. For all $i \in \{1, \dots, N_{\text{pol}}\}$, we set $T(i, i) = 0$. For all $i, j \in \{1, \dots, N_{\text{pol}}\}$ such that $i \neq j$, we set $T(i, j) = T(j, i) = 0$ if $B_c^i \cap B_c^j = \emptyset$. We now suppose that $B_c^i \cap B_c^j \neq \emptyset$. Let $\{\gamma_c^{i,\alpha}\}_{1 \leq \alpha \leq N_i}$ and $\{\gamma_c^{j,\beta}\}_{1 \leq \beta \leq N_j}$ be the edges of the skeleton that are included in B_c^i and B_c^j respectively. Then, by construction (see Theorem 5.16), $B_c^i \cap B_c^j = \gamma_c^{i,\alpha_0} = \gamma_c^{j,\beta_0}$ for some $\alpha_0 \in \{1, \dots, N_i\}$ and $\beta_0 \in \{1, \dots, N_j\}$, and, we set $T(i, j) = \alpha_0$ and $T(j, i) = \beta_0$ (see Figure 5.13). We conclude that $\mathcal{C} = (\{B_e^i\}_{1 \leq i \leq N_{\text{pol}}}, \{\varphi_e^i\}_{1 \leq i \leq N_{\text{pol}}}, T)$ is a Chebyshev net with conical singularities on M . ■

Piecewise smooth Chebyshev nets on broken half-surfaces

Let us notice that whenever all the broken half-surfaces $\{B_c^i\}_{1 \leq i \leq N_{\text{pol}}}$ obtained in Theorem 5.20 are smooth sectors (only one vertex), Theorem 5.1 follows from Propositions 5.9 and 5.23. In the general case, we need to prove that, for all $i \in \{1, \dots, N_{\text{pol}}\}$, the Chebyshev parametrization $\varphi_i : B_e^i = (\mathbb{R}^+)^2 \rightarrow B_c^i$ obtained from Theorem 5.15 on the geodesic broken half-surface B_c^i satisfying the conditions

$$\int_{B_c^i} K^+ < \pi - |\psi^i|_{l^1}, \quad \int_{B_c^i} K^- < |\psi^i|_{l^\infty}, \quad (5.30)$$

is piecewise smooth. With this purpose in mind, we proceed as in Section 5.2: we first consider the case of a piecewise smooth sector Q of exterior angle $\psi \in (0, \pi)$ satisfying the conditions

$$\tau_+(\eta_1) + \tau_+(\eta_2) + \int_Q K^+ < \pi - \psi, \quad (5.31a)$$

$$\tau_-(\eta_1) + \tau_-(\eta_2) + \int_Q K^- < \psi. \quad (5.31b)$$

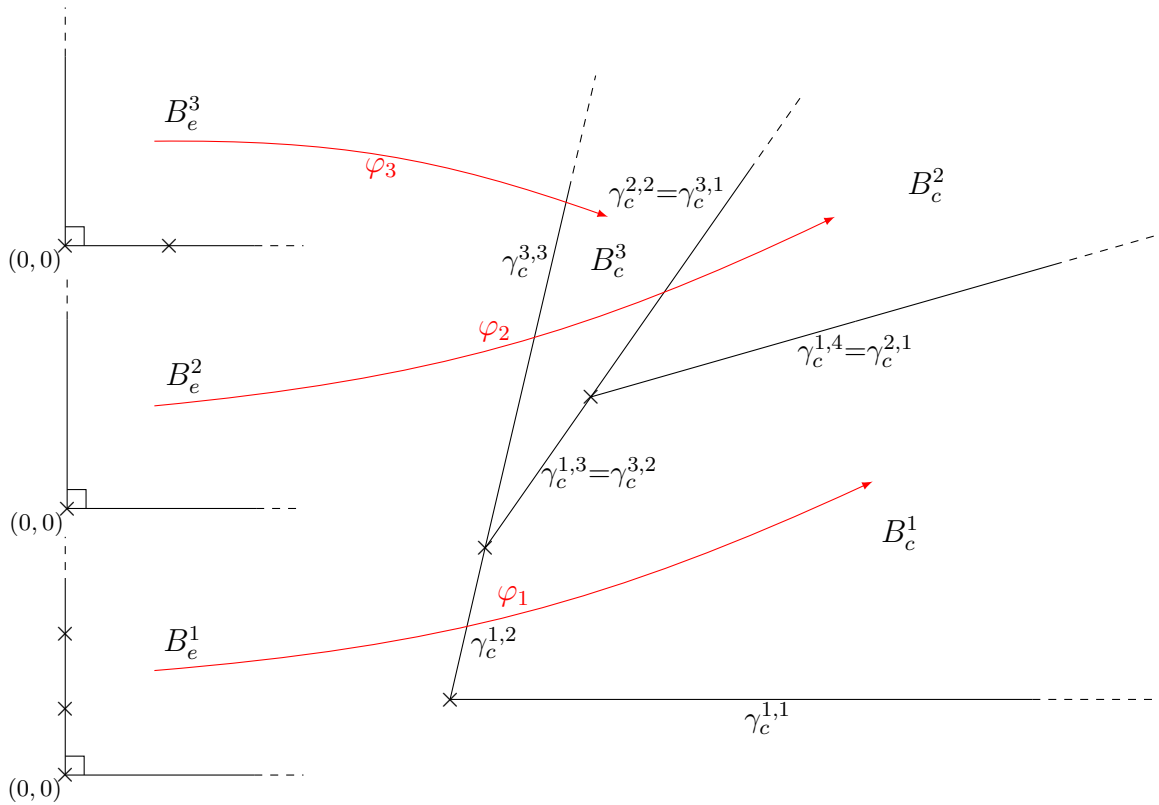


Fig. 5.13 Illustration of the construction of the Chebyshev net with conical singularities (the crosses are the vertices)

Before this, we state the following lemma on the geodesic curvature of parameter curves of a smooth Chebyshev net. The notations used in this lemma are depicted in Figure 5.14.

Lemma 5.24. *Let $a, b \in \mathbb{R}_*^+$ and let $\varphi: [0, a] \times [0, b] \rightarrow M$ be a smooth Chebyshev net on M such that $0 < \omega(u, v) < \pi$ for all $u, v \in [0, a] \times [0, b]$. We define $\Omega = \varphi([0, a] \times [0, b])$, $\eta_1(v) = \varphi(0, -v)$, $\sigma_1(v) = \varphi(a, -v)$ for all $v \in [-b, 0]$, and $\eta_2(u) = \varphi(u, 0)$, $\sigma_2(u) = \varphi(u, b)$ for all $u \in [0, a]$. Then, the geodesic curvatures κ_{η_1} , κ_{η_2} , κ_{σ_1} , and κ_{σ_2} of η_1 , η_2 , σ_1 , and σ_2 , respectively, are related by*

$$\int_0^a \kappa_{\sigma_2} = \int_0^a \kappa_{\eta_2} + \int_{\Omega} K, \quad \int_{-b}^0 \kappa_{\sigma_1} = \int_{-b}^0 \kappa_{\eta_1} + \int_{\Omega} K, \quad (5.32)$$

and satisfy

$$\int_0^a \kappa_{\eta_2}^+ - \int_0^a \kappa_{\sigma_2}^+ + \int_{\Omega} K^+ \geq 0, \quad \int_{-b}^0 \kappa_{\eta_1}^+ - \int_{-b}^0 \kappa_{\sigma_1}^+ + \int_{\Omega} K^+ \geq 0, \quad (5.33a)$$

$$\int_0^a \kappa_{\eta_2}^- - \int_0^a \kappa_{\sigma_2}^- + \int_{\Omega} K^- \geq 0, \quad \int_{-b}^0 \kappa_{\eta_1}^- - \int_{-b}^0 \kappa_{\sigma_1}^- + \int_{\Omega} K^- \geq 0. \quad (5.33b)$$

Proof. We only prove the lemma for the curves η_1 and σ_1 . The formulas for η_2 and σ_2 are obtained in a similar way. Using (5.7) and the Hazzidakis formula (5.8) with $u=a$ and $v=b$, we obtain

$$\omega(a, b) = \omega(0, 0) - \int_0^a \kappa_{\eta_2} - \int_{-b}^0 \kappa_{\eta_1} - \int_{\Omega} K = \omega(a, 0) - \int_{-b}^0 \kappa_{\eta_1} - \int_{\Omega} K,$$

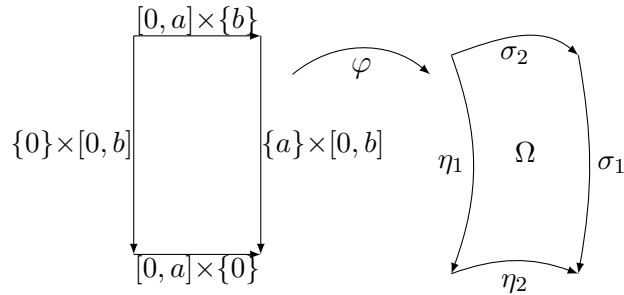


Fig. 5.14 Illustration of the notation of Lemma 5.24

so that

$$\int_{-b}^0 \kappa_{\sigma_1} = - \int_0^b \partial_v \omega(a, v) dv = \int_{-b}^0 \kappa_{\eta_1} + \int_{\Omega} K.$$

To prove the inequalities (5.33), we first note that (5.32) implies

$$\int_0^a \kappa_{\eta_1}^+ - \int_0^a \kappa_{\sigma_1}^+ + \int_{\Omega} K^+ = \int_0^a \kappa_{\eta_1}^- - \int_0^a \kappa_{\sigma_1}^- + \int_{\Omega} K^-.$$

Subdividing the curves η_1 and σ_1 according to the sign changes of κ_{η_1} and κ_{σ_1} , it is possible to assume that the sign of κ_{η_1} and κ_{σ_1} is constant on $[0, a]$. The discussion is then simplified to the two following cases:

- if κ_{η_1} and κ_{σ_1} have the same sign (say, nonnegative), then

$$\int_0^a \kappa_{\eta_1}^- - \int_0^a \kappa_{\sigma_1}^- + \int_{\Omega} K^- = \int_{\Omega} K^- \geq 0;$$

- if κ_{η_1} and κ_{σ_1} have different signs (say, $\kappa_{\eta_1} \geq 0$ and $\kappa_{\sigma_1} \leq 0$), then

$$\int_0^a \kappa_{\eta_1}^+ - \int_0^a \kappa_{\sigma_1}^+ + \int_{\Omega} K^+ = \int_0^a \kappa_{\eta_1}^+ + \int_{\Omega} K^+ \geq 0.$$

■

Theorem 5.25 (Existence of piecewise smooth Chebyshev nets on sectors). *Let Q be a sector delimited by the two piecewise smooth curves $\eta_1 : \mathbb{R}^- \rightarrow M$ and $\eta_2 : \mathbb{R}^+ \rightarrow M$. We denote $\pi - \theta_1 \in (0, \pi)$ the exterior angle of this sector and we suppose that Q satisfies the conditions (5.31). Then, there exist $N_{\text{piece}} \geq 1$ polygons $\{B_e^i\}_{1 \leq i \leq N_{\text{piece}}}$ such that $(\mathbb{R}^+)^2 = \bigcup_{i=1}^{N_{\text{piece}}} B_e^i$ and $\text{int}(B_e^i) \cap \text{int}(B_e^j) = \emptyset$ for all $i \neq j$, and Chebyshev coordinates φ on Q such that η_1 and η_2 are coordinate curves. Moreover, the angle $\omega = \angle(\partial_u \varphi, \partial_v \varphi)$ of the net satisfies the nonsmooth Hazzidakis formula*

$$\omega(u, v) = \theta_1 - \tau(\eta_2|_{[0, u]}) - \tau(\eta_1|_{[-v, 0]}) - \int_{\varphi([0, u] \times [0, v])} K, \quad (5.34)$$

for all $u, v \in \mathbb{R}^+$, and is bounded away from 0 and π by the positive real number

$$\min \left(\pi - \psi - \int_Q K^+ - \tau_+(\eta_1) - \tau_+(\eta_2), \psi - \int_Q K^- - \tau_-(\eta_1) - \tau_-(\eta_2) \right). \quad (5.35)$$

Finally, $\varphi|_{B_e^i} : B_e^i \rightarrow \varphi(B_e^i) \subset Q$ is a diffeomorphism, for all $1 \leq i \leq N_{\text{piece}}$.

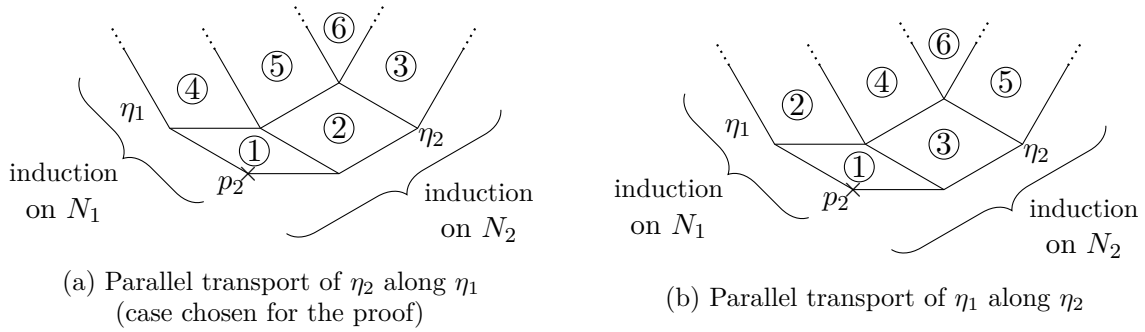


Fig. 5.15 Parallel transport of η_1 and η_2 along each other ($N_1 = 1, N_2 = 2$):
numbering of the double induction process

Proof. We first split the two curves η_1 and η_2 into smooth pieces. We denote $N_1 + 1 \geq 1$ and $N_2 + 1 \geq 1$ the number of smooth pieces of the curves η_1 and η_2 , respectively. Then, we parallel transport the curve η_2 along each smooth piece of η_1 . This is done recursively on N_1 . The parallel transport of η_2 along a piece of η_1 is obtained by induction on N_2 . Hence, we have two nested induction arguments (see Figure 5.15). We observe that, by symmetry, the role of the two curves can be switched, as can be seen in the same figure. Hence, we can always suppose that $N_1 \geq N_2$. Once the construction is over, we prove the nonsmooth Hazzidakis formula (5.34).

Step 1 (*Formulation of the first induction process (on $N_1 \geq 0$)*). We suppose that $N_2 \in \{0, \dots, N_1\}$ is a given fixed integer and we denote (\mathcal{H}_{N_1+1}) the following induction hypothesis:

for any sector Q of exterior angle $\pi - \theta_1 \in (0, \pi)$, delimited by the two curves η_1 and η_2 having respectively $N_1 + 1$ and $N_2 + 1$ smooth pieces and satisfying (5.31), there exist polygons $\{B_e^i\}_{1 \leq i \leq N_{\text{piece}}}$ and a Chebyshev net $\varphi: (\mathbb{R}^+)^2 \rightarrow Q$ such that:

- $(\mathbb{R}^+)^2 = \bigcup_{i=1}^{N_{\text{piece}}} B_e^i$ and $\text{int}(B_e^i) \cap \text{int}(B_e^j) = \emptyset$ for all $i \neq j$;
- η_1 and η_2 are coordinate curves;
- the angle $\omega = \angle(\partial_u \varphi, \partial_v \varphi)$ of φ satisfies the nonsmooth Hazzidakis formula (5.34);
- $\varphi|_{B_e^i}: B_e^i \rightarrow \varphi(B_e^i) \subset Q$ is a diffeomorphism, for all $i \in \{1, \dots, N_{\text{piece}}\}$.

Step 2 (*Proof of the first induction process (1st part of the construction)*). We firstly check that (\mathcal{H}_1) holds. Since $N_2 \leq N_1$, we have $N_2 = 0$. Hence, the sector Q is delimited by the two smooth curves η_1 and η_2 and (\mathcal{H}_1) holds, with $N_{\text{piece}} = 1$, by Proposition 5.9. Now, for $N_1 \geq 1$, we suppose that (\mathcal{H}_{N_1}) holds and we prove that (\mathcal{H}_{N_1+1}) also holds. Thus, we suppose that Q is delimited by two curves η_1 and η_2 having respectively $N_1 + 1 \geq 2$ and $N_2 + 1 \geq 1$ smooth pieces. Let

$$-\infty = a_{1,N_1+1} < \dots < a_{1,0} = 0 = a_{2,0} < \dots < a_{2,N_2+1} = \infty$$

be such that, for all $l = 1, 2$, η_l restricted to $[a_{l,i-1}, a_{l,i}]$ is a smooth curve, for all $i \in \{1, \dots, N_l + 1\}$. We denote $\eta_{l,i}: [a_{l,i-1}, a_{l,i}] \rightarrow M$ this piece of the curve η_l and $\kappa_{l,i}: [a_{l,i-1}, a_{l,i}] \rightarrow \mathbb{R}$ its geodesic curvature. We denote $\psi_{l,i} = (-1)^l \angle(\eta'_{l,i}(a_{l,i}), \eta'_{l,i+1}(a_{l,i}))$ for all $i \in \{1, \dots, N_l\}$ and $l \in \{1, 2\}$ (see Figure 5.16). To abbreviate the notation, we set $\tilde{\eta}_{1,1} = \eta_{1,1}$.

Step 3 (*Formulation of the second induction process (on $n \in \{1, \dots, N_2 + 1\}$)*). We parallel transport in what follows the curve η_2 along $\eta_{1,1}$. See Figure 5.16 for the notation and Figure 5.17

for an illustration of the construction. For all $n \in \{1, \dots, N_2 + 1\}$, we denote $(\tilde{\mathcal{H}}_n)$ the following induction hypothesis:

for all $j \in \{1, \dots, n\}$, let $\tilde{\eta}_{1,j} : [a_{1,1}, 0] \rightarrow Q$ be a smooth curve intersecting $\eta_{2,j}$ at $\eta_{2,j}(a_{2,j-1}) = \tilde{\eta}_{1,j}(0)$. If $n > 1$, for all $j \in \{1, \dots, n-1\}$, let $B_e^j = [a_{2,j-1}, a_{2,j}] \times [0, -a_{1,1}] \subset (\mathbb{R}^+)^2$ and assume that $\varphi_j : B_e^j \rightarrow B_c^j \subset Q$, with $B_c^j = \varphi_j(B_e^j)$, are Chebyshev nets such that

$$\begin{aligned}\varphi_j(a_{2,j-1}, v) &= \tilde{\eta}_{1,j}(-v), & \varphi_j(a_{2,j}, v) &= \tilde{\eta}_{1,j+1}(-v), & \forall v \in [0, -a_{1,1}], \\ \varphi_j(u, 0) &= \eta_{2,j}(u), & & & \forall u \in [a_{2,j-1}, a_{2,j}].\end{aligned}$$

Then, there exists a Chebyshev net $\varphi_n : B_e^n \subset (\mathbb{R}^+)^2 \rightarrow B_c^n \subset Q$, with $B_e^n = [a_{2,n-1}, a_{2,n}] \times [0, -a_{1,1}]$ and $B_c^n = \varphi_n(B_e^n)$. Moreover, the set B_c^n satisfies:

1. if $n > 1$, then $B_c^{n-1} \cap B_c^n = \tilde{\eta}_{1,n}$;
2. if $n > 2$, then $B_c^j \cap B_c^n = \emptyset$, for all $j \in \{1, \dots, n-2\}$.

Finally, suppose that $n < N_2 + 1$ and denote $\tilde{\eta}_{1,n+1} : [a_{1,1}, 0] \rightarrow Q$ the curve defined by $\tilde{\eta}_{1,n+1}(v) = \varphi_n(a_{2,n}, -v)$ for all $v \in [a_{1,1}, 0]$. This curve intersects $\eta_{2,n+1}$ at $\eta_{2,n+1}(a_{2,n}) = \tilde{\eta}_{1,n+1}(0)$, forming an interior angle denoted $\theta_{n+1} \in [0, \pi]$. Then, θ_{n+1} and the geodesic curvature $\tilde{\kappa}_{1,n+1} : [a_{1,1}, 0] \rightarrow \mathbb{R}$ of $\tilde{\eta}_{1,n+1}$ satisfy respectively

$$\theta_{n+1} = \theta_1 - \tau(\eta_2|_{[0, a_{2,n}]}) \in (0, \pi), \quad (5.36a)$$

$$\int_{-v}^0 \tilde{\kappa}_{1,n+1} = \int_{-v}^0 \kappa_{1,1} + \sum_{k=1}^n \int_{\varphi_k([a_{2,k-1}, a_{2,k}] \times [0, v])} K, \quad \forall v \in [0, -a_{1,1}]. \quad (5.36b)$$

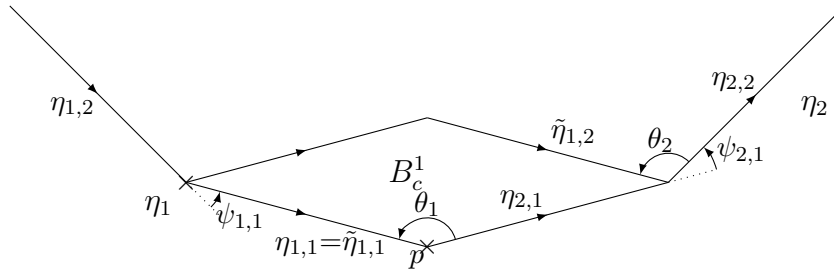


Fig. 5.16 Illustration of the parallel transport of $\eta_{2,1}$ along $\eta_{1,1}$ ($N_1 = 1, N_2 = 1$)

Step 4 (Proof of the second induction process). To prove that $(\tilde{\mathcal{H}}_1)$ holds, we apply Theorem 5.10 with the curves $\eta_{1,1}$ and $\eta_{2,1}$ of respective length $-a_{1,1}$ and $a_{2,1}$ and forming an interior angle $\theta_1 \in (0, \pi)$ by hypothesis. We obtain a mapping $\varphi_1 : B_e^1 \subset (\mathbb{R}^+)^2 \rightarrow B_c^1 \subset M$, with $B_e^1 = [a_{2,0}, a_{2,1}] \times [0, -a_{1,1}]$ and $B_c^1 = \varphi_1(B_e^1)$. Then, using the same argument as the proof of Lemma 5.8, we obtain that the mapping φ_1 is a Chebyshev net and that $B_c^1 \subset Q$. Using Lemma 5.24, we infer that $\tilde{\eta}_{1,2}$ has a geodesic curvature $\tilde{\kappa}_{1,2}$ satisfying

$$\int_{-v}^0 \tilde{\kappa}_{1,1} = \int_{-v}^0 \kappa_{1,1} + \int_{\varphi_1([0, a_{2,1}] \times [0, v])} K,$$

for all $v \in [0, -a_{1,1}]$. Moreover, we deduce from (5.7) that the interior angle $\theta_2 = \angle(\eta'_{2,2}(0), -\tilde{\eta}'_{1,2}(0))$ satisfies

$$\theta_2 = \theta_1 - \int_0^{a_{2,1}} \kappa_{2,1} - \psi_{2,2} = \theta_1 - \tau(\eta_2|_{[0, a_{2,1}]})$$

Since hypothesis (5.31) (with $\psi = \pi - \theta_1$) is satisfied by Q , we obtain that $\theta_2 \in (0, \pi)$. Hence, $(\tilde{\mathcal{H}}_1)$ holds. We now suppose that $(\tilde{\mathcal{H}}_{n-1})$ holds for $n \in \{0, \dots, N_2 + 1\}$. Let $\{\tilde{\eta}_{1,j}\}_{1 \leq j \leq n}$ and $\{\varphi_j\}_{1 \leq j \leq n-1}$ be respectively curves and Chebyshev nets as in the hypothesis of $(\tilde{\mathcal{H}}_n)$. Since $\theta_n \in (0, \pi)$, we apply Theorem 5.10 to the curves $\tilde{\eta}_{1,n}$ and $\eta_{2,n}$ to obtain a mapping $\varphi_n : B_e^n \subset (\mathbb{R}^+)^2 \rightarrow B_c^n \subset M$, with $B_e^n = [a_{2,n-1}, a_{2,n}] \times [0, -a_{1,1}]$ and $B_c^n = \varphi_n(B_e^n)$. Using the same argument as in the proof of Lemma 5.8, we obtain that φ is a Chebyshev net, that $B_c^n \subset Q$ and that B_c^n satisfies the statements 1 and 2 of $(\tilde{\mathcal{H}}_n)$.

We now suppose that $n < N_2 + 1$. Then, from Lemma 5.24 and from the assertion (5.36b) of $(\tilde{\mathcal{H}}_{n-1})$, we infer that the geodesic curvature $\tilde{\kappa}_{1,n+1}$ of $\tilde{\eta}_{1,n+1}$ satisfies

$$\int_{-v}^0 \tilde{\kappa}_{1,n+1} = \int_{-v}^0 \tilde{\kappa}_{1,n} + \int_{\varphi_n([a_{2,n-1}, a_{2,n}] \times [0, v])} K = \int_{-v}^0 \kappa_{1,0} + \sum_{k=1}^n \int_{\varphi_k([a_{2,k-1}, a_{2,k}] \times [0, v])} K,$$

for all $v \in [0, -a_{1,1}]$. Finally, from (5.7) and from the assertion (5.36a) of $(\tilde{\mathcal{H}}_{n-1})$, we infer that the interior angle $\theta_{n+1} = \angle(\eta'_{2,n+1}(a_{2,n}), -\tilde{\eta}'_{1,n+1}(0))$ satisfy

$$\theta_{n+1} = \theta_n - \int_{a_{2,n-1}}^{a_{2,n}} \kappa_{2,n} - \psi_{2,n} = \theta_1 - \tau(\eta_2|_{[0, a_{2,n}]}) .$$

Then, using hypotheses (5.31), we obtain that $\theta_{n+1} \in (0, \pi)$. This concludes the proof of the statement $(\tilde{\mathcal{H}}_n)$.

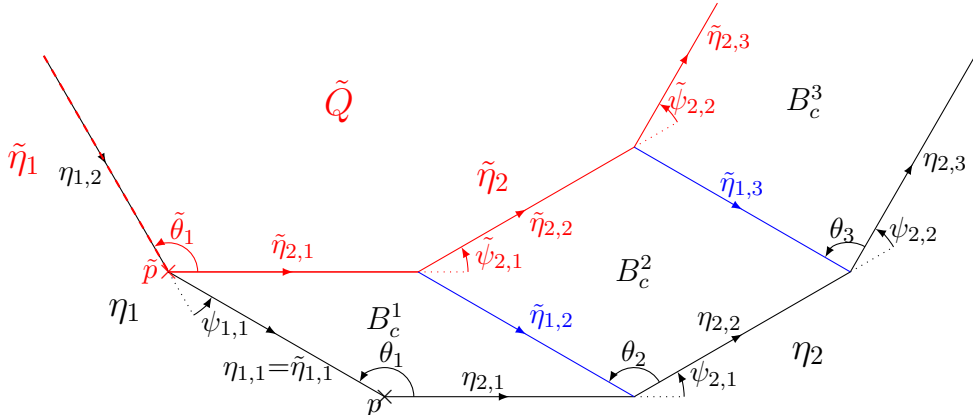


Fig. 5.17 Illustration of the recursive parallel transport of η_2 along $\eta_{1,1}$ ($N_1 = 1, N_2 = 2$)

Step 5 (Proof of the first induction process (2nd part of the construction)). By application of $(\tilde{\mathcal{H}}_n)$, for all $n \in \{1, \dots, N_2 + 1\}$, we obtain the existence of polygons $\{B_e^i\}_{1 \leq i \leq N_2+1}$ and, for all $i \in \{1, \dots, N_2 + 1\}$, of Chebyshev nets $\varphi_i : B_e^i \rightarrow B_c^i \subset Q$, with $B_c^i = \varphi_i(B_e^i)$. Then, for all $i \in \{1, \dots, N_2 + 1\}$, we denote $\tilde{\eta}_{2,i} : [a_{2,i-1}, a_{2,i}] \rightarrow Q$ the curve defined by $\tilde{\eta}_{2,i}(u) = \varphi_i(u, -a_{1,1})$, for all $u \in [a_{2,i-1}, a_{2,i}]$. We denote $\tilde{\eta}_2 : \mathbb{R}^+ \rightarrow Q$ the junction of the curves $\tilde{\eta}_{2,i}$, with $i \in \{1, \dots, N_2 + 1\}$, defined so that

$$\tilde{\eta}_2(\mathbb{R}^+) = \bigcup_{i=1}^{N_2+1} \tilde{\eta}_{2,i}([a_{2,i-1}, a_{2,i}]).$$

We denote $B_e^{\text{band}} = \mathbb{R}^+ \times [0, -a_{1,1}]$, $B_c^{\text{band}} = \bigcup_{i=1}^{N_2+1} B_c^i$ and $\tilde{Q} = Q \setminus B_c^{\text{band}}$. Let us construct the Chebyshev net on the half-band B_e^{band} . This mapping, denoted $\varphi_{\text{band}} : B_e^{\text{band}} \rightarrow B_c^{\text{band}}$, is defined

by

$$\varphi_{\text{band}}(u, v) = \varphi_i(u, v), \quad \text{whenever } (u, v) \in P_e^i \text{ for } i \in \{1, \dots, N_2 + 1\}. \quad (5.37)$$

Then, using that $\varphi_{\text{band}}|_{B_e^i}$ is a diffeomorphism for all $i \in \{1, \dots, N_2 + 1\}$ and using the statements 1 and 2 of $(\tilde{\mathcal{H}}_n)$, for all $n \in \{1, \dots, N_2 + 1\}$, we obtain that the mapping φ_{band} is a homeomorphism. We denote $\tilde{\eta}_1 : \mathbb{R}^- \rightarrow \eta_1[(-\infty, a_{1,1}]]$ the curve defined by $\tilde{\eta}_1(t) = \eta_1(t + a_{1,1})$. Then, \tilde{Q} is a sector delimited by the curves $\tilde{\eta}_1$ and $\tilde{\eta}_2$ with respectively N_1 and $N_2 + 1$ smooth pieces. We now prove that \tilde{Q} satisfies the hypotheses of (\mathcal{H}_{N_1}) (on the interior angle and on the total curvature). First note that, using (5.6), we obtain that the interior angle $\tilde{\theta}_1$ of \tilde{Q} satisfies

$$\tilde{\theta}_1 = \theta_1 - \int_{a_{1,1}}^0 \kappa_{1,1} - \psi_{1,1} = \theta_1 - \tau(\eta_1|_{[a_{1,1}, 0]}). \quad (5.38)$$

Then, using the hypotheses (5.31) on Q , we obtain that $\tilde{\theta}_1 \in (0, \pi)$.

To simplify the notation, we use in what follows the convention that $\sum_{k=1}^{i-1} (\dots) = 0$ when $i = 1$. As parallel transport preserves the angles, we have $\tilde{\psi}_{2,i} = \psi_{2,i}$, for all $i \in \{1, \dots, N_2\}$. Therefore, from (5.32) and the definition of φ_{band} , we infer that, for all $i \in \{1, \dots, N_2 + 1\}$ and $u \in [a_{2,i-1}, a_{2,i}]$,

$$\begin{aligned} \tau(\tilde{\eta}_2|_{[0,u]}) &= \sum_{k=1}^{i-1} \int_{a_{2,k-1}}^{a_{2,k}} \tilde{\kappa}_{2,k} + \int_{a_{2,i-1}}^u \tilde{\kappa}_{2,i} + \sum_{k=1}^{i-1} \tilde{\psi}_{2,k} \\ &= \sum_{k=1}^{i-1} \int_{a_{2,k-1}}^{a_{2,k}} \kappa_{2,k} + \sum_{k=1}^{i-1} \int_{B_c^k} K + \int_{a_{2,i-1}}^u \kappa_{2,i} + \int_{\varphi_i([a_{2,i-1}, u] \times [0, -a_{1,1}])} K + \sum_{k=1}^{i-1} \psi_{2,k} \\ &= \tau(\eta_2|_{[0,u]}) + \int_{\varphi_{\text{band}}([0,u] \times [0, -a_{1,1}])} K. \end{aligned} \quad (5.39)$$

Then, in the same manner as in Lemma 5.24, we deduce from (5.39) that

$$\tau_+(\tilde{\eta}_2) \leq \tau_+(\eta_2) + \int_{B_c^{\text{band}}} K^+ \quad \text{and} \quad \tau_-(\tilde{\eta}_2) \leq \tau_-(\eta_2) + \int_{B_c^{\text{band}}} K^-. \quad (5.40)$$

Moreover, we have

$$\tau_{\pm}(\tilde{\eta}_1) = \tau_{\pm}(\eta_1) - \tau_{\pm}(\eta_1|_{[a_{1,1}, 0]}). \quad (5.41)$$

We now prove that \tilde{Q} satisfies the condition (5.31a). First, we have

$$\begin{aligned} \tau_+(\tilde{\eta}_1) + \tau_+(\tilde{\eta}_2) + \int_{\tilde{Q}} K^+ + \pi - \tilde{\theta}_1 &\leq \tau_+(\eta_1) - \tau_+(\eta_1|_{[a_{1,1}, 0]}) + \tau_+(\eta_2) + \int_{B_c^{\text{band}}} K^+ \\ &\quad + \int_{\tilde{Q}} K^+ + \pi - \theta_1 + \tau(\eta_1|_{[a_{1,1}, 0]}) \\ &\leq \tau_+(\eta_2) + \tau_+(\eta_1) + \pi - \theta_1 + \int_Q K^+, \end{aligned} \quad (5.42)$$

using (5.38), (5.40) and (5.41) for the first inequality. Since hypothesis (5.31a) (with $\psi = \pi - \theta_1$) is satisfied by Q , we infer from (5.42) that

$$\tau_+(\tilde{\eta}_1) + \tau_+(\tilde{\eta}_2) + \int_{\tilde{Q}} K^+ + \pi - \tilde{\theta}_1 < \pi.$$

Finally, we prove that \tilde{Q} satisfies the condition (5.31b). From (5.40) and (5.41), we deduce that

$$\tau_-(\tilde{\eta}_1) + \tau_-(\tilde{\eta}_2) + \int_{\tilde{Q}} K^- \leq \tau_-(\eta_1) - \tau_-(\eta_1|_{[a_{1,1}, 0]}) + \tau_-(\eta_2) + \int_Q K^-. \quad (5.43)$$

Then, using the hypothesis (5.31b) on Q , we infer from (5.43) that

$$\tau_-(\tilde{\eta}_1) + \tau_-(\tilde{\eta}_2) + \int_{\tilde{Q}} K^- < \pi - \theta_1 - \tau_-(\eta_1|_{[a_{1,1},0]}).$$

Finally, using (5.38), we conclude that

$$\tau_-(\tilde{\eta}_1) + \tau_-(\tilde{\eta}_2) + \int_{\tilde{Q}} K^- \leq \pi - \tilde{\theta}_1 - \tau(\eta_1|_{[a_{1,1},0]}) - \tau_-(\eta_1|_{[a_{1,1},0]}) < \pi - \tilde{\theta}_1.$$

Hence, the hypotheses of (\mathcal{H}_{N_1}) are satisfied by \tilde{Q} . We obtain the existence of polygons $\{\tilde{B}_e^i\}_{1 \leq i \leq \tilde{N}_{\text{piece}}}$ such that $\text{int}(\tilde{B}_e^i) \cap \text{int}(\tilde{B}_e^j) = \emptyset$ for all $i \neq j$ and $\cup_{i=1}^{\tilde{N}_{\text{piece}}} \tilde{B}_e^i = (\mathbb{R}^+)^2$, and a Chebyshev parametrization of \tilde{Q} denoted $\tilde{\varphi}: (\mathbb{R}^+)^2 \rightarrow \tilde{Q}$. The translation of each polygon \tilde{B}_e^i by the vector $(0, -a_{1,1})$, i.e., the set $\{\tilde{B}_e^i + (0, -a_{1,1})\}_{1 \leq i \leq \tilde{N}_{\text{piece}}}$ is then joined to the set $\{B_e^i\}_{1 \leq i \leq N_2+1}$ to obtain $\{B_e^i\}_{1 \leq i \leq N_{\text{piece}}}$. Moreover, we define the mapping $\varphi: (\mathbb{R}^+)^2 \rightarrow Q$ by

$$\varphi(u, v) = \begin{cases} \varphi_{\text{band}}(u, v), & \text{if } (u, v) \in B_e^{\text{band}}, \\ \tilde{\varphi}(u, v + a_{1,1}), & \text{otherwise.} \end{cases}$$

We can show, in the same manner as for φ_{band} , that φ is a homeomorphism.

Step 6 (*Proof of the first induction process (nonsmooth Hazzidakis formula)*). Let $(u, v) \in (\mathbb{R}^+)^2$. First, we suppose that $(u, v) \in B_e^{\text{band}}$, so that $(u, v) \in B_e^j$ for some $j \in \{1, \dots, N_2+1\}$. By the Hazzidakis formula in the smooth setting (5.8), the angle ω_j between the parameter curves of φ_j satisfies

$$\omega_j(u, v) = \theta_j - \int_{a_{2,j-1}}^u \kappa_{2,j} - \int_{-v}^0 \tilde{\kappa}_{1,j} - \int_{\varphi_j([a_{2,j-1}, u] \times [0, v])} K. \quad (5.44)$$

Then, from (5.36) and (5.44), we infer that

$$\begin{aligned} \omega(u, v) &= \omega_j(u, v) = \theta_1 - \tau(\eta_2|_{[0, u]}) - \tau(\eta_1|_{[-v, 0]}) - \sum_{k=1}^{j-1} \int_{\varphi_k([a_{2,k-1}, a_{2,k}] \times [0, v])} K \\ &\quad - \int_{\varphi_j([a_{2,j-1}, u] \times [0, v])} K \\ &= \theta_1 - \tau(\eta_1|_{[-v, 0]}) - \tau(\eta_2|_{[0, u]}) - \int_{\varphi([0, u] \times [0, v])} K. \end{aligned}$$

We now suppose that $(u, v) \notin B_e^{\text{band}}$ and we denote $\bar{u} = u$ and $\bar{v} = v + a_{1,1}$. Then, $\bar{u}, \bar{v} \in \mathbb{R}^+$ and, by (\mathcal{H}_{N_1}) , the nonsmooth Hazzidakis formula (5.34) is satisfied by the angle $\tilde{\omega}$ between the coordinate curves of $\tilde{\varphi}$. Hence, using (5.34) on $\tilde{\omega}$ and (5.39), we obtain that

$$\begin{aligned} \omega(u, v) &= \tilde{\omega}(\bar{u}, \bar{v}) = \tilde{\theta}_1 - \tau(\tilde{\eta}_1|_{[-\bar{v}, 0]}) - \tau(\tilde{\eta}_2|_{[0, \bar{u}]}) - \int_{\tilde{\varphi}([0, \bar{u}] \times [0, \bar{v}])} K, \\ &= \theta_1 - \tau(\eta_1|_{[a_{1,1}, 0]}) - \tau(\eta_1|_{[-v, a_{1,1}]}) - \tau(\eta_2|_{[0, u]}) \\ &\quad - \int_{\varphi([0, u] \times [0, -a_{1,1}])} K - \int_{\varphi([0, u] \times [-a_{1,1}, v])} K \\ &= \theta_1 - \tau(\eta_1|_{[-v, 0]}) - \tau(\eta_2|_{[0, u]}) - \int_{\varphi([0, u] \times [0, v])} K. \end{aligned}$$

Hence, (\mathcal{H}_{N_1+1}) holds. This concludes the proof. ■

Remark 5.26 (Explicit value of $\mathcal{N}_{\text{piece}}$). We easily see from the proof that $\mathcal{N}_{\text{piece}} = (N_1 + 1)(N_2 + 1)$, where $N_1 + 1$ and $N_2 + 1$ are respectively the number of smooth pieces of η_1 and η_2 .

Corollary 5.27 (Existence of piecewise smooth Chebyshev nets on N -half-surfaces). *Let $N \geq 1$ and let B_c be a N -half-surface delimited by the curves $\{\gamma_c^i\}_{1 \leq i \leq N+1}$. We suppose that B_c satisfies the conditions*

$$\begin{aligned}\tau_+(\partial B_c) + \int_{B_c} K^+ &< \pi, \\ \tau_-(\partial B_c) + \int_{B_c} K^- &< |\psi|_{l^\infty}.\end{aligned}$$

Then, there exist $\mathcal{N}_{\text{piece}} \geq 1$ polygons $\{B_e^i\}_{1 \leq i \leq \mathcal{N}_{\text{piece}}}$ such that $(\mathbb{R}^+)^2 = \bigcup_{i=1}^{\mathcal{N}_{\text{piece}}} B_e^i$ and $\text{int}(B_e^i) \cap \text{int}(B_e^j) = \emptyset$ for all $i \neq j$, and Chebyshev coordinates φ on B_c such that $\{\gamma_c^i\}_{1 \leq i \leq N+1}$ are coordinate curves. Moreover, the angle $\omega = \angle(\partial_u \varphi, \partial_v \varphi)$ of the net is bounded away from 0 and π by the positive real number

$$\varepsilon = \min \left(\pi - \tau_+(\partial B_c) - \int_{B_c} K^+, \quad |\psi|_{l^\infty} - \tau_-(\partial B_c) - \int_{B_c} K^- \right).$$

Finally, the mapping $\varphi|_{B_e^i} : B_e^i \rightarrow B_c \subset B_c$, with $B_c^i = \varphi(B_e^i)$, is a diffeomorphism, for all $i \in \{1, \dots, \mathcal{N}_{\text{piece}}\}$.

Proof. The proof follows by combining Theorem 5.25 and Proposition 5.13. ■

Theorem 5.28 (Existence of piecewise smooth Chebyshev nets on geodesic N -half-surfaces). *Let $N \geq 1$ and let B_c be a geodesic N -half-surface delimited by the geodesic curves $\{\gamma_c^i\}_{1 \leq i \leq N+1}$. We suppose that B_c satisfies the conditions*

$$\begin{aligned}\int_{B_c} K^+ &< \pi - |\psi|_{l^1}, \\ \int_{B_c} K^- &< |\psi|_{l^\infty}.\end{aligned}$$

Then, there exist $\mathcal{N}_{\text{piece}} \geq 1$ polygons $\{B_e^i\}_{1 \leq i \leq \mathcal{N}_{\text{piece}}}$ such that $(\mathbb{R}^+)^2 = \bigcup_{i=1}^{\mathcal{N}_{\text{piece}}} B_e^i$ and $\text{int}(B_e^i) \cap \text{int}(B_e^j) = \emptyset$ for all $i \neq j$, and Chebyshev coordinates φ on B_c such that $\{\gamma_c^i\}_{1 \leq i \leq N+1}$ are coordinate curves. Moreover, the angle $\omega = \angle(\partial_u \varphi, \partial_v \varphi)$ of the net is bounded away from 0 and π by the positive real number

$$\min \left(\pi - |\psi|_{l^1} - \int_{B_c} K^+, |\psi|_{l^\infty} - \int_{B_c} K^- \right).$$

Finally, the mapping $\varphi|_{B_e^i} : B_e^i \rightarrow B_c \subset B_c$, with $B_c^i = \varphi(B_e^i)$, is a diffeomorphism, for all $i \in \{1, \dots, \mathcal{N}_{\text{piece}}\}$.

Chapter 6

Construction of discrete Chebyshev nets with singularities

We focus in this chapter on numerical applications of the results of the preceding chapters. We present the program we developed during this thesis which permits to construct discrete Chebyshev nets with singularities on a given surface M based on user's inputs (curves and angles). We linked our program to the Rhinoceros software, a commercial 3D computer graphics, and most of the figures presented in this chapter were created using Rhinoceros. Unless explicitly mentionned, the surface used for the illustrations of the different algorithms is the surface used for the conception of the forum of the Soliday's festival [3] presented in Figure 6.1. We implemented in this program a particular case of the algorithm presented in Chapter 5 that permits an automatic choice of the inputs ensuring that the angle between the coordinate curves of the discrete Chebyshev net with one conical singularity constructed on M is bounded away from 0 and π . This algorithm consists in splitting the suface into sectors that are meshed independently. The construction of discrete Chebyshev nets on sectors and the junctions of these discrete nets are considered in Section 6.1 and the algorithm is detailed in Section 6.2. We present in Section 6.3 some discrete Chebyshev nets obtained with our algorithm. Finally, we detail in Section 6.4 some additional functionalities of the program, that is, other types of boundary conditions permitting the construction of discrete Chebyshev nets and methods for the construction of the so-called rosette singularity.

Discrete Chebyshev nets with conical singularities

We construct in this section discrete Chebyshev nets on a surface M using the well-known compass method [12, 23, 40] with the primal boundary conditions. We then join discrete Chebyshev nets obtained using this algorithm to form discrete Chebyshev nets with conical singularities.

Compass method

The compass method is an algorithm that allows one to approximate the coordinate curves of a Chebyshev net $\varphi: U \subset \mathbb{R}^2 \rightarrow \Omega$, with $\Omega \subset M$. We denote $h > 0$ the step of this approximation. The purpose of the compass method is to approximate the grid $\varphi(U \cap h\mathbb{Z}^2)$ using a discretization of the conditions

$$|\partial_u \varphi(u, v)| = |\partial_v \varphi(u, v)| = 1,$$

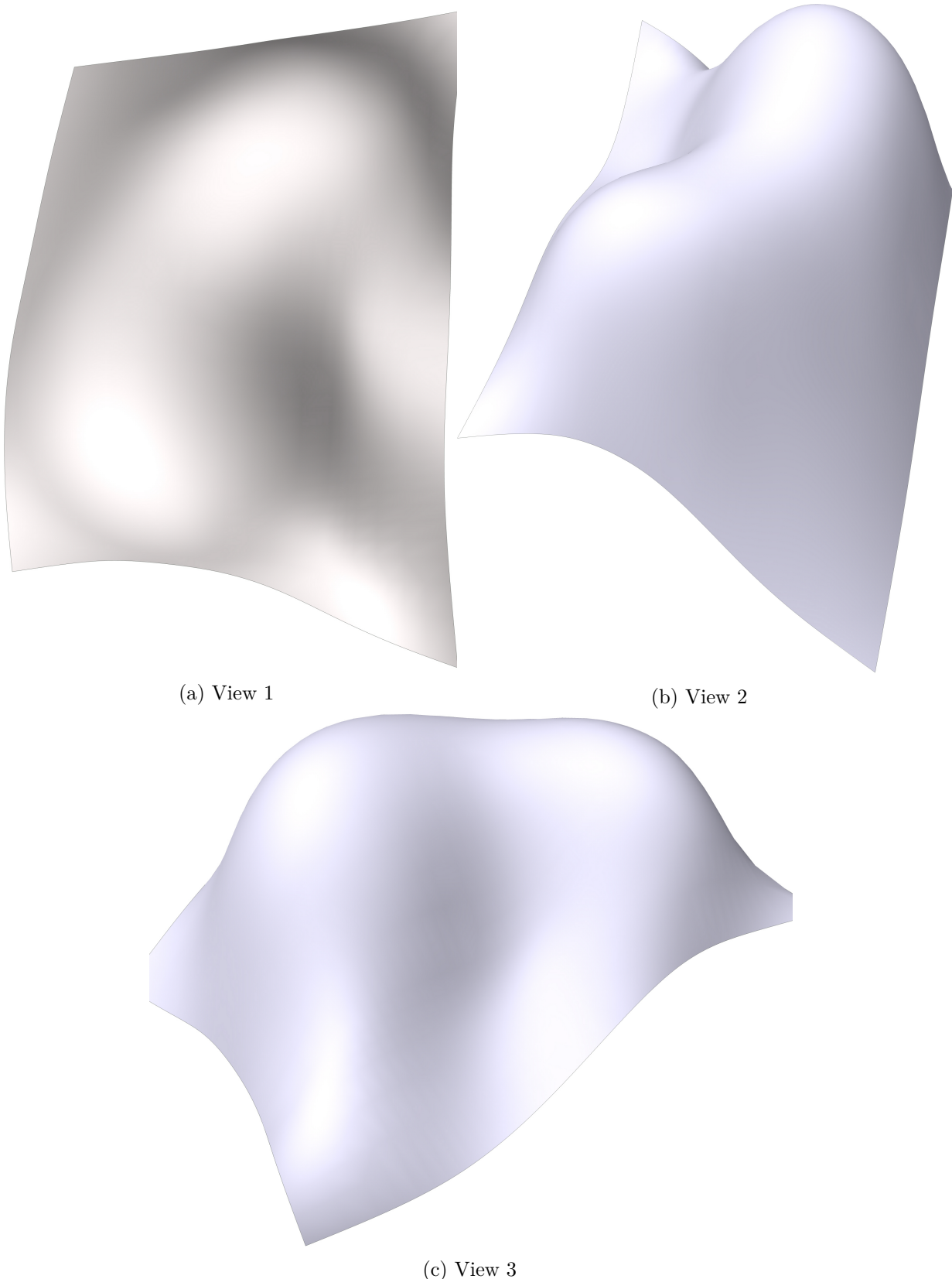


Fig. 6.1 The surface used for the conception of the forum constructed for the Soliday's festival (Rhinoceros software)

for all $(u, v) \in U$, defining Chebyshev nets. To illustrate this method, let

$$A = (u, v), \quad B = (u + h, v), \quad C = (u + h, v + h), \quad D = (u, v + h),$$

be four points in $U \subset \mathbb{R}^2$. Supposing that h is small enough, the point $\varphi(C)$ is approximated by a point of M at a distance h from both $\varphi(B)$ and $\varphi(D)$. We suppose moreover that h is small enough for the distances in the surface and the distances in \mathbb{R}^3 to be almost identical. Therefore, a good approximation of $\varphi(C)$ is given by the unique point of the surface (different from $\varphi(A)$) at the intersection of the two balls of radius h centered at $\varphi(B)$ and $\varphi(D)$. Thus, the points $\varphi(B)$, $\varphi(D)$ and $\varphi(A)$ allow one to define uniquely an approximation of $\varphi(C)$. We apply in what follows this method to primal boundary conditions.

Discrete Chebyshev nets given by two primal curves

We consider the primal boundary conditions given by the two primal curves $\gamma_1 : [0, L_1] \rightarrow M$, with $L_1 > 0$, and $\gamma_2 : [0, L_2] \rightarrow M$, with $L_2 > 0$, satisfying $\gamma_1(0) = \gamma_2(0)$ and $\angle(\gamma'_1(0), \gamma'_2(0)) \in (0, \pi)$. We set $U = [0, L_1] \times [0, L_2]$, $N_1 = \lfloor \frac{L_1}{h} \rfloor$ and $N_2 = \lfloor \frac{L_2}{h} \rfloor$. Then, the grid $\varphi(U \cap h\mathbb{Z})$ is given by a mapping $\mathcal{P} : \{1, \dots, N_1\} \times \{1, \dots, N_2\} \rightarrow M$ satisfying the primal boundary conditions

$$\begin{aligned}\mathcal{P}(i, 1) &= \gamma_1(ih), \text{ for all } i \in \{1, \dots, N_1\}, \\ \mathcal{P}(1, j) &= \gamma_2(jh), \text{ for all } j \in \{1, \dots, N_2\}.\end{aligned}\tag{6.1}$$

Now, let $\mathcal{P}_{i,j}^h \in M$, with $i \in \{1, \dots, N_1\}$ and $j \in \{1, \dots, N_2\}$, be an array satisfying the primal boundary conditions (6.1). Then, using the method described above, the three points $\mathcal{P}_{1,1}^h$, $\mathcal{P}_{1,2}^h$ and $\mathcal{P}_{2,1}^h$ determine uniquely the point $\mathcal{P}_{2,2}^h \in M$ such that the points $\mathcal{P}_{1,1}^h$, $\mathcal{P}_{2,1}^h$, $\mathcal{P}_{2,2}^h$ and $\mathcal{P}_{1,2}^h$ form a rhombus of length h in \mathbb{R}^3 . We denote d_E the Euclidean distance in \mathbb{R}^3 . Repeating the same operation, we entirely shape the grid \mathcal{P}^h using the conditions

$$\begin{aligned}d_E(\mathcal{P}_{i,j}^h, \mathcal{P}_{i+1,j}^h) &= h, \text{ for all } i \in \{1, \dots, N_1 - 1\} \text{ and } j \in \{1, \dots, N_2\}, \\ d_E(\mathcal{P}_{i,j}^h, \mathcal{P}_{i,j+1}^h) &= h, \text{ for all } i \in \{1, \dots, N_1\} \text{ and } j \in \{1, \dots, N_2 - 1\}.\end{aligned}\tag{6.2}$$

This method is illustrated in Figure 6.2. The grid \mathcal{P}^h is clearly an approximation of the grid \mathcal{P} associated with the Chebyshev net $\varphi : U \rightarrow M$. The inputs and the output of the compass method with primal boundary conditions are presented in Algorithm 1. We present an example of discrete Chebyshev net obtained with our program using primal boundary conditions in Figure 6.3.

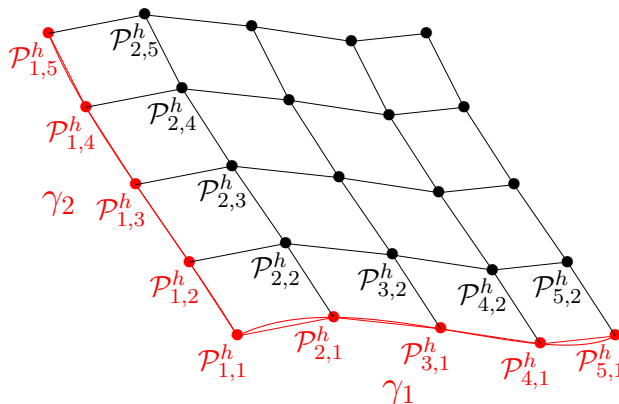


Fig. 6.2 Illustration of the compass method with the primal boundary conditions given by the red curves

Algorithm 1 Compass method with primal boundary conditions

Data: ε : the minimal angle accepted

 h : the step of the discretization

 M : the surface

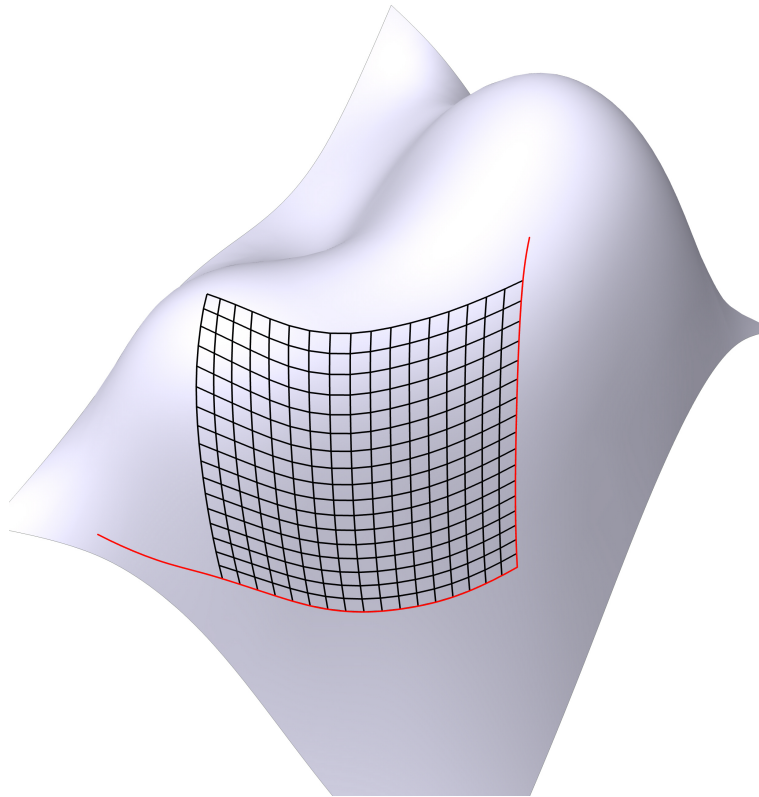
 γ_1 : a curve of M
 γ_2 : a curve of M
 N_1 : the number of points of the discretization of γ_1
 N_2 : the number of points of the discretization of γ_2
Result: \mathcal{P}^h : a discrete Chebyshev net


Fig. 6.3 A Chebyshev net constructed with the primal boundary conditions given by the red curves (view 2 of Figure 6.1)

Junction of discrete Chebyshev nets and conical singularities

We present in this section the junction of two different meshes defined using primal boundary conditions. To simplify the exposition, we switch to the continuous setting in this section. Junctions of Chebyshev nets are obtained by remarking that a curve in the boundary of some Chebyshev net $\varphi_1:U_1 \subset \mathbb{R}^2 \rightarrow \Omega_1 \subset M$ can be used as a boundary condition in order to construct a new Chebyshev net $\varphi_2:U_2 \subset \mathbb{R}^2 \rightarrow \Omega_2 \subset M$. Hence, we obtain a mapping $\varphi:U \rightarrow \Omega_1 \cup \Omega_2 \subset M$ which is the junction of these two Chebyshev nets. To illustrate this process, let $\gamma_1:[0, L_1] \rightarrow M$, with $L_1 > 0$, and $\gamma_2:[0, L_2] \rightarrow M$, with $L_2 > 0$, be two curves such that $\gamma_1(0) = \gamma_2(0)$ and $\angle(\gamma'_1(0), \gamma'_2(0)) \in (0, \pi)$. We denote $\varphi_1:[0, L_1] \times [0, L_2] \rightarrow M$ the Chebyshev net obtained using these boundary conditions. Then, let $u_0 \in [0, L_1]$ and let $\gamma_3:[0, L_1 - u_0] \rightarrow M$ be the curve defined by $\gamma_3(s) = \varphi_1(u_0 + s, L_2)$, for all $s \in [0, L_1 - u_0]$. Moreover, let $\gamma_4:[0, L_4] \rightarrow M$, with $L_4 > 0$, be a curve such that $\gamma_4(0) = \varphi_1(u_0, L_2) = \gamma_3(0)$ and $\angle(\gamma'_3(0), \gamma'_4(0)) \in (0, \pi)$. Then, there exists a Chebyshev net $\varphi_2:[0, L_1 - u_0] \times [0, L_2] \rightarrow M$ defined by the primal boundary conditions γ_3 and γ_4 .

Hence, we have constructed a mapping $\varphi: U \rightarrow M$, with $U = [0, L_1] \times [0, L_2] \cup [u_0, L_1] \times [L_2, L_2 + L_3]$ (see Figure 6.4). The inputs and the output of the algorithm joining two discrete Chebyshev nets defined by primal boundary conditions are presented in Algorithm 2.

Algorithm 2 Junction of two discrete Chebyshev nets

Data: ε : the minimal angle accepted
 h : the step of the discretization
 M : the surface
 \mathcal{P}^h : a discrete Chebyshev net
 p : a vertex in the boundary of \mathcal{P}^h
 γ : a curve of M such that $\gamma(0) = p$
 N : the number of points taken along γ
Result: \mathcal{P}_2^h : a discrete Chebyshev net

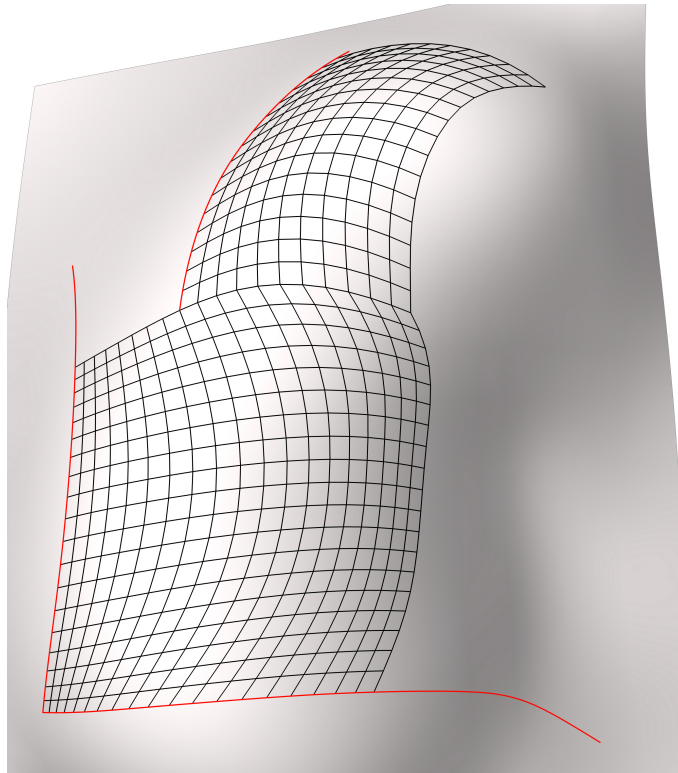


Fig. 6.4 Junction of two discrete Chebyshev nets (view 1)

We can now construct discrete Chebyshev nets with conical singularities by the junction of meshes defined by primal boundary conditions. Recall that the conical singularities of a discrete Chebyshev net are the points of the mesh with a valence different from 4. The connectivity of the mesh in a neighborhood of a conical singularity with valence 5 is shown in Figure 6.5. An example of discrete Chebyshev net with two conical singularities is presented in Figure 6.6.

An algorithm for Chebyshev nets with one conical singularity

In this section, given a surface M and a point $p \in M$, we construct a discrete Chebyshev net with a conical singularity of valence $N \geq 5$ at p . As all the singularity points considered in what follows are conical, the term conical will be omitted. Let us remark that a discrete Chebyshev

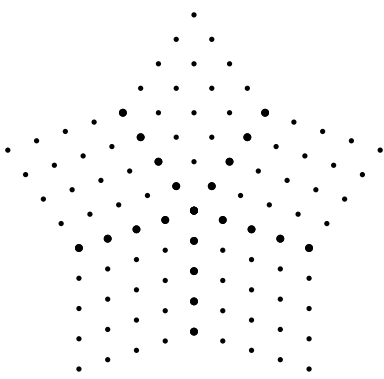


Fig. 6.5 Connectivity of a discrete Chebyshev net at a conical singularity point of valence 5

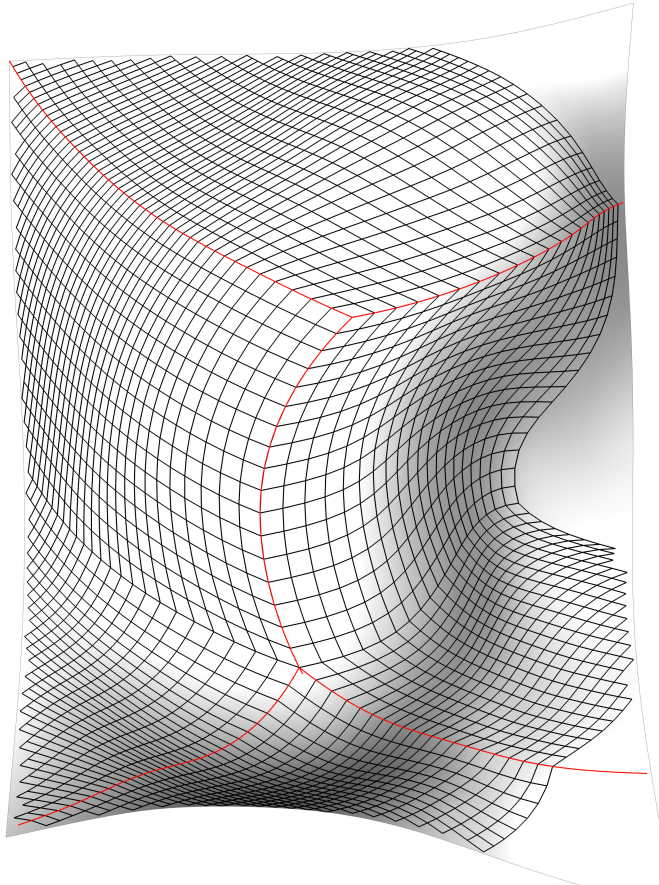


Fig. 6.6 Junction of 6 discrete Chebyshev nets defined by the primal boundary conditions given by the red curves forming two singularity points (view 1)

net with a singularity point at p is uniquely defined by the N coordinate curves starting from p , as each of the discrete nets joined to form the global net is uniquely defined by these curves (see Figure 6.7). We present an algorithm that consists in choosing efficiently these curves using the total Gaussian curvature of the surface.

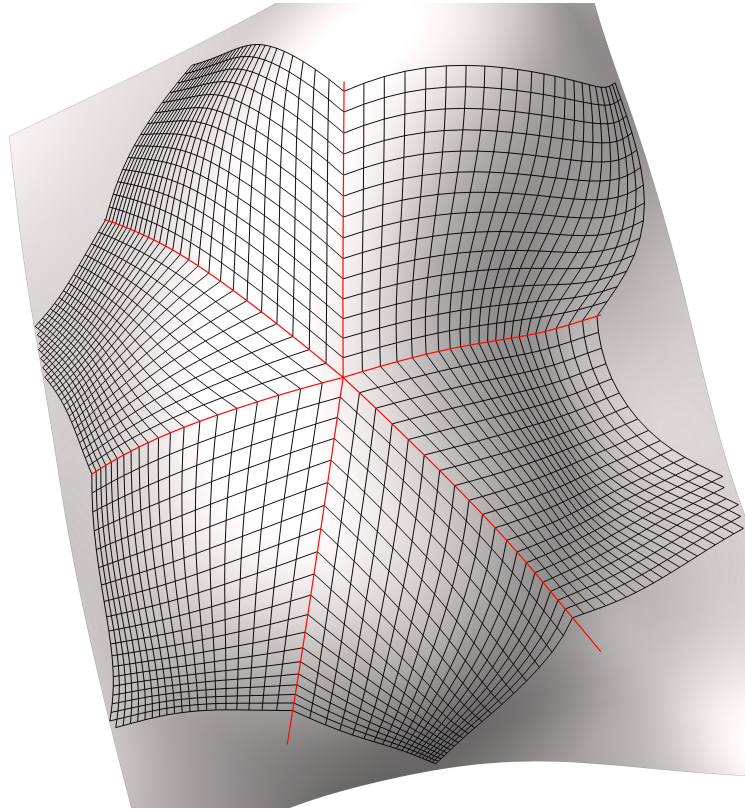


Fig. 6.7 A discrete Chebyshev net with one conical singularity of valence 6 (view 1)

Splitting the surface into sectors

Before we present the algorithm in the smooth setting, let us recall the Hazzidakis formula [28] on a parallelogram $ABCD$ formed by coordinate curves (see Figure 6.8):

$$\omega_A + \omega_C = \omega_B + \omega_D - \int_{ABCD} K dA, \quad (6.3)$$

where K is the Gaussian curvature of M . To simplify the construction, we only consider geodesic

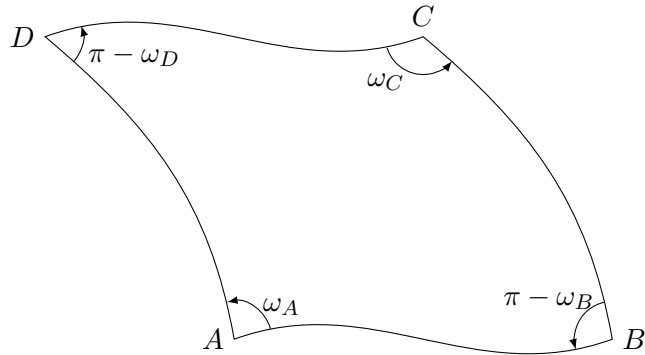


Fig. 6.8 Illustration of the Hazzidakis formula on the parallelogram $ABCD$

curves starting from p . Let $\{\gamma_i\}_{1 \leq i \leq N}$, with $N \geq 3$, be these geodesic curves and define

$$\begin{aligned}\psi_i &= \angle(\gamma'_i(0), \gamma'_{i+1}(0)), \quad \text{for } 1 \leq i \leq N-1, \\ \text{and } \psi_N &= \angle(\gamma'_N(0), \gamma'_1(0)).\end{aligned}$$

For all $i \in \{1, \dots, N-1\}$, we suppose that the curves γ_i and γ_{i+1} delimit a sector denoted Ω_i . We also suppose that the curves γ_N and γ_1 delimit a sector denoted Ω_N (see Figure 6.9). The sector Ω_i will be said to be with interior angle ψ_i , for all $i \in \{1, \dots, N\}$, in the sequel. We denote $K^+ = \max(K, 0)$ and $K^- = \max(-K, 0)$ the positive and the negative parts of the Gaussian curvature K of M . Let $\varphi_i : U_i \subset \mathbb{R}^2 \rightarrow \Omega_i$ be the Chebyshev net defined using the curves γ_i and γ_{i+1} as primal boundary conditions, for all $i \in \{1, \dots, N-1\}$. Let $\varphi_N : U_N \subset \mathbb{R}^2 \rightarrow \Omega_N$ be the Chebyshev net defined by the curves γ_N and γ_1 . From the Hazzidakis formula (6.3), we remark that the angle between the coordinate curves of the net φ_i is bounded away from 0 and π in the sector Ω_i whenever

$$\int_{\Omega_i} K^+ < \psi_i \quad \text{and} \quad \int_{\Omega_i} K^- < \pi - \psi_i, \quad (6.4)$$

for all $i \in \{1, \dots, N\}$. Hence, under these conditions, the angle ω between the coordinate curves of the Chebyshev net φ obtained by the junction along the geodesic curves of the Chebyshev nets $\{\varphi_i\}_{1 \leq i \leq N}$ is bounded away from 0 and π . We emphasize that the conditions (6.4) allow one to parametrize, in the best case, surfaces with curvature satisfying $\int_M K^+ < 2\pi$ and $\int_M K^- < \infty$. However, for these conditions on the total curvature to hold, the positive curvature should be evenly distributed among the sectors in order to satisfy (6.4) and this cannot be obtained in general (consider for example a portion of the ellipsoid). We cannot therefore expect, in general, to mesh a surface satisfying these conditions with only one singularity point and geodesic curves. Therefore, we suppose in what follows that the positive curvature is small enough (or well distributed) so that the condition $\int_{\Omega_i} K^+ < \psi_i$, for all $i \in \{1, \dots, N\}$, is always satisfied.

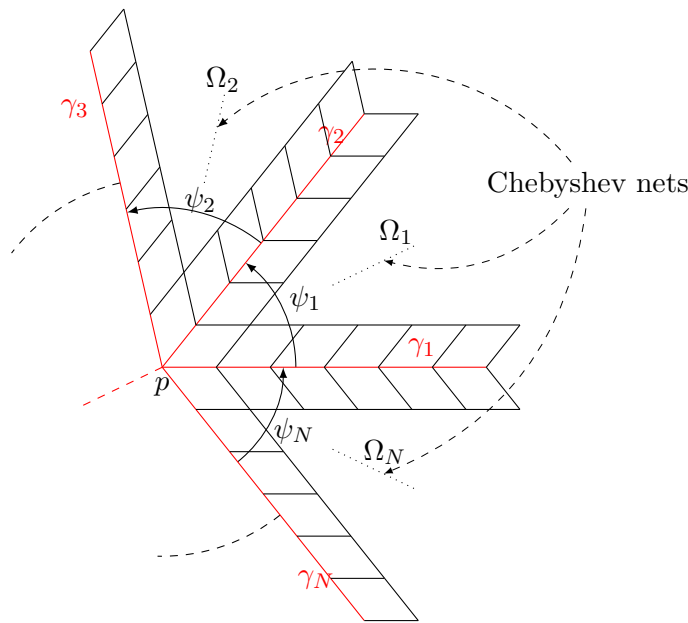


Fig. 6.9 Illustration of the surface splitting into sectors

Algorithm

The algorithm for the construction consists in choosing the interior angles $\{\psi_i\}_{1 \leq i \leq N}$ of the sectors $\{\Omega_i\}_{1 \leq i \leq N}$ so as to minimize the number N of sectors under the constraint that none of the angles of the Chebyshev net becomes flat in each sector. Let $\pi - \varepsilon$, with $\varepsilon \in (0, \pi)$, be the maximal angle accepted. The angle ψ_i is then chosen by dichotomy so that the condition $\int_{\Omega_i} K^- = \pi - \psi_i - \varepsilon$ holds true for all $i \in \{1, \dots, N\}$. Note that in this case the condition (6.4) is satisfied for all $i \in \{1, \dots, N\}$. This algorithm is summarized in Algorithm 3.

Numerical results

We apply in this section the algorithm described in Section 6.2.2 to surfaces that cannot be parametrized by a Chebyshev net without a singularity. Typical examples are Enneper surfaces of order $n \geq 2$ [15]. The total Gaussian curvature of these surfaces is $-4(n-1)\pi$, which exceeds the maximal -2π negative total curvature that can be parametrized without singularity. The Chebyshev net obtained is shown on Figure 6.10 for $n=3$ and on Figure 6.11 for $n=5$. The red curves are the geodesic curves $\{\gamma_i\}_{1 \leq i \leq N}$, with $N \geq 3$, delimiting the N sectors. Let us notice that the Chebyshev net is not smooth, since the second coordinate curves have a kink across these curves.

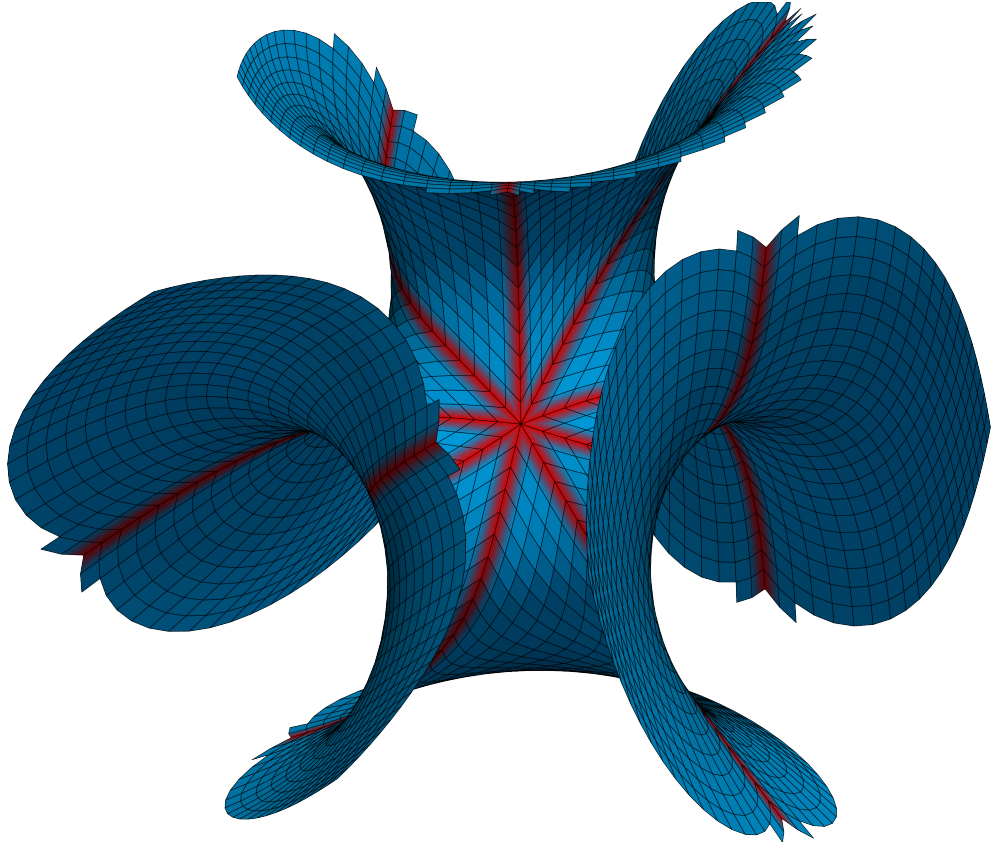


Fig. 6.10 A Chebyshev net with one singularity on Enneper's surface of order 3

We observe that a singularity point with valence 9 is sufficient to mesh the Enneper surface of order $n=3$ (with total Gaussian curvature $\int_M K = -8\pi$). A singularity point with valence 15 is sufficient for the Enneper surface of order $n=5$ with total Gaussian curvature $\int_M K = -16\pi$.

Algorithm 3 Construction of a discrete Chebyshev net with one singularity

Data: ε : the minimal angle accepted
 M : the surface
 K : the Gaussian curvature of the surface
 p : a point of the surface, position of the singularity
 v : the direction of the first geodesic

Result: \mathcal{P}^h : a Chebyshev net with one singularity point

```

 $\mathcal{P}^h \leftarrow$  empty net
 $tol \leftarrow \varepsilon/2$ 
 $\gamma_{\text{init}} \leftarrow$  geodesic curve starting at  $p$  in the direction  $v$ 
 $\gamma_1 \leftarrow \gamma_{\text{init}}$ 
add primal curve( $\mathcal{P}^h$ ,  $\gamma_1$ )
 $\psi_{\text{tot}} \leftarrow 0$ 
while  $\psi_{\text{tot}} < 2\pi$  do
     $\psi_{\text{min}} \leftarrow 0$ 
     $\psi_{\text{max}} \leftarrow \pi$ 
     $\psi \leftarrow \frac{\pi}{2}$ 
     $\Omega \leftarrow$  empty set
     $finished \leftarrow NO$ 
    while not  $finished$  do
        if  $\psi < 2\pi - \psi_{\text{tot}}$  then
             $\gamma_2 \leftarrow$  geodesic curve starting at  $p$  and forming an angle  $\psi$  with  $\gamma_1$ 
        else
             $\psi \leftarrow 2\pi - \psi_{\text{tot}}$ 
             $\gamma_2 \leftarrow \gamma_{\text{init}}$ 
        end if
         $\Omega \leftarrow$  sector delimited by  $\gamma_1$  and  $\gamma_2$ 
        if  $\int_{\Omega} K^- > \pi - \psi - \varepsilon$  then
             $\psi_{\text{max}} \leftarrow \psi$ 
             $\psi \leftarrow \max(\frac{\psi_{\text{min}} + \psi}{2}, \varepsilon)$ 
        else if  $\int_{\Omega} K^- < \pi - \psi - \varepsilon - tol$  then
             $\psi_{\text{min}} \leftarrow \psi$ 
             $\psi \leftarrow \min(\frac{\psi_{\text{max}} + \psi}{2}, \pi - \varepsilon, 2\pi - \psi_{\text{tot}})$ 
        else
             $finished \leftarrow YES$ 
        end if
    end while
    add primal curve( $\mathcal{P}^h$ ,  $\gamma_2$ )
     $\mathcal{P}_i^h \leftarrow$  Discrete Chebyshev net built on the sector delimited by  $\gamma_1$  and  $\gamma_2$ 
     $\mathcal{P}^h \leftarrow \{\mathcal{P}^h, \mathcal{P}_i^h\}$ 
     $\gamma_1 \leftarrow \gamma_2$ 
     $\psi_{\text{tot}} \leftarrow \psi_{\text{tot}} + \psi$ 
end while

```

Note that if we were to try meshing these surfaces with a Chebyshev net without singularity, folds would appear very quickly near the multiple necks of the surface where the negative Gaussian curvature is concentrated. The use of singularity points enables us to propagate the mesh further along the necks while keeping acceptable angles, thereby ensuring the constructibility of the mesh.

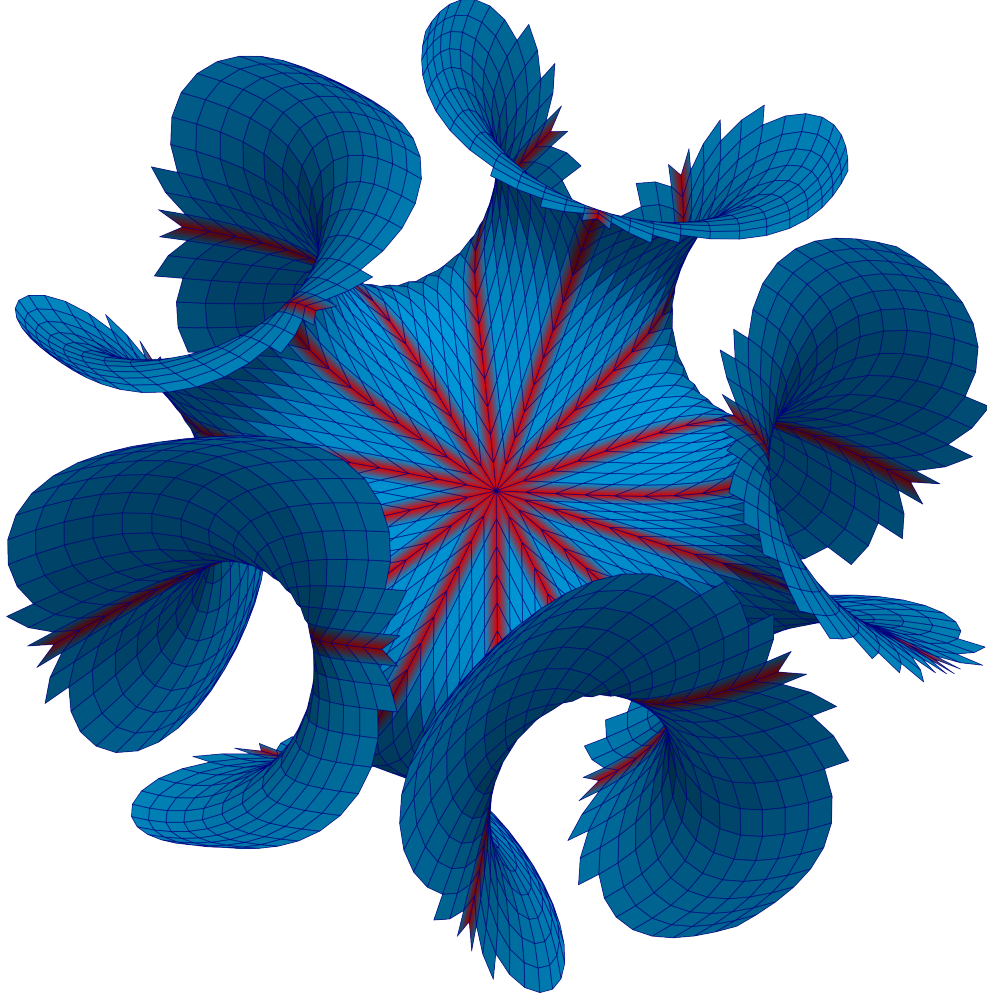


Fig. 6.11 A Chebyshev net with one singularity on Enneper's surface of order 5

An example of Chebyshev net with one singularity point obtained on a surface M with a well-distributed positive curvature is presented in Figure 6.12. This surface is obtained by the junction of a half-sphere and an Enneper surface of type $n=4$ ($\int_M K^+ = 2\pi$ and $\int_M K^- = -12\pi$). The singularity of the Chebyshev net has valence 15. We notice that angles rapidly decrease on the positively curved part of the surface and increase once negative Gaussian curvature takes over. The initial angles around the singularity should therefore not be taken too small to prevent the occurrence of a fold in the mesh.

Additional functionalities

Other types of boundary conditions

We now present two types of boundary conditions that can be used for defining discrete Chebyshev nets. As for the primal boundary conditions, we use the compass method for their discretization.

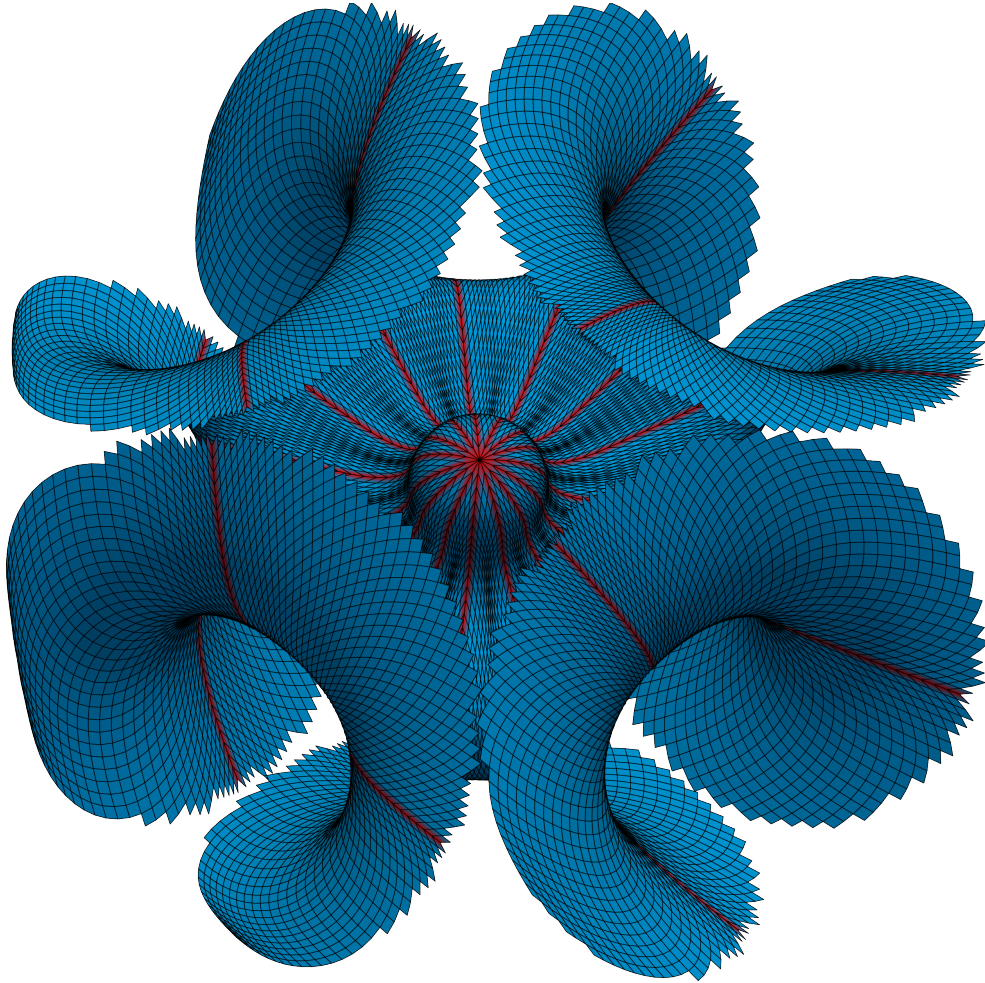


Fig. 6.12 A Chebyshev net with one singularity on a surface with positive and negative curvature

Dual boundary conditions

We present the compass method applied to the dual boundary conditions given by a dual curve $\gamma: \mathbb{R}^+ \rightarrow M$ and a set of angles $\{\bar{\omega}_i\}_{1 \leq i \leq N_1}$ in $(0, \pi)$, with $N_1 \geq 2$. Let $\mathcal{P}_{i,j}^h$, with $i, j \in \{1, \dots, N_1\}$, be a grid satisfying the following dual boundary conditions:

$$\mathcal{P}_{i,i}^h = \gamma \left(2h \sum_{k=1}^i \sin\left(\frac{\bar{\omega}_k}{2}\right) \right), \quad \text{for all } i \in \{1, \dots, N_1\}.$$

In the first stage of the construction, for all $i \in \{1, \dots, N_1 - 1\}$, we compute using the compass method the two uniquely defined points $\mathcal{P}_{i+1,i}^h$ and $\mathcal{P}_{i,i+1}^h$ such that $\mathcal{P}_{i,i}^h \mathcal{P}_{i+1,i}^h \mathcal{P}_{i+1,i+1}^h \mathcal{P}_{i,i+1}^h$ form a rhombus in \mathbb{R}^3 . We then repeat the construction with the points $\{\mathcal{P}_{k,1+k}^h\}_{1 \leq k \leq N_1-1}$ above γ and with the points $\{\mathcal{P}_{k,k-1}^h\}_{1 \leq k \leq N_1}$ below γ (see Figure 6.13). We construct the discrete Chebyshev net symmetrically on each side of the dual curve γ , so that we only consider the construction above this curve. In the same manner, we construct the discrete Chebyshev net level by level, each level $l \in \{0, \dots, N_1 - 1\}$ corresponding to a dual curve defined by the points $\{\mathcal{P}_{k,l+k}^h\}_{1 \leq k \leq N_1-l}$. In conclusion, the grid \mathcal{P}^h is well defined and \mathcal{P}^h satisfies (6.2) with $N_2 = N_1$. The inputs and the output of the compass method with dual boundary conditions are presented

in Algorithm 4. We present an example of discrete Chebyshev net obtained with our program using dual boundary conditions in Figure 6.14.

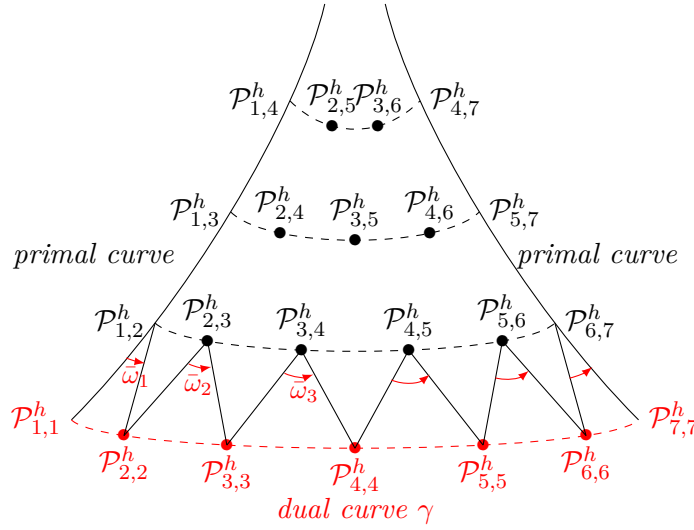


Fig. 6.13 Illustration of the one-sided compass method with the dual boundary conditions given by the curve and the angles in red

Algorithm 4 Compass method with dual boundary conditions

Data: ε : the minimal angle accepted

h : the step of the discretization

M : the surface

γ : a curve of M

N : the number of points of the discretization of γ

$\{\bar{\omega}_i\}_{1 \leq i \leq N}$: an angle distribution along γ

Result: \mathcal{P}^h : a discrete Chebyshev net

Note that a closed dual curve can be used as a dual boundary condition. We present an example of discrete Chebyshev net on a sphere obtained using a closed dual curve in Figure 6.15. The domain D of the discrete Chebyshev net $\mathcal{P}^h : D \rightarrow M$ is in this case the grid formed by the diagonals of the discrete cylinder (see Figure 6.16).

Mixed boundary conditions

We finally present the compass method with the mixed boundary conditions given by the dual curve $\gamma_1 : \mathbb{R}^+ \rightarrow M$ and the primal curve $\gamma_2 : [0, L_2] \rightarrow M$, with $L_2 > 0$. We suppose that $\gamma_1(0) = \gamma_2(0)$ and $\angle(\gamma'_1(0), \gamma'_2(0)) \in (0, \frac{\pi}{2})$, and we set $\gamma_1^{\text{set}} = \gamma_1(\mathbb{R}^+)$ and $N_2 = \lfloor \frac{L_2}{h} \rfloor$. Let $\mathcal{P}_{i,j}^h$, with $i, j \in \{1, \dots, N_2\}$, be a grid satisfying the following boundary conditions induced by the primal curve γ_2 :

$$\mathcal{P}_{1,j}^h = \gamma_2(jh), \quad \text{for all } j \in \{1, \dots, N_2\}.$$

Note that there exists a unique point (different from $\mathcal{P}_{1,1}^h$), say $\mathcal{P}_{2,2}^h \in \gamma_1^{\text{set}}$, such that $d_E(\mathcal{P}_{2,2}^h, \mathcal{P}_{1,2}^h) = h$. The point $\mathcal{P}_{2,2}^h$ allows one to define uniquely $\mathcal{P}_{2,j}^h \in M$, for all $j \in \{3, \dots, N_2\}$. Indeed, we first compute the unique point $\mathcal{P}_{2,3}^h$ such that $\mathcal{P}_{1,2}^h \mathcal{P}_{2,2}^h \mathcal{P}_{2,3}^h \mathcal{P}_{1,3}^h$ form a rhombus using the compass method. The remaining points $\{\mathcal{P}_{2,j}^h\}_{3 < j \leq N_2}$ are obtained in the same manner (see Figure 6.17). Reproducing this algorithm, we construct the discrete Chebyshev net \mathcal{P}^h level by level, each level $l \in \{2, \dots, N_2\}$ corresponding to a primal curve defined by the points

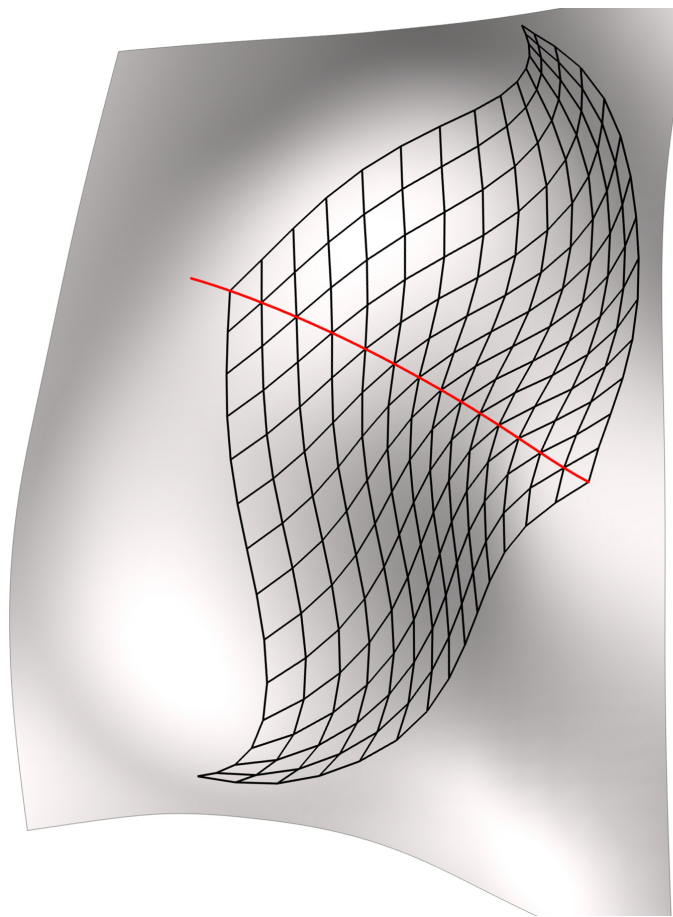


Fig. 6.14 A Chebyshev net constructed with the dual boundary conditions given by the red curve and a constant angle (view 1)

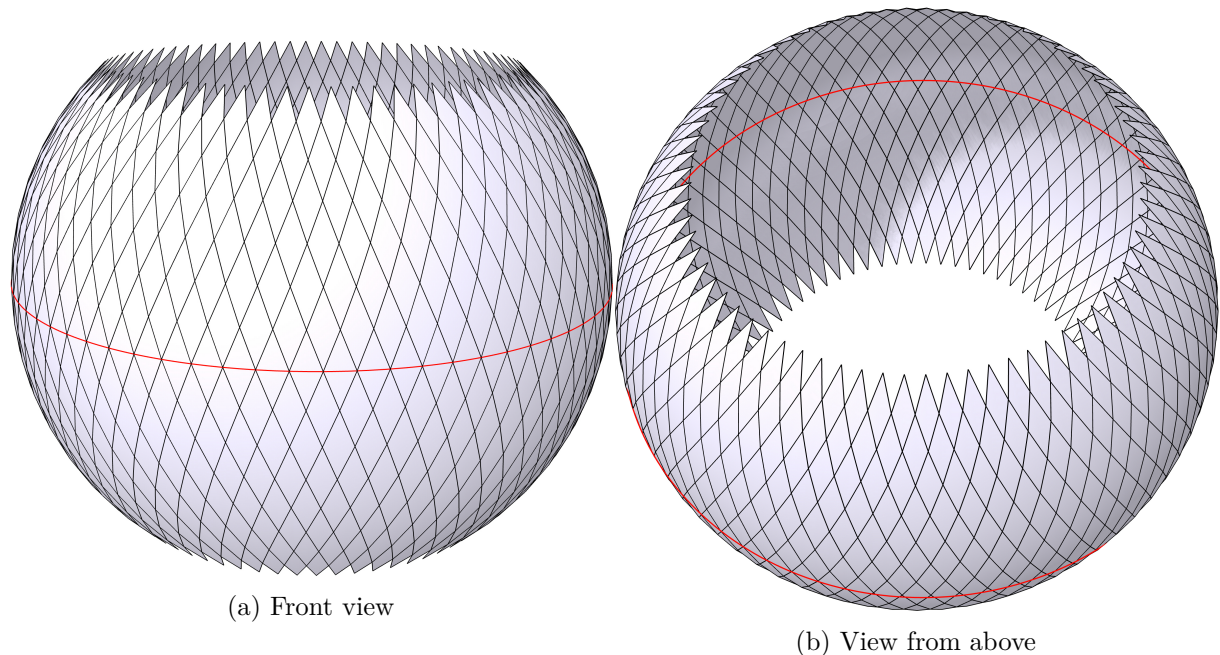


Fig. 6.15 A discrete Chebyshev net defined by a closed dual curve (in red) on the sphere

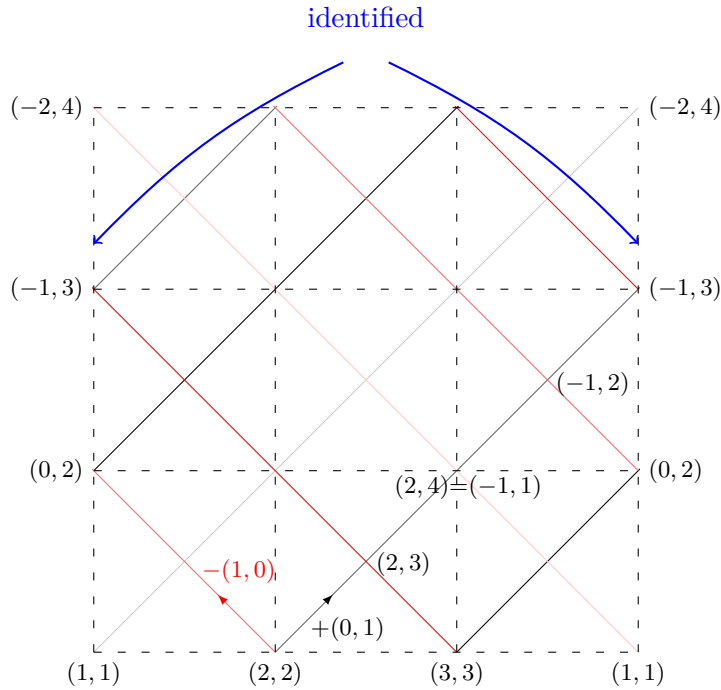


Fig. 6.16 Grid formed by the diagonals of the discrete cylinder

$\{\mathcal{P}_{l,l+k}^h\}_{0 \leq k \leq N_2-l}$. We remark that the points $\mathcal{P}_{i,i}^h$, with $i \in \{1, \dots, N_2\}$, define a dual boundary condition. Therefore, the points $\mathcal{P}_{l+k,l}^h$, with $l \in \{1, \dots, N_2-1\}$ and $k \in \{1, \dots, N_2-l\}$, are uniquely determined using the method of Subsection 6.4.1.1. Hence, the grid \mathcal{P}^h is entirely shaped and \mathcal{P}^h satisfies (6.2) with $N_1 = N_2$. The inputs and the output of the compass method with mixed boundary conditions are presented in Algorithm 5. We present an example of discrete Chebyshev net obtained with our program using mixed boundary conditions in Figure 6.18.

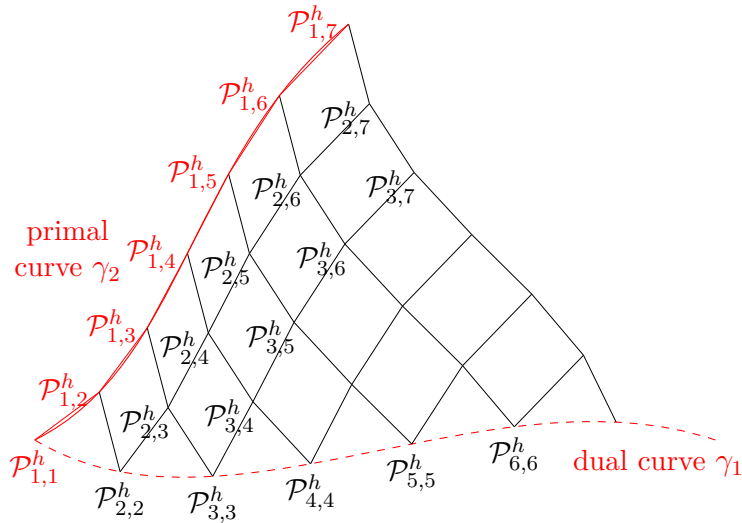


Fig. 6.17 Illustration of the one-sided compass method with mixed boundary conditions

Rosette singularities

We focus in this section on the construction of discrete Chebyshev nets with so-called rosette-type singularities. We first define discrete Chebyshev nets with a rosette singularity as discrete nets

Algorithm 5 Compass method with mixed boundary conditions

Data: ε : the minimal angle accepted

h : the step of the discretization

M : the surface

γ_1 : a curve of M (dual curve)

γ_2 : a curve of M (primal curve)

N_2 : the number of points of the discretization of γ_2

Result: \mathcal{P}^h : a discrete Chebyshev net

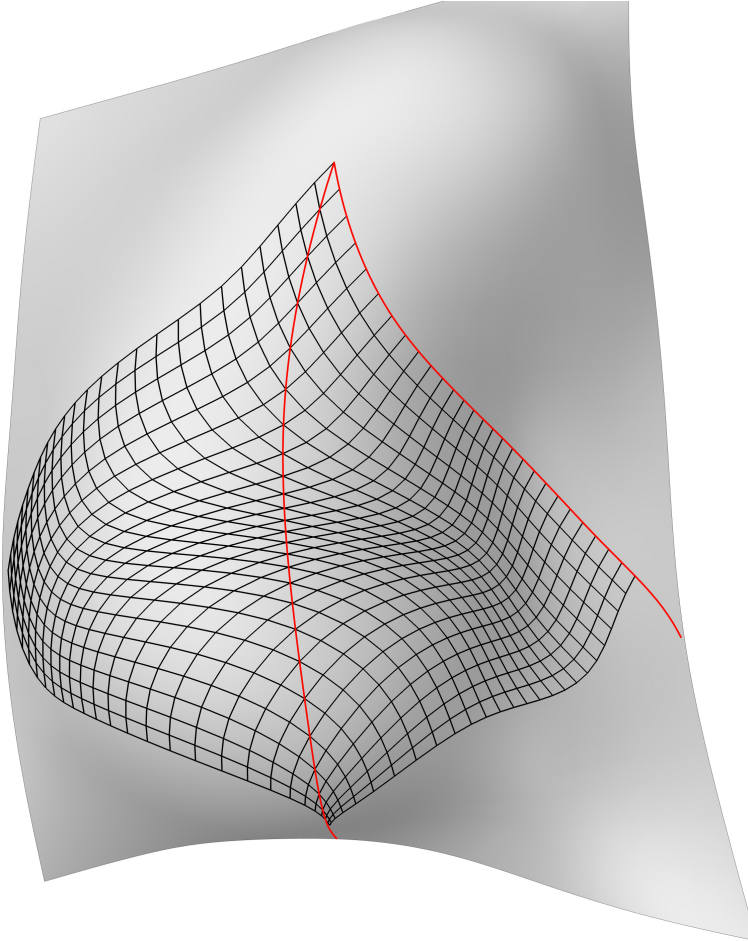


Fig. 6.18 A Chebyshev net constructed with the mixed boundary conditions given by the red curves (view 1)

obtained using the one-sided compass method with a small enough closed dual curve. We present an example of these discrete nets in Figure 6.19. The mesh in the neighborhood of the closed dual curve is depicted in Figure 6.20. Note that, for technical reasons, we displayed in this figure whole rhombi along the closed dual curve (in red), whereas the compass method should be only one-sided.

We then restrict to discrete Chebyshev nets with a rosette singularity reduced to a point $p \in M$. In other words, we suppose that the mesh covers any small enough neighborhood of p in M (see Figure 6.21). We observe in this figure that the point p is a conical singularity of valence $N \geq 5$ of the mesh surrounded by N conical singularity points of valence 3. We therefore call this set of conical singularity points a rosette-type singularity. An example of rosette-type conical singularity on an ellipsoid is presented in Figure 6.22.

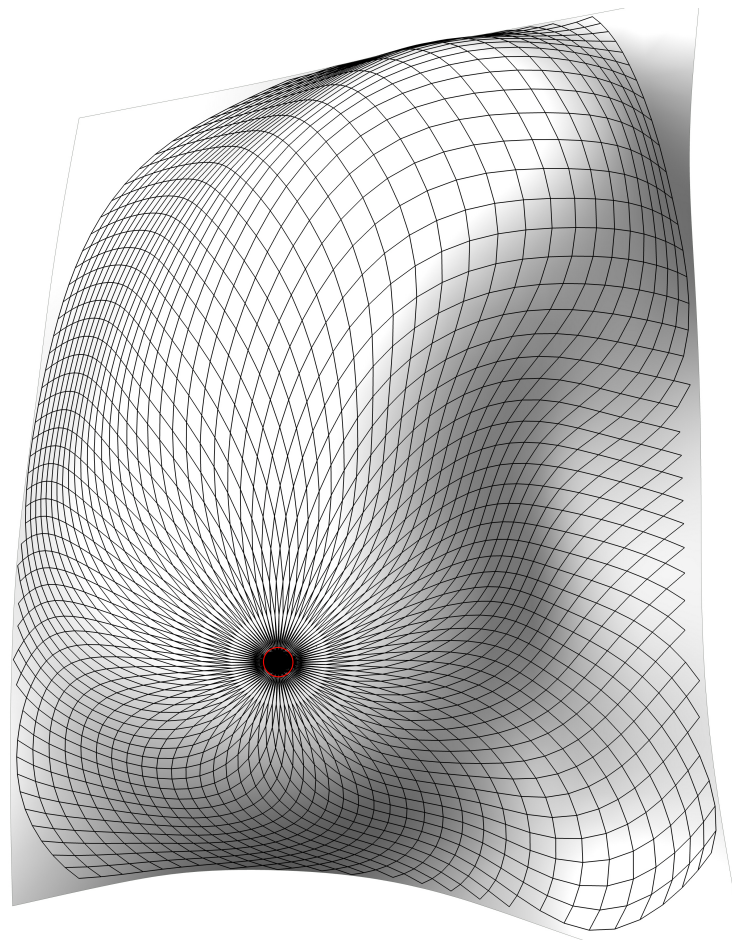


Fig. 6.19 A discrete Chebyshev net with a rosette singularity defined by a small closed dual curve (view 1)

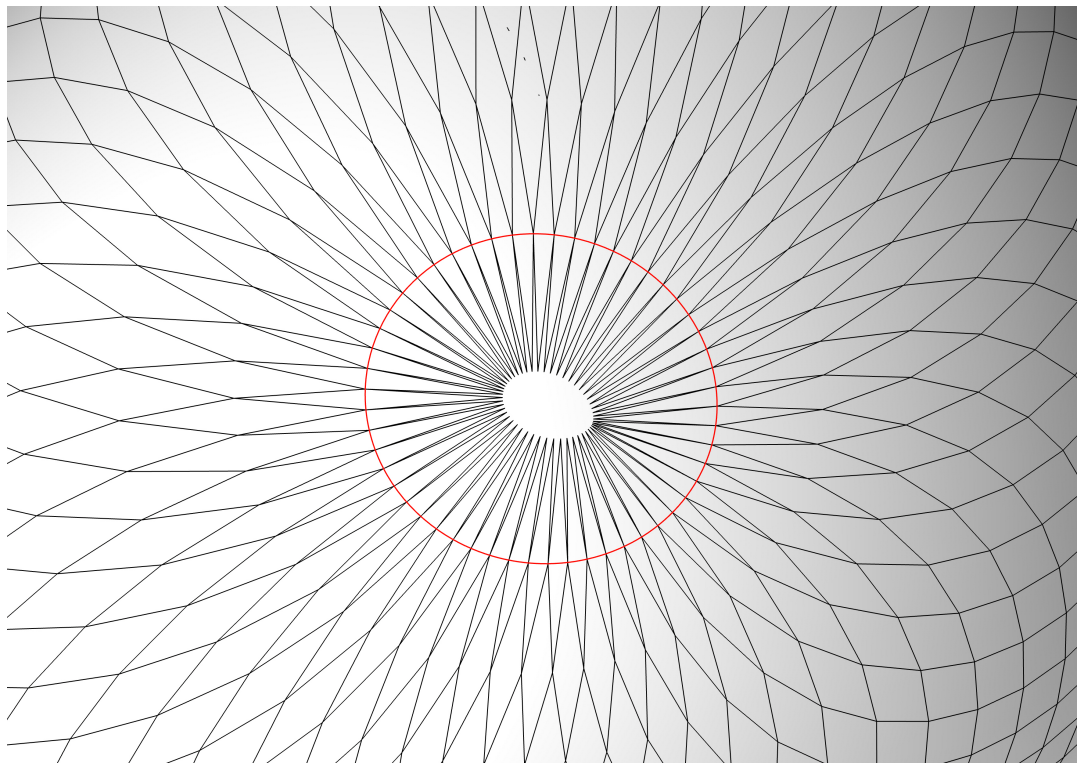


Fig. 6.20 A neighborhood of a rosette singularity

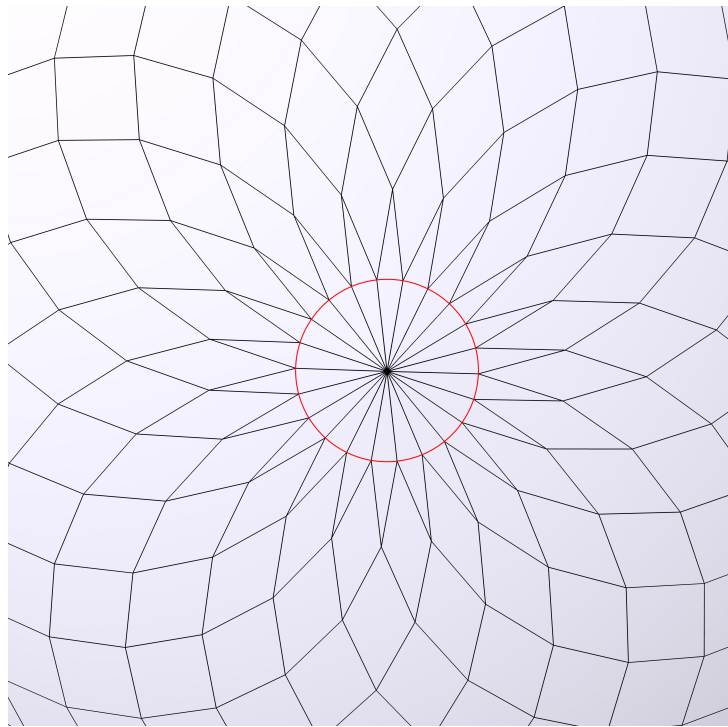


Fig. 6.21 A rosette singularity reduced to a point

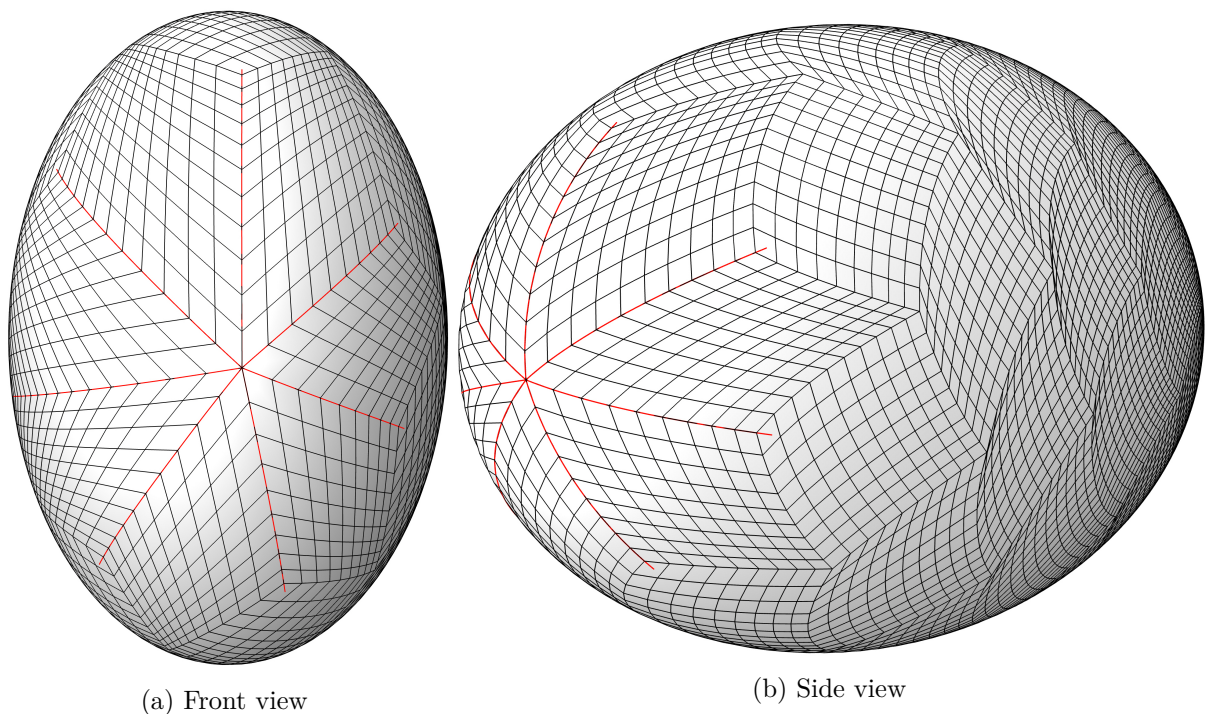


Fig. 6.22 A junction of discrete Chebyshev nets defined by the primal boundary conditions given by the red curves forming a rosette-type singularity

Chapter 7

Perspectives

In this short conclusive chapter, we present some open problems identified during this thesis which we think can be of interest. First, we present some possible extensions of our results. Then, we address open problems related to the existence of Chebyshev nets on general surfaces. These theoretical perspectives concern the construction of singularities with positive indices, such as rosette singularities (see Section 6.4.2) and conical singularities of valence three, and the construction of Chebyshev nets on surfaces with dominant positive curvature. Finally, we present open problems more directly related to the construction of Chebyshev nets for practical applications like gridshells. In particular, we elaborate on algorithms that would permit to construct Chebyshev nets in practical cases.

Possible extensions of our results

In this thesis, we have constructed Chebyshev nets with piecewise smooth conical singularities. With an eye to architectural applications, the construction of smooth Chebyshev nets is of great interest. In this context, we remarked that the conical singularities can be easily smoothed, up to an introduction of small holes on the surface. Therefore, we conjecture the following extension of Theorem 5.1 proved in Chapter 5:

Conjecture 7.1 (Smoothing of Chebyshev nets with singularities). *Let M be a smooth, complete, and simply connected surface satisfying*

$$\int_M K^+ < 2\pi \quad \text{and} \quad \int_M K^- < \infty.$$

Then, there exists $N_{\text{sing}} \in \mathbb{N}$ such that, for all $\varepsilon > 0$, there exist non-intersecting open balls $\{\mathcal{O}_1^\varepsilon, \dots, \mathcal{O}_{N_{\text{sing}}}^\varepsilon\}$ of radius lower than ε and a Chebyshev GC atlas on $M \setminus \{\mathcal{O}_1^\varepsilon, \dots, \mathcal{O}_{N_{\text{sing}}}^\varepsilon\}$.

Our preliminary work on this conjecture indicates that it holds, but the proof is still open. Moreover, in the case where the Chebyshev net has no singularity point, a similar smoothing argument can be applied to the construction introduced in [14] to prove the following conjecture:

Conjecture 7.2 (Global smooth parametrization of surfaces). *Let M be a smooth, complete, and simply connected surface satisfying*

$$\int_M K^+ < 2\pi, \quad \int_M K^- < 2\pi.$$

Then, there exist global smooth Chebyshev coordinates on M .

Another possible extension concerns the numerical applications of our results. Note that only a subcase of the result of Chapter 5 has been implemented and a first extension would be to implement the algorithm presented in Chapter 5, dealing in particular with the splitting of the surface. Then, in the case where multiple Chebyshev nets can be constructed on M , it would be interesting to focus on the construction of Chebyshev nets preserving a given structural layout [?]. Construction of Chebyshev nets with a given symmetry and control over the alignment of these nets with a given direction field such as principal directions of curvature or asymptotic directions can be other sources of investigation. We finally notice that an implementation of the above mentioned smoothing of conical singularities is also a possible extension of the numerical applications.

Existence and construction of Chebyshev nets

Let us consider the construction of Chebyshev nets on surfaces with dominant positive curvature. We observed in this thesis that conical singularities of valence greater than four are adapted to surfaces with dominant negative curvature. It appears that rosette singularities and conical singularities of valence three can be used for the parametrization of surfaces with dominant positive curvature. But, since the angle is preserved along the coordinate curves (see Figure 7.1), it seems that we cannot construct a Chebyshev GC atlas with more than three conical singularities of valence three. One way to circumvent this restriction is the introduction of a

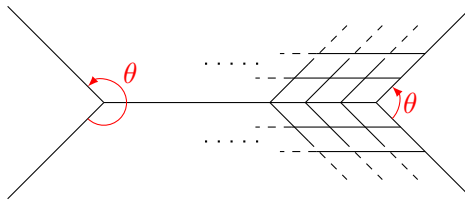


Fig. 7.1 Illustration of a Chebyshev net with two conical singularities of valence 3 joined by a coordinate curve

conical singularity of valence greater than four to form a so-called rosette-type singularity, in the same manner as in Section 6.4.2. This problem is then related to the construction of rosette singularities. One way to tackle the general problem of constructing Chebyshev nets on surfaces with dominant positive curvature is then to gain a deeper understanding of the rosette singularity. We can raise in this context the following two questions:

- can we construct a Chebyshev GC atlas on the sphere with two rosette singularities that are not antipodal?
- can we construct a Chebyshev GC atlas with two rosette singularities on any ellipsoid?

We finally mention that, more generally, the construction of Chebyshev nets on ellipsoids seems to be a challenging problem (see the conference of E. Ghys [24] where this problem is addressed).

Conception of Algorithms

In this manuscript, our algorithms for the construction of Chebyshev nets are mostly based on the worst case scenario. Indeed, to ensure the feasibility of the construction, we did not exploit the

possibility that the positive and the negative parts of the curvature could counterbalance. But, in most applications like form-finding for gridshells, the principal issue is to find a Chebyshev net such that the positive and the negative curvature counterbalance as much as possible. To achieve this goal, it appears that the total curvature of the surface (used in this manuscript) may not be the most relevant information to consider. This is due to the unpredictability of the position of the coordinate curves which prevents an accurate estimation of the curvature to be used in the Hazzidakis formula. Then, other information on the geometry of the surface such as geodesic curves (or the direction of principal curvatures) can be more relevant. We expect that an algorithm splitting the surface (such as in Chapter 5) based on this information can give better results in practical cases.

Finally, in this thesis we always considered a fixed surface M . With a view to applications such as form-finding for gridshells, it would be of great interest to consider (small) modifications of the surface. For example, the Chebyshev net φ can be separated from the surface whenever the angle ω is near 0 or π . This can be achieved by defining an angle distribution ω not satisfying the Hazzidakis formula everywhere on the surface. Then, the main issue in this perspective is to determine the cases where one can construct a surface \tilde{M} embedded in \mathbb{R}^3 and a Chebyshev net $\tilde{\varphi}$ on \tilde{M} with the prescribed angle distribution ω .

References

- [1] Aleksandrov, A. D. and Zalgaller, V. A. (1967). *Intrinsic geometry of surfaces*. Translated from the Russian by J. M. Danskin. Translations of Mathematical Monographs, Vol. 15. American Mathematical Society, Providence, R.I.
- [2] Bakelman, I. Y. (1967). Chebyshev nets in manifolds of bounded curvature, *Trudy Math. Inst. Steklov.* 76 (1965) 124–129. English transl. In *Proc. Steklov Inst. Math.*, volume 76, pages 154–160.
- [3] Baverel, O., Caron, J.-F., Tayeb, F., and Du Peloux, L. (2012). Gridshells in composite materials: Construction of a 300 m² forum for the solidays' festival in paris. *Structural Engineering International*, 22(3):408–414.
- [4] Ben-Chen, M., Gotsman, C., and Bunin, G. (2008). Conformal flattening by curvature prescription and metric scaling. In *Computer Graphics Forum*, volume 27, pages 449–458. Wiley Online Library.
- [5] Bianchi, L. (1902–1903). *Lezione di geometria differenziale*, volume 1,2. Spoerri, Pisa, second edition.
- [6] Bobenko, A. and Pinkall, U. (1996). Discrete surfaces with constant negative Gaussian curvature and the Hirota equation. *J. Differential Geom.*, 43(3):527–611.
- [7] Bobenko, A. I. and Klein, C. (2011). *Computational approach to Riemann surfaces*. Springer.
- [8] Bobenko, A. I. and Pinkall, U. (1999). Discretization of surfaces and integrable systems. *Oxford lecture series in mathematics and its applications*, 16:3–58.
- [9] Bobenko, A. I. and Suris, Y. B. (2008). *Discrete differential geometry*, volume 98 of *Graduate Studies in Mathematics*. American Mathematical Society, Providence, RI. Integrable structure.
- [10] Bommes, D., Campen, M., Ebke, H.-C., Alliez, P., and Kobbelt, L. (2013). Integer-grid maps for reliable quad meshing. *ACM Transactions on Graphics (TOG)*, 32(4):98.
- [11] Bonk, M. and Lang, U. (2003). Bi-Lipschitz parameterization of surfaces. *Mathematische Annalen*, 327(1):135–169.
- [12] Bouhaya, L., Baverel, O., and Caron, J.-F. (2010). Mapping two-way continuous elastic grid on an imposed surface: Application to grid shells. In *Symposium of the International Association for Shell and Spatial Structures (50th. 2009. Valencia). Evolution and Trends in Design, Analysis and Construction of Shell and Spatial Structures: Proceedings*. Editorial Universitat Politècnica de València.
- [13] Bouhaya, L., Baverel, O., and Caron, J.-F. (2014). Optimization of gridshell bar orientation using a simplified genetic approach. *Structural and Multidisciplinary Optimization*, 50(5):839–848.
- [14] Burago, Y. D., Ivanov, S. V., and Malev, S. G. (2005). Remarks on Chebyshev coordinates. *Zap. Nauchn. Sem. S.-Peterburg. Otdel. Mat. Inst. Steklov. (POMI)*, 329(Geom. i Topol. 9):5–13, 195.
- [15] Dierkes, U., Hildebrandt, S., and Sauvigny, F. (2010). *Minimal surfaces*, volume 339 of *Grundlehren der Mathematischen Wissenschaften [Fundamental Principles of Mathematical Sciences]*. Springer, Heidelberg, second edition. With assistance and contributions by A. Küster and R. Jakob.

References

- [16] Do Carmo, M. P. (1976). *Differential geometry of curves and surfaces*. Prentice-Hall, Inc., Englewood Cliffs, N.J. Translated from the Portuguese.
- [17] Douthe, C. (2007). *Etude de structures élancées précontraintes en matériaux composites, application à la conception des gridshells*. Theses, Ecole des Ponts ParisTech.
- [18] Douthe, C., Baverel, O., and Caron, J.-F. (2006). Form-finding of a grid shell in composite materials. *J. Int. Assoc. Shells Spatial Struct.*, 150:53–62.
- [19] Du Peloux, L., Caron, J.-F., Tayeb, F., and Baverel, O. (2015). The ephemeral cathedral of Créteil : a 350m² lightweight structure made of a GFRP composite gridshell. In *19èmes Journées Nationales sur les Composites*, Proceedings of the "19èmes Journées Nationales sur les Composites", Villeurbanne, France. JNC.
- [20] Du Peloux, L., Tayeb, F., Baverel, O., and Caron, J.-F. (2013). Faith can also move composite gridshells. In *IASS Symposium 2013: "Beyond the Limits of Man"*, Proceedings of the International Association for Shell and Spatial Structures Symposium 2013, Wrocław, Poland. International Association for Shell and Spatial Structures.
- [21] Du Peloux, L., Tayeb, F., Baverel, O., and Caron, J.-F. (2016). Construction of a Large Composite Gridshell Structure: A Lightweight Structure Made with Pultruded Glass Fibre Reinforced Polymer Tubes. *Structural Engineering International: Journal of the International Association for Bridge and Structural Engineering (IABSE)*, 26(2):160–167(8).
- [22] Gallot, S., Hulin, D., and Lafontaine, J. (1990). *Riemannian geometry*, volume 3. Springer.
- [23] Garg, A., Sageman-Furnas, A., Deng, B., Yue, Y., Grinspun, E., Pauly, M., and Wardetzky, M. (2014). Wire mesh design. *ACM Trans. Graph.*, 33(4):66:1–12.
- [24] Ghys, É. (2011a). La coupe des vêtements selon chebyshev. <http://podcast.grenet.fr/episode/%C2%AB-la-coupe-des-vetements-selon-tchebychev-%C2%BB-par-etienne-ghys/>.
- [25] Ghys, É. (2011b). Sur la coupe des vêtements: variation autour d'un thème de Tchebychev. *Enseign. Math.* (2), 57(1-2):165–208.
- [26] Goldman, W. (2010). Geometric structures on manifolds. <http://www.math.umd.edu/~wmg/gstom.pdf>.
- [27] Hartman, P. (1964). *Ordinary differential equations*. John Wiley & Sons, Inc., New York-London-Sydney.
- [28] Hazzidakis, J. N. (1880). Ueber einige Eigenschaften der Flächen mit constantem Krümmungsmaass. *J. Reine Angew. Math.*, 88:68–73.
- [29] Hirota, R. (1977). Nonlinear partial difference equations. III. Discrete sine-Gordon equation. *J. Phys. Soc. Japan*, 43(6):2079–2086.
- [30] Hoffmann, T. (1999). Discrete Amsler surfaces and a discrete Painlevé III equation. In *Discrete integrable geometry and physics (Vienna, 1996)*, volume 16 of *Oxford Lecture Ser. Math. Appl.*, pages 83–96. Oxford Univ. Press, New York.
- [31] Kälberer, F., Nieser, M., and Polthier, K. (2007). Quadcover – surface parameterization using branched coverings. *Computer Graphics Forum*, 26(3):375–384.
- [32] Kharevych, L., Springborn, B., and Schröder, P. (2005). Cone singularities to the rescue: Mitigating area distortion in discrete conformal. In *ACM SIGGRAPH/Eurographics Symposium on Geometry Processing*.
- [33] Kharevych, L., Springborn, B., and Schröder, P. (2006). Discrete conformal mappings via circle patterns. *ACM Transactions on Graphics (TOG)*, 25(2):412–438.
- [34] Lafuente Hernández, E., Gengnagel, C., Sechelmann, S., and Rörig, T. (2011). On the materiality and structural behaviour of highly-elastic gridshell structures. In *Computational Design Modelling*, pages 123–135. Springer.

- [35] Lafuente Hernandez, E., Sechelmann, S., Rörig, T., and Gengnagel, C. (2012). Topology optimisation of regular and irregular elastic gridshells by means of a non-linear variational method. In *Proc. Advances in Architectural Geometry*, pages 147–160. Springer.
- [36] Lee, J. M. (2011). *Introduction to topological manifolds*, volume 202 of *Graduate Texts in Mathematics*. Springer, New York, second edition.
- [37] Masson, Y. and Monasse, L. (2016). Existence of global Chebyshev nets on surfaces of absolute Gaussian curvature less than 2π . *J. Geom.*
- [38] Nieser, M. and Polthier, K. (2009). Parameterizing singularities of positive integral index. In *IMA International Conference on Mathematics of Surfaces*, pages 265–277. Springer.
- [39] Otto, F. (1974). Il10 gitterschalen. *Institut für leichte Flächentragwerke (IL)*.
- [40] Otto, F., Hennicke, J., and Matsushida, K. (1974). Gitterschalen gridshells. *Institut für leichte Flächentragwerke (IL)*.
- [41] Pinkall, U. (2008). Designing cylinders with constant negative curvature. In *Discrete differential geometry*, pages 57–66. Springer.
- [42] Ray, N., Li, W. C., Lévy, B., Sheffer, A., and Alliez, P. (2006). Periodic global parameterization. *ACM Transactions on Graphics (TOG)*, 25(4):1460–1485.
- [43] Samelson, S. L. and Dayawansa, W. P. (1995). On the existence of global Tchebychev nets. *Trans. Amer. Math. Soc.*, 347(2):651–660.
- [44] Stoker, J. (1969). *Differential Geometry*, volume XX of *Pure and Applied Mathematics*. Interscience Publishers John Wiley & Sons, New-York-London-Sydney.
- [45] Tong, Y., Alliez, P., Cohen-Steiner, D., and Desbrun, M. (2006). Designing quadrangulations with discrete harmonic forms. In *Proceedings of the fourth Eurographics symposium on Geometry processing*, pages 201–210. Eurographics Association.
- [46] Troyanov, M. (1986). Les surfaces euclidiennes à singularités coniques. *Ens. Math.*, 32:79–94.
- [47] Wolff, M. (2012). Travaux dirigés de master 2 : Groupes fuchsiens et représentation de groupes de surfaces. <https://webusers.imj-prg.fr/~maxime.wolff/ExosM2Hyp.pdf>.

